A N N U A L R E P O R T

1 9 7 0

U. S. WATER CONSERVATION LABORATORY
Southwest Branch
Soil and Water Conservation Research Division
Agricultural Research Service
United States Department of Agriculture
Phoenix, Arizona

FOR OFFICIAL USE ONLY

This report contains unpublished and confidential information concerning work in progress. The contents of this report may not be published or reproduced in any form without the prior consent of the research workers involved.

TABLE OF CONTENTS

	Title	Page
Introduction	Changes in Personnel	iv
SWC-012-gG-1	Methods for water quality improvement and its storage underground	
Ariz.-WCL 66-1	Experimental and analytical studies of the flow and oxygen regimes in soil intermittently inundated with low quality water	1-1
Ariz.-WCL 67-4	Waste-water renovation by spreading treated sewage for groundwater recharge	2-1
Ariz.-WCL 68-3	Column studies of the chemical, physical, and biological processes of wastewater renovation by percolation through the soil	3-1
Ariz.-WCL 70-2	Characterization of the soil microflora and biological processes occurring in soil used for waste water renovation	4-1
SWC-018-gG-2	Increasing and conserving farm water supplies	
Ariz.-WCL 60-7	Soil treatment to reduce infiltration and increase precipitation runoff	5-1
Ariz.-WCL 64-6	Dispersion and flocculation of soil and clay materials as related to the Na and Ca status of the ambient solution	6-1
Ariz.-WCL 65-2	Materials and methods for water harvesting and water storage in the State of Hawaii	7-1
Ariz.-WCL 67-2	Physical and chemical characteristics of hydrophobic soils	8-1
Ariz.-WCL 67-3	Use of floating solid and granular materials to reduce evaporation from water surfaces	9-1
Ariz.-WCL 68-1	Evaporation of water from soil	10-1

	Title	Page
Ariz.-WCL 68-2	Fabricated-in-place, reinforced reservoir linings	11-1
SWC-019-gG-3	Efficient irrigation and agricultural water use	
Ariz.-WCL 58-2	Consumptive use of water by crops grown in Arizona	12-1
Ariz.-WCL 62-10	Plant response to changes in evaporative demand and soil water potential, as shown by measurement of leaf resistance, transpiration, leaf temperature, and leaf water content	13-1
Ariz.-WCL 66-2	Irrigation outlet structures to distribute water onto erosive soils	14-1
Ariz.-WCL 67-1	Flow measurement in open channels with critical depth flumes	15-1
Ariz.-WCL 68-5	Assessing the energy environment of plants	16-1
Ariz.-WCL 70-1	Computer simulation of greenhouses	17-1
Ariz.-WCL 70-3	Design and performance of trickle irrigation systems	18-1
Appendix I	Summation of Important Findings	AI-1
Appendix II	List of Publications	AII-1
Appendix III	Summary Table of Status of Research Outlines	AIII-1

CHANGES IN PERSONNEL

The Laboratory has been strengthened during 1970 by the addition of six new members. They are as follows.

D. A. Bucks, Agricultural Engineer (Return from military furlough)
R. G. Gilbert, Research Soil Scientist
L. Hankins, Summer Aid
D. Ruiz, Summer Aid
R. Valdez, Mathematics Aid
K. K. Watson, Research Civil Engineer, Visiting Scientist from Australia

During 1970 there were two departures. They are as follows:

L. Hankins, Summer Aid
D. Ruiz, Summer Aid

LABORATORY STAFF

Professional:

H. Bouwer, B.S., M.S., Ph.D., P.E., Research Hydraulic Engineer
D. A. Bucks, B.S., M.S., Agricultural Engineer
K. R. Cooley, B.S., M.S., Ph.D., Research Hydrologist
W. L. Ehrler, B.A., M.S., Ph.D., Research Plant Physiologist
L. J. Erie, B.S., M.S., P.E., Agricultural Engineer
D. H. Fink, B.S., M.S., Ph.D., Research Soil Scientist
G. W. Frasier, B.S., M.S., Research Hydraulic Engineer
R. G. Gilbert, B.S., M.S., Ph.D., Research Soil Scientist
S. B. Idso., B.Phys., M.S., Ph.D., Research Soil Scientist
R. D. Jackson, B.S., M.S., Ph.D., Research Physicist
B. A. Kimball, B.S., M.S., Ph.D., Research Soil Scientist
J. C. Lance, B.S., M.S., Ph.D., Research Soil Scientist
L. E. Myers, B.S., M.S., P.E., Research Hydraulic Engineer and Director
F. S. Nakayama, B.S., M.S., Ph.D., Research Chemist
R. J. Reginato, B.S., M.S., Research Soil Scientist
J. A. Replogle, B.S., M.S., Ph.D., P.E., Research Hydraulic Engineer
R. C. Rice, B.S., M.S., P.E., Agricultural Engineer
K. K. Watson, B.E., M.E., Ph.D., Research Civil Engineer
F. D. Whisler, B.S., M.S., Ph.D., Research Soil Scientist

Technicians:

E. D. Escarcega, Hydraulic Engineering Technician
O. F. French, Agricultural Research Technician
L. Hankins, Summer Aid
L. P. Girdley, Engineering Draftsman
J. R. Griggs, Physical Science Technician
R. S. Linebarger, Biological Laboratory Technician
J. M. R. Martinez, Engineering Aid
H. L. Mastin, Physical Science Technician
J. B. Miller, Physical Science Technician
S. T. Mitchell, Physical Science Technician
K. G. Mullins, Physical Science Technician
J. M. Pritchard, Physical Science Technician
B. A. Rasnick, Physical Science Technician
M. S. Riggs, Laboratory Technician (Salt River Project)
D. Ruiz, Summer Aid
C. C. Stetter, Laboratory Technician (Salt River Project)
R. Valdez, Mathematics Aid

Administrative, Clerical, and Maintenance:

O. J. Abeyta, Gardener
I. G. Barnett, Janitor
E. D. Bell, General Machinist
E. E. De La Rosa, Maintenance Worker
B. E. Fisher, Library Technician
C. G. Hiesel, General Machinist
R. C. Klapper, Refrigeration and Air Conditioning Mechanic
A. H. Morse, Secretary-Dictating Machine Transcriber
M. E. Olson, Clerk-Stenographer
L. J. Orneside, Clerk-Stenographer
M. A. Seiler, Clerk-Stenographer
M. F. Witcher, Clerk-Stenographer

TITLE: EXPERIMENTAL AND ANALYTICAL STUDIES OF THE FLOW AND OXYGEN REGIMES IN SOIL INTERMITTENTLY INUNDATED WITH LOW QUALITY WATER.

CRIS WORK UNIT: SWC-012-gG-1 CODE NO.: Ariz.-WCL 66-1

INTRODUCTION:

The need for this study and the preliminary results are given in the 1966 Annual Report. A soil column was used to study the effect of entrapped air on the flow of water into a layered sand and gravel system, such as occurs at the Flushing Meadows recharge site. There are at least three situations which might occur during flooding and subsequent drainage:

(1) At the edges of the spreading basins water can enter and drain from the soil with free escape and access of air all along the profile.

(2) Further toward the center of the basins, water may enter the soil with air free to escape, but during drainage air might not have free access to all parts of the profile except through the surface.

(3) In the center of wide spreading basins, water might enter the soil but the air might not be free to escape except through the surface or by being collected in high pressure pockets within the profile with some depression of the water table. The drainage would be like number (2).

Since items (2) and (3) might mean a slower movement of water under intermittent flooding, it seems worthwhile to study this in the laboratory.

PROCEDURE:

A 4" I.D. leucite column (Figure 1), which can be used with gamma scintillation, was packed with 97.5 cm of coarse sand and gravel and then another 72.5 cm of fine sand from the Salt River bed near Flushing Meadows. The column had the sides machined to

flat surfaces and ports for tensiometers every centimeter. This was the same column reported in the 1966 annual report. All of the Baird Atomic gamma scintillation equipment has been replaced by Hamner Electronics equipment. All of the tensiometers which in the 1966 report were of an O-ring, slip-fit type were replaced during the year by copper tubing, Swagelok fitting type described in last year's Annual Report. The slip-fit type tensiometer holders and plugs for unused ports were screwed into the column with fiber washers as seals. All of these fiber washers were replaced by greased O-ring seals.

The column was packed dry but as uniformly as possible. A dry scan of the column was made immediately after packing and counts were also taken through the leucite, both empty and full of water, so that some calculation of the bulk density and absorption coefficient could be made.

For the first few trials the air pressure buildup was measured by inserting tensiometer-type fittings into the O-ring, slip-fit holders and using the same transducers as the tensiometers used by means of a scanivalve. (The ceramic for a tensiometer was replaced by a brass screen.) During the year it appeared that this connection system leaked; therefore, two pressure transducers were mounted directly into the columns at 70 and 157 cm above the base of the column.

Air pressure relief ports were provided all along the column. They could be plugged to simulate the condition of no air escape or access.

All of the work was carried out in a constant temperature room set at 24.5 $\pm$ 0.5 C.

Water was applied to the top of the column at a constant head supplied by Mariotte siphon, burettes. Thus, the inflow rates could be measured.

Five different sets of boundary conditions were imposed on the column:

1. The water table at 10 cm, and
   a. air allowed to escape and enter freely from the sides;
   b. air allowed to escape freely but not enter except from the top;
   c. air not allowed to escape or enter freely except from the top or by displacing the water table;
   d. air not allowed to escape or enter freely except from the top and all outflow prevented until the wetting front reached 30 cm; and
2. a. The water table at 60 cm, and the air not allowed to escape or enter freely except from the top or by displacing the water table (like 1c).

RESULTS AND DISCUSSION:

There has been very little in the way of meaningful results achieved by this experiment to date. The cases of restricted air movement have all been frustrated by leaks. In a column of 180 cm with 175 ports, it seems to be impossible to prevent all leaks. Several different schemes for detecting the location of the leaks have been tried, but the leaks seem to be too small for the usual type of detection. They also seem to get worse with time; i.e., at one stage the column leaked only 10 cm water pressure/hour (This was the best value.), but 6 to 8 weeks later the rate was 40-50 cm/hour.

The internal packing of the column also appeared to change over the year, even though several cycles of wetting and drying were made before any data taking occurred. Figure 2 illustrates this effect. In this figure, the amount of infiltration versus time is plotted for several different runs of type 1a in the Procedure Section. The run on 10 March was made after several weeks of drainage and evaporation (loss from the surface and

through the leucite walls); thus, it was infiltration into a dry column. The runs on 12 and 16 March were infiltration into wet and intermediate initial conditions. As expected, the infiltration into a dry column occurred at a higher rate initially than the other two runs, but after about an hour the slopes of the curves, or flow rates, were the same. On 29 December this same experiment was repeated on an initial wet condition. The initial rate of inflow was higher than on 12 March, but the final rate was slower; i.e., the slope was less. Thus the packing, probably at the soil surface, had changed.

The amount of drainage versus time shown in Figure 3 was the same for all runs of experiment 1a. The single curve plotted in this figure is the best representation of the data. A similar plot for the case of experiment 2a where the water table was at 60 cm instead of 10 cm is shown in Figure 4. It is given only to show the difference in total amount of water drained from the column due to water table height. It appears that most of the water stored in the column during an infiltration is stored in the coarser sand and gravel layer. The finer sand does not appear to drain much by gravity flow. This situation may or may not be real. Possibly the coarse layer will never fill because the flow rate of the entire column is controlled by the fine sand. Thus there is not really much of a continuous water column hanging on the upper layer to cause drainage of the upper layer. On the other hand, the column may leak in such a way that the bottom can always drain without pulling air through the surface layer.

SUMMARY AND CONCLUSIONS:

Only the results of the experiments where air could have free escape and access all along the soil column are valid. All other cases examined are suspect due to air leaks along the column. New columns with only ports for four or five tensiometers and two air pressure transducers are being constructed and will be used to

repeat the experiments outlined in this report.

PERSONNEL: Herman Bouwer and Frank D. Whisler

CURRENT TERMINATION DATE: December 1970

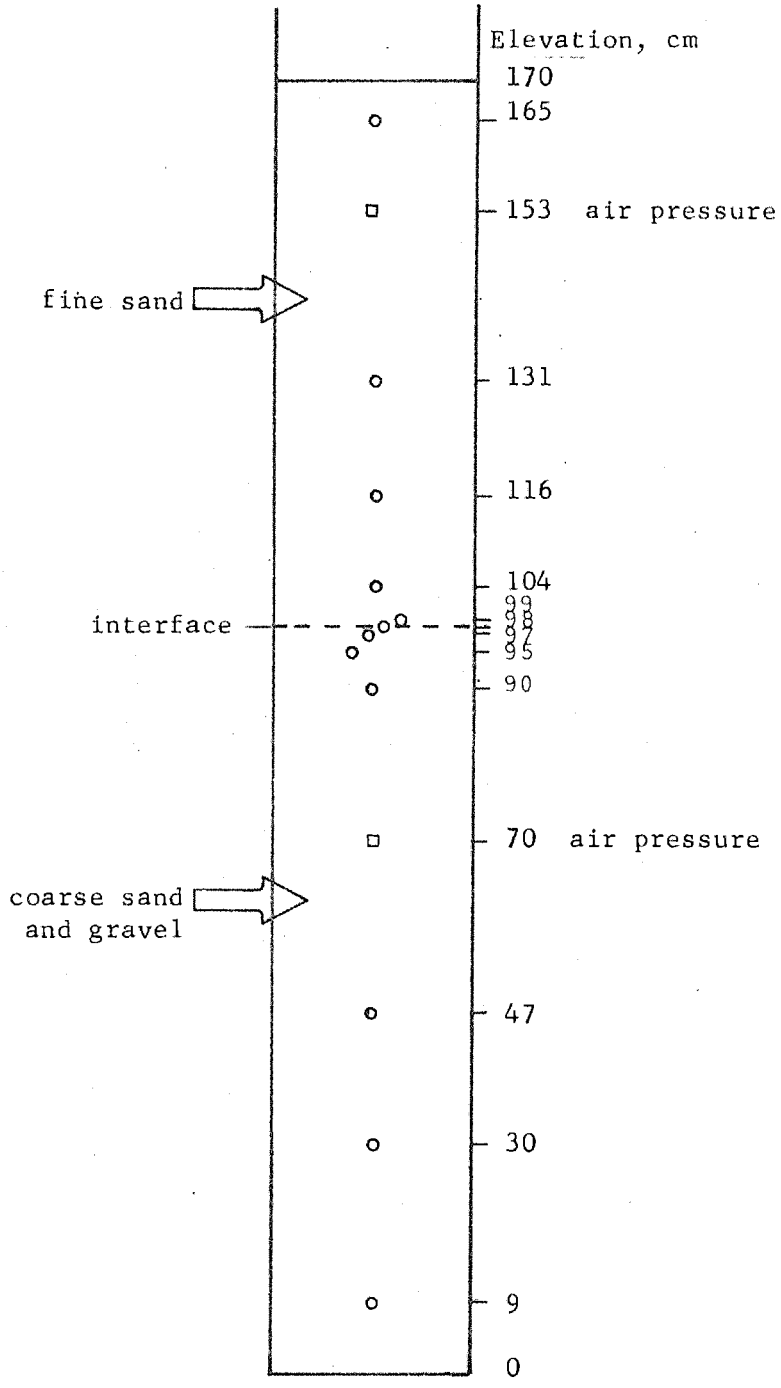

Figure 1. Schematic of 4" I.D. leucite column with tensiometers and air pressure ports.

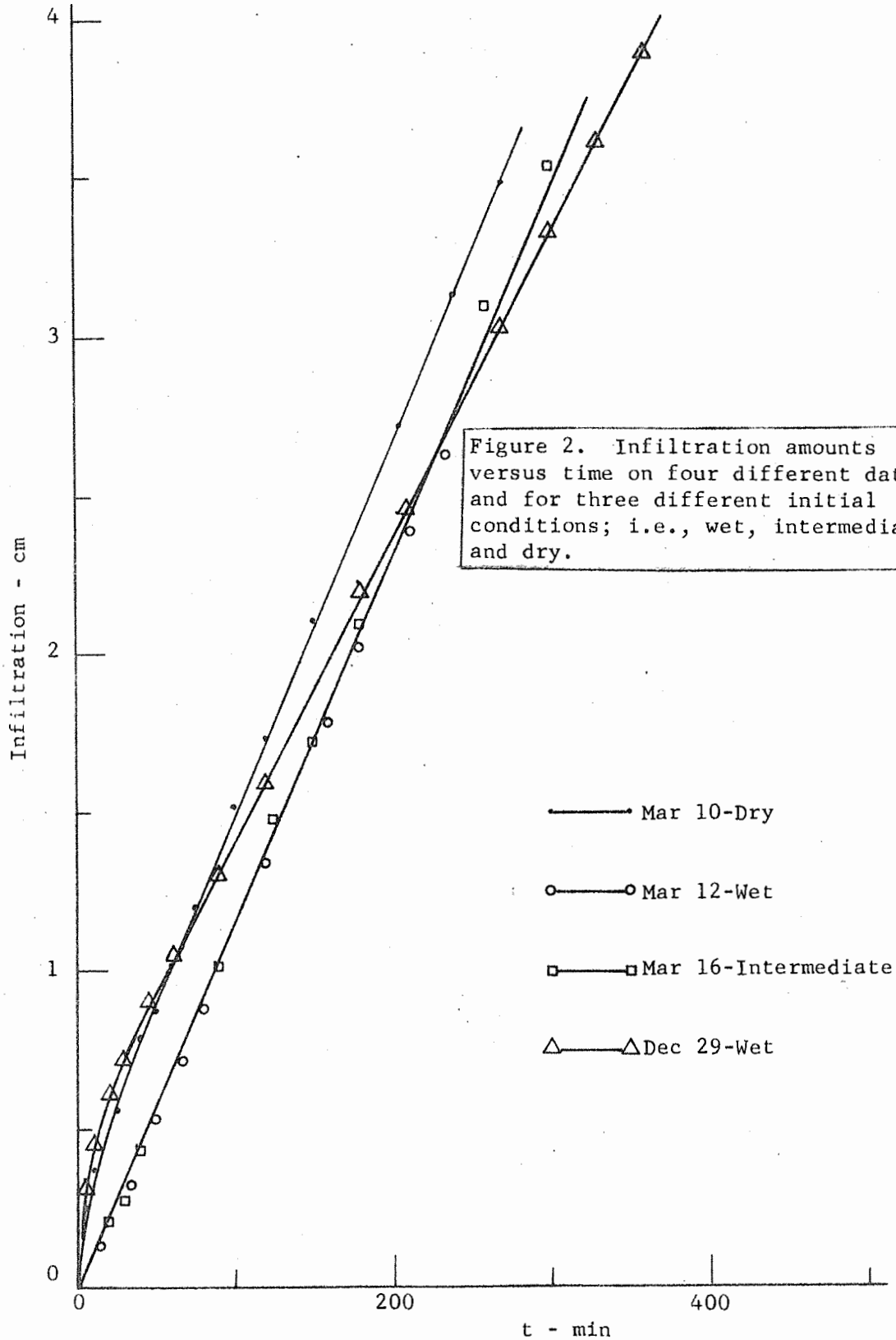

Figure 2. Infiltration amounts versus time on four different dates and for three different initial conditions; i.e., wet, intermediate, and dry.

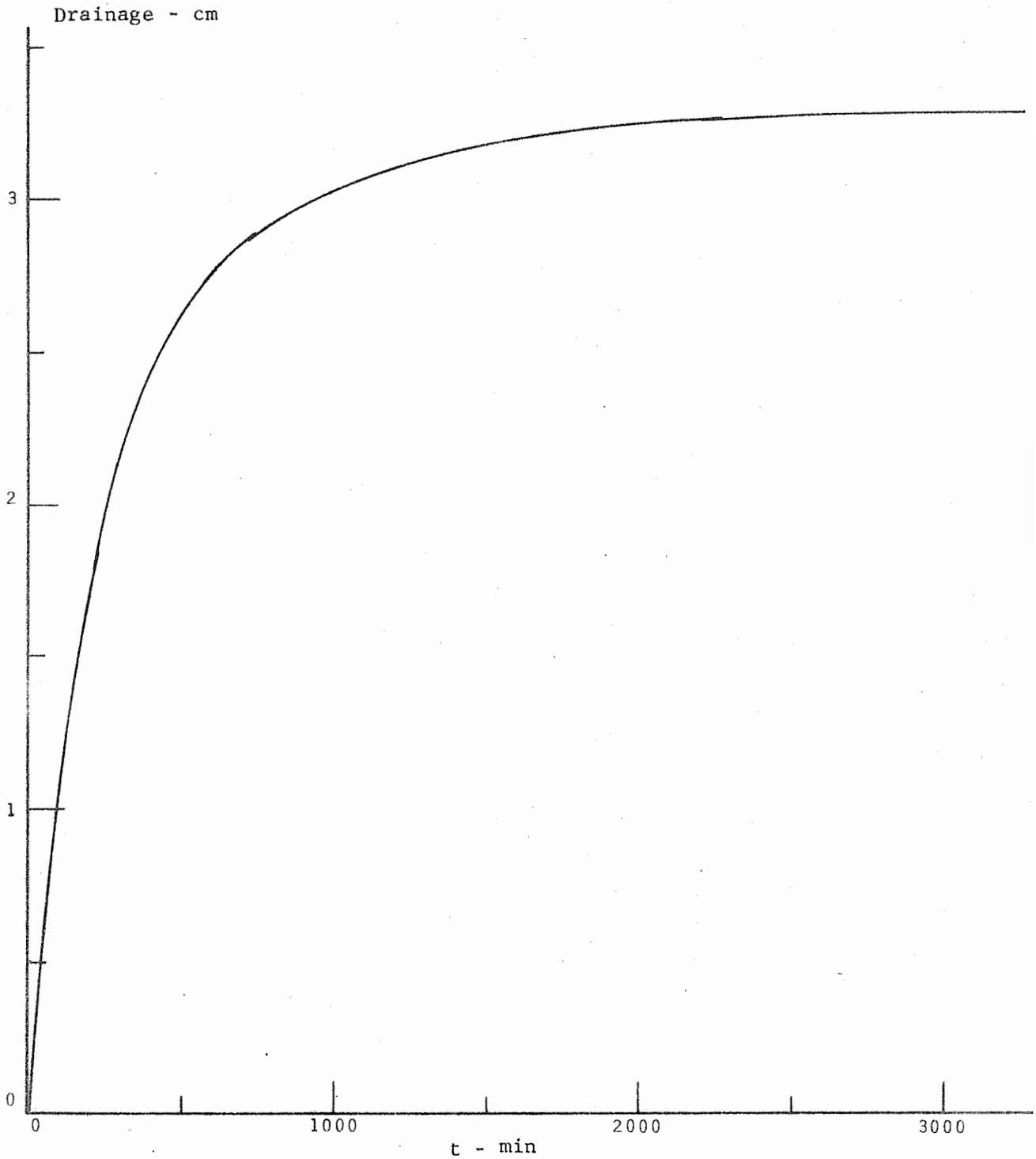

Figure 3. Drainage amount versus time for the cases of Figure 2. The water table was at 10 cm above the base of the column.

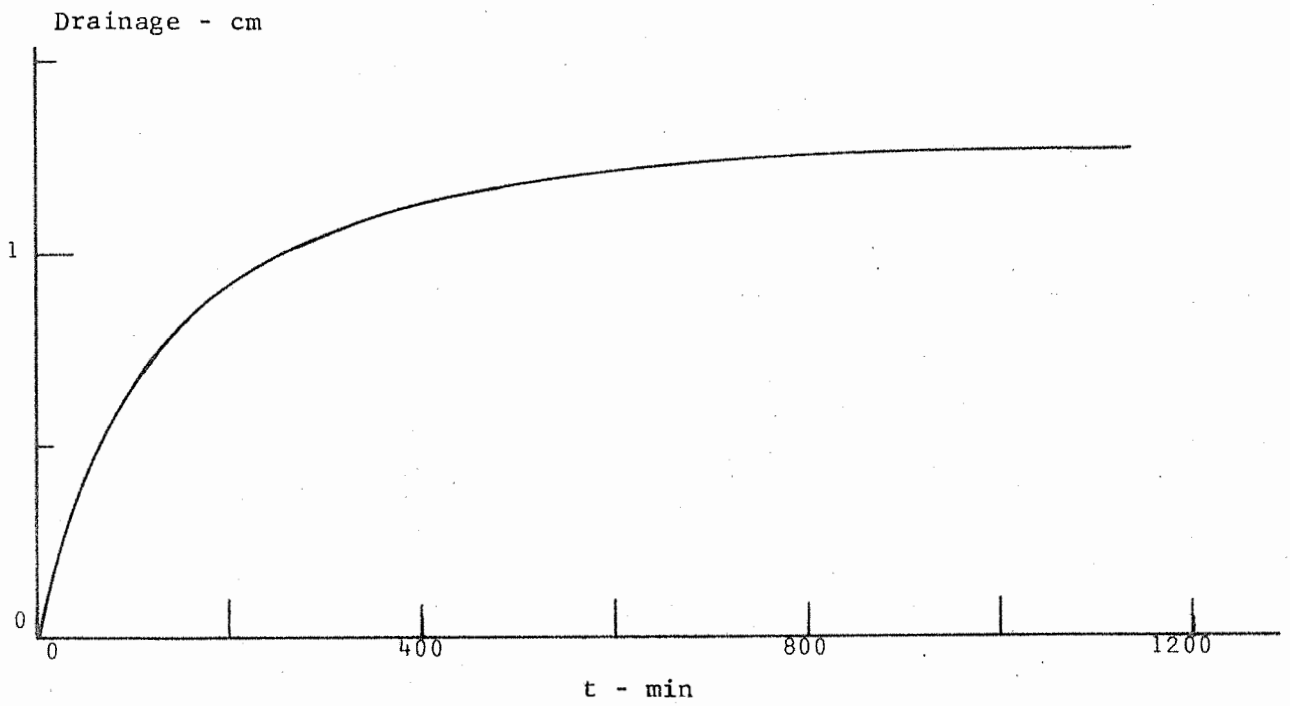

Figure 4. Drainage amount versus time for restricted air access to the column and the water table at 60 cm above the base of the column.

TITLE: WASTE-WATER RENOVATION BY SPREADING TREATED SEWAGE FOR GROUND-WATER RECHARGE

CRIS WORK UNIT: SWC-012-gG-1 CODE NO.: Ariz.-WCL 67-4

INTRODUCTION:

The year of 1970 was the third full year of operation of the Flushing Meadows Project, which is an experimental project for renovating secondary sewage effluent by ground-water recharge with infiltration basins. The project is located in the Salt River bed about 1½ miles downstream (west) from the 91st Avenue Phoenix Sewage Treatment Plant. The project was constructed in 1967 and the basins have been intermittently inundated since September 1967.

The excellent cooperation with the Salt River Project, which received a grant from the Federal Water Quality Administration for partial support of the project, was continued in 1970. The grant terminated in December 1969, at which time the financial support for the two laboratory technicians was assumed by the Salt River Project. A welcome addition to the cooperative effort is the work started in 1970 by Dr. G. A. Cole and Miss Joyce Foster of Arizona State University, who are studying the development and behavior of the biomass in the reclaimed sewage water in ponds.

The operation of the basins in 1970 was aimed at maximizing annual infiltration. Thus, relatively long inundation periods of 2 - 3 weeks rotated with dry-up periods of about the same length were held throughout the year. To facilitate orderly presentation of the results, the report is divided into six sections:

I. Infiltration Studies.
II. Water Quality Studies.
III. Aquifer Studies.
IV. Pond Studies.
V. Laboratory Infiltration Studies.
VI. Summary and Conclusions.

I. INFILTRATION STUDIES

1. Recharge Basin Management.

A plan of the Flushing Meadows Project showing infiltration basins, observation wells, and fish ponds, is presented in Figure 1.

On 20 November 1969, the vegetation was mowed and bailed in basins 1, 3, and 6. Thus, at the start of the year 1970, the basin bottoms were in the following condition:

Basin 1. Stubble of sprangle top, barnyard grass, and other native grasses that were allowed to "volunteer" in 1969.

Basin 2. Bottom covered by 2-inch layer of coarse sand topped by 4-inch layer of 3/8-inch gravel (placed in spring 1968).

Basin 3. Stubble of bermuda and native grasses and occasional patches of straw.

Basin 4. Four-inch layer of bermuda straw.

Basin 5. Four-inch layer of rice straw.

Basin 6. Stubble of rice and occasional patches of straw.

Throughout the year of 1970, inundation periods were usually 2 - 3 weeks and dry-up periods were of about the same length. Inundation depths were held at 1 ft. This schedule prevented the growth of new vegetation in the basins. In October 1970, the condition of the basin bottoms was as follows:

Basin 1. No vegetation, ½-inch layer of sludge and algae which became white upon drying.

Basin 2. Clean gravel, coated with sludge and algae drying white. Organic solids also present between gravel particles.

Basin 3. As No. 1, but about 10% of the bottom covered with bermuda straw from 1969 growing season.

Basin 4. Two-inch layer of bermuda straw, covered by sludge and algae crust of ¼-inch thickness.

Basin 5. As No. 4, but with rice straw instead of bermuda straw.

Basin 6. As No. 1, but with occasional patches of rice straw.

On 29 October, after a dry-up of 20 days, the straw, sludge, and algae layers in basins 3, 4, 5, and 6 were removed by "shaving" the bottom with a front-end loader, leaving essentially bare soil.

The quality of the secondary sewage effluent followed the usual annual pattern. High suspended solids concentrations (20-50 mg/l) prevailed in the first few months of 1970. Improvement in the quality was observed in April and May, and during the summer and early fall, the effluent was very clear with suspended solid contents of only 1-3 mg/l. In November and December, the suspended solids content was again in the 20-50 mg/l range. In the winter months, the effluent was sometimes almost black with a depth of visibility of about 1 inch!

2. Infiltration Rates.

The infiltration rates for the basins, all for a water depth of about 13 inches, are shown in Figure 2. The rates were obtained from continuous records of the inflow and outflow, as measured with critical-depth flumes for each basin. For each inundation period, infiltration rates were plotted for every 6 hours. The resulting points usually fitted a straight or broken line which are the lines shown in Figure 2.

Inundation periods were generally 2 - 3 weeks and the dry-up periods were of about the same length. Considerable increases in infiltration were obtained with the 21-day dry-up period from 23 March to 13 April, the 21-day dry-up from 27 July to 17 August, and the 18-day dry-up period from 4 to 22 September. The infiltration rates after the 24-day dry-up from 9 October to 3 November, in which basins 3, 4, 5, and 6 were also cleaned, were not as high as might be expected because of the increased suspended solids content of the effluent water. The fact that the cleaned basins

show an infiltration recovery whereas the infiltration rate in basin 1, which was not cleaned, showed no increase after this dry-up period, indicates that the cleaning operation did have a favorable effect on the infiltration rates.

Infiltration rates were in the range of 1 to 2 ft/day during the winter months with low quality effluent, and in the range of 2 to 4 ft/day during the summer and early fall when the effluent was very clear. The infiltration rates generally decreased linearly with time. Of interest is the inundation period 13-27 April, when the infiltration rate increased with time for all basins. This could have been caused by a decrease in the suspended solids content of the effluent during that period and decomposition of solids deposited on the soil surface.

Accumulated infiltration amounts for the year 1970 are shown in Figure 3. The line with the dots is the average of all basins and it shows that an average infiltration of 400 ft was obtained for the year. Thus, one acre of recharge basin can renovate 400 acre-ft of sewage effluent per year, or 0.36 mgd.

In comparing the infiltration curves for the individual basins, the original infiltration rates of the basins when the effluent was first applied and all basins were in the same condition (bare, virgin soil), should be taken into account. These rates, measured for the period 21-26 September 1967 with clear effluent, are shown in the second column of Table 1. Because clogging of the surface and biological action in the soil had not yet taken place, the different infiltration rates in September 1967 must be attributed to a difference in average hydraulic conductivity of the bottom soil, as caused by slight textural differences. The highest original infiltration rates were observed in basin 2, the lowest in basin 6. The third column in Table 1 shows the accumulated infiltration amounts for 1970. In the fourth column these values are divided by the September 1967 infiltration rates. Setting the highest value in the fourth column at 100, and adjusting the

other values accordingly, yields indexes of relative infiltration which are shown in the last column. These data show that the lowest relative infiltration rate occurred in basin 2, which was covered by a gravel layer in the spring of 1968. The adverse effect of the gravel layer may be due to the fact that the gravel layer acts as a mulch and thus prevents drying of the underlying soil. Also, suspended solids and fine soil particles blown in as "dust," may have settled at the gravel-soil interface and caused clogging of the soil surface. As mentioned in Annual Report 1969, the clogging effect of the gravel layer was concentrated at the gravel-soil interface. The highest relative infiltration rates occurred in basins 1, 3, and 4, which had grass vegetation in 1969. Apparently, type of grass or removal of straw did not have a significant effect on infiltration, as indicated by the similarity between the indexes for the native-grass stubble in basin 1, the bermuda stubble in basin 3, and the bermuda straw in basin 4. Basins 5 and 6, which had rice in 1969, showed somewhat lower infiltration indexes in 1970. The removal of the straw in basin 6 did not have much effect on the infiltration, since the index in basin 6 with the rice stubble is about the same as the index in basin 5 where the rice straw was not removed.

3. Inundation scheduling for maximum long-term infiltration.

Inspection of the infiltration rates in the basins since the start of the project in September 1967 shows that, generally, (a) the infiltration rates decrease linearly with time, (b) dry-up periods of a few days are not effective in restoring infiltration rates, and (c) significant infiltration recoveries are obtained only with dry-up periods of at least 10 to 20 days.

The infiltration recovery during dry-up is illustrated in Figure 4, which is based on cylinder infiltrometer measurements in basin 1. Each point in the graph is the average for six infiltrometers, which were installed about 10 ft apart. The infiltrometers were about 8 inches in diameter and they were driven about 6

inches into the soil. The data indicate the final infiltration rate and they apply to a water depth of 6 inches. The starting point for the curves in Figure 4 was obtained from the infiltration rate in the entire basin at the end of the preceding inundation period (Figure 2). The curves show that most of the restoration of the infiltration rate occurs between the 5th and 10th day after the start of the dry-up period. The data for Figure 4 were obtained in March-April and June-July. In the winter months, a slower recovery can be expected.

Schematic curves of the decrease in infiltration rate during inundation and the recovery in infiltration during dry-up are presented in Figure 5. These curves are based on the infiltration behavior observed since September 1967 (such as presented in Figure 2 for 1970) and on Figure 4. The infiltration rate is expressed on a relative basis, taking a value of 100 for the infiltration rate at the beginning of an inundation period. Generally, the infiltration rate decreases linearly with time for about a month, after which it approaches an essentially constant "residual" value. Infiltration recovery starts after about 4 days dry-up and is essentially completed after about 12 days in the summer, and about 20 days in the winter.

Assuming full infiltration recovery after 12 days dry-up in the summer and 20 days in the winter, long-term infiltration rates (which include the time that the basins are not inundated) were calculated for different lengths of inundation periods. The results, plotted in Figure 6 with the infiltration rate at the start of the inundation period again taken as 100, show a flat peak with a maximum at inundation periods of 24 days in the summer and 30 days in the winter. Near-maximum long-term rates are obtained as long as the inundation periods are in the 20 - 40 day range, however. Because the infiltration recovery may be slower after a long inundation than after a short inundation,

it would probably be best to use inundation periods that are closer to 20 than to 40 days. Thus, maximum long-term infiltration would probably be obtained with inundation periods of 16 - 24 days, alternated with dry-up periods of 12 days in the summer and 20 days in the winter.

Since complete infiltration recovery to the original values may not always be obtained, an occasional extra long dry-up period may be desirable. The best time for such an extended dry-up period is when drying conditions are favorable. For the Phoenix area, such times are probably spring, to restore the infiltration after the winter season, and fall, to start the winter season with high rates.

To illustrate the use of the curves in Figure 6, they will be applied to the 1970 infiltration of basin 5, which has an infiltration behavior that is very close to the average of all six basins (Figure 3). The period 13 April - 1 November will be considered as summer, and the rest of the year as winter. For the 201-day summer period, the infiltration rate at the start of each inundation period averaged 2.9 ft/day. For the 164-day winter period, this average was 2.1 ft/day. The average length of inundation was 16.1 days for the summer and 16.8 days for the winter. According to Figure 6, the average long-term infiltration rate for these inundation periods would be 48% of the average intake rate at the start of the inundation periods in the summer, and 38% in the winter. Thus, the accumulated infiltration during the summer period would be 0.48 x 2.9 x 201 = 280 ft and during the winter period 0.38 x 2.1 x 164 = 131 ft. This gives a total infiltration of 411 ft for the entire year, which is close to the measured infiltration of 406 ft as shown in Figure 3. Thus, the inundation schedules practiced in 1970 yielded an accumulated infiltration that was close to the theoretical maximum. The agreement also supports the validity of the schematic relationships for infiltration decline and recovery presented in Figure 5.

II. WATER QUALITY STUDIES

1. Sampling, Observation Wells, and Analytical Techniques.

Sampling schedules and techniques in 1970 were the same as described for 1969 (See Annual Report 1969). The observation wells (see Figure 1 for locations), which are cased and open at the bottom, are 20 ft deep, except the East Center Well (ECW) which is 30 ft deep, and the West Center Well (WCW) which is 100 ft deep. The East Well (EW) is 250 ft deep, but water is obtained from the 10-30 ft depth level where the casing is perforated. The static ground-water table was at a depth of about 9 ft throughout 1970.

Starting 15 November 1970, the nitrogen analyses were performed with the Technicon AutoAnalyzer. A Beckman 915 Total Organic Carbon Analyzer was acquired and made operational. In 1971, COD and BOD will be replaced by TOC content. In the last months of 1970, coliform densities were also determined with the membrane filter technique, which will probably be used in 1971 instead of the multiple-tube fermentation method employed so far.

2. Chemical Oxygen Demand.

The COD of the secondary sewage effluent, which was the influent for the recharge basins, showed a similar trend in 1970 as it did in 1969, with values generally near 40 mg/l in the summer and near 50 mg/l in the winter (Figure 7). Some winter values were well in the 50-100 mg/l range. The COD of the renovated water in wells 1-2, ECW, and 5-6 was usually in the 10-20 mg/l range, with the values from well 1-2 most of the time being slightly higher than the others (Figure 7).

COD-values for the renovated water in the other wells were also usually in the 10-20 mg/l range (Table 2). The 91st Avenue well is an irrigation well which is located about 1½ miles east from the project area and yields native ground water. Well 8 began yielding renovated water in October 1970, when the salt concentration had reached the 900-1100 mg/l range of the sewage effluent (see "Dissolved Salts"). The West Center Well began

yielding renovated water no longer mixed with native ground water in about August 1970 (see Figure 12).

3. Biochemical Oxygen Demand.

BOD-values for the East Center Well were determined in the 91st Avenue Treatment Plant laboratory almost weekly for the period April-July. The BOD_5 of this renovated water was well below 1 mg/l (Figure 7). The BOD_5 of the influent is usually in the 10-20 mg/l range.

4. Nitrogen.

The total nitrogen content of the influent in 1970, obtained by adding organic N (usually about 1 mg/l) to NH_4-N, is shown in Figure 8 (nitrate and nitrite are negligible in the sewage effluent). The total nitrogen content of the influent was 25-35 mg/l for the winter period and around 20 mg/l for the summer. This annual trend may be due to the increased use of water for showers and washing machines in the hot Phoenix summer.

A reverse trend occurred for the NH_4-N content of the renovated water from ECW (Figure 8), which is in the 5-10 mg/l range for the winter months but higher in the summer period with a peak of about 15 mg/l in May-June. This trend is difficult to explain, especially since vegetation was not allowed to develop in the basins. Perhaps greater microbiological activity in the summer resulted in the fixation of ammonia, either directly in the biomass, or by some of the stable organic compounds produced in the decay of microorganisms and other organic matter. These compounds and part of the biomass could then slowly break down in late fall and winter with resulting mobilization of NH_4-N. A similar trend was observed in 1969, but at a somewhat lower level (about 5 mg/l in the winter and 10 mg/l in the summer with a peak in June; see Annual Report 1969).

Since 2-3 week inundation periods were held throughout the year, NO_3-N concentrations were very low in the renovated water,

except for a period of a few days about 1 week after the start of a new inundation period, when NO_3-N concentrations were higher (Figure 8). These "peaks" in the NO_3-N content are due to arrival of nitrified sewage effluent held as capillary water during the preceding dry-up period, and pushed down by the newly infiltrated water when inundation was resumed. Also, nitrogen stored in the soil as adsorbed ammonium, may be converted to nitrate during the dry period and contribute to the NO_3-peaks. This explains why the NO_3-N content of the peaks sometimes exceeds the total N-content of the influent. Since the peaks tended to occur around weekends, when no samples were taken, maximum NO_3-N concentrations were sometimes left undetected. Thus, low peaks such as the ones in June, July, and November, may in actuality have been as high as those observed in February, April, and May. In the future, inundation periods will be scheduled so as to reduce the chance that NO_3-peaks will occur on weekends.

Nitrite concentrations in influent and renovated water were negligibly low. Thus, according to Figure 8, nitrogen removals by the soil percolation process after the passage of the nitrate peak were about 75% in January, 50% in April, 23% in June, 42% in September, and 75% in November. The main mechanisms of this removal process probably are denitrification and ammonium fixation.

The NO_3-N concentrations for wells 1-2 and 5-6 are shown in Figure 9. The peaks were higher in well 1-2, and occurred somewhat sooner, than in well 5-6, especially during the first half of the year. This may be due to the fact that well 1-2 is in more permeable soil material than well 5-6. The additional travel time could have resulted in a reduction of the NO_3-peak in well 5-6. The NO_3-peaks in September, October, and November were apparently missed due to insufficient frequency of sampling. The NO_3-N concentrations after passage of the nitrate peak were higher in well 1-2 than in well 5-6 or ECW (Figure 8). This could be partly due

to the fact that basins 1 and 2, in which the water yielded by well 1-2 has infiltrated, had little (basin 1) or no (basin 2) vegetation. In contrast, basins 3 and 4, from which ECW-water is derived, had bermuda-grass stubble and straw, respectively. Basins 5 and 6, where the water for well 5-6 infiltrates, had rice straw and stubble, respectively. Thus, the vegetation remnants in basins 3, 4, 5, and 6 may have caused increased removal of nitrogen, possibly by increasing the organic matter in the soil.

The NO_3-N concentrations of the renovated sewage water from the other wells are shown in Table 3 (91st Avenue yielding native ground water). Due to the greater underground travel distances, the NO_3-peaks in the renovated water from the wells are more dispersed. With the monthly sampling program, peaks would be difficult to detect anyway. Though occasionally NO_3-N concentrations in excess of 10 mg/l were observed, the concentrations were mostly below 10 mg/l.

The NH_4-N concentrations were highest in wells 1-2 and 5-6, less in wells 1, 7, and EW, and lowest in well 8 and WCW where the concentration was about the same as that of the native ground water from 91st Avenue well (Table 4). Thus, the NH_4-N concentrations were lower in the renovated water that had longer underground travel and detention times. Wells 1, 5-6, 7, and EW show a similar annual trend in the NH_4-N concentrations as ECW (Figure 8).

As regards mechanisms for nitrogen removal, as the sewage water moves through the soil, most of this removal was attributed to biodenitrification and adsorption or fixation of ammonium in the soil (see Annual Report 1969). Denitrification is a true loss of nitrogen from the system, since the end products are nitrogen or nitrogen oxides, which escape to the atmosphere. With ammonium fixation or adsorption, however, nitrogen is stored in the soil. This should have an upper limit and sooner or later nitrogen removal by fixation or adsorption of ammonium must become insignificant. Because of an error discovered in the 1969 determination

of the nitrogen concentrations of the soil from the recharge basins, the amount of nitrogen that can be fixed or adsorbed in the soil is much less than previously reported.

The nitrogen concentrations in the soil from the recharge basins, as reported in Table 7 of Annual Report 1969, should be divided by a factor 10. Thus, the soil in the recharge basins after 2.3 years of recharge contained only 0.1 mg N more per gram of dry soil than the natural soil. For the 3-ft layer of loamy sand, which covers the coarse sand and gravel layers in the Salt River bed, this would mean a total nitrogen storage of 13.5 mg/cm^2 surface area. This amount of nitrogen is contained in about 0.5 liter of sewage effluent, which for 1 cm^2 surface area corresponds to total infiltration of 500 cm or 17 ft. Since the accumulated infiltration in December 1969 (when the soil nitrogen analyses were made) was about 460 ft, the removal of nitrogen by fixation and adsorption of ammonia in the soil was rather insignificant.

The nitrogen concentrations in the soil (Kjeldahl method) for January 1971, and the corrected values for December 1969, are shown in Table 4a. The dual columns for basins 1 and 4 in January 1971 refer to different sets of samples, taken about 10 days apart. The data show that the nitrogen content in the natural soil outside the recharge basins has not changed much in the 13-month period separating the samples. The same is true for the soil from basin 1, where the average for the two sets of samples for January 1971, i.e., 0.145 mg N/g of dry soil, is almost the same as the average of 0.148 mg N/g soil for December 1969. The soil from the first 24 inches in basin 4 also shows little change in nitrogen content. Thus, despite the fact that in 1970 an average amount of 400 ft of sewage effluent infiltrated in the recharge basins, the soil in the basins continued to contain only about 0.1 mg more N/g dry soil than the soil outside the basins which was never flooded with sewage effluent. The 0.1 mg N/g soil represents only

a small fraction of the nitrogen removed from the sewage effluent (Figure 8). Since storage of nitrogen in the coarse sands and gravels underlying the 3-ft layer of loamy sand seems unlikely, most of the nitrogen removal must be attributed to denitrification.

5. Phosphates.

In the fall of 1970, it was discovered that the calculated concentration of the potassium phosphate solution used for preparing standards, was off by a factor 2. Thus, all phosphate-phosphorus concentrations shown in previous reports and papers must be divided by two.

The concentrations of PO_4-P of the water from wells 1-2 and ECW were about 45% less than the influent concentration in 1970 (Figure 10). The water from well 5-6 had about 70% less PO_4-P than the influent, probably due to the finer soil materials below that well. The removal of PO_4 from the water continued as it moved further through the ground, as indicated by the lower PO_4-P concentrations in wells 1, 7, and 8 (Figure 11). The PO_4-P concentrations for WCW, EW, and 91st Avenue well are shown in Table 5.

6. Fluorides.

The average F-content of the influent for 1970 was 4.07 mg/liter (Table 6). The F-content of the renovated water was highest for wells 1-2, ECW, and 5-6, which are between the recharge basins (Figure 1). Wells 1, 7, and EW showed lower F-concentrations, due to the increased distance of underground travel for the water. Well 8 and WCW showed the lowest F-concentrations in the renovated water.

7. Boron.

Boron concentrations in the renovated water are about the same as in the influent (Table 7), due to the absence of boron-fixing materials such as iron and aluminum oxides in the soil and aquifer material. The boron concentration has shown an increasing trend. In 1968 and 1969, B-concentrations were generally in the 0.4-0.5 mg/l range.

8. Metals.

Metal analyses of three water samples were carried out by the Robert S. Kerr Water Research Center of the Federal Water Quality Administration, Ada, Oklahoma. The results (Table 8) show that Zn, Fe, Cu, and Ni are the metals in the sewage effluent that were above the detection limits. Zn was reduced by 76%, Cu by 83%, and Ni by at least 89% as the water moved from the basins to the 30-ft deep ECW. Iron was below the detection limit in the renovated water. More metal analyses, including mercury determinations, will be done in the future.

9. Dissolved Salts.

The dissolved-salts concentrations for 1970 (Table 9) indicate that all observation wells in the project area yielded renovated sewage water. The water from well 8 reached sewage-effluent salt levels in October 1970. The salt concentration in the water from WCW, which is 100 ft deep and located in the center of the basin area (Figure 1), started to show a reduction in August 1969, and continued to drop in 1970. The 1100-ppm level, which indicates that native ground-water (salt content about 4000 ppm) has been essentially completely displaced by renovated sewage water, was reached in September 1970. Thus, the displacement of native ground water below WCW took about 3 years, 2 years for the first traces of sewage water to arrive (see Annual Report 1969), and 1 year for complete displacement. Since nitrate peaks and relatively high nitrate levels due to frequent, short inundation periods were observed in the renovated water at the beginning of the project (see nitrate levels for ECW water, Annual Reports 1967 and 1968), the arrival of renovated sewage water at WCW could be expected to cause an increase in the nitrate concentration in WCW water. So far, however, increased nitrate concentrations in WCW have not been observed (Figure 12).

10. pH.

The pH of the sewage effluent in 1970 ranged between 7 and 8 (Table 10). The pH of the renovated water was somewhat lower and generally around 7. This lower pH is probably due to the bacterial activity in the soil and resultant production of CO_2.

11. Coliform Densities.

Fecal coliform densities in the sewage effluent (recharge basin influent) were generally in the 100,000 to 1,000,000 range (Most Probable Number per 100 ml) with a median of about 200,000.

Presumptive and fecal coliform densities in the renovated sewage water from ECW, expressed as MPN per 100 ml, are shown in Figure 13. The MPN in this water showed a tendency to increase after the start of an inundation period, when newly infiltrated water reached the intake of ECW, and to decrease during dry-up periods. The median MPN for the fecal coliforms in ECW-water was 20, with a normal range of 0-300 and a few values between 300 and 1000. For well 7, which is 90 ft from the nearest recharge basin (Figure 1), the median MPN for the fecal coliforms was 10 with a normal range of 0-100 and a few values between 100 and 500. Well 8, which is 290 ft from the nearest basin, did not have any coliform bacteria since November 1970, when renovated water had arrived and testing for coliforms was begun.

III. AQUIFER STUDIES

1. Response of Water Table to Ground-Water Recharge.

Intensive water-level measurements in all observation wells (see Figure 1 for location) were made for the inundation period 22 September - 9 October. The results (Figure 14) show piezometric heads at the 20-ft depth level with respect to a local bench mark. As was done previously, the water-level rises in the 30-ft deep East Center Well were multiplied by 1.26 to obtain the piezometric levels for the 20-ft depth level (see Annual Report 1969). The piezometric head profiles show a North-South slope prior to the inundation. This is probably due to natural recharge from the effluent stream north of the basins (Figure 1), which carried large amounts of rainfall runoff and exceeded its banks for several days following the heavy rains on the Labor Day weekend (5 September). Standing water in the low areas near the effluent channel persisted for several weeks.

Considerable rise of the water levels in the observation wells was already observed on 23 September, one day after inundation of the basins was started. Maximum levels occurred on about 25 September, after which the water levels receded because of decreasing infiltration rates. Inundation was stopped on 9 October, and the water levels dropped to eventually lower levels than at the start of the inundation period. This indicates a general lowering of the "static" water levels due to dissipation of the recharge mound caused by the 5 September flood in the effluent channel. Well 5-6 responded in similar manner as the other wells, indicating that the "opening up" of the bottom of the well by driving in a rod, as was done in October 1969, was effective in improving the response of this well.

Another measurement of the static water level in the wells was made on 2 December, prior to the inundation period of 2-30 December. The levels were lower than the static levels on 22 September and 19 October, and the profile again was essentially a horizontal

line, indicating that the local effect of the flood in the effluent channel on the ground-water table had disappeared.

2. Hydraulic Conductivity of Aquifer.

The response of the water level in the ECW to infiltration for the period 2-30 December is shown in Figure 15. An essentially constant water level prevailed from 9 to 14 December at an elevation of 1.45 ft above the static level of 2 December. The average infiltration rates in the basins was 2.07 ft/day on 9 December and 1.87 ft/day on 14 December. Taking the average of the two values, i.e., 1.97 ft/day, the equilibrium rise of the water level in ECW per 1 ft/day infiltration rate can be calculated as 1.45/1.97 = 0.73. The resulting value is, for a given set of boundary conditions, a function of the aquifer hydraulic conductivity only. Thus, it can be used to detect possible changes in the hydraulic conductivity, for example, due to recharge with sewage effluent. The lower the water table rise per unit infiltration rate, the higher the hydraulic conductivity would be. The following values, along with the static water level elevations in ECW, have thus far been obtained:

	Static water level in ECW	equilibrium rise / infiltration rate
	feet local BM	ft/ft/day
Sept 1967	-6.0	0.77
Oct 1968	-2.0	0.71
Nov 1969	-1.5	0.72
Dec 1970	-1.3	0.73

The above data indicate that the hydraulic conductivity of the aquifer has remained essentially unchanged since 1968. From 1967 to 1968, the hydraulic conductivity actually shows an increase! This apparent increase may, at least in part, be attributed to the 4-ft rise in static ground-water level from 1967 to 1968, which could have caused the inclusion of some permeable strata

into the aquifer. Most of the water table rise from 1967 to 1968 was probably due to a prolonged flow in the Salt River due to release of water from the storage dams in the spring of 1968. After that, the water table in the project area has shown only a minor rise. Since the elevation of the basins is about 8 ft local BM (Figure 14), the static water-table depth in 1970 was about 9 ft.

IV. POND STUDIES

In 1969, four ponds were constructed, one unlined pond near the East Well receiving renovated sewage water from EW, two lined ponds in the northeast corner of the project also receiving water from EW, and an unlined pond near the effluent pump in the northwest corner receiving secondary sewage effluent (Figure 1).

1. Unlined Ponds.

The unlined pond receiving secondary sewage effluent, referred to as the permanent effluent pond in Figure 1, is about 30 x 40 ft in size and 5 ft deep in the center. The pond was filled in the fall of 1969, and constant water level was maintained. Once a week, the inflow was stopped for 24 hours to measure the rate of fall of the water level. This rate was about 5 ft/day when the pond was just filled. The seepage then decreased to a "residual" value of about 0.4 ft/day, which was maintained for most of 1970 (Figure 16). Because most of the soil clogging can be expected to be concentrated at the bottom surface, the seepage per foot of depth would be approximately 0.04 ft/day. The results thus show that the infiltration rates become very low under continuous inundation with the effluent. For the same reason, seepage from the 1 - 2 ft deep effluent channel running north of the project (Figure 1) should be insignificant. This is also evidenced by the horizontal position of the static water table (Figure 14). Only with intermittent inundation can significant infiltration rates be maintained.

The unlined pond near the East Well, called the East Pond, is about 10 x 18 ft in size and 4 ft deep. This pond was installed to determine how the seepage from an unlined lake filled with reclaimed sewage water would change with time, due to "aging" of the pond. Initially, the seepage rates were more than 6 ft/day, but decreased to about 0.5 ft/day as algae and sediments formed on the bottom (Figure 17). The seepage increase in the beginning of July was caused by a tadpole "explosion," which thoroughly

cleaned the bottom of the pond. In August, conditions were back to normal and the seepage returned to the 0.4 ft/day level. On 14 October, the pond was treated with Dow Pond Sealer 703, which reduced the seepage to about 0.1 ft/day. The treatment, which was applied by J. B. Miller of the U. S. Water Conservation Laboratory, consisted of applying the sealer evenly over the water surface at a rate of 2000 lbs/acre.

2. Lined Ponds.

The lining for the two lined ponds in the northeast corner (Figure 1) consisted of a fiberglass-asphalt material developed at the U. S. Water Conservation Laboratory and was installed under the supervision of Mr. G. W. Frasier. The lined ponds, which were designated as the East Lined Pond (ELP) and the West Lined Pond (WLP), are about 30 x 40 ft each with 2:1 side slopes. They were filled with renovated water from the EW in March 1970. When full, each pond was approximately 5.5 ft deep with a capacity of about 21,000 gal of water (ELP - 5.8 ft; 19,500 gal: WLP-5.2 ft; 23,000 gal). Sandy soil from the area around the ponds was used to cover the bottom of each lined pond with a 6-inch layer of sediment. The sediment provided an environment for spawning of fish and the establishment of bottom fauna important to the nutrient food chain of fish.

The lined ponds were connected with an overflow pipe from the ELP into the WLP. Water lost from the ponds by seepage and evaporation was replaced by renovated water from the EW. This make-up water was introduced into the ELP only and the overflow water from the ELP filled the WLP (Refer to Tables 2-10, except for Table 7, for the quality of the make-up water from the EW).

From March through December various chemical and biological components were monitored by the staff of the U. S. Water Conservation Laboratory and by Miss Joyce Foster and Dr. Gerald Cole from the Zoology Department at Arizona State University. The preliminary data reported for 1970 will serve as a basis for

evaluating and formulating more detailed investigations on eutrophication and primary productivity in fresh water ponds containing sewage water reclaimed by ground-water recharge through surface spreading.

Nitrogen and Phosphorus. Water samples (duplicate 500 ml) were collected from each pond and analyzed by procedures previously described for nitrate-N, ammonium-N, phosphorus, chemical oxygen demand (COD), total dissolved salts (TDS) and pH. The results obtained are summarized in Table 11. Due to the primary productivity of these ponds, the concentrations of nitrate-N, ammonium-N, and phosphorus decreased with time after the March filling of the ponds until a stabilized concentration level was reached in each pond. The ELP reached this level about 8 July, whereas the WLP had reached it by 1 June, approximately 1 month earlier. This probably resulted from the addition of the make-up water from the EW into the ELP only, with the WLP being replenished from the ELP. Thus, the nutrients were periodically replenished in the ELP by the make-up water.

Chemical Oxygen Demand and Total Dissolved Salts. The COD increased in each pond until August. Then the COD decreased and stabilized between 64 to 74 ppm in the WLP and between 30 to 38 ppm in the ELP. Also, the TDS showed similar trends with the ELP changing only periodically whereas the WLP increased and stabilized at the higher level after 17 June. The differences in COD and TDS between the ponds may partly be explained by the greater fish production and population present in the WLP (refer to later section on Fish). Since the WLP received its water through the ELP, evaporation may also have contributed to the higher TDS level in the WLP.

pH. Initially, the pH of the pond water was 7.1, equal to that of the EW, and it was saturated with CO_2. Because of CO_2-consumption by the algae, the pH increased to between 8.9 and 9.3 in each pond.

Coliform Bacteria. Water samples collected for chemical analysis were also analyzed for coliform bacteria populations. Numbers of presumptive and fecal coliform bacteria were determined by the most probable numbers method using the standard multiple-tube fermentation technique. Data was collected periodically from 29 April to 5 November (Table 12). Fecal coliforms were detected occasionally in both ponds, but their populations died off rapidly. Presumptive coliform populations survived well in the ponds and maintained a relatively constant population density in both ponds. The sporadic occurrence of fecal coliforms in each pond probably resulted from the introduction of them in the make-up water from the EW. The fecal coliform populations in the EW changed in accordance with the inundation periods of the basins.

Algae. Secchi disk measurements for evaluation of algal growth were made from May until December in each pond. Figure 18 shows that a dense algal development occurred in May and June and early July. Then from 15 to 25 July a die-back of algae was observed in both ponds. The die-back occurred first in the ELP on 15 July followed by the WLP on 22 July. However, the regrowth of algae was very rapid within 4 to 5 days. Similar die-back and regrowth cycles occurred periodically in an apparent monthly pattern in August and September. Lower temperatures in October and November may have prevented the occurrence of prominent die-back and regrowth cycles of algae. It should be noted that these algal die-backs did not result in a putrified or polluted pond condition; and no fish deaths resulted from them in either pond.

The gross primary productivity (GPP) and chlorophyll content in ELP and WLP were analyzed by Miss Joyce Foster on several occasions. Results for 5 November are summarized in Table 13. These results show that the ELP had the highest GPP and chlorophyll A content. The Secchi disk readings (Figure 18) also indicated a higher density of algae in ELP than WLP on 5 November.

Chlorophyll B was present in trace amounts in both ponds and chlorophyll C was not detected. The absence of chlorophyll C indicated that no diatoms were present in these ponds.

A qualitative characterization of the algal population in ELP only is summarized on Table 14. Five known genera of green algae were present with Chlorogonium being the most predominant. Ankistrodesma was common and this is a genera associated with fresh water and is not present in polluted waters. Three unknown species of green algae were detected and only one genera of blue green algae, Oscillatoria, was present. Also, no diatoms were detected, confirming the absence of Chlorophyll C.

Fish. Tilapia mossambica was introduced into the ponds on 6 May. Each pond received 30 adults weighing about 220 grams each. The fish were visibly injured before or during shipment and the survival was consequently low, especially in the WLP. For the purposes of spawning the number of adults surviving on 18 May was 20 in the ELP and 8 in the WLP. Second generation fish about ½ inch long were detected in the WLP on 9 July.

Fish deaths were recorded until date of harvest on 5 November. In the WLP, 26 of the adult fish and 13 second generation fish died. In the ELP 12 adults and 6 second generation fish died. When the fish were harvested wet weights were recorded. The WLP contained 96.59 lbs and the ELP had only 48.65 lbs. Many more second generation fish were observed in WLP; however, actual population structures and size distributions of the fish in both ponds will be examined in 1971. Also, stomach contents will be analyzed to determine the predominant food utilized by the fish in each pond. The fish production of WLP corresponds to a rate of about 4000 lbs per acre. This is a high production, considering that it took place in 5 months and that it started from spawns rather than from stocking with young fish.

The differences in fish wet weight between the ELP and WLP can not be explained by the number of surviving adults, since the ELP

had the greatest number of surviving adult fish. Possibly many of the small second generation fish were carried through the overflow pipe from the ELP into the WLP during fill-up periods.

Other Biological Observations. Several other micro- and macro-animal forms were detected. The protozoans included several species of Amoeboid forms, Heliozoans and Protomonads. The predominant arthropods were crustaceans with the sole predominant zooplankter being *Cyclops vernalis*. Its density was very great in ELP. The insects included bottom fauna primarily *Chironomid* larvae. The population density was 578 mg/m^2 (dry wgt) and 1459 mg/m^2 (dry wgt) in the WLP and ELP, respectively. Besides benthic *Chironomid* larvae, there are two predominant free swimming insect species: *Notonecta* (water boatman) and *Hydrophilus* (beetle). Other insect larvae that are probably present include dragonfly and mayfly larval forms. No nocturnal observations of insect activity were made.

V. LABORATORY INFILTRATION STUDIES

Studies were continued to determine the soil clogging effect that occurs during infiltration of sewage effluent containing suspended solids.

Soil columns 61 cm long and 10 cm in diameter were filled with 50 cm of soil. Two different soil materials were used, a sandy loam and a coarse sand. Sewage effluent of different suspended-solids concentrations was applied to the columns. Low suspended-solids concentrations were obtained by filtering the effluent through a mixed-media filter. The columns were covered to prevent algal growth. Suspended-solids concentrations were measured by filtering the water through 1 μ fiberglass filter paper. Different hydraulic gradients were maintained in the columns by controlling the height of the tail water level. Tensiometers were installed at 1, 4, 10, and 30 cm from the soil surface.

Table 15 shows the different gradients, suspended-solids concentrations, and days of inundation for the two soils used. The columns were inundated until a clogged surface layer had developed, as indicated by high hydraulic impedance in the first centimeter of soil. The relation between the impedance of the clogged or "sealed" layer and the total-solids load is shown in Figure 19 for the sandy loam. Each point represents an average of the 6 columns. At unit gradient the impedance increases rapidly with total-solids load for all three suspended-solids concentrations. The columns with the lowest suspended-solids concentrations (1.8 mg/liter) had less total load for an equal impedance change than the higher concentrations. This may be the result of additional clogging due to bacterial growth during the long inundation period.

A total-solids load between 10 and 16 mg/cm^2 was required to form a clogged layer with the impedance of 1,000 minutes. When using filtered water (1.8 mg/liter suspended-solids concentration), infiltration of 56 meters of water was required to reach this

impedance. The columns receiving the high suspended-solids concentration (108 mg/liter) received only 1.4 m of water. Removing the suspended solids from the effluent, then, increases the infiltration rate and permits longer inundation periods.

Clogging occurred at a slower rate with a gradient of 0.2 (Figure 19). The initial infiltration rate at unit gradient was from 0.045 to 0.06 cm/min as compared to 0.009 cm/min at 0.2 gradient. The higher gradient results in higher initial infiltration rate and, because of the greater seepage force, in a more compact seal. Thus, for the same total-solids load applied, the impedance of the seal is greater for the system with the high hydraulic gradient than with the low gradient.

When the gradient was first held at 0.2 and then increased to 1 and water free from suspended solids was added to the column, the impedance of the seal did not change. This indicated that once the seal is formed, increasing the gradient will not compress, and hence increase the impedance of, the clogged layer.

The impedance versus total-solids load for the coarse sand is shown in Figure 20. Each point represents an average of three columns. The impedance increases rapidly with load for the gradients of 0.6 and 1. These curves are very similar to the curve for unit gradient in the loamy sand. The high infiltration rate, even at the 0.6 gradient, results in the suspended solids being forced into the surface pores of the soil. Results at lower gradients are incomplete at this time for the coarse sand.

Clogging occurred mostly at the surface, but there appears to be a slow long-term clogging with depth in the loamy sand soil. This is shown in Figure 21 where hydraulic conductivity (K) for 4- to 10-cm and 10- to 30-cm intervals is plotted with time. The initial K values were obtained with tap water. After 1-1/2 years of intermittent inundation the hydraulic conductivity was reduced

by 60%. The cause of the reduction may at least partly be due to bacterial growth within the column.

The results so far indicate that, when using filtered water, a higher infiltration rate will be maintained for a longer period of time than when using unfiltered water. At a given gradient, the total-solids load required for clogging is about the same regardless of the suspended-solids concentration of the water. The effect of filtering, then, increases as the suspended-solids concentration increases. Clogging occurs at a slower rate when the initial infiltration rate was decreased sufficiently by imposing a lower gradient on the soil. Most of the clogging occurs at the soil surface. However, a slow long-term reduction in hydraulic conductivity occurred throughout the soil profile during 1-1/2 years of intermittent inundation.

VI. SUMMARY AND CONCLUSIONS

In 1970 the Flushing Meadows Project was operated to obtain maximum long-term infiltration rates for the secondary sewage effluent in the recharge basins. Inundation periods were 2 - 3 weeks, alternated with dry-up periods of about 2 weeks in the summer and 3 weeks in the winter. The water depth in the basins was held at 13 inches and new vegetation did not develop. The accumulated infiltration for all six basins averaged 400 ft for the year. The infiltration relative to the original infiltration capacity of the basins was highest in the basins with grass stubble or straw left from the 1969 season. Next came the basins with rice straw or stubble left from 1969. The gravel-covered basin had the lowest relative infiltration rate.

The measured accumulated infiltration of 400 ft in 1970 was very close to the theoretical maximum calculated from the infiltration behavior during inundation and dry-up. The infiltration rate decreased almost linearly with time to some residual value. The infiltration recovery during dry-up was S-shaped with little or no recovery during the first 5 days of dry-up and most of the recovery taking place between the 5th and 12th day after dry-up. Using these relationships, the inundation schedule yielding maximum long-term infiltration was evaluated. This schedule would require inundation periods of 2 to 3 weeks alternated with dry-up periods of about 12 days in the summer and 20 days in the winter.

The effect of suspended solids content in the effluent on infiltration rate and hydraulic impedance of the surface layer was studied in the laboratory using soil columns. Variables included soil type, hydraulic gradient, and suspended solids content. For an initial hydraulic gradient of one in the column, the impedance of the surface layer for a given total solids load was greater if the suspended solids concentration was low than when it was high. For an initial hydraulic gradient of 0.2, the impedance

of the surface layer was initially higher, but at the end much lower than for an initial gradient of 1, for the same total solids load on the soil surface. After about 1½ years intermittent inundation, the hydraulic conductivity of the entire soil below the clogged surface layer was reduced by about 60%. The studies indicate the importance of keeping the suspended solids in the effluent as low as possible. Infiltration can then be maximized by using high hydraulic gradients (high water depths).

At the end of 1970, the total depth of effluent that has moved into the soil since the beginning of the project was 860 ft. The response of the water table to recharge, evaluated each fall, indicated that the hydraulic conductivity of the aquifer has essentially remained unchanged. The static ground-water table was at a depth of about 9 ft below the bottom of the basins, which is about the same as in 1969.

The suspended solids content of the secondary sewage effluent, which was the influent for the infiltration basins, showed the usual annual pattern with values of 0 - 5 mg/l for the period May - October, and values of 20 - 50 mg/l for the rest of the year. Comparing the quality of the sewage water after it has percolated downward to the ground water and moved an additional distance of about 30 ft below the water table (to the well in the center of the project) with that of the secondary effluent, shows that the BOD has been reduced from 15 to 0.5 mg/l and the COD from 45 to 17 mg/l. Fecal coliforms were reduced from a median of 200,000 per 100 ml to a median of 20 per 100 ml. The coliform density in the renovated water usually increased after a new inundation period, when newly infiltrated water reached the bottom of the well. During dry-up, the coliform decreased and reached values close to zero in a few weeks. Lower fecal coliform concentrations were observed in the renovated water from wells 90 ft and 290 ft away from the basins (median densities of 10 and 0 per 100 ml, respectively).

The total nitrogen content of the secondary effluent was about 25 mg/l, mostly as ammonium. The ammonium-nitrogen concentration in the renovated water gradually increased from 7 ppm in January to 15 ppm in May and June, after which it gradually decreased to 7 ppm in October and November. In the middle of December, it began to increase again. This behavior can perhaps be explained by increased bacterial activity in the summer and fall when temperatures are higher, and a decrease in the activity and decay of organic matter with mobilization of ammonium starting in the winter when temperatures in the soil are lower. The nitrate-nitrogen concentration of the renovated water showed the usual behavior when long inundation periods are held, i. e., NO_3-N concentrations of about 0.1 mg/l with peaks of 30 mg/l or more occurring for a few days (about 1 week) after the start of a new inundation period. These peaks are caused by the arrival of nitrified effluent held as capillary water during the preceding dry-up period. Nitrogen removals after the passage of the nitrate peak ranged from 25% to 75%, depending on the ammonium level in the renovated water.

The Kjeldahl nitrogen content of the loamy sand in the infiltration basins, which forms a layer of about 3 ft thick, was about 0.1 mg higher per gram of dry soil than that of the loamy sand outside the basins that had never been flooded with sewage effluent. This was about the same as observed in 1969, and it can only account for a small fraction of the nitrogen removed from the sewage water as it passes through the soil. Since nitrogen storage in the gravel, boulder, and coarse-sand materials underlying the loamy-sand layer is unlikely, the main mechanism for the nitrogen removal must have been denitrification.

Phosphate-phosphorus in the water was reduced from about 11 ppm in the effluent to 7 ppm in the renovated water after about 40 ft of movement through soil. This concentration was further reduced to about 3 ppm as the water traveled to a well 90 ft from the basins, and to 0.05 ppm as it moved to a well 290 ft from the basins.

Fluorides were reduced from 4.0 ppm to 2.6 ppm for the well in the center of the project and to 1.9 ppm for the well 90 ft away from the recharge basins. Boron concentrations were about 0.7 ppm in the effluent and since the soil lacks iron and aluminum oxides which would remove boron, the B-concentration in the renovated water is also about 0.7 ppm. Salts increased from about 1000 ppm in the effluent to 1020 ppm in the renovated water due to evaporation from the basins, and the pH changed from 7.4 to 7.0 due to bacterial activity and CO_2 production in the soil.

Metals above limits of detection include copper, which was reduced from 0.096 ppm in the effluent to 0.016 ppm in the renovated water from the well in the center of the project; nickel, which was reduced from 0.088 to < 0.01 ppm; zinc, which was reduced from 0.075 to 0.018 ppm; and iron, which was reduced from 0.013 to < 0.01 ppm.

Seepage in relation to time was studied for two unlined ponds, one kept full with secondary sewage effluent, the other with reclaimed sewage water pumped from 10 to 30 ft depth. The ponds were about 5 ft deep. Initially, the seepage (expressed as rate of fall of the water surface) was more than 5 ft/day, but after a few months reached a "residual" value of about 0.5 ft/day for both ponds. This is low for renovating secondary effluent by ground-water recharge, but high for recreational lakes filled with reclaimed sewage water. Application of a pond sealer to the pond receiving renovated sewage water reduced the seepage by about 75%, to a value of about 0.1 ft/day.

The behavior of the renovated sewage water, pumped from 10-30 ft depth from a well 50 ft from the nearest recharge basin, was studied in two ponds, 30 x 40 x 5 ft in size and lined with an asphalt-fiberglass lining material. The ponds were filled in March 1970. N and P levels dropped to low values because of the development of the biomass. Consumption of CO_2 by algae resulted in a pH-increase to about 9. Depth of visibility in the ponds as

determined with a Secchi disk was usually in the 20 - 40 cm range. On several occasions, algae die-backs occurred and Secchi disk readings of 100-160 cm were obtained. Following such clearing-up periods, the algae recovered rapidly. Gross primary productivity of the pond water was as high as 4.72 mg O_2/l/hr. Five known genera of green algae were present with Chlorogonium predominant and Ankistrodesma common. Adult Tilapia fish were introduced in May in each pond as brood stock. Spawning took place, and in November, the fish were harvested. The average production of fish for the two ponds was about 3000 lbs/acre of surface area. The studies indicate that the reclaimed water is suitable for recreational lakes. The water will support algae growth and will have a high productivity, but fish-killing oxygen depletions did not occur and the water was aesthetically acceptable.

PERSONNEL: Herman Bouwer (Sections I, II, III, and VI), R. G. Gilbert (Section IV), R. C. Rice (Section V), E. D. Escarcega, J. C. Lance, and F. D. Whisler.

CURRENT TERMINATION DATE: 1972.

Table 1. Calculation of relative index of infiltration for 1970.

Basin	Infiltration rate Sept 1967 ft/day	Accumulated Infiltration 1970 ft/yr	Infiltration 1970 / Infiltration 1967	Index of infiltration for 1970
1	3.2	433	135	99
2	4.0	338	84	61
3	3.2	408	127	93
4	3.6	492	137	100
5	3.9	406	104	76
6	3.1	335	108	79

Table 2. COD in mg/l for various wells (1970).

Date	1	7	EW	WCW	8	91st Ave.
29 Jan	16	15	14	15	16	22
25 Feb	18	18	19	12	15	-
26 Mar	15	16	13	14	13	23
22 Apr	16	13	11	6	5	17
21 May	19	16	18	18	11	-
17 June	16	9	10	10	7	-
22 July	8	12	12	6	8	-
26 Aug	8	5	20	9	8	-
7 Oct	24	23	26	14	23	-
29 Oct	23	16	19	18	20	-
2 Dec	14	15	14	14	15	-
31 Dec	6	5	8	10	3	-

Table 3. Nitrate-nitrogen concentrations in mg/l for various wells (1970).

Date	1	7	8	EW	WCW	91st Ave.
29 Jan	0.8	0.5	0.4	5.5	5.5	5.5
25 Feb	1.8	13.5	0.5	9.7	2.3	-
26 Mar	2.8	11.3	0.5	8.7	4.9	5.5
22 Apr	11.5	28.4	0.4	15.0	4.7	5.6
21 May	4.4	22.6	1.3	8.9	5.0	-
17 June	12.0	14.8	1.9	4.8	3.5	-
22 July	1.8	3.7	1.6	1.7	3.1	-
26 Aug	1.6	12.6	5.0	6.7	3.4	-
7 Oct	0.2	1.2	1.3	0.1	2.0	-
29 Oct	0.6	0.2	1.0	2.4	0.1	-
2 Dec	0.2	0.5	2.3	4.1	0.2	-
31 Dec	0.4	0.4	0.6	4.3	0.2	-

Table 4. Ammonium-nitrogen concentrations in mg/l for various wells (1970).

Date	1	1-2	5-6	7	8	EW	WCW	91st Ave.
29 Jan	4.8	11.9	10.5	2.9	4.3	4.0	0.3	0.1
25 Feb	5.5	10.7	10.9	4.7	2.0	4.2	0.0	-
26 Mar	6.9	9.7	12.5	6.1	1.2	5.6	0.5	0.3
22 Apr	7.2	9.9	14.1	6.3	0.1	5.7	0.2	0.4
21 May	8.5	11.5	13.7	5.6	1.5	7.0	0.2	-
17 June	9.5	9.9	13.6	7.5	1.1	9.5	0.0	-
22 July	7.9	8.8	11.5	7.1	0.2	8.2	0.0	-
26 Aug	6.2	8.3	9.6	6.4	0.1	7.8	0.0	-
7 Oct	5.0	9.6	7.5	4.6	0.3	6.1	0.1	-
29 Oct	4.5	9.4	8.3	3.9	0.1	5.7	0.1	-
2 Dec	1.8	8.6	8.4	4.4	0.3	6.2	0.4	-
31 Dec	3.8	10.0	15.0	5.7	0.6	9.9	0.7	-

Table 4a. Kjeldahl nitrogen concentrations for soil outside and inside recharge basins (mg N per gram of dry soil).

Outside soil (NE corner) depth, inches	December 1969	January 1971	
0-12	0.077	0.097	
12-24	0.068	0.040	
24-36	0.058	0.048	
36-48	0.039	0.042	
48-60	0.049	0.024	
Avg	0.058	0.050	
Basin 1			
0-12	0.192	0.252	0.186
12-24	0.185	0.186	-
24-36	0.156	0.088	0.111
36-48	0.089	0.145	0.088
48-60	0.118	0.182	0.090
Avg	0.148	0.171	0.119
Basin 4			
0-12	0.208	0.201	0.230
12-24	0.127	0.120	0.097
24-36	-	0.142	0.098
36-48	-	0.115	-
Avg [a]	0.167	0.160	0.162

[a] for first 24 inches only

Table 5. Phosphate-phosphorus concentration in mg/l for various wells (1970).

Date	WCW	EW	91st Ave.
29 Jan	0.0	3.1	0.0
25 Feb	0.1	-	-
26 Mar	0.1	5.8	0.1
22 April	0.0	6.3	0.0
21 May	0.1	7.6	-
17 June	0.1	7.9	-
22 July	0.1	4.0	-
26 Aug	0.0	5.0	-
7 Oct	0.2	0.8	-
29 Oct	0.1	3.3	-
2 Dec	0.0	4.3	-
31 Dec	0.0	9.1	-

Table 6. Fluoride concentration in mg/l for effluent and wells (1970).

Date	Effl.
1- 2 Jan	3.6
2- 9 Jan	4.4
9-14 Jan	4.2
2- 6 Feb	5.1
6-13 Feb	5.6
13-16 Feb	4.4
13-20 Mar	4.5
20-23 Mar	4.7
13-24 April	5.2
24-27 April	5.4
13-15 May	5.4
15-22 May	4.4
22-26 May	4.2
8-12 June	4.4
12-19 June	4.5
25-26 Aug	4.1
1- 4 Sept	3.7
22-25 Sept	3.6
25-30 Sept	3.0
1- 2 Oct	3.0
2- 9 Oct	3.2
3- 6 Nov	4.1
6-17 Nov	3.6
2-11 Dec	3.7
11-18 Dec	3.8
18-22 Dec	2.6
24-29 Dec	2.3
29-30 Dec	3.3
AVG.	4.07

Date	1	1-2	ECW	5-6	7	8	EW	WCW	91st Ave.
25 Feb	2.1	2.8	2.6	2.9	2.2	0.9	1.9	0.5	0.6
26 Mar	-	-	3.1	-	-	-	-	-	0.6
17 June	2.5	3.1	3.0	7.2	2.9	0.8	2.9	0.7	-
26 Aug	2.0	2.4	2.3	2.9	2.4	0.9	2.2	0.5	-
29 Oct	1.5	2.1	2.0	2.2	2.0	0.8	1.9	0.3	-
31 Dec	1.3	2.5	2.8	2.2	2.0	0.8	2.3	0.7	-
AVG.	1.88	2.58	2.63	3.48	2.3	0.84	2.24	0.54	0.6

Table 7. Boron concentration in mg/l for effluent and wells (1970).

Date	Effl.	1	1-2	ECW	5-6	7	8	EW	WCW
22 April	0.74	0.79	0.76	-	0.77	-	-	-	0.87
17 June	0.77	-	0.75	0.68	0.73	0.77	0.84	0.73	-
26 Aug	0.75	0.79	0.73	0.69	-	-	-	0.73	0.94
29 Oct	-	-	0.75	0.75	0.75	0.74	0.82	-	-
30 Dec	0.73	0.71	-	0.69	0.70	-	-	-	0.68

Table 8. Dissolved metal concentrations (mg/l) in water filtered through 0.45μ membrane. Samples taken 19 February 1970.

	Influent	ECW	WCW
Zinc	0.075	0.018	0.014
Cadmium	< 0.01	< 0.01	< 0.01
Boron	0.88	0.89	0.86
Iron	0.013	< 0.01	< 0.01
Molybdenum	< 0.01	< 0.01	< 0.01
Manganese	< 0.01	< 0.01	< 0.01
Copper	0.094	0.016	0.025
Silver	< 0.01	< 0.01	< 0.01
Nickel	0.088	< 0.01	< 0.01
Lead	< 0.05	< 0.05	< 0.05
Chromium	< 0.01	< 0.01	< 0.01

Table 9. Total salt concentration in effluent and in water from wells, mg/l (1970).

Date	Effl.	1	1-2	ECW	5-6	7	8	EW	91st Ave.
2- 5 Jan	1056	-	960	896	896	-	-	1024	-
29 Jan	-	1069	1100	1088	1088	1050	1587	1171	-
4- 5 Feb	1152	-	1088	1024	1024	-	-	-	2432
25 Feb	-	1088	1152	1088	1120	1139	1568	1165	-
26 Mar	-	960	1024	980	966	1018	1440	1024	2432
21-22 April	1024	1056	960	1120	992	1088	1440	992	2240
20-21 May	1120	1024	1030	1024	1024	1056	1440	1024	-
16-17 June	1152	1229	1203	1126	1152	1203	1523	1120	-
21-22 July	960	1088	992	1024	1024	1056	1344	1024	-
25-26 Aug	1088	1082	1056	960	1043	998	1357	1043	-
28 Sept	-	-	-	1024	-	-	-	-	-
6- 7 Oct	902	947	902	960	909	954	1184	954	-
29 Oct	-	992	960	1024	960	960	1152	1024	-
2 Dec	-	960	896	896	928	960	1088	960	-
29-30 Dec	960	960	960	960	960	960	1120	1024	-

Table 10. pH of effluent and water from wells (1970).

Date	Effl.	1	1-2	ECW	5-6	7	8	EW	91st Ave.
2- 5 Jan	7.8	-	7.4	7.2	7.5	-	-	7.2	7.2
29 Jan	-	7.6	7.2	7.3	7.5	7.3	7.5	7.4	-
25 Feb	-	7.6	7.0	7.1	7.2	7.0	7.5	7.0	-
26 Mar	-	7.5	7.3	7.3	7.4	7.8	7.6	7.1	7.2
21-22 Apr	7.9	7.6	7.1	7.1	7.3	7.0	7.4	7.0	7.2
20-21 May	7.2	7.2	6.8	6.8	7.2	6.9	7.3	6.9	-
16-17 June	7.2	7.2	6.8	6.5	7.0	6.5	7.2	6.8	-
21-22 July	6.9	7.1	6.9	6.6	6.9	6.7	7.3	6.7	-
25-26 Aug	7.4	7.4	7.0	6.9	7.3	6.8	7.1	6.8	-
28 Sept	-	-	-	6.9	-	-	-	-	-
6- 7 Oct	7.5	7.3	7.2	6.8	7.2	6.8	7.3	7.1	-
29 Oct	-	7.2	7.1	6.8	7.2	7.1	7.3	6.7	-
2 Dec	-	7.8	7.0	7.1	7.4	7.2	7.2	6.8	-
29-30 Dec	7.5	7.4	6.8	6.9	7.3	7.1	7.4	6.9	-

Table 11. Analysis of Chemical Components of Renovated Sewage Water in the Fiberglass-Asphalt-Lined Ponds from March to November 1970.

Analytical Data - East Pond

Date	Nitrate ppm-N	Ammonium ppm-N	Phosphorus ppm-P	COD ppm	TDS ppm	pH
26 Mar	8.7	5.6	5.8	13	1024	7.1
22 Apr	12.6	4.3	4.3	28	1030	7.8
11 May	9.0	0.7	-	48	1024	9.1
21 May	12.4	0.5	1.3	49	1037	9.0
1 Jun	4.6	0.5	-	62	1043	9.2
17 Jun	2.6	0.6	0.6	92	1210	8.9
8 Jul	0.3	0.9	-	73	1152	8.7
22 Jul	0.1	2.0	0.8	87	1408	8.4
3 Aug	0.1	0.3	0.5	37	1088	9.1
17 Aug	0.4	1.1	0.8	38	1024	8.9
14 Sep	0.2	0.1	0.3	30	960	9.0
28 Sep	1.0	0.5	0.6	33	1024	8.9
5 Oct	0.8	0.4	0.6	35	1088	8.9
26 Oct	0.2	0.6	0.3	38	1088	9.1
24 Nov	0.1	0.3	0.3	32	1024	9.1

Analytical Data - West Pond

Date	Nitrate ppm-N	Ammonium ppm-N	Phosphorus ppm-P	COD ppm	TDS ppm	pH
26 Mar	8.7	5.6	5.8	13	1024	7.1
22 Apr	9.4	2.3	2.0	50	1011	9.0
11 May	6.8	0.7	-	68	1088	8.9
21 May	4.2	0.0	0.5	83	1069	9.8
1 Jun	0.6	0.4	-	87	1088	9.5
17 Jun	0.1	0.5	0.4	66	1280	9.1
8 Jul	0.1	0.3	-	95	1280	9.0
22 Jul	1.1	1.1	1.0	42	1216	8.9
3 Aug	0.1	0.4	0.4	69	1280	9.3
17 Aug	0.1	0.4	0.7	69	1222	9.1
14 Sep	0.1	0.2	0.5	66	1216	8.9
28 Sep	0.1	0.3	0.5	64	1280	8.9
5 Oct	0.1	0.2	0.3	68	1344	9.1
26 Oct	0.1	0.6	0.4	74	1408	9.3
24 Nov	0.1	0.4	0.2	70	1280	9.3

Table 12. Presumptive and fecal coliform bacteria populations in lined ponds from May to November 1970. Multiple-tube fermentation technique was used to determine most probable numbers (MPN) per 100 ml.

Date	EAST LINED POND		WEST LINED POND	
	Presumptive Coliform	Fecal Coliform	Presumptive Coliform	Fecal Coliform
	MPN/100 ml		MPN/100 ml	
6 May	13	2	130	0
20 May	∞ [a]	0	1,611	14
3 June	∞	0	905	0
30 June	∞	22	1,611	17
8 July	∞	13	1,611	46
22 July	1,720	330	1,410	50
5 Aug	16,110	20	∞	0
12 Aug	34,800	0	∞	20
26 Aug	161,100	0	∞	0
9 Sept	34,800	0	181,000	0
30 Sept	∞	400	174,000	0
14 Oct	174,000	0	174,000	0
28 Oct	271,000	0	65,000	0
4 Nov	65,000	0	120,000	0

[a] ∞ - Indicates all fermentation tubes were positive for dilution used and proper dilution was not analyzed.

Table 13. Analysis of Algal Growth and Activity in Renovated Sewage Water of the East and West Lined Ponds When the Fish (*Tilapia Mossambica*) Were Harvested 5 November 1970.[a]

Analysis	East Lined Pond	West Lined Pond
Gross Primary Productivity[b]	4.72 mg O_2/l/hr	1.43 mg O_2/l/hr
Chlorophyll A	471.14 mg/m^3	76.84 mg/m^3
Chlorophyll B	Trace	Trace
Chlorophyll C	None	None

[a] Data collected by Miss Joyce Foster, Zoology Department, Arizona State University.

[b] Photosynthesis rate minus respiration rate.

Table 14. Qualitative Characterization of the Algal Population in Renovated Sewage Water of the East Lined Pond.[a]

Green Algae

Name	Number of Species	Frequency
Chlorogonium	2	Predominant
Ankistrodesmus	3	Common
Scenedesmus	5	Rare
Euglenoids	Various	Rare
Pediastrum	1	Rare
Unknown	3	Rare

Blue-Green Algae

Name	Number of Species	Frequency
Oscillatoria	2	Rare

[a] Data collected by Miss Joyce Foster, Zoology Department, Arizona State University.

Table 15. Hydraulic gradient, suspended-solids concentrations and length of inundation period for two soils.

Soil	Gradient	Suspended-solids concentrations mg/l	Length of inundations, days
	1	1.8	106
Loamy	1	32	11
Sand	1	108	4
	0.2	40	77
Coarse	1	14	5
Sand	0.6	18	6

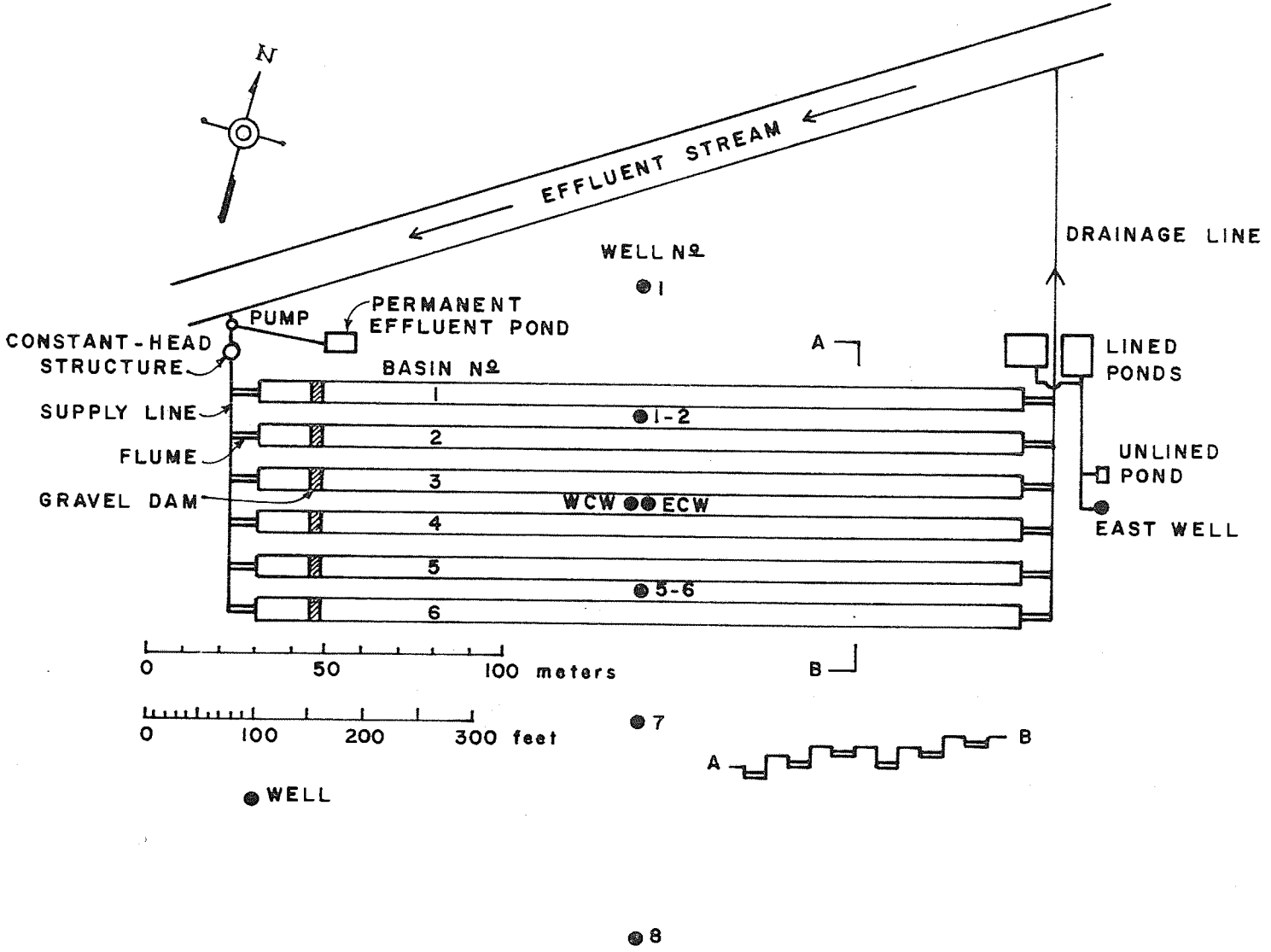

Figure 1. Schematic of Flushing Meadows Project.

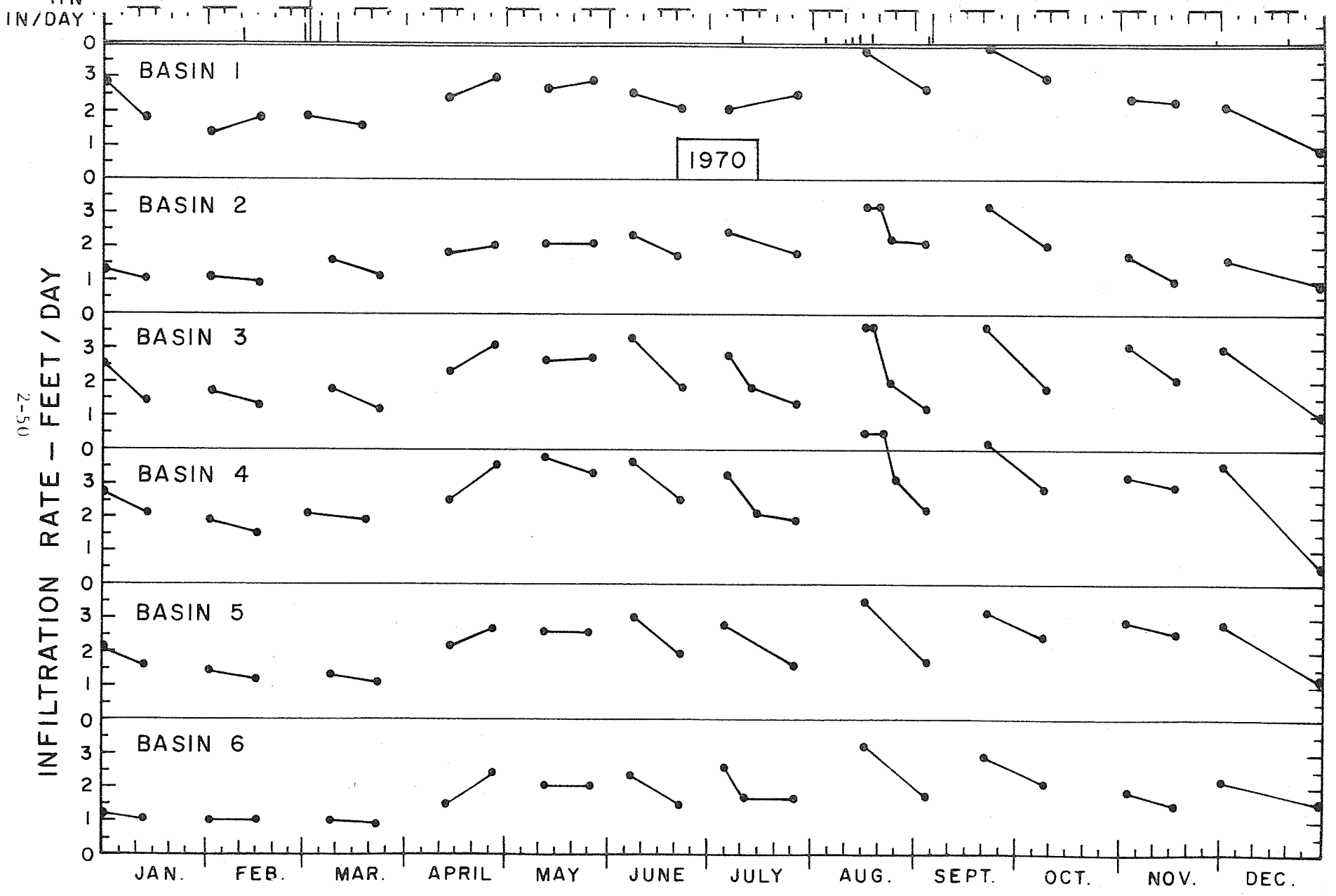

Figure 2. Infiltration rates for the six ba

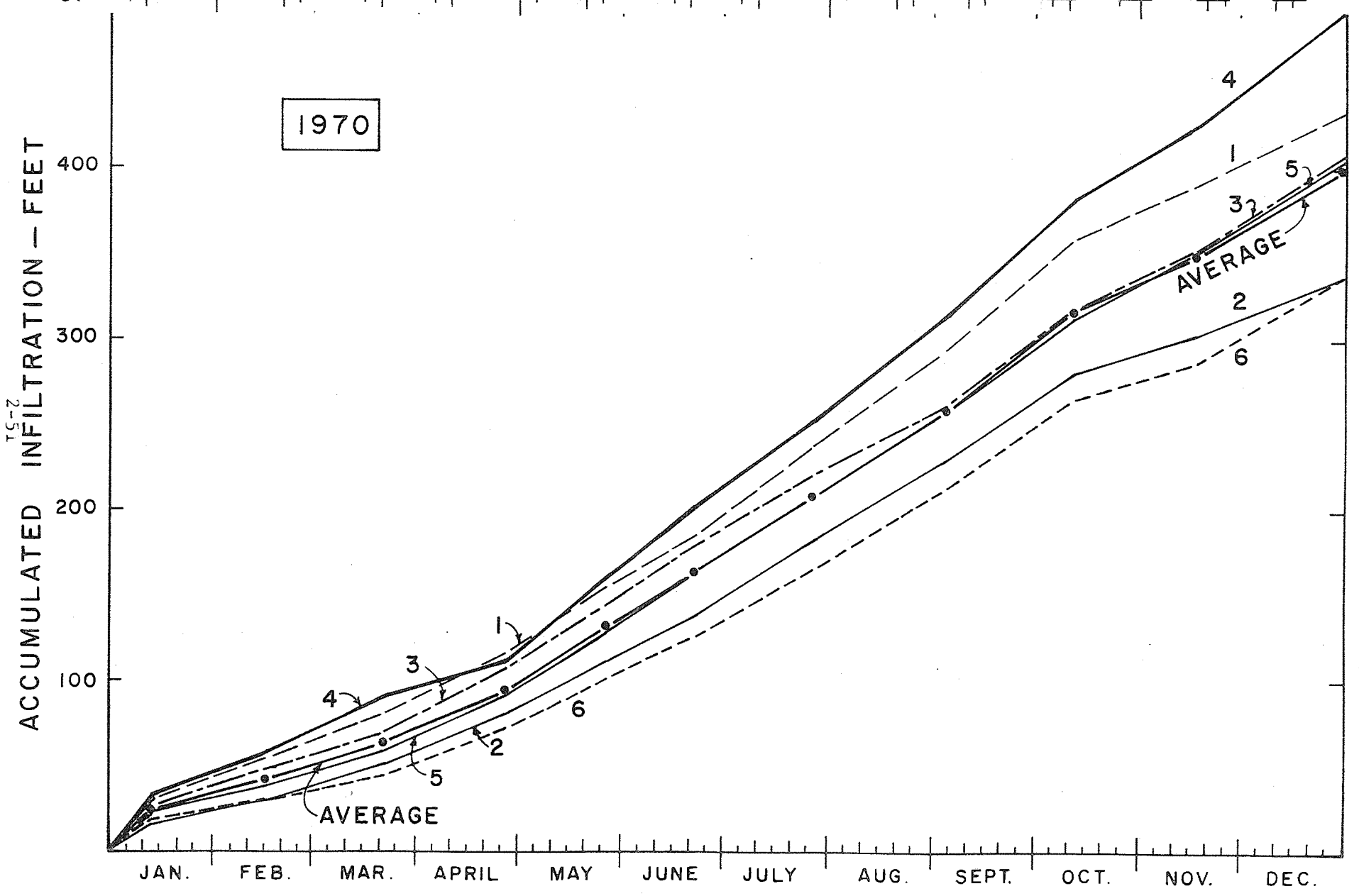

Figure 3. Accumulated infiltration for the six basins.

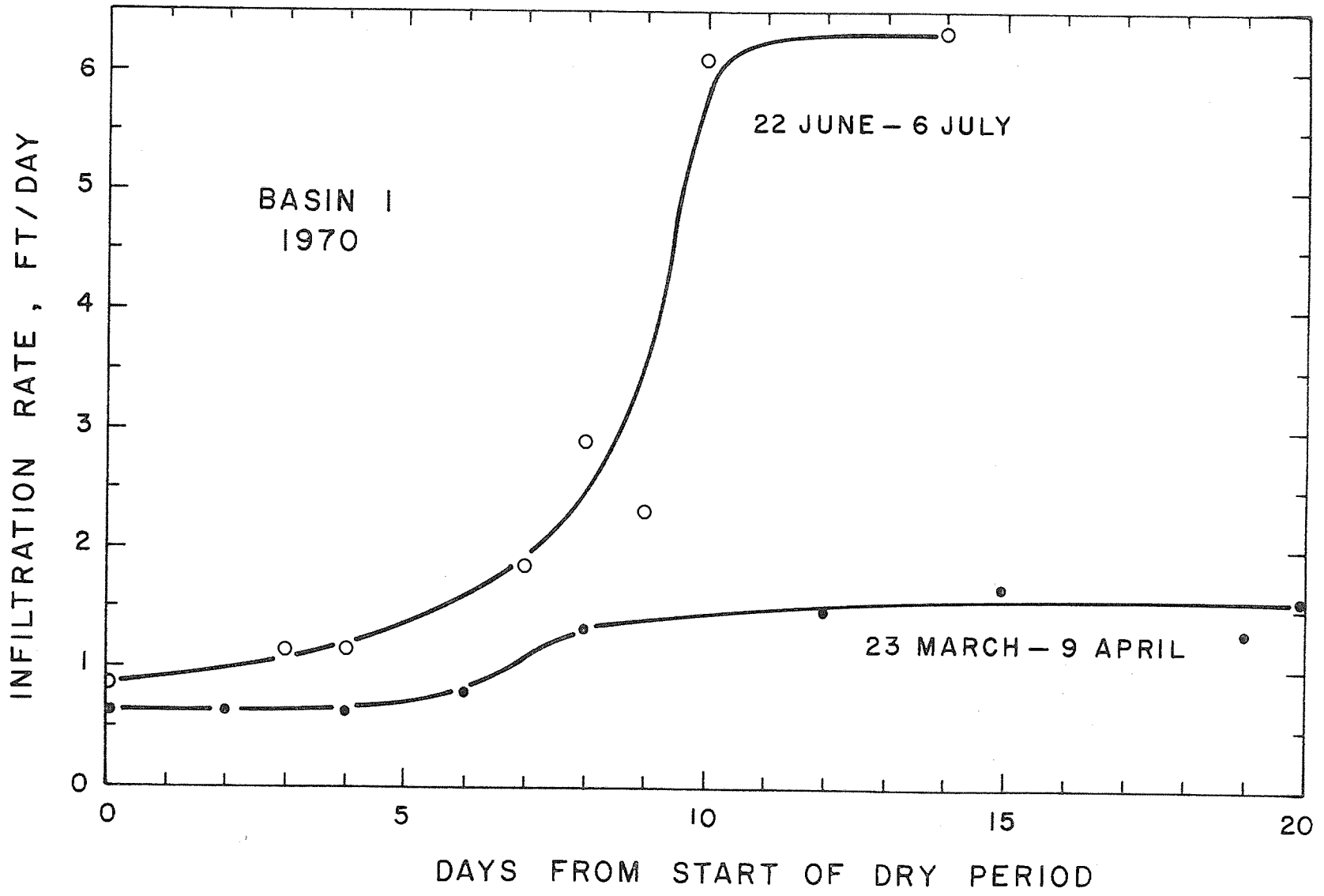

Figure 4. Infiltration recovery during dry-up.

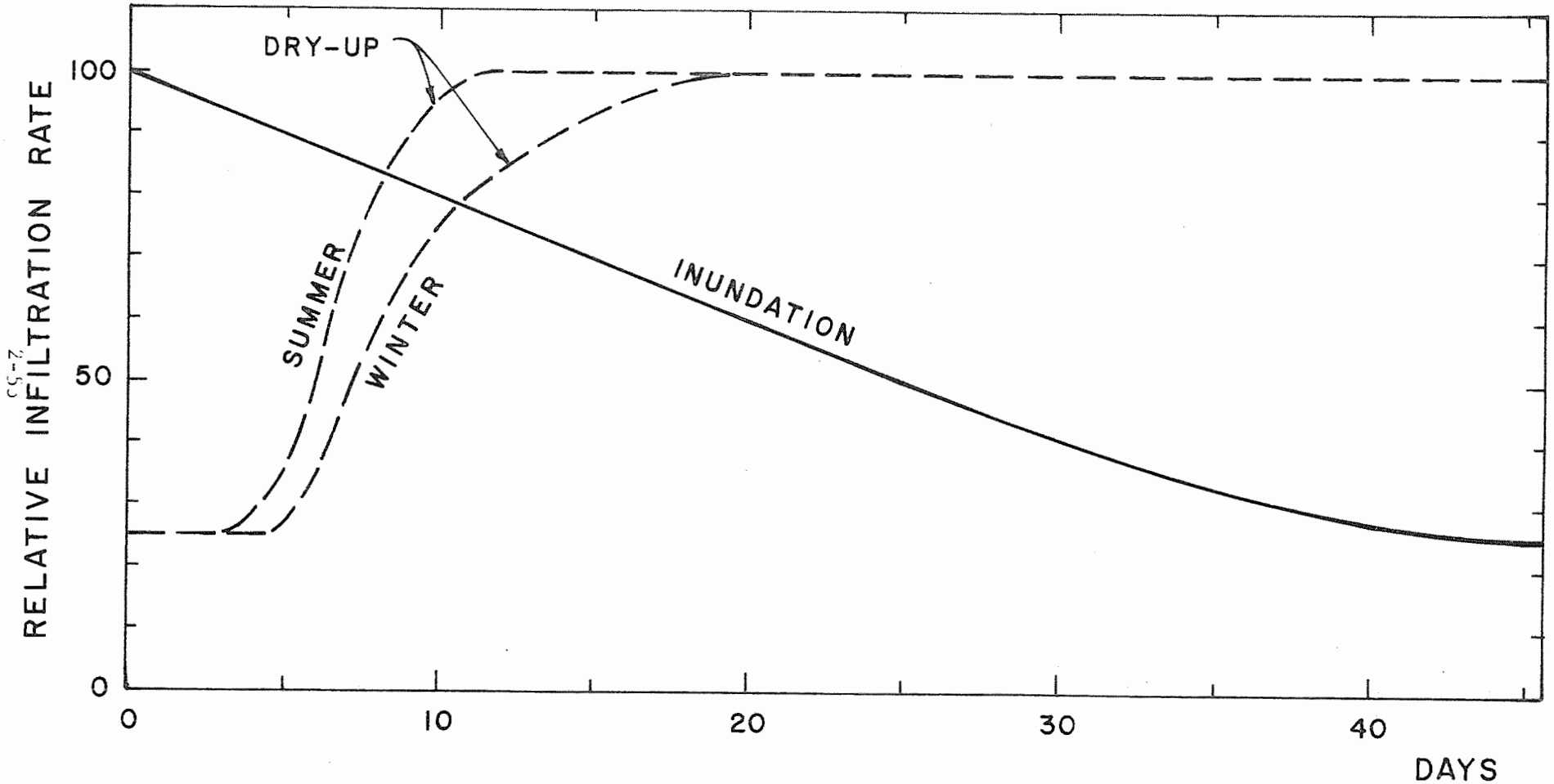

Figure 5. Schematic infiltration-time relationships.

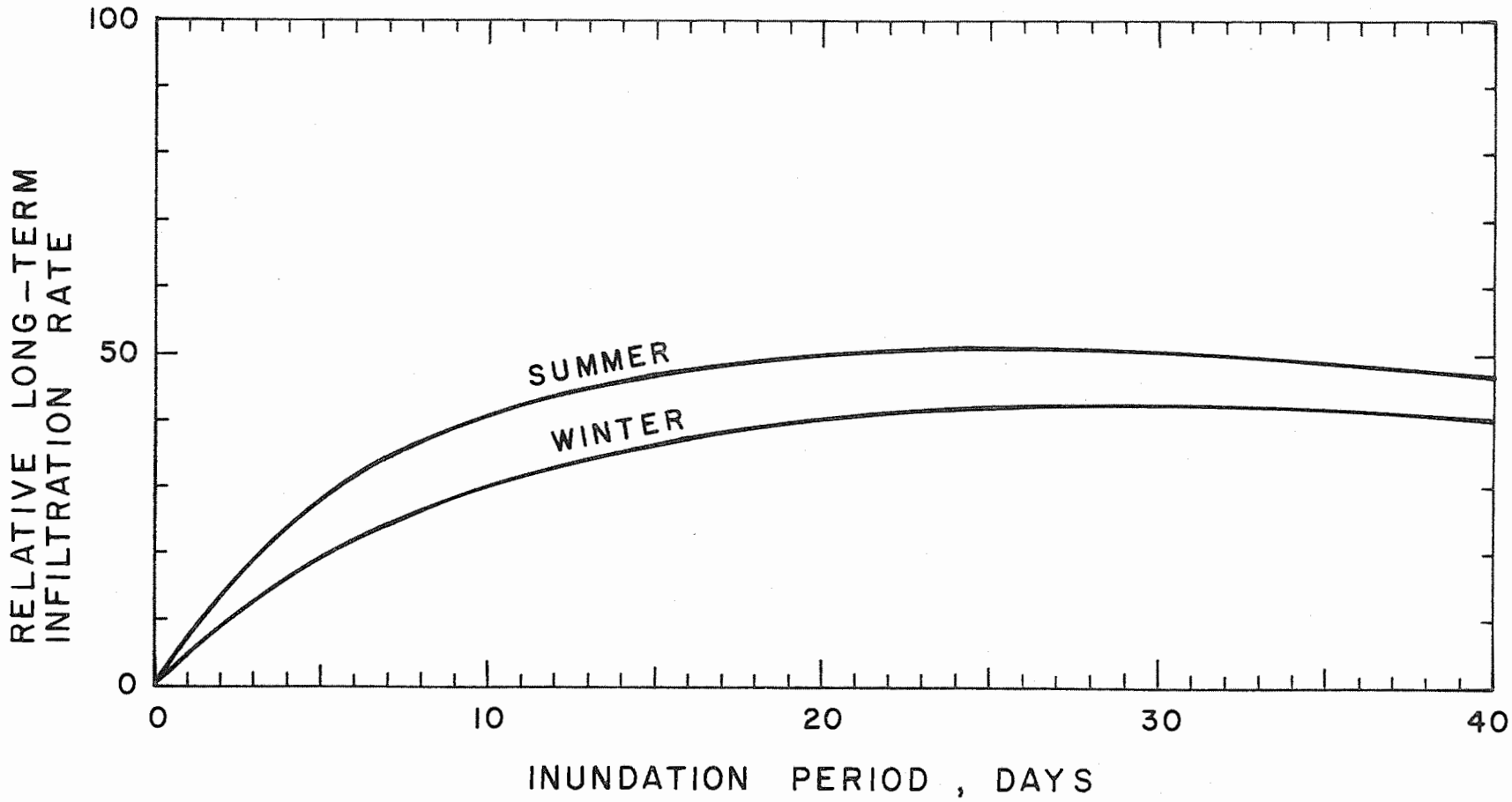

Figure 6. Long-term infiltration rate versus length of inundation periods.

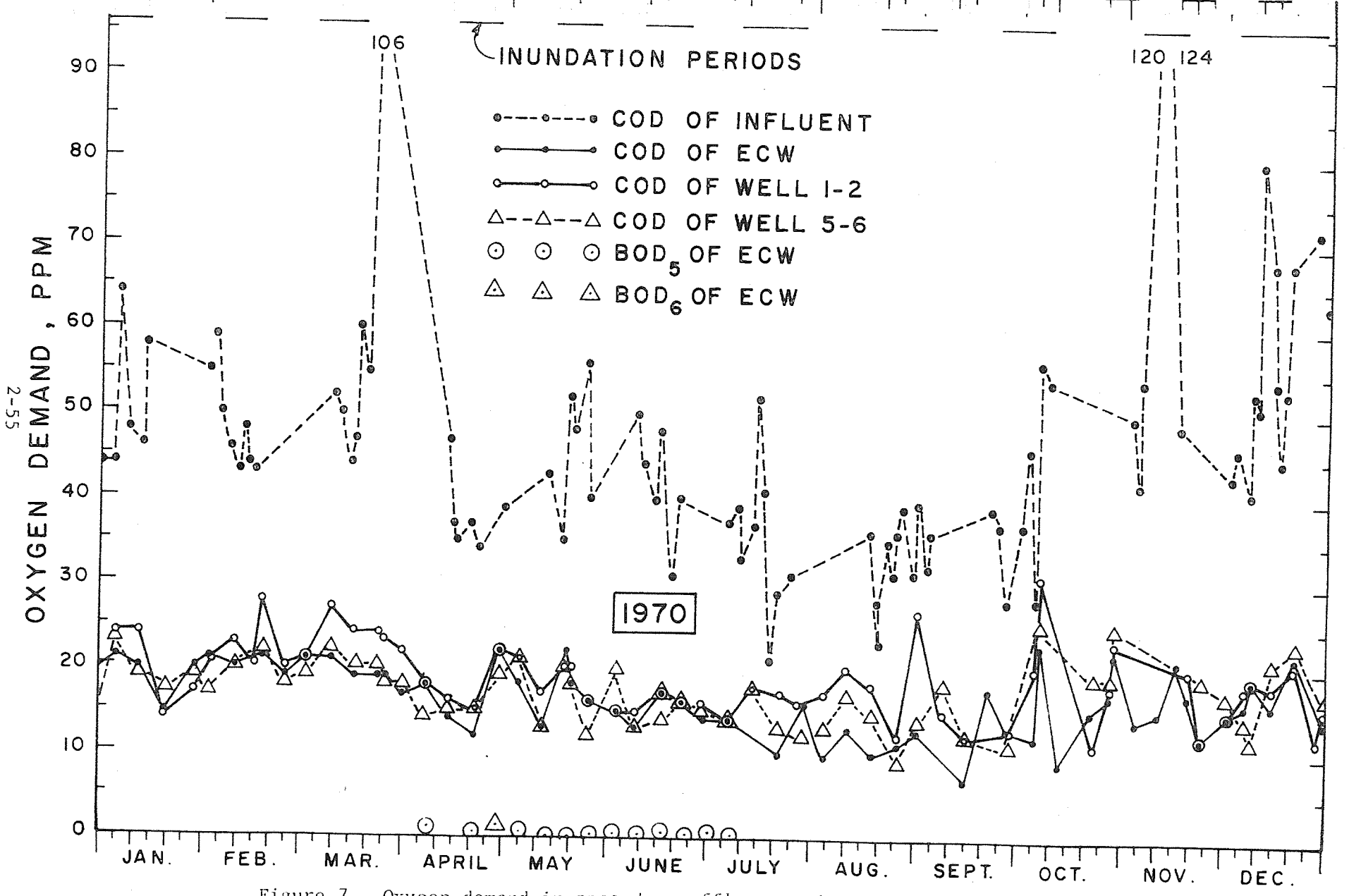

Figure 7. Oxygen demand in secondary effluent and renovated water.

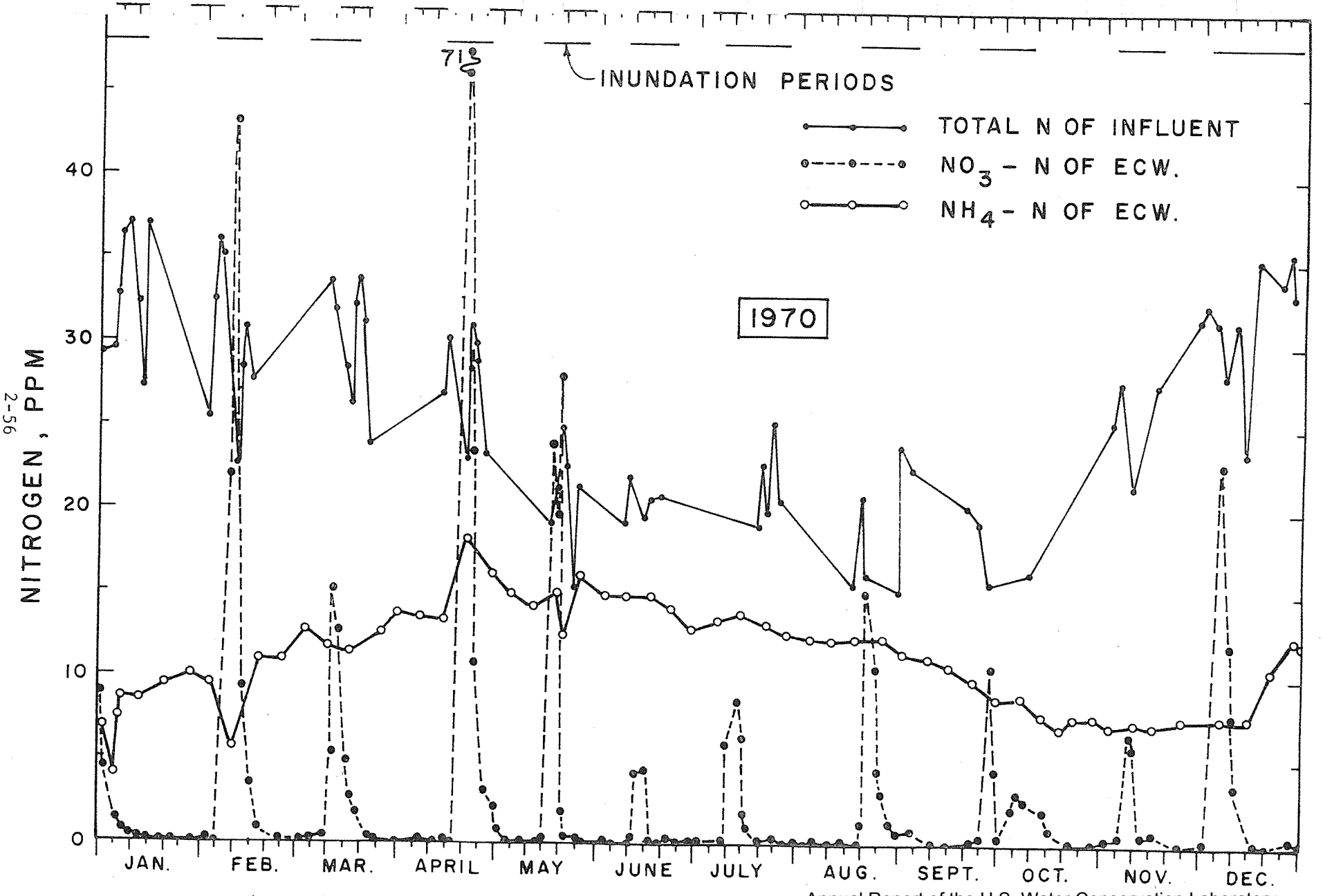

Figure 8. Nitrogen in secondary effluent and renovated water.

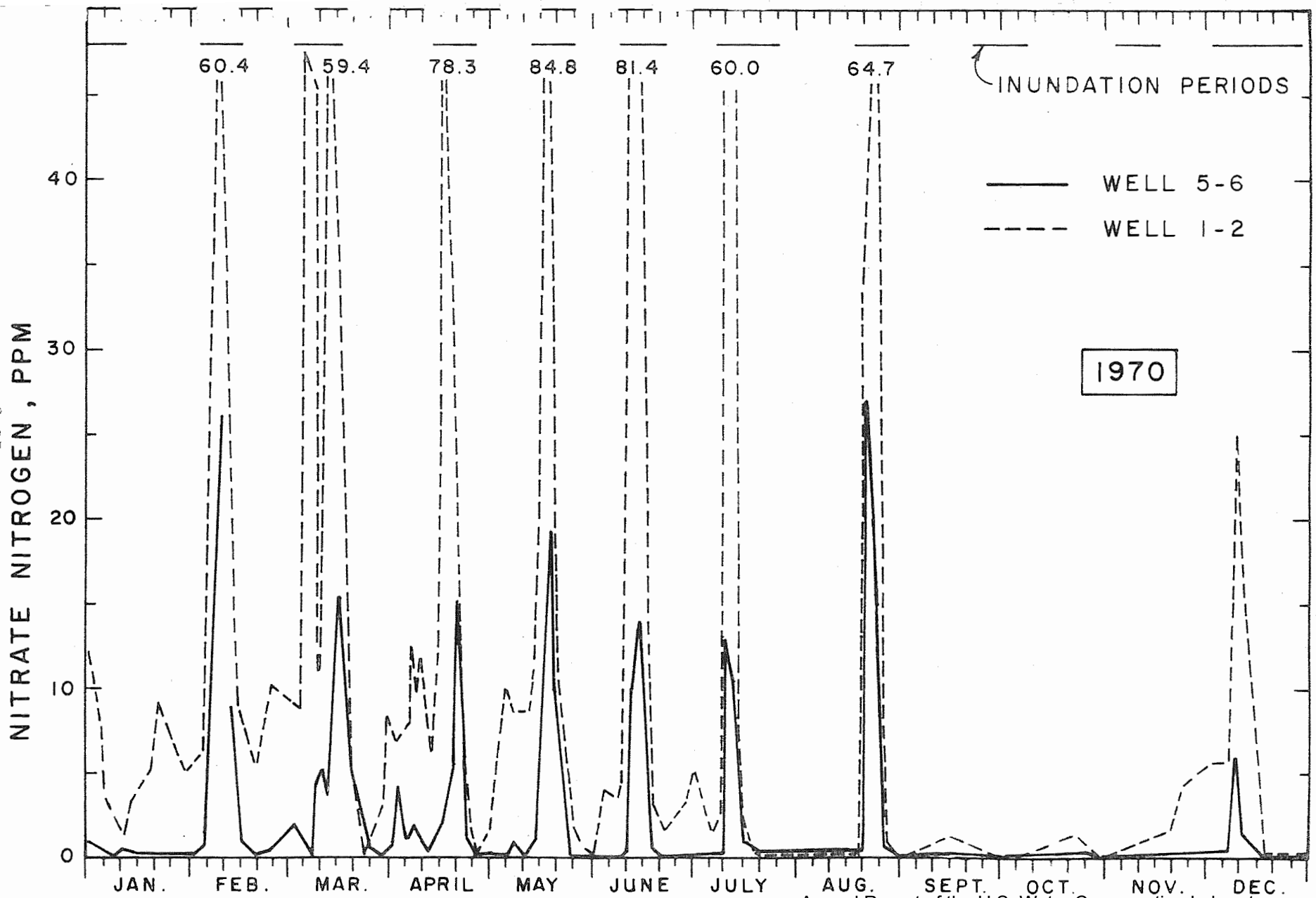

Figure 9. Nitrate nitrogen in renovated water from wells 1-2 and 5-6.

Annual Report of the U.S. Water Conservation Laboratory

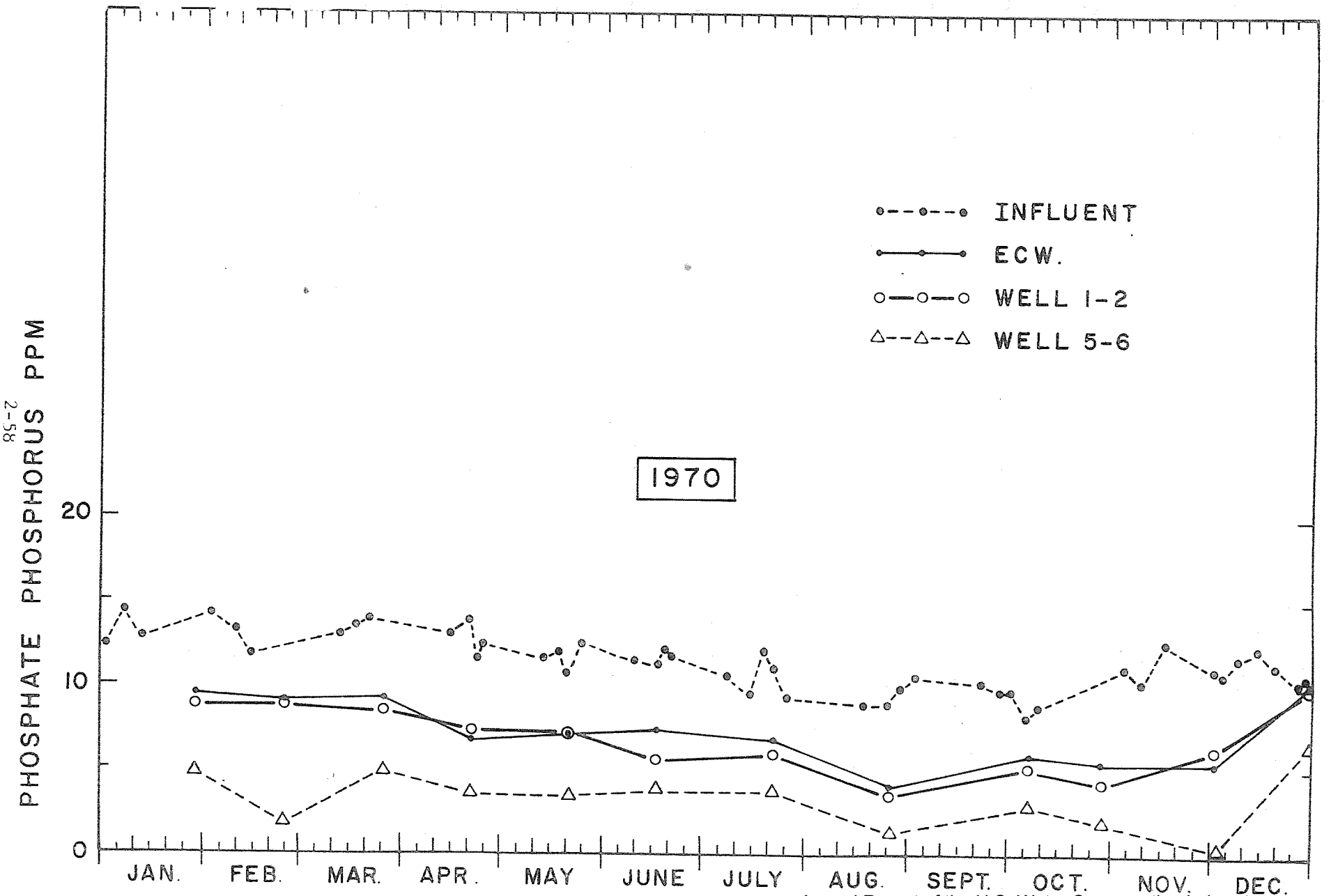

Figure 10. Phosphates in secondary effluent and renovated water from wells inside project.

Annual Report of the U.S. Water Conservation Laboratory

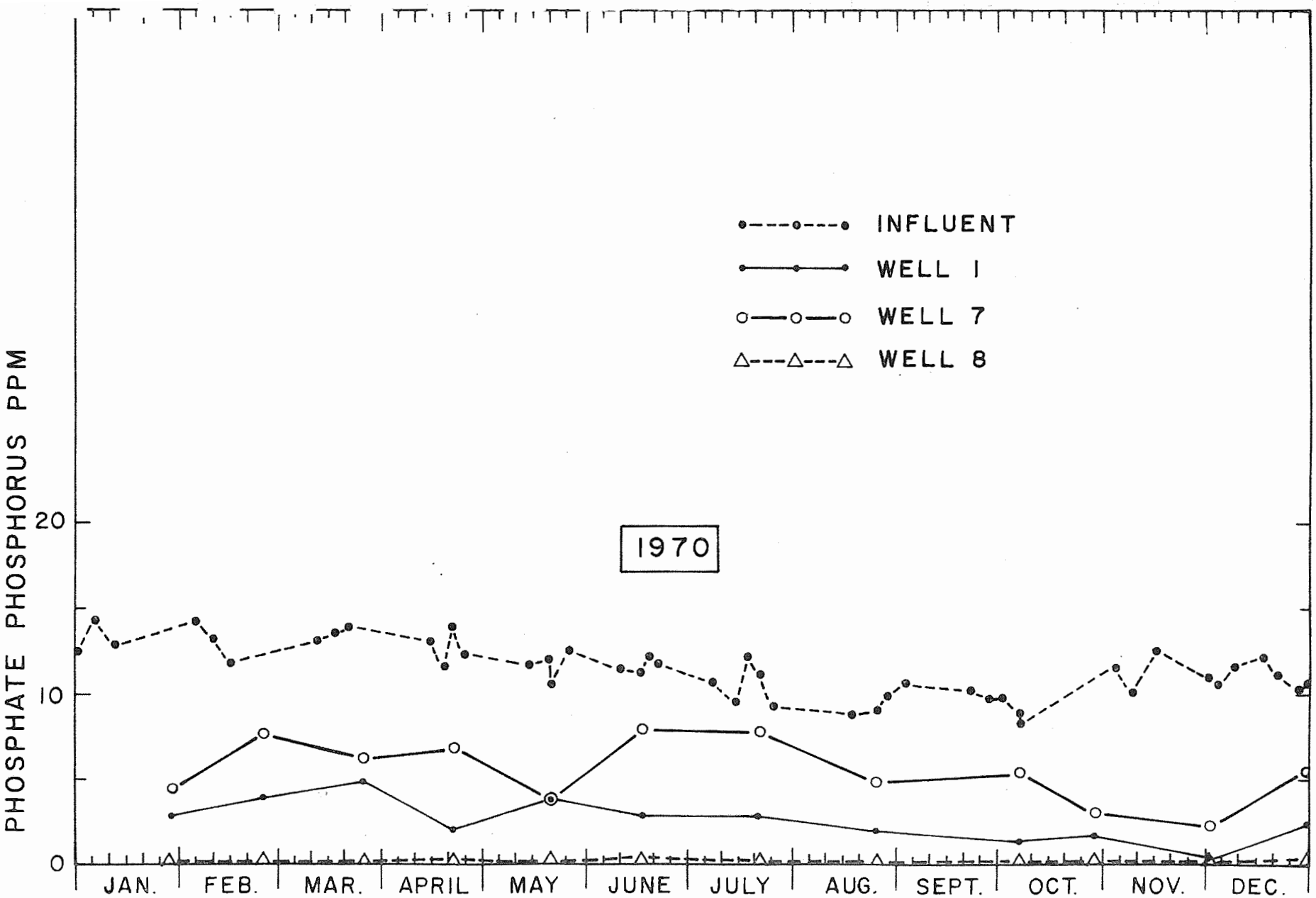

Figure 11. Phosphates in secondary effluent and renovated water from wells outside project.

Annual Report of the U.S. Water Conservation Laboratory

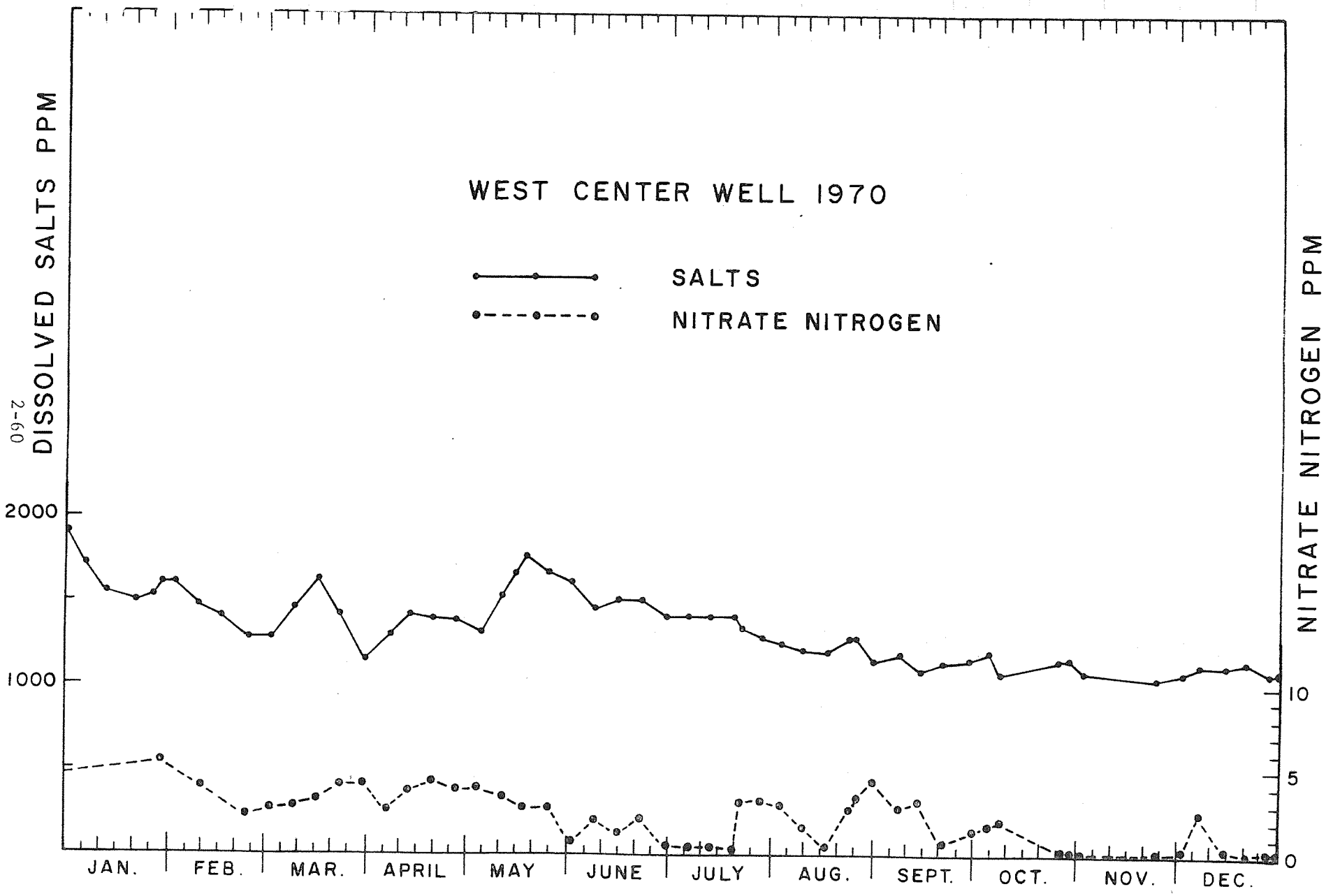

Figure 12. Salts and nitrates in water from West Center Well.

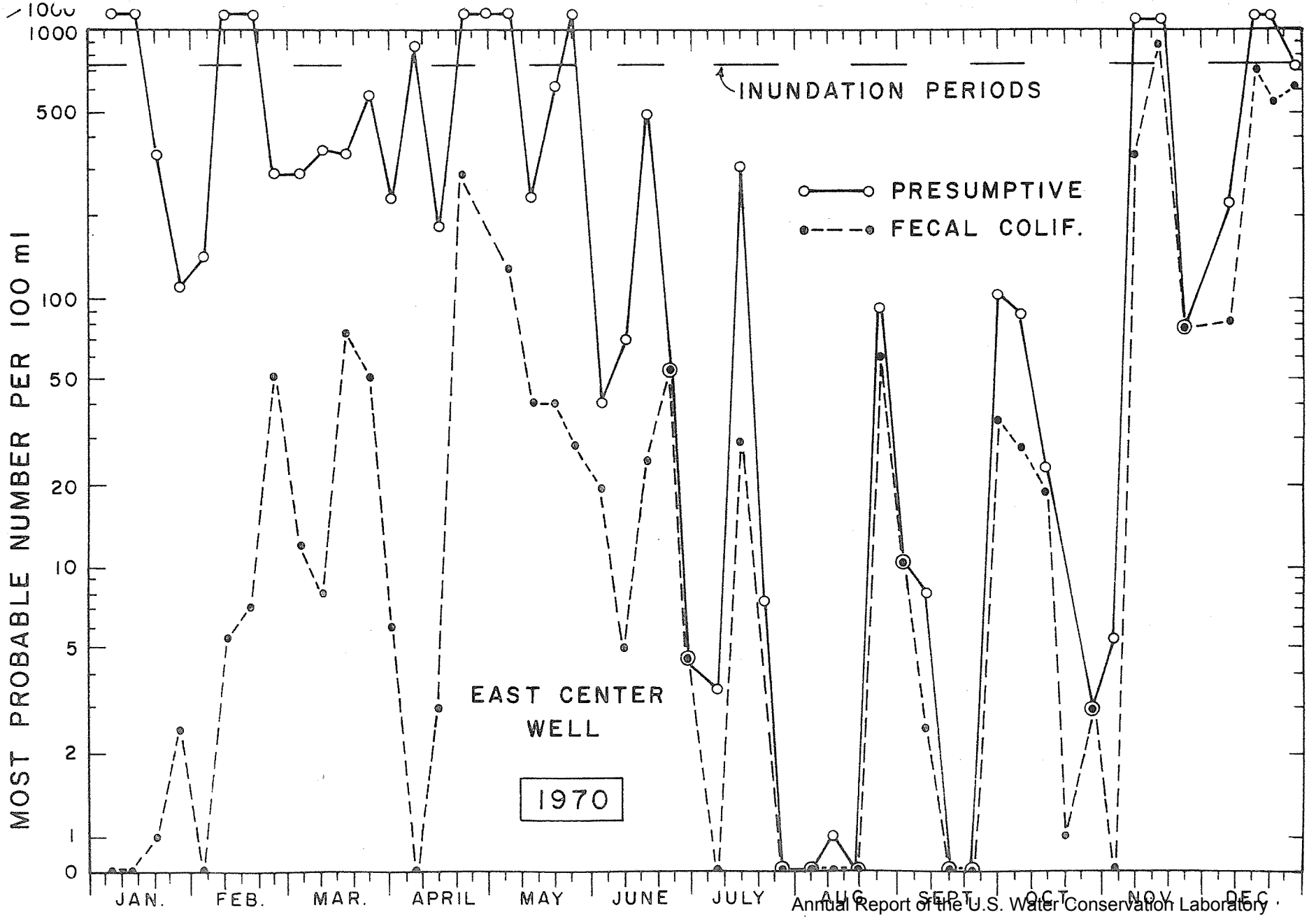

Figure 13. Presumptive and fecal coliform counts in renovated water from East Center Well.

Annual Report of the U.S. Water Conservation Laboratory

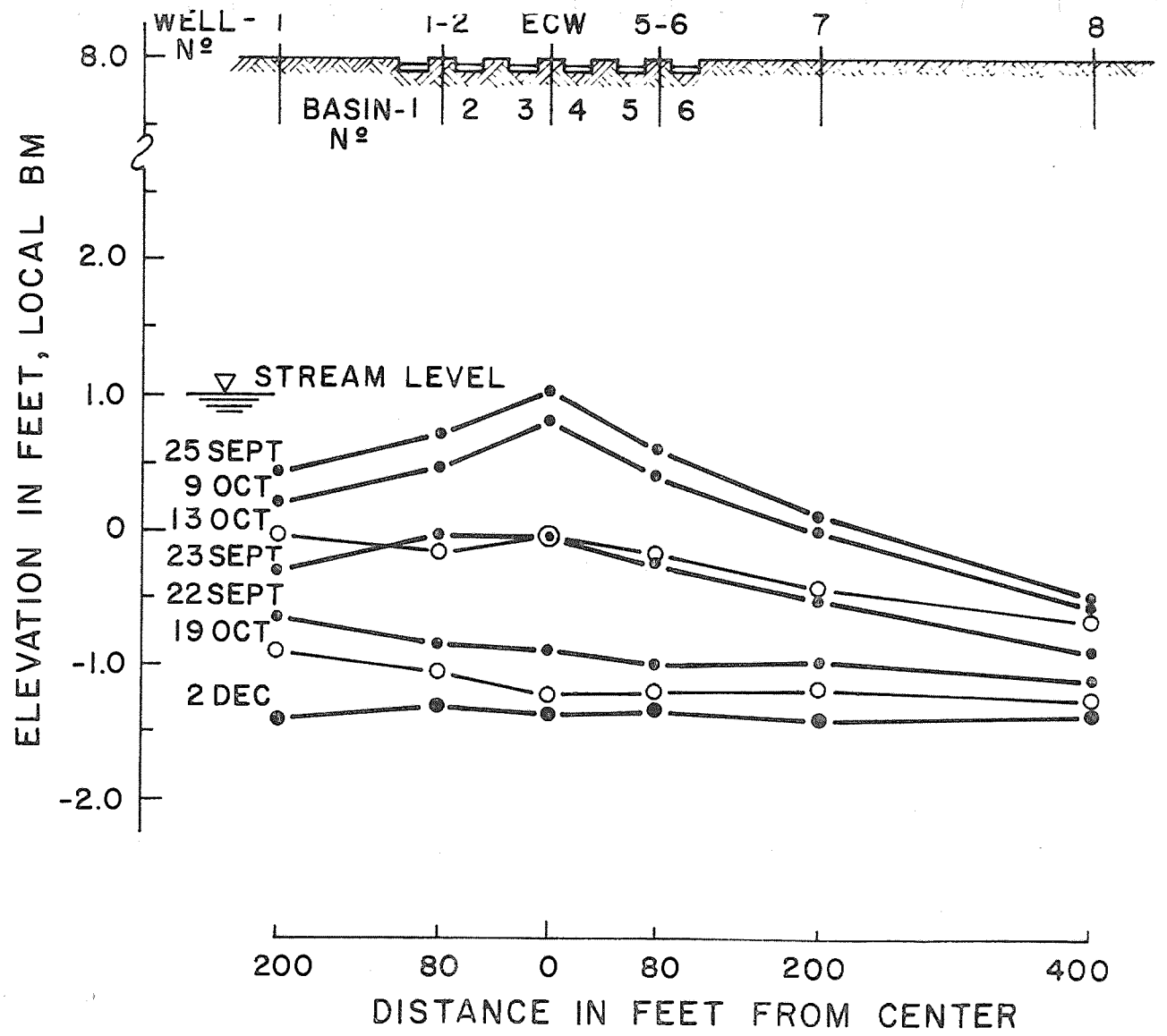

Figure 14. Piezometric heads at 20-ft depth before, during, and after inundation period.

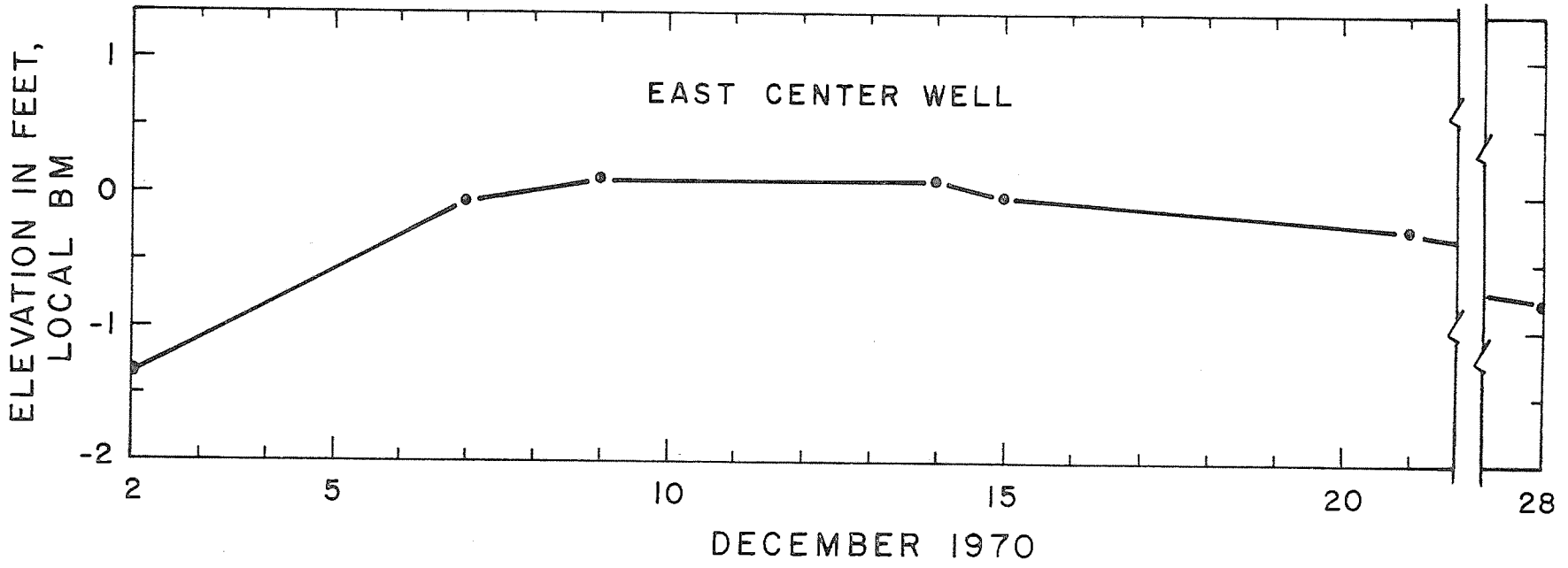

Figure 15. Response of water level in ECW to ground-water recharge

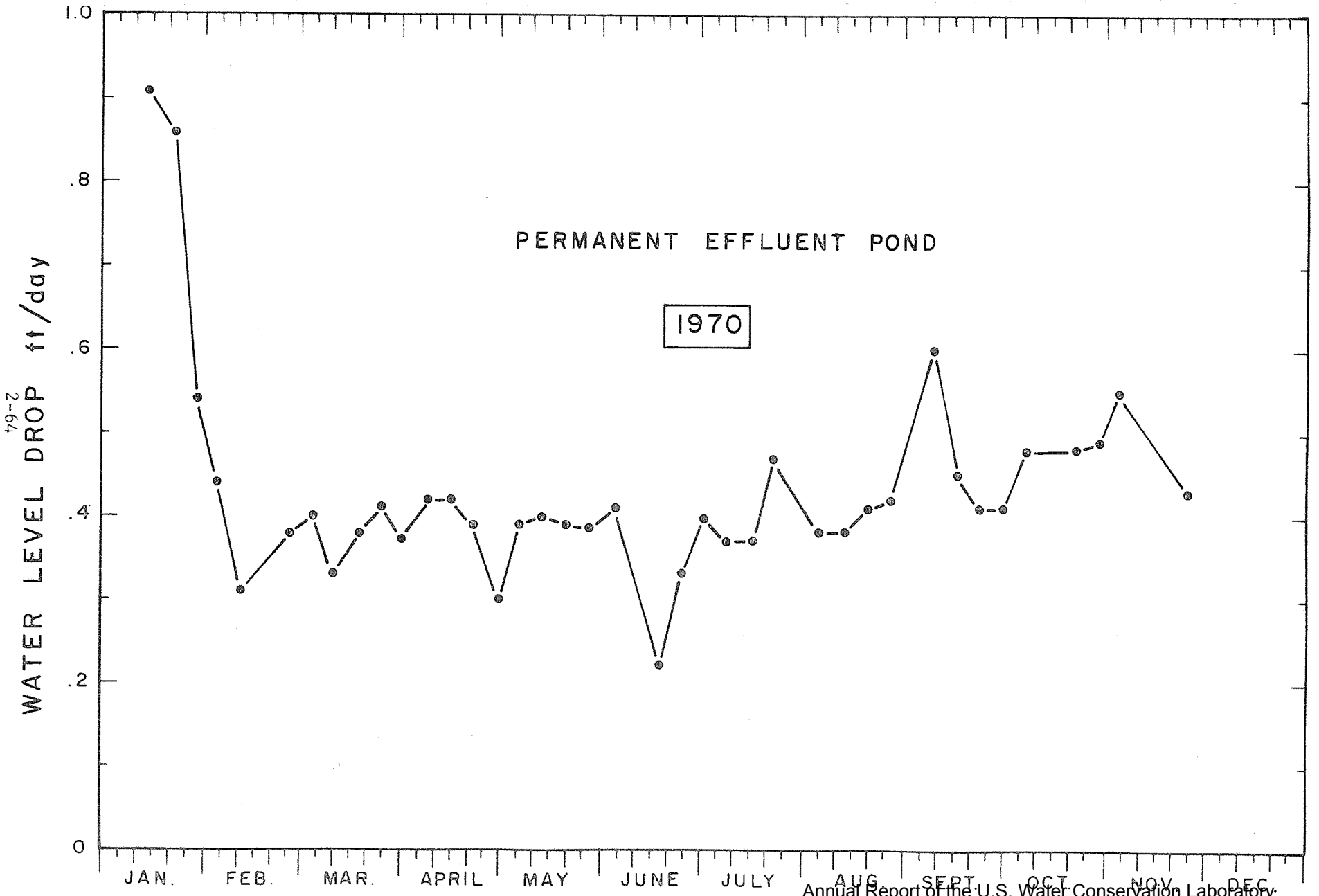

Figure 16. Seepage versus time in permanent effluent pond.

Annual Report of the U.S. Water Conservation Laboratory

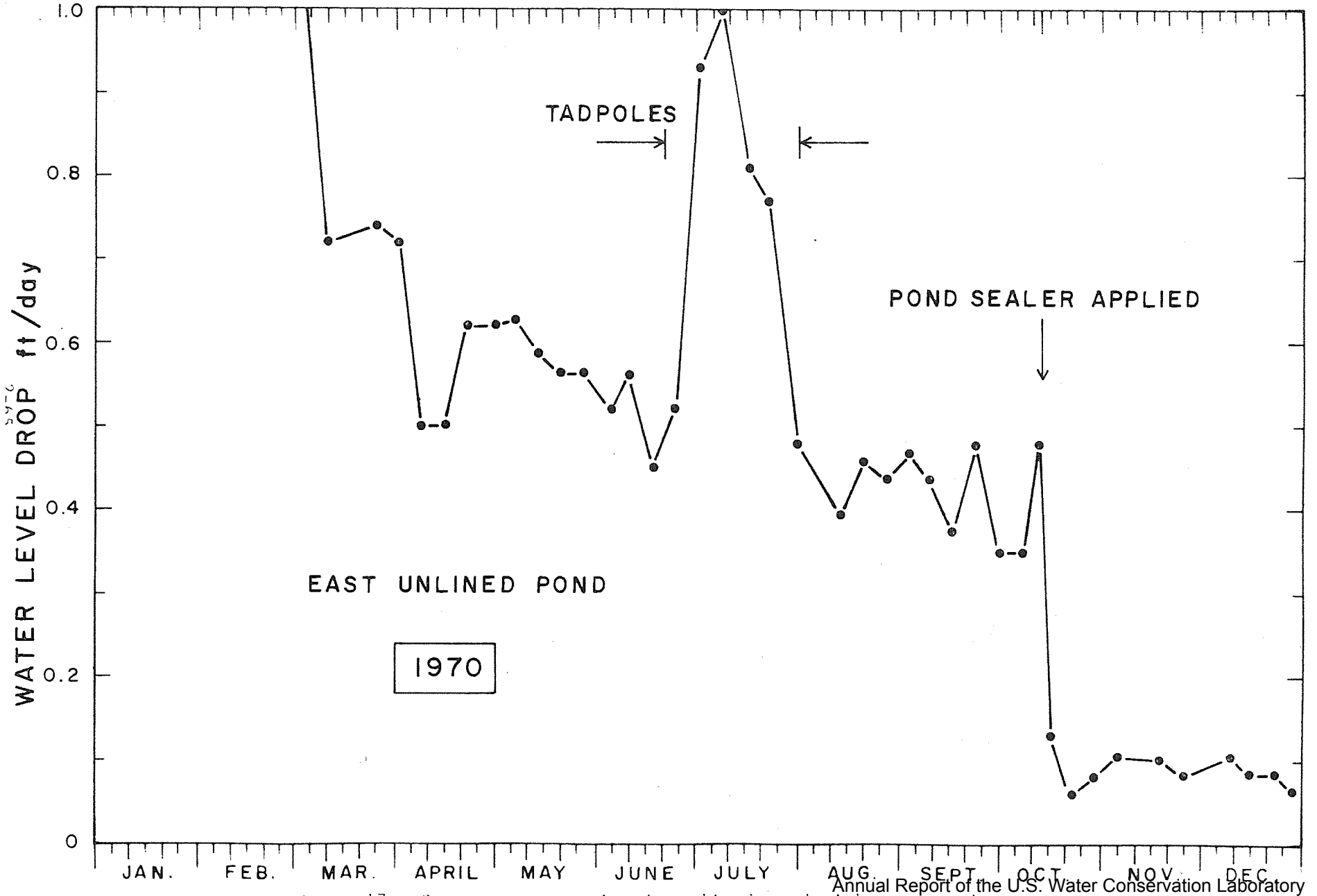

Figure 17. Seepage versus time in unlined pond with renovated water.

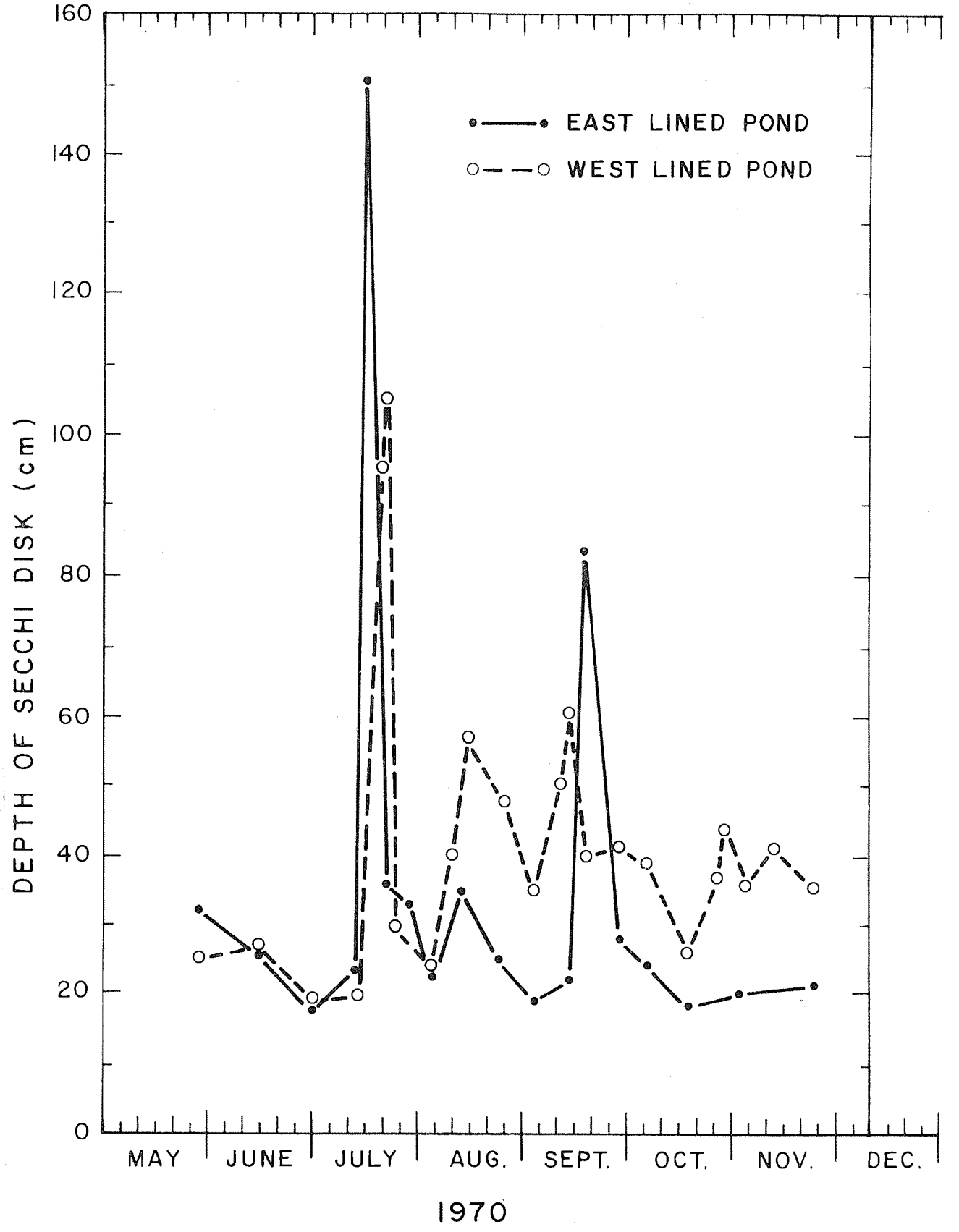

Figure 18. Secchi disk measurements for evaluation of algal growth and density in ponds containing renovated secondary sewage effluent water.

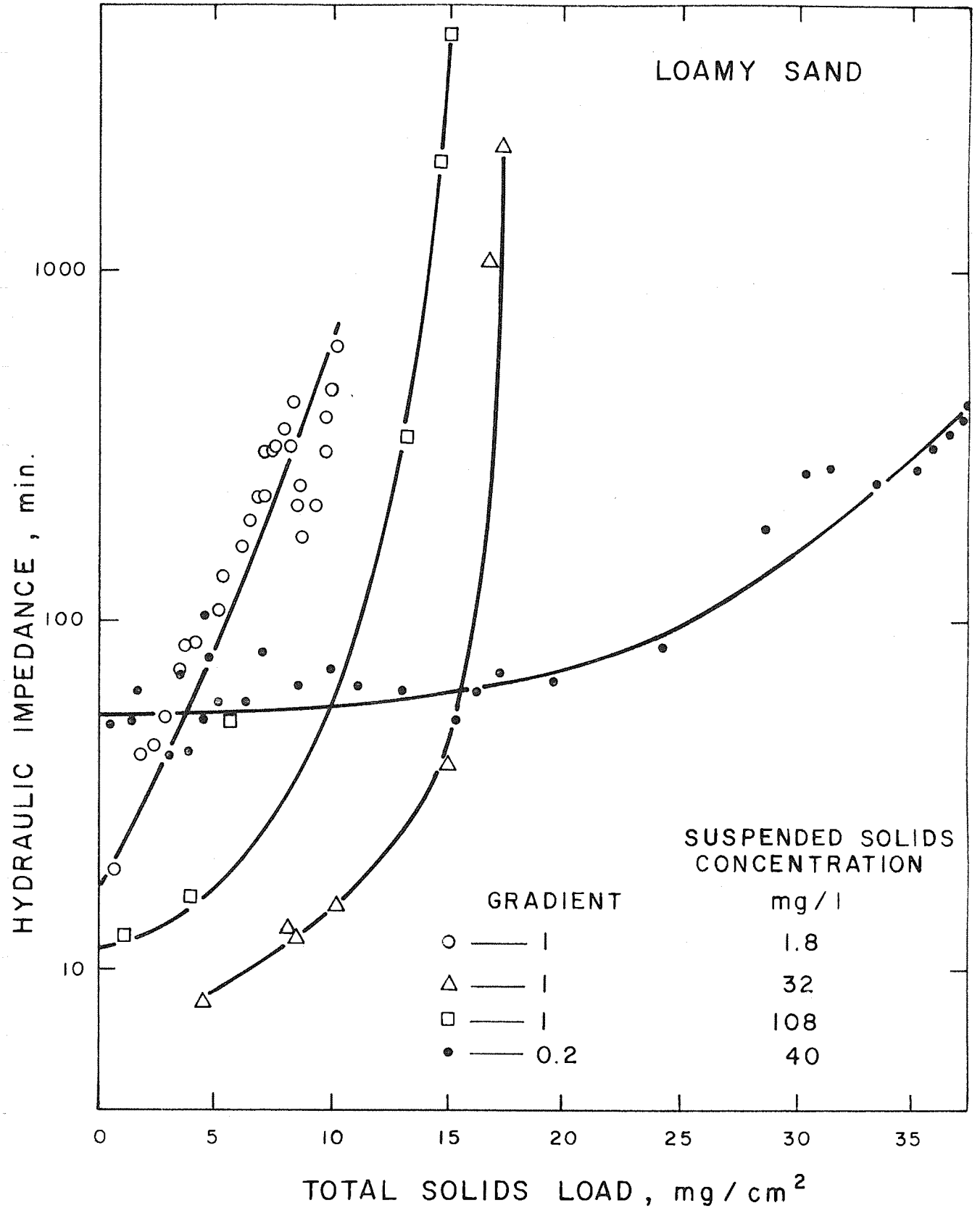

Figure 19. Hydraulic impedance in relation to total-solids load for loamy sand.

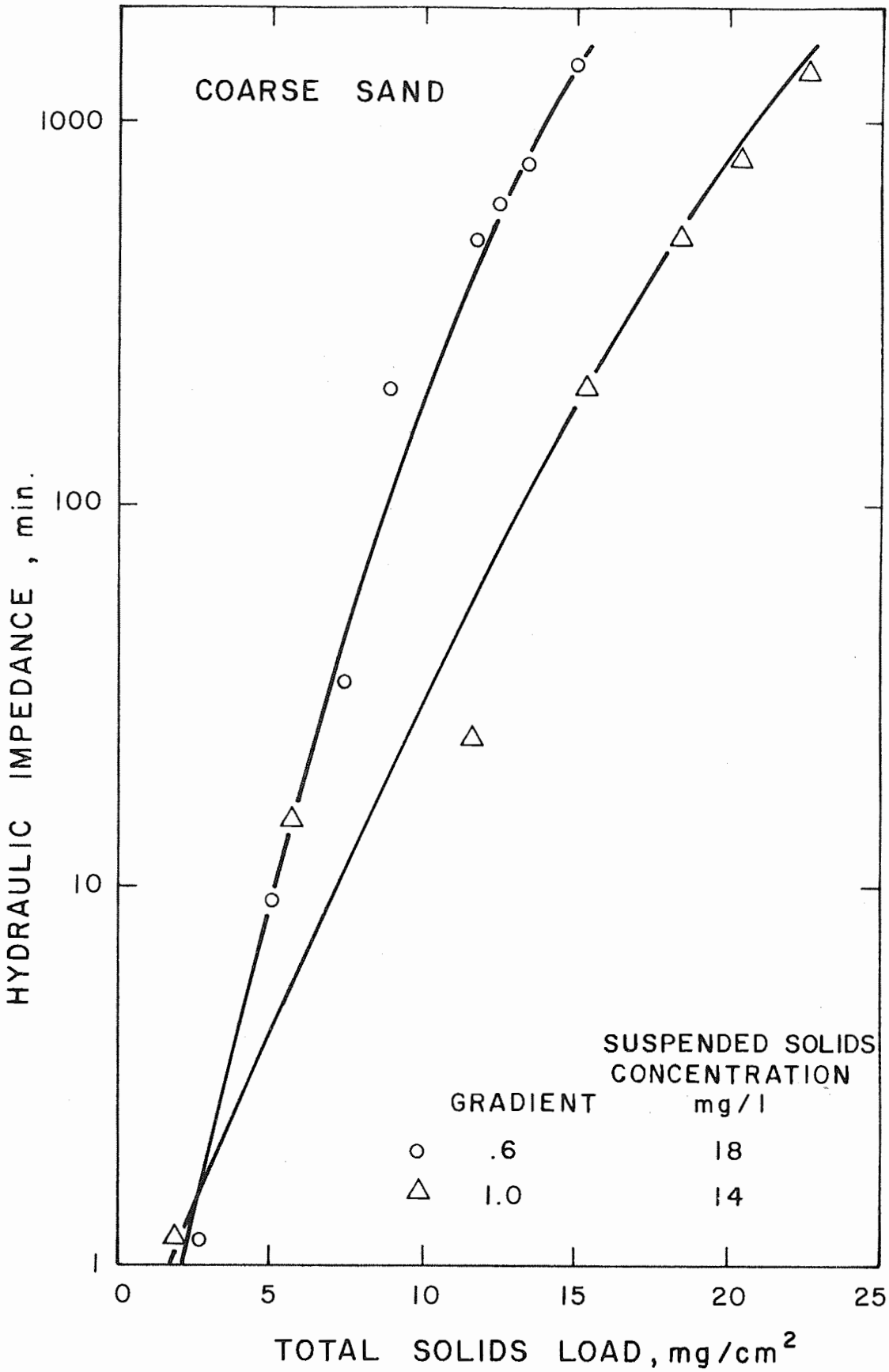

Figure 20. Hydraulic impedance in relation to total-solids load for coarse sand.

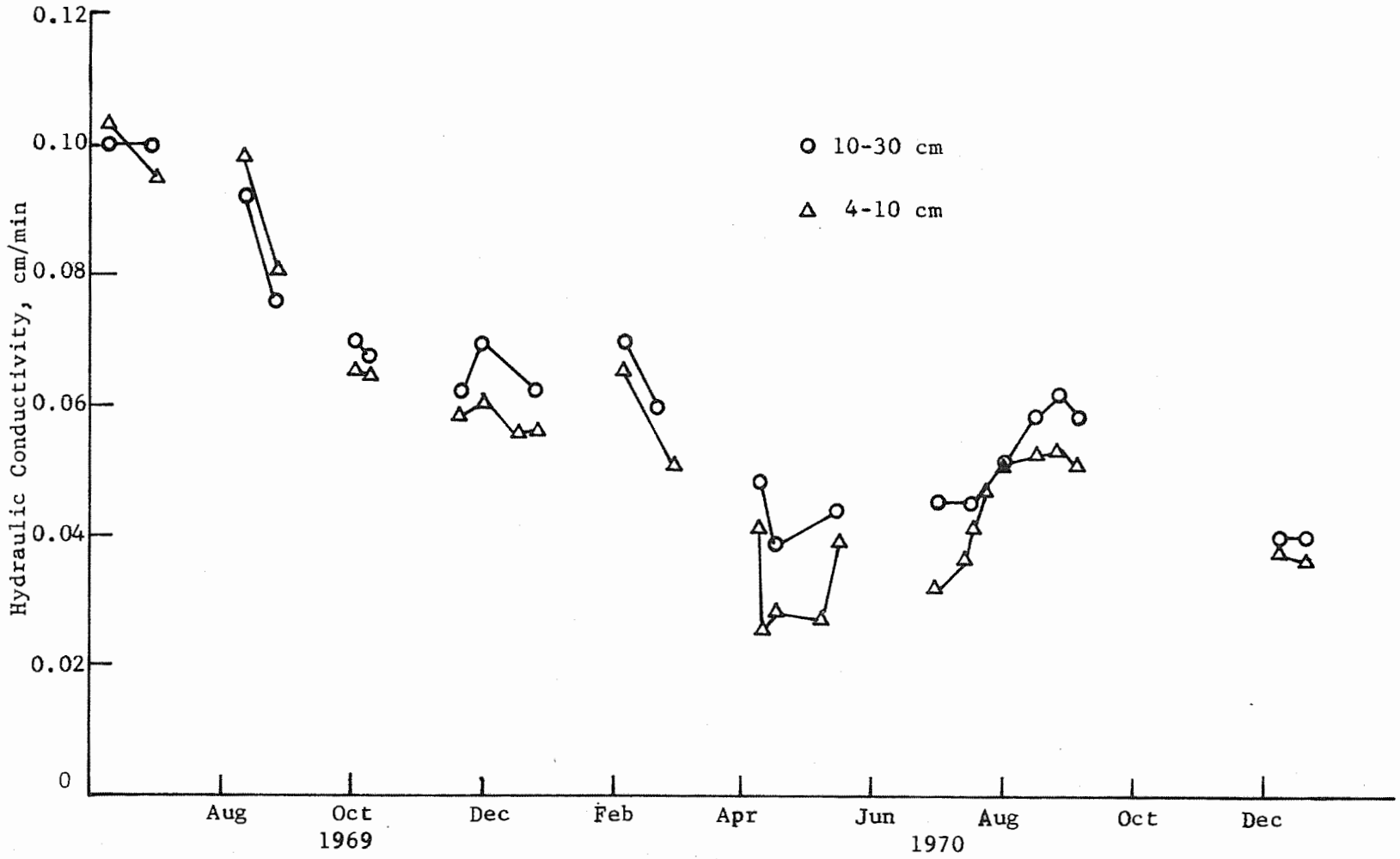

Figure 21. Average hydraulic conductivity of six columns at two depths with time.

TITLE: COLUMN STUDIES OF THE CHEMICAL, PHYSICAL, AND BIOLOGICAL PROCESSES OF WASTEWATER RENOVATION BY PERCOLATION THROUGH THE SOIL.

CRIS WORK UNIT: SWC-012-gG-1 CODE NO.: Ariz.-WCL 68-3

INTRODUCTION:

Experiments on the renovation of secondary sewage effluent with the soil columns described in the 1969 Annual Report were continued in 1970. The research emphasis during 1970 was on characterizing the oxygen utilization by the soil columns and determining the mechanisms responsible for the nitrogen loss observed in 1969.

PART I. CHEMICAL AND BIOLOGICAL PROCESSES DURING RENOVATION

PROCEDURE:

Secondary sewage effluent was passed through 8 polyvinyl chloride columns packed with soil from the basins at Flushing Meadows. The soil columns were 250 cm in length and 10 cm in diameter. A constant head of water was maintained above the columns with a Mariotte siphon. The sewage water and column effluent were analyzed for NO_3, NH_4, and COD.

Oxygen movement into the columns by mass flow was calculated by assuming that the water drained from the soil during the dry period was replaced by an equal volume of air. The movement of oxygen into the columns by diffusion was measured by stopping the column drainage for periods of 1 to 3 hours, while oxygen depletion in a closed air space above the column was measured by chromatographic analysis. The difference between oxygen contents of the air space at the beginning and end of the diffusion time indicated the amount of oxygen entering the column by diffusion. The diffusion rate could be calculated and plotted vs. length of drainage period, so that the area under the curve represented the total amount of oxygen entering by diffusion during the drainage period. The oxygen content of the

soil atmosphere at various depths in the soil columns was determined by extracting samples from ports along the column for analysis with the gas chromatograph. The ports were constructed by drilling holes through the PVC pipe, inserting hypodermic needles through the holes into the soil, sealing around the needles with epoxy, and placing a serum cap over the hub of the needle. Samples of the soil atmosphere were also extracted from the ports during unsaturated flow through the columns. Oxidation reduction electrodes described in the 1969 Annual Report were also inserted at various depths in these two soil columns.

The two columns with oxidation reduction electrodes and sampling ports were operated on various flooding cycles in order to further study the gas production observed in 1969 which was thought to be due to denitrification.

Three soil columns which were continuously flooded in 1969 until they ceased to remove nitrogen from sewage water at about 120 days were maintained on an intermittent flooding schedule for 12 cycles after an initial 2-week dry period to see if their ability to remove nitrogen could be restored.

Three other soil columns were flooded continuously for 165 days to determine if nitrogen removed from the water was being stored in the soil. The soil was analyzed for Kjeldahl nitrogen before and after the long flooding period.

After the 165-day flooding period the columns were drained for for 6 days and cut into 10 equal sections in order to estimate the respiration rate at various depths by measuring the rate of CO_2 evolution. In a preliminary study alternate sections of one column were purged with nitrogen gas and air immediately after division, and 50 ml of sewage water was added to each section. The increase in CO_2 content in a closed air space above the soil was measured daily for 3 days by chromatographic analysis

of samples withdrawn through a septum. The other two columns were divided, and all sections of one column were purged with N_2 to maintain anaerobic conditions while the sections of the other column were purged with air to maintain aerobic conditions. No sewage water was added to these sections, and the CO_2 evolution from these sections was again measured for 3 days. All of the gas samples were also analyzed for N_2O and CH_4. Soil samples were taken at the surface and at 25-cm intervals along the column for plate counts of soil bacteria, fungi, and actinomycetes and water content determinations.

RESULTS AND DISCUSSION:

Oxygen Entry. The oxygen content of the soil atmosphere steadily increased in the zone above 140 cm, but changed very little at lower depths (Figure 1). This indicates that the soil remains an anaerobic environment below 140 cm even at the end of the 5-day dry period. The oxidation reduction potentials confirm these observations. The electrode at the 130-cm depth indicated reduced conditions for about 3 days before changing, and the lower electrodes indicated reduced conditions throughout the dry period (Figure 2). The low oxygen environment could be maintained below 140 cm for more than 10 days and below 190 cm for at least 21 days (Figure 3). These data indicate that a considerable portion of the soil profile provides a suitable environment for denitrification even during the dry part of an intermittent flooding schedule. The nitrates formed in the upper section of the soil profile then must pass through a zone which is favorable for denitrification from the standpoint of the anaerobic requirement. The fact that high nitrate concentrations are found in the water collected from soil columns immediately following the dry period must be due to the lack of a sufficient amount of carbon in the anaerobic zone to support a high enough population of denitrifying bacteria to utilize all of the nitrate passing through that zone. It seems

likely that nitrogen removal by denitrification could be increased if the supply of carbon in the anaerobic zone could be increased. More work will be done on supplying carbon to anaerobic zones in the immediate future.

The oxygen concentrations at various depths during the drainage period were measured in a soil column which was closed at the top except for a pinhole (Figure 4). Oxygen could enter the column by mass flow in response to drainage, but not by diffusion. A considerable amount of oxygen entered the column, but the oxygen concentrations were much lower than in the open columns where both mass flow and diffusion occurred. This supports the conclusion from previous data that both mass flow and diffusion are important mechanisms of oxygen entry.

Another column was closed at the top and air was pumped through the open space above the soil with a slight positive pressure exerted on the column. Analysis from samples at different depths indicated that oxygen concentrations were still very low below 180 cm (Figure 5).

The diffusion of oxygen into two soil columns following a 16-day flooding period was measured for comparison with other data following 2-day flooding periods.

The diffusion of oxygen appeared to level off at about 8 mg/hr by the fifth day of the dry period following a 16-day flooding period, as compared to a rate of 4 mg/hr for the fifth day following a 2-day flooding period (Figure 6). This apparent increase in oxygen diffusion may instead be due to a decrease in the proportion of oxygen in the air above the soil caused by the diffusion of nitrogen into this space from the soil. The data cited earlier indicate that a large section of the column remains anaerobic during the dry period, providing a suitable environment for nitrogen production by denitrification.

Respiration of Column Sections. The increase in CO_2 content of the air space above the sections of columns which had previously been flooded by 165 days did not vary much with the depth of the column (Tables 1 and 2). This is in agreement with the data from plate counts of microorganisms which indicated that their numbers also did not change with the depth of the column (Table 3). These data indicate that the columns were quite uniform. The sections which were purged with nitrogen produced only slightly less CO_2 than those purged with air. The difference between the aerobic and anaerobic sections appeared to increase, however, with time, and this effect was more marked in the column sections which were enriched with sewage water. This indicated that a number of days of drainage is necessary for soils to develop an aerobic population with a respiration rate higher than that observed for anaerobic soils. More work needs to be done in this area with waste water which has a high organic matter content.

Traces of methane were observed in a few anaerobic columns while N_2O concentrations ranging from a trace to about 1.5% were observed in several sections, some of which were aerobic as well as anaerobic. This indicates that denitrification was occurring in both aerobic and anaerobic sections, and that denitrification may occur during the dry periods between floods.

COD Removal Processes. The COD of water collected from 2 columns which had been flooded with secondary sewage effluent for 120 days averaged about 17 mg/l. The COD of the sewage water applied averaged about 50 mg/l. The COD of the water from the columns was about the same at the end of the long flooding period as it was at the beginning (Figure 7). It was also about the same as the COD of water collected when the same two columns were flooded for short frequent periods, which is essentially aerobic treatment. This indicated that the absence of oxygen did not affect the COD reduction of the sewage water used in these

studies. More work is needed to determine if oxygen is still not needed as the COD of the water applied is increased, and this will be studied during the next year.

Nitrogen Removal. The soil columns which were continuously flooded for 120 days last year released some of the nitrogen stored during that period when they were operated on an intermittent flooding schedule. The columns fluctuated between net nitrogen removal and net nitrogen release for 4 cycles before consistently releasing nitrogen for 5 cycles (Table 4). The column's ability to consistently remove large quantities of nitrogen from sewage water appeared to be restored, however, after the soil stopped releasing nitrogen. During the last 2 cycles the columns removed 60 and 43% of the nitrogen from the sewage water. The amount of nitrogen removed during these cycles shows that rejuvenation of the nitrogen removal ability of the columns is more than simply the freeing of sites for more adsorption. These data indicate that the alternate flooding and drying periods are essential for the development of the proper environment and microbial population for extensive nitrogen removal by processes such as denitrification.

The columns released an average net total of 1,080 mg of N. The average amount of nitrogen which had been removed from sewage water by the columns during the long flooding period was 2,380 mg. Nitrogen could have also been released from the columns in the gaseous form. Gases were never released in sufficient quantity to be forced out as bubbles and collected, but some N_2 could have left the columns in solution. The sewage water entering the columns should be in equilibrium with air (79% N_2) with respect to dissolved N_2. If nitrogen gas is produced inside the columns, the water would instead be in equilibrium with 100% N_2. Samples of the soil atmosphere which were collected from soil columns where unsaturated flow occurred as a result of surface clogging

had a nitrogen content of 94.2% (Table 5). Water in equilibrium with this atmosphere, rather than air, could dissolve an additional 2 mg of N_2 per liter of water.

The analysis of soil samples from columns which were flooded continuously for 165 days this year showed no increase in soil Kjeldahl-N (Table 6). The average net nitrogen removal from these columns, however, was only 339 mg (Table 7). This amount of nitrogen could have been lost as N_2. Also, some nitrogen could be stored in the columns, but if evenly distributed it would be difficult to detect in these quantities. The soil used to pack these columns was taken from the basins at Flushing Meadows where its capacity for fixing nitrogen had probably been saturated.

PART II. PHYSICAL PROCESS DURING RENOVATION

PROCEDURE:

The same columns which were reported on last year were maintained and observed for most of this year. Since last year's report was based upon only 2 or 3 cycles, several 1-, 2-, 3-, and 4-week cycles of infiltration of effluent, plus 5-days drainage, were run through the columns. Redox potential and pressure head were observed in columns 7 and 8 during these cycles.

RESULTS AND DISCUSSION:

In general, this study confirmed our previous observations. These observations are:

1. When denitrification within the column does occur, the flux of water through the column is slowed until most of the N_2 gas is expelled; then the flux returns to a high rate.
2. The redox potential appears to increase in the zone of denitrification, and then decrease when the gases are expelled.
3. The pressure gradients confirm the plugging of the pores within the soil column.

In addition, it was observed this year that some gases could be expelled from the column without an attendent increase in flux, etc.; however, after 3 or 4 days of slow gas production, the rate of flow did increase.

The pressure-head profiles also show that much of the reduction in flow rate over long inundation periods is due to surface clogging or plugging.

SUMMARY AND CONCLUSIONS:

Eight columns filled with 250 cm of soil from the Flushing Meadows recharge basins were again intermittently flooded with secondary sewage effluent during 1970.

Oxygen entry and utilization were studied in two columns equipped with gas sampling ports and oxidation reduction electrodes. Three columns which had previously been flooded continuously for 120 days were placed on an intermittent flooding schedule to see if their ability to remove N from sewage water could be restored. Three other columns were continuously flooded for 165 days to study fixation of N by the soil. These columns were then divided and respiration of the column sections under aerobic and anaerobic conditions was estimated by measuring CO_2 evolution. Samples from the sections were analyzed for Kjeldahl-N, and plate counts of soil microorganisms were made.

The oxygen profiles obtained for soil columns during the dry period indicate that a large section of the column remained anaerobic throughout dry periods up to 21 days in length. The comparison of profiles of open columns with columns closed except for pinholes supports the earlier conclusion that both mass flow and diffusion are important mechanisms of oxygen entry.

The COD reduction by soil columns continuously flooded with sewage water for long periods was equal to that obtained with short frequent flooding periods. This indicates that anaerobic reactions

were as effective as aerobic reactions for COD reduction of secondary sewage effluent.

CO_2 production by sections of columns which had previously been flooded for 165 days did not vary much with the depth of the column, and microbial populations were also uniform. Anaerobic sections produced almost as much CO_2 as aerobic sections during a 3-day period. This indicates that the columns were quite uniform and that the potential for anaerobic activity was almost equal to that for aerobic activity even during the dry period.

Denitrification may account for a considerable amount of nitrogen removal in soil columns even though gases were usually not produced in sufficient quantity to be forced out of the columns and collected. As much as 10% of the nitrogen entering the column in the sewage water could leave the column as dissolved N_2. An analysis of samples of the soil atmosphere in columns during unsaturated flow due to surface clogging showed a nitrogen content of about 95%. The change from equilibrium with air to equilibrium with an atmosphere of this composition would result in dissolving an additional 2 mg of N_2 per liter of water.

The oxygen profiles and oxidation reduction potentials indicate that a large section of the column remains anaerobic during the dry period providing a suitable environment for denitrification. Nitrogen produced during the dry period could diffuse from the open column without being detected. The detection of N_2O in sections of columns divided after a long flooding period indicates that denitrification does occur during the dry period. Also, the apparent increase in the oxygen diffusion rate during dry periods following long floods as compared to diffusion rates following brief floods may be due to the production of nitrogen by denitrification. The diffusion of nitrogen into the air space above the columns would reduce the proportion of oxygen in the samples.

The columns flooded intermittently after being continuously flooded for 120 days released about 35% of the nitrogen which had been removed from sewage water during the long flooding period. The ability of the columns to remove considerable quantities of nitrogen appeared to be restored after they released stored nitrogen for several cycles. The amount of nitrogen removal from sewage water after the rejuvenation was more than could be explained by the freeing of adsorption sites. Thus, intermittent flooding seems to be a requirement for consistent nitrogen removal. The soil adsorbs NH_4^+ from sewage water and holds it until the dry period when it can be nitrified. The flooding period must be long enough to develop a good population of denitrifying bacteria, but not long enough to exceed the soil's capacity to adsorb NH_4^+.

The adsorption of NH_4 in a stable form was probably significant when the soil was initially flooded, but columns packed with soil from basins used for groundwater recharge for 2 years did not show an increase in nitrogen content after 165 days of flooding and 5-day drainage. This is in agreement with results from soil samples taken from basins in the field.

PERSONNEL: J. C. Lance, F. D. Whisler, Herman Bouwer, R. C. Rice, R. G. Gilbert, R. S. Linebarger, E. D. Escarcega.

CURRENT TERMINATION DATE: 1971

Table 1. The increase in percent CO_2 content in a 400-cc closed compartment above sections of a soil column which had been flooded with secondary sewage effluent

Section*	Day 1		Day 2		Day 3	
	Aerobic	Anaerobic	Aerobic	Anaerobic	Aerobic	Anaerobic
1	0.65	0.55	1.10	1.03	1.43	1.43
2	1.60	1.38	0.92	1.35	2.17	2.62
3	1.60	1.45	1.03	0.75	4.95	2.88
4	1.25	1.40	1.05	1.02	2.35	2.75
5	1.52	0.85	0.88	1.05	3.10	2.0
6	1.72	1.40	1.0	0.75	3.02	2.0
7	1.80	1.95	1.0	0.73	3.0	2.20
8	1.60	1.55	0.92	0.80	3.40	2.20
9	1.45	1.05	1.40	0.60	2.70	1.10
10	0.98	0.45	0.57	0.30	1.25	0.30

* Two 250-cm soil columns cut into ten sections, with sections from one column maintained aerobic and the other column sections anaerobic.

Table 2. Increase in percent CO_2 content in a 400-cc closed compartment above sections of a soil column which had been previously flooded for 165 days*

Section	Day 1		Day 2		Day 3	
	Aerobic	Anaerobic	Aerobic	Anaerobic	Aerobic	Anaerobic
1	1.0	1.2	1.6	0.3	3.3	2.0
2	1.5	1.5	0.6	0.3	3.8	1.4
3	1.6	0.9	0.4	0.3	4.1	2.0
4	0.7	0.4	1.7	1.3	4.1	1.0
5	0.7	0.2	0.0	0.3	4.6	0.6

* One 250-cm column divided into ten alternate aerobic and anaerobic sections. Fifty ml of secondary sewage effluent was added to each section immediately after the columns were divided.

Table 3. Profiles of soil moisture and microbial numbers in soil columns flooded for 165 days with secondary sewage effluent[1/]

Column section number	Numbers of microorganisms/g of soil[2/]			Soil moisture percentage
	Fungi $\times 10^2$	Bacteria $\times 10^4$	Actinomycetes $\times 10^4$	
1 (top)	17	260	27	9.48
2 (25 cm)	5	317	43	11.56
3 (50 cm)	16	208	48	12.74
4 (75 cm)	9	120	49	13.53
5 (125 cm)	16	170	47	14.71
6 (150 cm)	17	250	48	15.10
7 (175 cm)	16	167	45	15.86
8 (200 cm)	13	180	52	18.92
9 (225 cm)	16	190	48	19.10
10 (250 cm)	17	211	42	19.36
11 (botton)	17	216	57	20.10

1/ Data are averages of results from 3 columns.

2/ Culture media used were Littman-Oxgall agar for fungi and plate count agar for bacteria and actionmycetes.

Table 4. Net nitrogen removal from sewage water by soil columns intermittently flooded with sewage water after being continuously flooded for several months[1/]

Cycle length Flooded	Dry	Net N removal/cycle Col 1	Col 2	Col 3	Avg
days	days	mg	mg	mg	mg
23	12	517.7	22.6	-136.6[2/]	134.6
3	4	-533.0	-682.9	-516.5	-577.4
23	5	433.7	278.1	502.8	404.8
17	4	111.6	204.9	256.1	190.9
9	5	-230.7	-748.3	-197.1	-392.0
9	5	-332.5	-198.4	-178.8	-236.6
16	5	-176.8	-130.1	-190.4	-165.8
21	5	-81.0	-5.0	-398.6	-161.5
16	5	-108.1	-44.0	37.6	-38.2
16	7	437.3	418.5	508.1	454.6
22	4	790.8	917.9	1220.8	976.5
16	5	676.5	623.0	515.1	604.8

1/ Column 1 was flooded for 105 days and columns 2 and 3 were flooded for 180 days.

2/ Negative numbers indicate that the soil was adding N to the water.

Table 5. The composition of the soil atmosphere during unsaturated flow of sewage water through soil columns

Column depth	N_2	O_2	CO_2	CH_4	Total
cm	%	%	%	%	%
130	95.8	1.0	3.6	Tr*	100.4
160	93.2	3.5	2.6	-	99.3
190	93.6	1.7	3.9	-	99.2
Avg	94.2	2.1	3.4		99.7

* Trace is detectable, but < 0.05%.

Table 6. Kjeldahl-N content of soil from columns flooded for 165 days with secondary sewage effluent

Section*	Col 1	Col 2	Col 3	Ave
		mg N/g of dry soil		
1	0.28	0.27	0.31	0.29
2	-	0.28	0.33	0.31
3	0.32	0.35	0.32	0.33
4	0.32	0.29	0.29	0.30
5	0.33	0.29	0.32	0.31
6	0.32	0.32	0.36	0.33
7	0.31	0.37	0.29	0.32
8	0.40	-	0.34	0.37
9	0.34	0.34	0.38	0.35
10	0.37	0.32	0.36	0.35
11	0.35	0.34	0.36	0.35
Avg	0.33	0.32	0.33	0.33

* Columns sampled at 25-cm intervals beginning at surface.

Table 7. Net N removal from soil columns continuously flooded for 165 days

Column	N removal
	mg
1	269.8
2	448.2
3	300.2
Avg	339.4

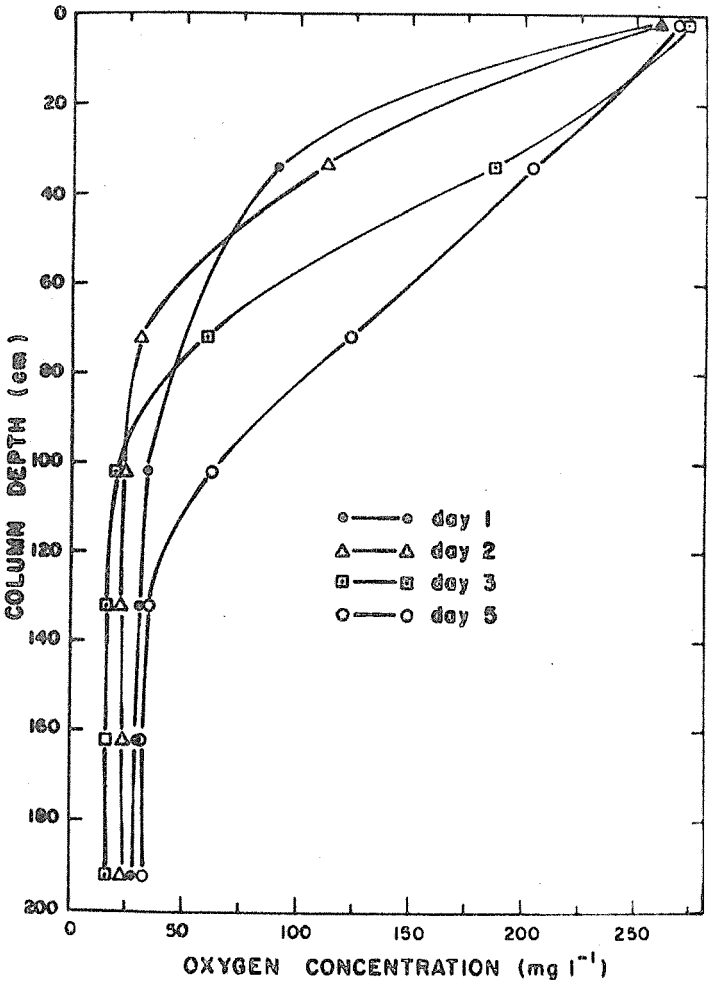

Figure 1. Oxygen concentration at different depths in a soil column during a 5-day dry period following 2 days of flooding. (Data from 2 columns were averaged.)

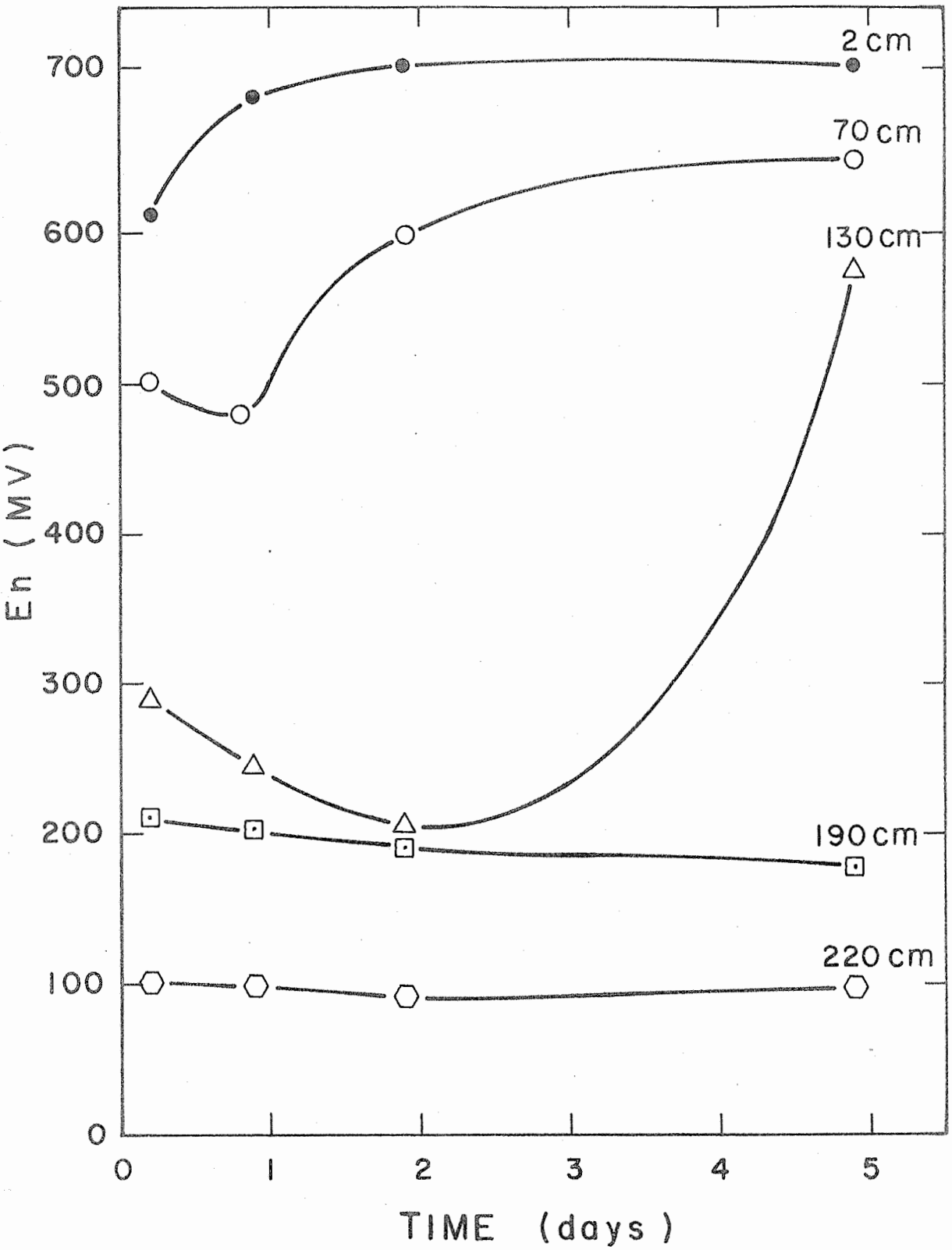

Figure 2. The oxidation-reduction potential at various depths in a soil column during a 5-day dry period following 2 days of flooding. (Data from 2 columns were averaged.)

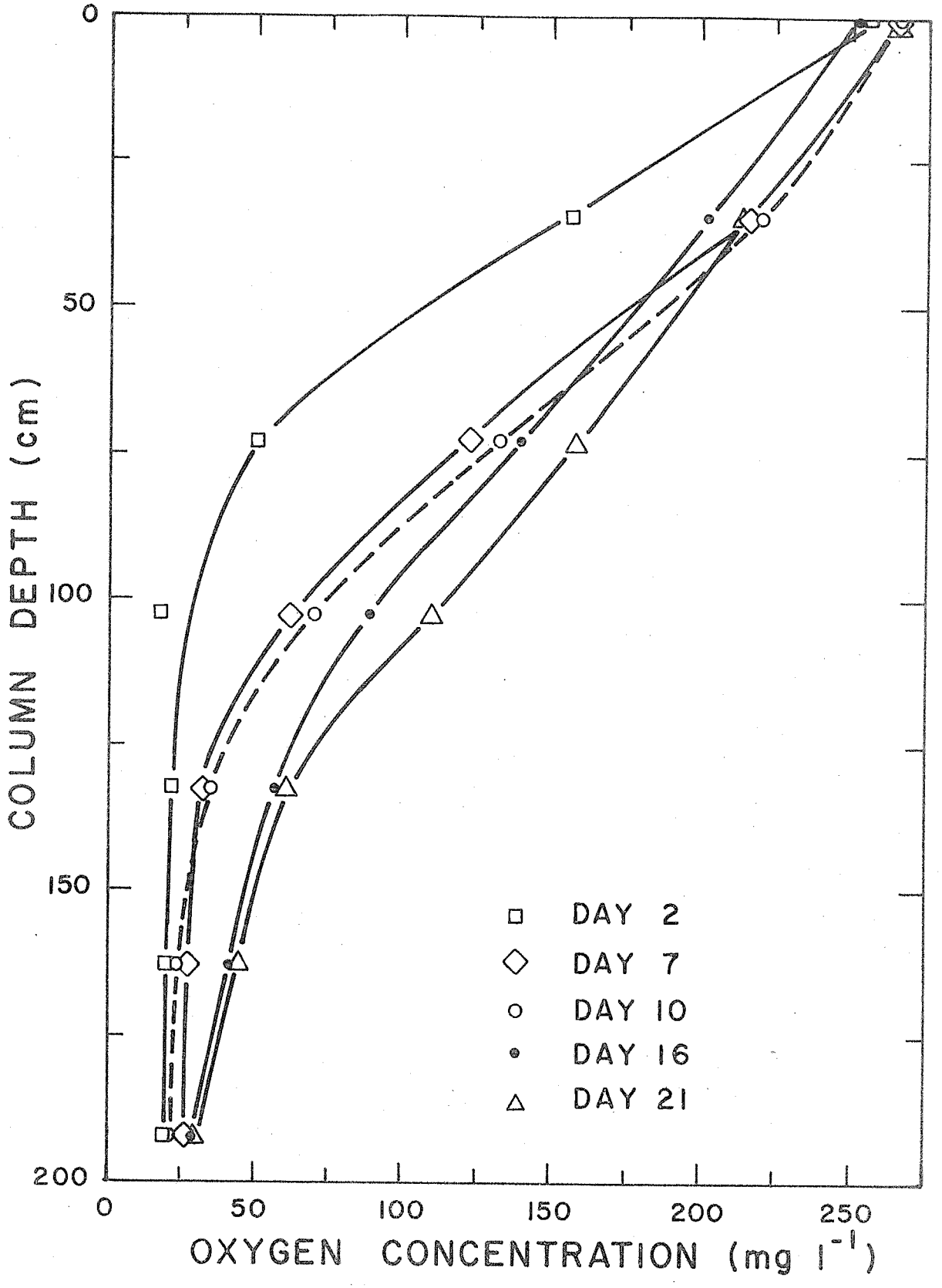

Figure 3. Oxygen concentration at different depths in a soil column during a 21-day dry period following 2 days of flooding. (Data from 2 columns were averaged.)

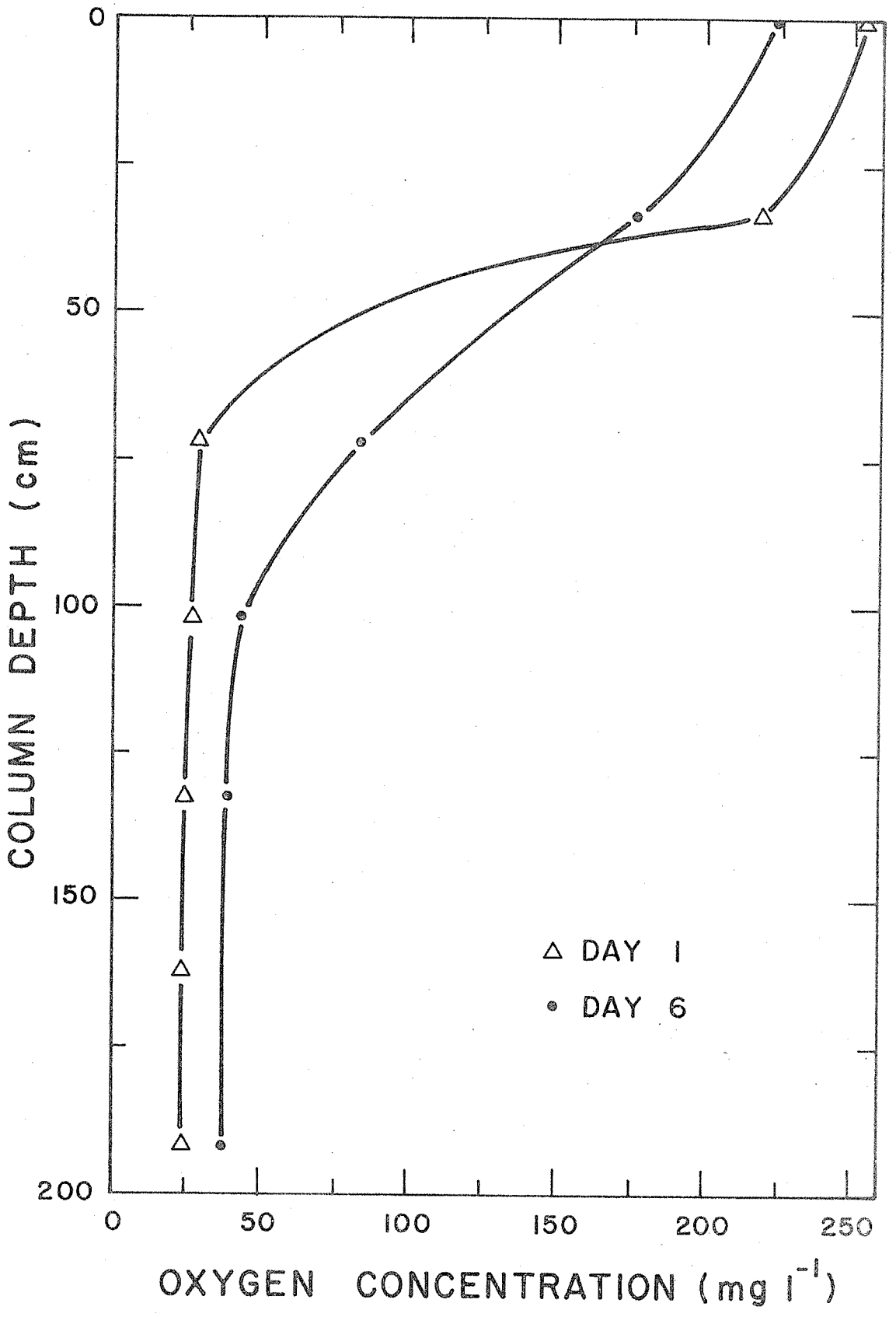

Figure 4. Oxygen concentration at different depths in a soil column closed at the top except for a pinhole during the drainage period.

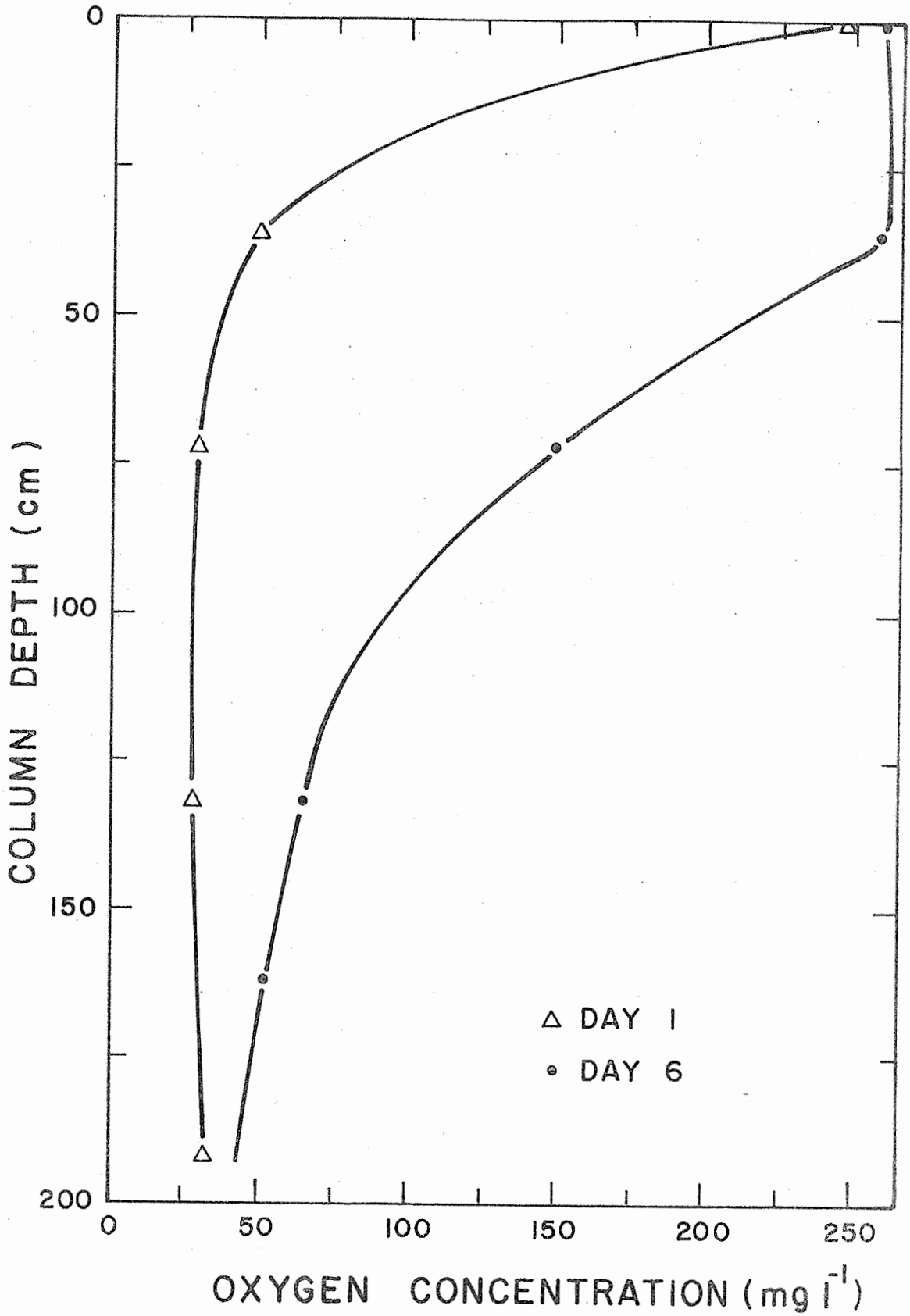

Figure 5. Oxygen concentration at different depths in a soil column when air was pumped through during the drainage period.

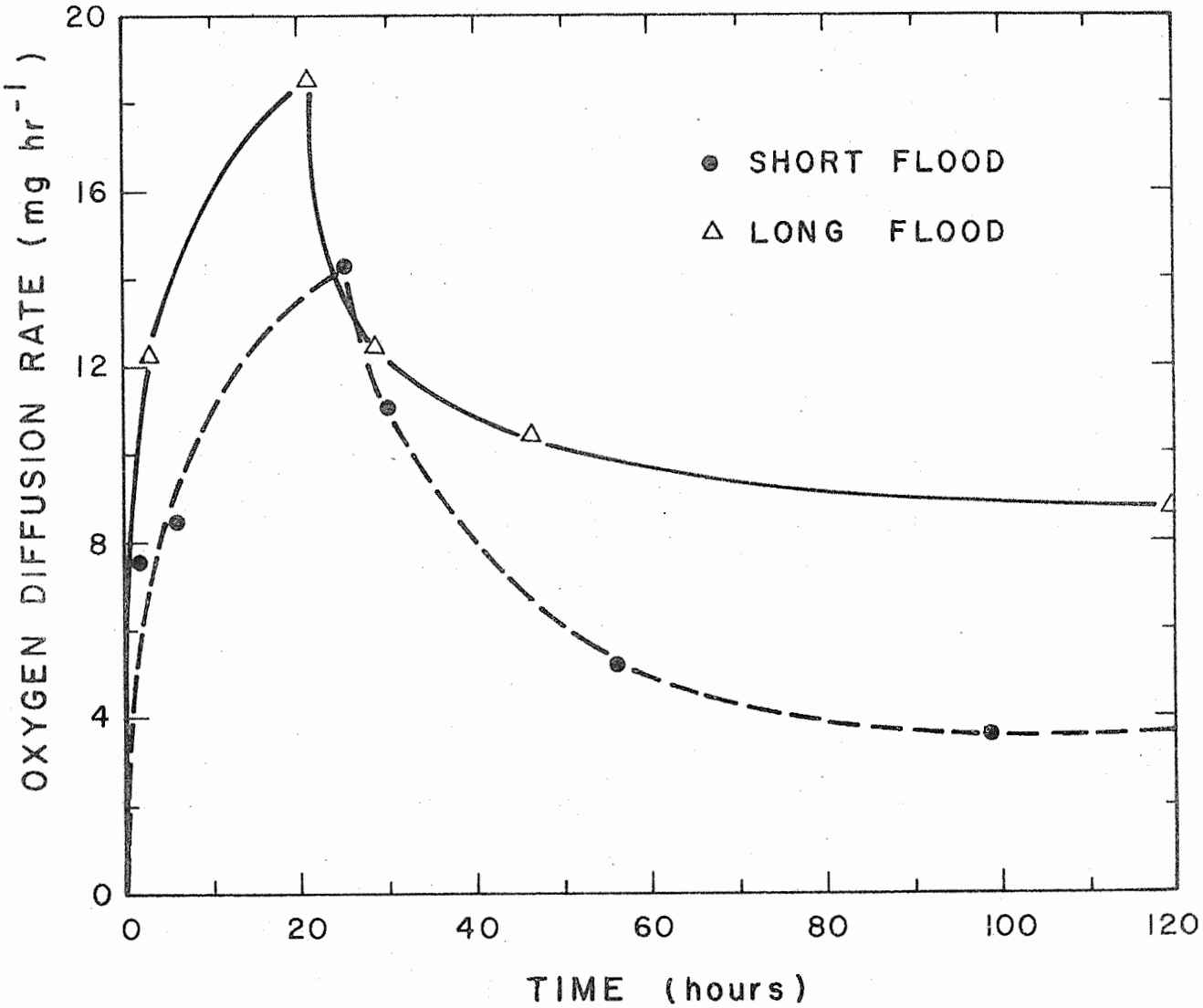

Figure 6. The rate of oxygen diffusion into soil columns during 5-day dry periods following 2- and 16-day flooding periods.

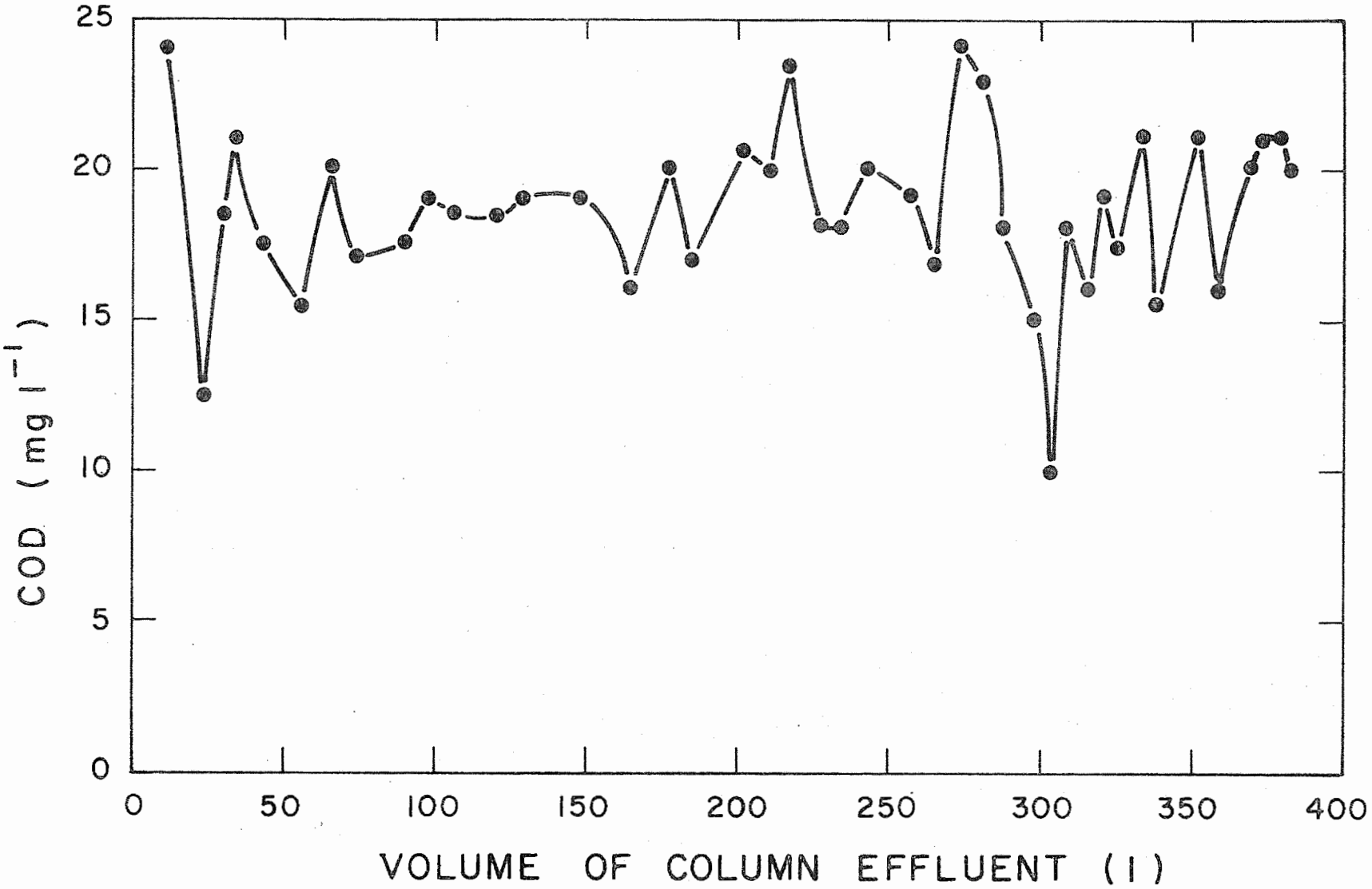

Figure 7. The COD of water from soil columns flooded with sewage water continuously for 120 days. (Data from 2 columns were averaged. COD of sewage water averaged 50 mg/l.)

TITLE: CHARACTERIZATION OF THE SOIL MICROFLORA AND BIOLOGICAL PROCESSES OCCURRING IN SOIL USED FOR WASTE WATER RENOVATION.

CRIS WORK UNIT: SWC-012-gG-1 CODE NO.: Ariz.-WCL-70-2

INTRODUCTION:

Laboratory research has been initiated to determine the effects of microbial activity on the performance and management of spreading basins for reuse and renovation of secondary sewage effluent by means of ground-water recharge. The first objective was to characterize the aerobic and anaerobic microbial population in the soil profile of sewage spreading basins and laboratory soil columns. Secondly, microbial activity and biological processes related to removal of excess nutrients, i.e., nitrogen, phosphorus, carbon and BOD, from sewage water with sewage spreading basins will be determined. Lastly, the influence of vegetation, chemical treatments and selected management practices on the biological processes, i. e., nitrification and denitrification, will be evaluated. The results obtained will aid in the formulation of management practices which will yield the optimum combination of quality and quantity of renovated water that can be used for unrestricted irrigation, recreation, and other purposes.

PROCEDURE:

The influence of microbial activity and biological processes throughout the soil profile related to removal of nitrogen will be studied in detail in sewage spreading basins and laboratory soil columns. Measurements of microbial activity of sewage basins and column soils will include Warburg respiration studies in aerobic and anaerobic atmospheres and ATP and enzyme activity measurements. Numbers of microbial populations in aerobic and anaerobic environments will be determined by standard soil dilution techniques. Existing concepts and methods will be evaluated and modified as necessary to meet experimental requirements; and new concepts, research techniques, devices, and methods will be developed when necessary.

RESULTS AND DISCUSSION:

Laboratory facilities for studying soil microorganisms and biological processes have been established. Experiments for soil column studies have been designed and are being constructed. Concurrent field studies will also be initiated. Only preliminary data on microbial numbers of soil columns flooded for 165 days with secondary sewage effluent has been collected. This data will be incorporated into the annual report of cooperating personnel, WCL 68-3.

PERSONNEL: R. G. Gilbert, J. C. Lance, Herman Bouwer, R. C. Rice, F. D. Whisler, and E. Escarcega.

CURRENT TERMINATION DATE: October 1975.

TITLE: SOIL TREATMENT TO REDUCE INFILTRATION AND INCREASE PRECIPITATION RUNOFF

CRIS WORK UNIT: SWC-018-gG-2 CODE NO.: Ariz.-WCL 60-7

INTRODUCTION:

Measurements of rainfall and runoff were continued on the large watersheds at the Monument Tank testing site, on plots at the Granite Reef testing site, and at the Seneca catchment. Laboratory studies were concerned with evaluation of low-cost soil stabilizer, water repellent treatments. Treatments which were satisfactory in the Laboratory tests were placed on small test plots at Granite Reef to evaluate weathering characteristics.

PART I. GRANITE REEF TESTING SITE

The 30 mil non-reinforced butyl linings in the water storage pits for the three watersheds have shown increasing signs of deterioration in recent years. The butyl material, installed in December 1963, began developing small holes, particularly on the upper edges of the bank where the sheeting was under maximum tension. The tear resistance around the holes was very low, indicating a deterioration of material. In April 1970 the linings were replaced. The storage area for W-1 was lined with new 32 mil non-reinforced butyl sheeting, and the storage area for W-2 was lined with a 20 mil modified polyethylene sheeting. The storage area for W-3 was lined with an asphalt-fiberglass material. This lining is discussed further in Annual Report section titled "Fabricated-In-Place, Reinforced Reservoir Linings," WCL 68-2.

A total of 173.4 mm of rainfall was measured in 18 separate storms. Over 30% of this precipitation occurred in one storm on 5-6 September 1970, when 63.5 mm of rain was collected in a 14 hour period. Following are the results of the rainfall-runoff measurements from the different storms for each plot, compared to the standard U.S. Weather Bureau raingage.

Paved or Covered Plots. The treatments applied to the plots are listed in Table 1 and the runoff results presented in Table 2.

Runoff from the three plots covered with thin films, L-1, (30 mil chlorinated polyethylene), L-4 (15 mil butyl) and L-7 (1 mil aluminum foil) averaged 98.2%, 90.5%, and 84.1% for the year. These runoff results are slightly higher than were measured in 1969. The physical appearance of the aluminum foil and the chlorinated polyethylene has not changed in the past year. The 15 mil butyl shows severe deterioration and has developed several small tears.

The two-phase asphalt treatments on plots L-5 and L-6 averaged 94.0% and 96.7%, respectively, for the year. Weathering of the asphalt had allowed numerous small pock marks and cracks to develop in the pavements. On 26 February 1970, water equivalent to a 5 mm rain was sprinkled on the plots and the runoff measured. Loss of water through cracks or retained on the plots was 0.55 mm on L-5 and 0.38 mm on L-6. On 22 April 1970 both plots were given a seal coat of modified SSKH asphalt emulsion to seal the cracks and smooth the pavement surface. Prior to treatment, L-5 averaged 85.2% runoff and L-6 averaged 93.9% runoff from 77.6 mm of rain. After application of the seal coat, L-5 averaged 98.0% and L-6 averaged 98.9% runoff from 95.8 mm of rain. These results show the importance of a periodic maintenance program for a high level of efficiency from asphalt pavement catchments.

The vinyl-coated asphalt-fiberglass plot A-1 averaged 94% runoff. This treatment is very smooth and should yield 100% rainfall runoff. Plot A-2, standard gravel roof covering, averaged 77.3% runoff. The plot continues to lose approximately 2 mm of rainfall runoff per storm by retention in the gravel layer and evaporation into the atmosphere. The concrete plot A-5 averaged 75.4% runoff for the year. The concrete slab retains some water in the porous surface, but it is believed the majority of the loss occurs through lateral cracks in the plot. Attempts to seal the cracks in January 1970 with an asphaltic crack sealer were only partially successful. Runoff continued to decline during the year.

On 19 March 1970, plot A-4 was covered with a 2 mil thick, tan acrylic film bonded to the soil with asphalt emulsions. The film was reported to have excellent weathering characteristics. The treatment failed in less than one month without collecting any water. Subsequent examination of the film showed that tear and puncture resistance was too low to prevent mechanical or wind damage.

Bare Soil Plots: The bare soil plots are all treatments where the soil is not completely covered or paved. The treatments are listed in Table 3 and the runoff results presented in Table 4.

Rainfall runoff from the two uncleared watersheds W-1 and W-2 averaged 10.1% and 6.9%, respectively, for the year. Watershed W-3, hand cleared of brush in 1963, yielded 15.3% runoff. Approximately 50% of the water collected from these areas occurred during the 5 September 1970 storm. The significance of the differences in the total runoff from the three areas is difficult to evaluate with the limited number of storms during the year which produced runoff. Generally, storms of relatively high intensities and rainfall quantities in excess of 8 mm are required before runoff occurs.

The two smoothed untreated plots, L-2 and A-3, averaged 20.6% and 29.2% runoff, respectively. The runoff from these plots is still significantly higher than the runoff from the three watersheds. Runoff from the smoothed plot L-3, treated with a silicone water repellent, averaged 73.7% for the year, a decrease of approximately 15% since retreatment. These runoff values are similar to the runoff measured after the original treatment in 1965. A gravel layer has developed on this plot which may be reducing runoff by retaining water similar to the gravel covered plot A-2.

PART II. MONUMENT TANK TESTING SITE

Total rainfall the past year was 208 mm for the period 6 January 1970 through 16 December 1970. Preliminary analysis of monthly rainfall totals from the raingage network shows a random variation of 10 to 20% in areal distribution over the 30 hectare test site. The

precipitation variation is accounted for in the analysis of the runoff from the watersheds by using the Thiessen polygon method of weighted averages. Analysis of rainfall by individual storms has not been completed.

A preliminary analysis has been completed by individual storm event of all the runoff data collected from each of the watersheds. The total rainfall and runoff results from the areas for the period 13 November 1967 through 16 December 1970 is presented in Table 5(a). The results are slightly misleading because the majority of the runoff occurred during one 30 day period, 11 December 1967 through 10 January 1968. During this 30 day interval, runoff was 11.9 mm, 82.5 mm. 113.7 mm, and 20.4 mm from watershed 1 through 4, respectively. The total measured precipitation was approximately 100 mm and occurred as both rain and snow. It is believed that raingages did not accurately measure the snowfall. Table 5(b) presents the results of rainfall and runoff with the precipitation and runoff data omitted for the period of 11 December 1967 through 10 January 1968. These results show the runoff from the four watersheds is much lower than was originally expected. Runoff from areas 1 and 4 with the natural channels was less than 1% of the total precipitation. Areas 2 and 3 with the lined collection ditches averaged 3.5 to 4.5% runoff.

A comparison of the soil types at the Monument Tank test site and the Granite Reef test site is presented in Table 6. This comparison shows the Monument Tank soils are finer textured than Granite Reef soil and might be expected to have larger runoff, especially on watersheds 2 and 3 which have the lined channels. The reasons for the low runoff are not known, but factors such as surface roughness and distance of overland flow are believed to be of major importance. Studies to better define the effect of these variables will be initiated.

PART III. OPERATIONAL FIELD CATCHMENTS

With the exception of the Seneca catchment, all operational field units have been turned over to the respective cooperating agencies. The Metate catchment was the only unit visited the past year and was in excellent condition. No reports were received on the performance of any of the other operational units.

Total precipitation at the Seneca catchment was 522.7 mm for the period 1 December 1969 through 17 December 1970. Preliminary analysis has been completed by individual storms of all the runoff data collected. The results show the runoff from the catchment has averaged less than 2% since installation in July 1967. These results include runoff when the area was treated. (See previous Annual Reports.)

Comparison of the soil type with Granite Reef, Table 6, would suggest runoff similar to the two untreated Granite Reef watersheds. The Seneca plot is on a uniform 8% natural slope. Plant growth on the plot consists of grasses growing in small clumps. It was originally thought that rainfall runoff, occurring over a period of many years, had eroded small rills or microchannels to produce a surface drainage system for the area. Debris from grass killed during 1969 showed that this was not true. Following rainstorms in 1970, grass debris collected on the lower edges of small basins and depressions to provide a clear outline of the depressions. The entire area was covered with these basins that obviously retain most of the rain that falls. Creation of a waterproof soil surface cannot cause high rainfall runoff unless the soil surface is modified to reduce the present high retention.

PART IV. SOIL STABILIZATION

Soil stabilizing materials examined during 1970 are listed in Table 7 with resin type, where known, plus particle size, particle charge, and contact angle.

Particle size was measured with a calibrated grid on a microscope. All materials except 4, 5, 15 and 16 had particles of 4 microns or less diameter. Material 4 was an old sample and new material may have smaller particles. Materials 5, 15 and 16 did not penetrate undisturbed soil surfaces satisfactorily, indicating that particle size less than 12 microns is required.

Particle charge was determined by applying 6 volts, DC current to two 7 mm diameter brass rod electrodes spaced 15 mm apart and noting which electrode became coated. Cationic or positively charged particles, for example, migrate to and coat the negatively charged electrode. Only two materials, 2 and 5, were cationic. Although material 5 did not infiltrate satisfactorily, material 2 did. Under the test conditions, particle charge was not a factor.

Contact angle between a water drop and a soil surface treated with test materials was measured by the large drop method described in the 1969 Annual Report. Soils were treated with 1.7 kg m^{-2} distilled water containing 2% dispersed or dissolved test resin. All treatments except material 5 also contained 3% sodium methyl siliconate. The lowest contact angle measured on smoothed Granite Reef soil in petri dishes was 92 degrees for material 7. Contact angle increases, up to a point, with surface roughness. Field tests of material 7 applied to relatively rough, natural Granite Reef soil showed that it was sufficiently hydrophobic to prevent water infiltration.

Material tests on soil in petri dishes were used only for preliminary screening purposes. Attempts to develop trays of soil representative of field conditions were not successful and so procedures were devised for evaluating 1 m^2 areas of natural, undisturbed soil treated with test materials. The areas were outlined with paint sprayed around a 1 m^2 mask and materials were applied with a small sprinkling can. The dripper used on petri dishes was modified to make it portable and was used to evaluate erosion resistance of treated areas. One thousand drops, 5 mm

diameter, falling from a 2 meter height were applied in a period of 5 minutes, and the number of drops required to initiate erosion was recorded.

Materials were applied at a rate of 0.64 liters m^{-2} in water dispersions or solutions containing 2% resin and 3% sodium methyl siliconate. Application rate and SMS concentration were based on previous field and laboratory investigations. Numerous small plot trials showed that concentrations exceeding 2% resin frequently did not adequately penetrate field soil surfaces. Materials must soak in rapidly to avoid runoff and should stabilize the soil to a depth of at least 5 mm.

Performance of 10 materials applied to 1 m^2 plots at Granite Reef on 14 July 1970 is summarized in Table 8. Dripper tests were made on 31 July and 21 October 1970. Eight of the materials were in good condition after 3 months exposure. Additional materials will be applied to similar plots. The major question to be answered is the ability of test materials to resist degradation by photo-oxidations, chemical reaction with the soil, and erosion by natural rainfall.

SUMMARY AND CONCLUSIONS:

A total of 174 mm rainfall was measured in 18 separate storms at the Granite Reef test site. Over 30% of this precipitation occurred in one storm on 5-6 September 1970, when 64 mm of rain fell in a 14 hour period. Runoff of precipitation from 200 m^2 covered plots averaged: chlorinated polyethylene - 98%, butyl - 90%, and aluminum foil - 84%. The 9-year old, 15 mil butyl rubber sheeting is now in poor condition and is developing small holes and tears. Small cracks and pock marks had developed in a 3-year old seal coat on two asphalt pavement plots, reducing rainfall runoff to about 85-94%. A new seal coat increased runoff to 98-99%. Runoff from other covered and paved catchments was about the same as in 1969. Only one new material, 2-mil acrylic film

bonded to the soil with asphalt, was installed. This failed in less than one month because of low puncture and tear resistance.

Runoff from two 500 m^2 uncleared watersheds at Granite Reef averaged only 7-10%. A similar area, cleared of brush in 1963, averaged 15%. Approximately half the runoff from these three areas occurred during one storm. A smoothed, compacted soil catchment averaged 29%. The smoothed soil plot treated with a silicone water repellent averaged 74% for the year. As previously reported, water is retained on this catchment by a gravel layer resulting from erosion of the finer soil fractions.

Preliminary analysis of rainfall and runoff data for the Seneca catchment has been completed. Runoff from this 2,000 m^2, uncleared area with a 10% slope has averaged less than 2% of the 500 mm average annual rainfall since installation in July 1967. Debris from grass killed in 1969 collected on the lower edges of small basins or depressions following rainstorms during 1970. The debris collections showed that the entire area is covered with small depressions that retain most of the precipitation. Creation of a waterproof soil surface cannot cause high precipitation runoff unless the surface is modified to reduce the present retention.

Total precipitation measured at the Monument Tank test site during 1970 was 208 mm. Monthly precipitation totals from the raingage network showed a random variation of 10-20% in areal distribution over the 30 hectare test site. A preliminary analysis of runoff for individual storm events has been completed for all four watersheds. Totals for the period 13 November 1967 through 16 December 1970 show precipitation of 977 to 1009 mm, and runoff from the watersheds as follows: 1 - 1.9%, 2 - 11.5%, 3 - 15.1%, and 4 - 2.1%. Watersheds 2 and 3 have lined collection ditches so that there are only minor channel losses. During one 30 day period, 11 December 1967 through 10 January 1968, runoff from watershed 3 was 114 mm while measured precipitation was only 100 mm. Most of

this precipitation occurred as snow which was not accurately measured. If this period is deleted from the record, precipitation runoff from the watersheds was: 1 - 0.7%, 2 - 3.4%, 3 - 4.3%, and 4 - < 0.1%. Runoff from watersheds 2 and 3, with essentially no channel losses, was much less than had been expected. Runoff from 500 m^2 uncleared plots at Granite Reef with coarser soils, flatter slopes and less precipitation averages 10-20%. The major difference is length of slope and surface roughness. Studies are planned to better define the effect of these two factors on precipitation runoff.

Nineteen soil stabilizing materials were examined during 1970 and were characterized by resin type, particle size, particle charge, and soil-water contact angle. Correlation with field trials on small plots of undisturbed, natural Granite Reef soil indicated that particle size must be less than 12 microns and should be less than 5 microns for adequate penetration into the soil. Both cationic and anionic materials were satisfactory, as were contact angles exceeding 92 degrees. Ten materials were applied to small plots at Granite Reef and erosion resistance was measured by applying 1,000 water drops, 5 mm in diameter, falling from a height of 2 meters. Eight of the materials showed no erosion after 6 months exposure.

PERSONNEL: L. E. Myers, G. W. Frasier and K. R. Cooley.

CURRENT TERMINATION DATE: December 1970.

Table 1. Treatments on paved or covered plots at Granite Reef.

Plot	Treatment Date	Treatment
L-1	8 Aug 1967	Basecoat. MC-250 at 1.5 kg asphalt m^{-2}
	22 Aug 1967	Topcoat. RSK asphalt emulsion at 0.7 kg asphalt M^{-2}
	20 May 1968	Top Sheeting. 30-mil chlorinated black polyethylene
L-4	30 Nov 1961	Butyl Rubber Sheeting. 15-mil
L-5	18 Sep 1962	Basecoat. S-1 at 1.04 kg asphalt m^{-2}
	16 Mar 1966	Topcoat. RSK asphalt emulsion at 0.6 kg asphalt m^{-2}
	22 Apr 1970	Sealcoat. Modified SSKH asphalt emulsion at 0.6 kg asphalt m^{-2}
L-6	19 Apr 1963	Basecoat. RC-special at 1.5 kg asphalt m^{-2}
	8 May 1963	Topcoat South Half. SS-2 special asphalt emulsion at 0.65 kg asphalt m^{-2} with 3% butyl latex
	9 Jul 1963	Topcoat North Half. S-1 at 0.5 kg asphalt m^{-2} with 3% butyl latex
	22 Apr 1970	Sealcoat. Modified SSKH asphalt emulsion at 0.6 kg asphalt m^{-2}
L-7	3 Aug 1967	Basecoat. MC-250 at 1.5 kg asphalt m^{-2}
	22 Aug 1967	Top Sheeting. 1-mil aluminum foil bonded with RSK asphalt emulsion at 0.7 kg asphalt m^{-2}
A-1	3 Aug 1967	Basecoat. MC-250 at 1.5 kg asphalt m^{-2}
	22 Aug 1967	Top Sheeting. 3/4 oz chopped fiberglass matting bonded with RSK asphalt emulsion at 1.4 kg asphalt m^{-2}
	Jan 1968	Top Spray. Vinyl aluminum coating at 0.1 gal yd^{-2}

Table 1. (continued) Treatments on paved or covered plots at Granite Reef.

Plot	Treatment Date	Treatment
A-2	3 Aug 1967	Basecoat. MC-250 at 1.5 kg asphalt m^{-2}
	12 Sep 1967	Top Sheeting. Standard rag felt-rock roofing treatment
A-5	Sep 1968	Concrete slab

Table 2. Rainfall and runoff for paved or covered plots at Granite Reef.

Date	Total Rainfall	L-1 Runoff		L-4 Runoff		L-5 Runoff		L-6 Runoff	
1970	mm	mm	%	mm	%	mm	%	mm	%
17 Jan	1.5	1.8	120.0	1.5	100.0	1.3	86.7	1.4	93.3
10/11 Feb	9.5	9.2	96.8	8.5	89.5	7.7	81.1	8.6	90.5
1/2 Mar	16.8	16.0	95.2	14.9	88.7	13.8	82.1	14.8	88.1
2/3 Mar	22.1	21.4	96.8	20.0	90.5	19.4	87.8	21.4	96.8
5 Mar	15.7	15.3	97.5	14.5	92.4	14.6	93.0	16.6	105.7
10 Mar	8.5	8.0	94.1	7.4	87.1	7.0	82.4	7.6	89.4
17 Apr	3.5	2.9	82.9	2.8	80.0	2.3	65.7	2.5	71.4
4 Jul	3.3	3.5	106.1	3.4	103.0	3.4 2/	103.4	3.4 2/	103.4
18 Jul	1.8	2.0	111.1	2.3	127.8	1.9	105.6	2.4	133.3
21 Jul	1.6	1.2	75.0	1.0	62.5	1.1	68.8	.7	43.8
11 Aug	9.9	9.6	97.0	9.6	97.0	9.7	98.0	10.4	105.1
5/6 Sep	63.5	63.5 1/	100.0	59.7	94.0	63.5 1/	100.0	63.5 1/	100.0
12 Sep	2.5	2.7	108.0	1.9	76.0	2.9	116.0	2.2	88.0
3 Oct	4.8	5.3	110.4	3.9	81.3	4.4	91.7	4.5	93.8
30 Nov	1.8	1.9	105.6	1.2	66.7	1.6	88.9	1.6	88.7
18 Dec	.8	.6	75.0	.4	50.0	.5	62.5	.5	62.5
20 Dec	2.8	2.5	89.3	1.8	64.3	2.3	82.1	2.6	92.9
21 Dec	3.0	2.8	93.3	2.1	70.0	2.6	86.7	3.0	100.0
Total	173.4	170.2	98.2	156.9	90.5	160.0	94.0	167.7	96.7

1/ Storage overflowed, runoff estimated at 100%.
2/ New sealcoats applied 22 Apr 1970.

Table 2. (continued) Rainfall and runoff for paved or covered plots at Granite Reef.

Date	Total Rainfall	L-7 Runoff		A-1 Runoff		A-2 Runoff		A-5 Runoff	
1970	mm	mm	%	mm	%	mm	%	mm	%
17 Jan	1.5	1.4	93.3	1.4	93.3	.6	40.0	.9	60.0
10/11 Feb	9.5	7.4	77.9	7.9	83.2	7.0	73.7	6.7	70.5
1/2 Mar	16.8	13.4	79.8	15.7	93.5	12.8	76.2	13.0	77.4
2/3 Mar	22.1	19.4	87.8	21.5	97.3	19.9	90.0	21.7	98.2
5 Mar	15.7	13.6	86.6	14.9	94.9	14.4	91.7	16.5	105.1
10 Mar	8.5	6.6	77.6	8.0	94.1	6.8	80.0	6.6	77.6
17 Apr	3.5	2.0	57.1	3.1	88.6	1.6	45.7	2.6	74.3
4 Jul	3.3	2.9	87.9	3.4	103.0	1.6	48.5	1.4	42.4
18 Jul	1.8	2.1	116.7	1.7	94.4	.6	33.3	0	0
21 Jul	1.6	.7	43.8	.9	56.3	.3	18.8	.7	43.8
11 Aug	9.9	9.1	91.9	9.6	97.0	8.3	83.8	6.8	68.7
5/6 Sep	63.5	56.1	88.3	58.4	92.0	54.0	85.0	48.2	75.9
12 Sep	2.5	1.8	72.0	2.5	100.0	1.1	44.0	1.0	40.0
3 Oct	4.8	4.0	83.3	4.4	91.7	2.3	47.9	2.4	50.0
30 Nov	1.8	1.1	61.1	1.4	77.8	.1	5.6	.7	38.9
18 Dec	.8	.2	25.0	.4	50.0	0	0	0	0
20 Dec	2.8	2.1	75.0	2.4	85.7	.9	32.1	0	0
21 Dec	3.0	1.9	63.3	2.4	80.0	1.7	56.7	1.5 3/	50.0
Total	173.4	145.8	84.1	160.0	94.0	134.0	77.3	130.7	75.4

3/ Missing data, runoff estimated at 50%.

Table 3. Treatments of bare soil plots at Granite Reef.

Plot	Treatment Date	Treatment
L-2	30 Nov 1961	Smoothed soil, 14.14 m × 14.14 m plot
L-3	4 Aug 1965	Smoothed soil, 14.14 m × 14.14 m plot treated with R-9 at 0.057 kg m^{-2}
	6 Nov 1969	Retreated with R-9 at 0.04 kg m^{-2}
A-3	1 Aug 1967	Smoothed soil, 6 m × 30 m plot
W-1	1 Dec 1963	Uncleared watershed
W-2	1 Dec 1963	Uncleared watershed
W-3	1 Dec 1963	Cleared watershed
R-2	1 Mar 1965	Ridge and furrow - 10% side slope
R-4	13 May 1966	Ridge and furrow - 10% side slope treated with 44.9 g m^{-2} sodium carbonate
	3 Nov 1970	Treated with 3% silicone water repellent and 2% soil stabilizer-1.2 liters of solution m^{-2}

Table 4. Rainfall and runoff for bare soil plots at Granite Reef.

Date	Total Rainfall	L-2 Runoff		L-3 Runoff		A-3 Runoff		W-1 Runoff	
1970	mm	mm	%	mm	%	mm	%	mm	%
17 Jan	1.5	0	0	.6	40.0	0	0	0	0
10/11 Feb	9.5	0	0	7.8	82.1	.7	7.4	0	0
1/2 Mar	16.8	.5	3.0	13.6	81.0	4.2	25.0	.3	1.8
2/3 Mar	22.1	4.2	19.0	19.8	89.6	7.3	33.0	2.6	11.8
5 Mar	15.7	5.5	35.0	14.5	92.4	8.2	52.2	2.1	13.4
10 Mar	8.5	.4	4.7	7.0	82.4	1.9	22.4	.2	2.4
17 Apr	3.5	0	0	1.3	37.1	0	0	0	0
4 Jul	3.3	0	0	1.6	48.5	.7	21.2	0	0
18 Jul	1.8	0	0	0	0	0	0	0	0
21 Jul	1.6	0	0	0	0	0	0	0	0
11 Aug	9.9	4.2	42.4	6.3	63.6	5.0	50.5	1.9	19.2
5/6 Sep	63.5	21.0	33.1	51.1	80.5	22.3	35.1	10.5	16.5
12 Sep	2.5	0	0	1.2	48.0	0	0	0	0
3 Oct	4.8	0	0	2.5	52.1	.3	6.3	0	0
30 Nov	1.8	0	0	0	0	0	0	0	0
18 Dec	.8	0	0	0	0	0	0	0	0
20 Dec	2.8	0	0	0	0	0	0	0	0
21 Dec	3.0	0	0	.5	16.7	0	0	0	0
Total	173.4	35.8	20.6	127.8	73.7	50.6	29.2	17.6	10.1

Table 4. (continued) Rainfall and runoff for bare soil plots at Granite Reef.

Date	Total Rainfall	W-2 Runoff		W-3 Runoff		R-2 Runoff		R-4 Runoff	
1970	mm	mm	%	mm	%	mm	%	mm	%
17 Jan	1.5	0	0	0	0	0	0	0	0
10/11 Feb	9.5	0	0	.3	3.2	.4	4.2	0	0
1/2 Mar	16.8	.5	3.0	1.3	7.7	3.6	21.4	2.6	15.5
2/3 Mar	22.1	1.1	5.0	3.5	15.8	7.0	31.7	5.7	25.8
5 Mar	15.7	1.6	10.2	4.0	25.5	6.9	43.9	6.0	38.2
10 Mar	8.5	0	0	.6	7.1	1.3	15.3	.8	9.4
17 Apr	3.5	0	0	0	0	0	0	0	0
4 Jul	3.3	0	0	0	0	.8	24.2	.4	12.1
18 Jul	1.8	0	0	0	0	0	0	0	0
21 Jul	1.6	0	0	0	0	0	0	0	0
11 Aug	9.9	2.9	29.3	1.1	11.1	4.5	45.5	4.0	40.4
5/6 Sep	63.5	5.9	9.3	15.7	24.7	23.7	37.3	21.0	33.1
12 Sep	2.5	0	0	0	0	0	0	0	0
3 Oct	4.8	0	0	0	0	.7	14.6	.3	6.3
30 Nov	1.8	0	0	0	0	0	0	0	0
18 Dec	.8	0	0	0	0	0	0	0 1/	0
20 Dec	2.8	0	0	0	0	0	0	2.0	70.0
21 Dec	3.0	0	0	0	0	0	0	2.1	70.0
Total	173.4	12.0	6.9	26.5	15.3	48.9	28.2	44.9	25.9

1/ Retreated 3 Nov 1970.

TABLE 5. Total rainfall and runoff results from the four watersheds at the Monument Tank testing site for the period 13 November 1967 through 16 December 1970.

(a)

Watershed No.	Total Precipitation	Total Runoff	
	(mm)	(mm)	(%)
1	1001.0	18.6	1.9
2	977.1	112.2	11.5
3	1009.0	152.5	15.1
4	1005.5	20.6	2.1

(b)

Watershed No.	Total Precipitation 1/	Total Runoff 1/	
	(mm)	(mm)	(%)
1	899.8	6.7	0.7
2	876.2	29.7	3.4
3	910.6	38.8	4.3
4	907.1	.3	<.1

1/ Data of period 11 December 1967 through 10 January 1968 omitted.

Table 6. Physical analysis of soils from Monument Tank testing site, Granite Reef testing site and Seneca catchment.

Location	Sand	Silt	Clay	Soil Classification
	%	%	%	
Monument Tank Area 1	34	53	13	Loam
Monument Tank Area 2	35	36	29	Clay Loam
Monument Tank Area 3	49	38	13	Loam
Granite Reef	58	35	7	Sandy Loam
Seneca	56	33	11	Sandy Loam

Table 7. Description of soil stabilizing materials.

	Manufacturer	Material Designation	Resin Type	Particle Size	Particle Charge	Contact Angle
				microns		degrees
1.	National Starch	Resyn 2813	Vinyl acrylic	0.6-1.8	-	142
2.	National Starch	Resyn 1251	Vinyl acrylic	0.6-2.5	+	136
3.	Union Carbide	DCA-70	Polyvinyl acetate	0.6-3.7	-	136
4.	American Cyanamid	Aerospray Binder 52	Unknown	14-70	-	112
5.	Phillips	Petroset 55	Modified SBR	12	+	155
6.	Dow Chemical	Latex 305	SBR	0.8-2.5	-	124
7.	Dow Chemical	Latex 460	SBR	0.6-1.8	-	92
8.	Dow Chemical	Latex 620	SBR	0.6-1.8	-	126
9.	Dow Chemical	Latex 636	SBR	0.8-1.0	-	119
10.	Dow Chemical	Latex 880	SBR	1.2-2.5	-	126
11.	Dow Corning	4-3543	Acrylic-silicone	0.2-5.0	0	100
12.	Dow Corning	4-0219	Silicone	0.6-2.5	-	140
13.	Morton Chemical	Serfene 400	Acrylic	0.6-2.5	-	115
14.	Morton Chemical	Latex MC 561-6	Acrylic	0.6-2.5	-	109
15.	Hercules	Dresinate 1978	Rosin derived	2.5-12.5	-	135
16.	Hercules	Dresinate 60W80F	Rosin derived	2.5-12.5	0	100
17.	DuPont	Elvanol 72-60	Polyvinyl alcohol	Solution	0	141
18.	DuPont	Elvanol 46-22	Polyvinyl alcohol	Solution	0	145
19.	Soil Seal	Soil Seal	Unknown	1.0-4.0	-	130

Table 8. Erosion resistance of soil stabilizers applied 14 July 1970 to one square meter plots of undisturbed natural soil at Granite Reef.

	Material 1/	Erosion 2/	
		31 July 70	21 Oct 70
1.	2% 2813 + 3% SMS 3/	None	None
3.	2% DCA70 + 3% SMS	None	None
3.	2% DCA70 + 5% Mobilcer 46 4/	350 drops 5/	None 6/
7.	2% 460 + 3% SMS	None	None
8.	2% 620 + 3% SMS	None	1000 drops 5/
9.	2% 636 + 3% SMS	None	None
14.	2% MC561-6 + 3% SMS	None	None
16.	2% Dresinate 80F + 3% SMS	Immediate	Immediate
17.	2% 72-60 + 3% SMS	None	None
18.	2% 46-22 + 3% SMS	None	None

Notes: 1/ Application 0.64 liter fluid per square yard.

2/ After application of 1,000 drops, 5 mm diam. falling 2 meters.

3/ Sodium Methyl Siliconate water repellent

4/ Paraffin wax emulsion

5/ Erosion initiated after indicated number of drops.

6/ No longer water repellent.

TITLE: DISPERSION AND FLOCCULATION OF SOIL AND CLAY MATERIALS AS RELATED TO THE Na AND Ca STATUS OF THE AMBIENT SOLUTION

CRIS WORK UNIT: SWC-018-gG-2 CODE NO.: Ariz.-WCL-64-6

The importance of understanding the chemical nature of the soil solution for studying dispersion-flocculation behavior of soil colloids has been explained and demonstrated in the preceding annual reports for 1965-1969. Three aspects of the properties of the chemical constituents in solution were investigated and listed under Parts I to III. In Part I the solubility behavior of gypsum, which is extensively used in soil reclamation and management, is described from the standpoint of its solubility in various salts to ascertain the interactions of calcium with other anions. Also, the interaction of sodium with carbonates, continuing the work of the previous year, is reported in Part II and that of calcium with carbonate is presented in Part III.

PART I. CALCIUM COMPLEXING AND THE ENHANCED SOLUBILITY OF GYPSUM ($CaSO_4 \cdot 2H_2O$) IN CONCENTRATED SODIUM-SALT SOLUTIONS

INTRODUCTION:

Solubility product principles are used extensively to define solution equilibrium conditions of sparingly soluble calcium soil mineral constituents such as gypsum ($CaSO_4 \cdot 2H_2O$) at low salt concentrations (10, 17). However, at increasingly higher electrolyte concentrations (> 0.2M) that are associated with saline soils and groundwater, brine and sea water, the solubility prediction using standard computational procedures is unreliable. Presumably, this failure is caused by several interrelated factors including the inapplicability of the extended Debye-Hückel theory for estimating the activity coefficients of the ions, and the neglection of the increased interaction of Ca^{2+} and SO_4^{2-} with other dissolved constituents to form complexes.

The purpose of this study was to develop a reliable and practical method for predicting gypsum solubility in concentrated mixed-salt solutions and includes the measurement of gypsum solubility in $NaClO_4$, NaCl, $NaNO_3$, and NaOAc solutions and their mixtures and the establishment of the dissociation constant for $CaCl^+$, $CaNO_3^+$, and $CaOAc^+$ and other forms as required from the solubility behavior.

THEORY:

The solubility of a solid is usually increased when a noncommon ion salt is present in the saturated solution. This phenomenon is explained on the basis of the solubility product principle. Since the activity coefficients are decreased with increasing salt concentration, the dissolution of the solid must increase in order to maintain an unvarying ion-activity solubility product constant. If there is an interaction between the supposedly "neutral" electrolyte and the dissolved solid to give associated or complex forms, an increase in solid solubility over and above any ionic strength effect occurs.

This solubility enhancement of solids in "neutral" electrolytes can be advantageously adapted to estimate the associative properties of the cation or anion of the solid species with the added anion or cation. Thus, the association of Ca^{2+} with SO_4^{2-} to form $CaSO_4^o$ was determined from the solubility increase of $Ca(IO_3)_2$ in sulfate solution (3). Gypsum dissolves differently in different Na-salts at the same salt concentration (15), and this behavior can be used for measuring the interaction of Ca with a variety of anions and also for explaining one aspect of solubility enhancement.

Dissociation Constant Determination.-The apparent dissociation constant of $CaCl^+$, $CaNO_3^+$, and $CaOAc^+$ can be determined by studying $CaSO_4 \cdot 2H_2O$ in NaCl, $NaNO_3$, and NaOAc solutions, respectively. The mass and charge balance relationships using the $NaNO_3$ system as an example are as follows:

$$[NO_3]_T = [CaNO_3^+]? + [NO_3^-] + [NaNO_3^o]? \quad [1]$$

$$[Na]_T = [Na^+] + [NaSO_4^-] + [NaNO_3^o]? \quad [2]$$

$$[Ca]_T = [Ca^{2+}] + [CaSO_4^o] + [CaNO_3^+]? \quad [3]$$

$$2[Ca^{2+}] + [Na^+] + [CaNO_3^+]? = 2[SO_4^{2-}] + [NaSO_4^-] + [NO_3^-], \quad [4]$$

where the subscript T is the total concentration of the particular element. The presence of the $CaNO_3^+$ and particularly $NaNO_3^o$ as indicated by the question mark has not been clearly established before and will be discussed further with the experimentally determined gypsum solubility in the different Na-salts.

For the NaCl or the NaOAc solutions, appropriate substitutions for their respective complex $CaCl^+$, $CaOAc^+$, $NaOAc^o$ are made in equations [1] through [4]. Association of Ca^{2+} with NO_3^- and OAc^- has been reported previously (5, 11, 12), but either at temperatures other than 25 C, or at different ionic strengths. The associated forms $CaSO_4^o$ and $NaSO_4^-$ are well documented by several independent measurements (16, p. 235-236).

Subtracting equations [1] and [2] and adding 2 times equation [3] to equation [4] while assuming $NaNO_3^o = 0$ yields a relation which is devoid of $[CaNO_3^+]$ as

$$2[Na^+] + 2[Ca]_T - 2[CaSO_4^o] = 2[SO_4^{2-}] + [NO_3]_T + [Na]_T, \quad [5]$$

but which is usable for estimating $[CaNO_3^+]$.

Equations [2] and [5] can be modified to include only the sulfate constituent by introducing the dissociation constants for $NaSO_4^-$ ($\underline{K}_{NaSO_4^-}$) and $CaSO_4^o$ ($\underline{K}_{CaSO_4^o}$) and the solubility product constant for gypsum ($\underline{K}_{sp}$):

$$\underline{K}_{NaSO_4^-} = [Na^+][SO_4^{2-}]\gamma_{Na}\gamma_{SO_4}/[NaSO_4^-]\gamma_{NaSO_4},$$

$$\underline{K}_{CaSO_4^o} = [Ca^{2+}][SO_4^{2-}]\gamma_{Ca}\gamma_{SO_4}/[CaSO_4^o]\gamma_{CaSO_4}, \text{ and}$$

$$\underline{K}_{sp} = [Ca^{2+}][SO_4^{2-}]\gamma_{Ca}\gamma_{SO_4}.$$

The brackets, [ ], represent the concentration and the gamma, γ, represents the activity coefficient.

Using the definition of $\underline{K}_{NaSO_4^-}$ in equation [2] gives

$$[Na^+] = [Na]_T/(1 + [SO_4^{2-}]\gamma_{Na}\gamma_{SO_4}/(\underline{K}_{NaSO_4^-}\ \gamma_{NaSO_4})) \qquad [6]$$

for which the $[Na^+]$ constituent can be substituted into equation [5].

The concentration of $CaSO_4^o$ can be computed as

$$[CaSO_4^o] = \underline{K}_{sp}/(\underline{K}_{CaSO_4^o}\ \gamma_{CaSO_4}) \qquad [7]$$

and substituted into equation [5] resulting in equation [8] which is then solvable in terms of the single constituent $[SO_4^{2-}]$ as

$$2[Na]_T/(1 + [SO_4^{2-}]\gamma_{Na}\gamma_{SO_4}/(\underline{K}_{NaSO_4^-}\ \gamma_{NaSO_4}))$$
$$+ 2[Ca]_T - 2\underline{K}_{sp}/(\underline{K}_{CaSO_4^o}\ \gamma_{CaSO_4}) = 2[SO_4^{2-}] + [NO_3]_T + [Na]_T \qquad [8]$$

Note that in both equations [7] and [8], the activity coefficient γ_{CaSO_4} of the uncharged $CaSO_4^o$ species is not assumed to be 1 as is usually done for dilute solutions, and instead, γ_{CaSO_4} will be developed in this study as a function of ionic strength.

The following Davies relation (7) was used for estimating the activity coefficients of the ionic species:

$$-\log \gamma_i = Az_i^2(\mu^{1/2}/(1 + \mu^{1/2}) - 0.2\ \mu) \qquad [9]$$

where z_i = valence of species i, A = Debye constant, and μ = ionic strength = $1/2 \sum_i m_i z_i^2$.

The solution for $[SO_4^{2-}]$ in equation [8] thus requires a knowledge of (a) the quantities $[Na]_T$, $[Ca]_T$, and $[NO_3]_T$ which are obtainable from solubility measurements of $CaSO_4 \cdot 2H_2O$ in known concentrations of the Na-salt solution, (b) the constants $\underline{K}_{sp}$, $\underline{K}_{NaSO_4^-}$, and $\underline{K}_{CaSO_4^o}$ which are available in the literature, and (c) the activity coefficients of the ionic species which are computable from ionic strength dependent functions. After $[SO_4^{2-}]$ is obtained, $[Ca^{2+}]$, $[CaNO_3^+]$, and $[NO_3^-]$, which make up part of the factors in the dissociation constant of $[CaNO_3^+]$ as $\underline{K}_{CaNO_3^+} = [Ca^{2+}][NO_3^-]\gamma_{Ca}\gamma_{NO_3}/([CaNO^+]\gamma_{CaNO_3})$, and $[Na^+]$ and $[NaSO_4^-]$ can be obtained with proper manipulation of the constants and mass balance equations.

Gypsum Solubility Prediction.-If the dissociation constants for the various Ca-complexes are known, then the solubility of $CaSO_4 \cdot 2H_2O$ in mixed Na-salts solutions such as $NaClO_4$-NaCl-$NaNO_3$-NaOAc can be computed. The necessary mass and charge balance relations are

$$[Cl]_{total} = [CaCl^+]? + [Cl^-] \qquad [10]$$

$$[NO_3]_{total} = [CaNO_3^+]? + [NO_3^-] + [NaNO_3^o]? \qquad [11]$$

$$[OAc]_{total} = [CaOAc^+]? + [OAc^-] + [NaOAc^o]? \qquad [12]$$

$$[Na]_{total} = [NaSO_4^-] + [Na^+] + [NaNO_3^o]? + [NaOAc^o]? \qquad [13]$$

$$2[Ca^{2+}] + [Na^+] + [CaCl^+]? + [CaNO_3^+]? + [CaOAc^+]? =$$

$$[Cl^-] + [NO_3^-] + [OAc^-] + [NaSO_4^-] + 2[SO_4^{2-}] + [ClO_4^-] \quad [14]$$

Equations [10] to [14] are a set of five equations with five unknowns; namely, $[Cl^-]$, $[NO_3^-]$, $[OAc^-]$, $[Na^+]$, and $[SO_4^{2-}]$. Note that $[Ca^{2+}]$ can be related to $[SO_4^{2-}]$ through the solubility product constant. These equations can be solved in a manner similar to the preceding sets for determining the dissociation constants or by the Newton-Raphson method involving nonlinear simultaneous equations (14).

The solution to the simultaneous equations then gives the Ca constituents which, when combined, gives the solubility of gypsum in mixed salt solutions as

$$[Ca]_{total} = [Ca^{2+}] + [CaCl^+]? + [CaNO_3^+]? + [CaOAc^+]? + [CaSO_4^o] \quad [15]$$

EXPERIMENTAL PROCEDURE:

The amount of $CaSO_4.2H_2O$ dissolved in a range of concentrations (2.5×10^{-2} to 1 M) of $NaClO_4$, NaCl, $NaNO_3$, and NaOAc solutions and mixtures of these Na-salts was determined at 25 ± 0.5 C with the versenate complexometric titration technique. Saturated solutions were equilibrated for at least one week with occasional shaking. The pH of the solutions containing NaOAc was also measured. Duplicate measurements were made for each of the solution combinations.

RESULTS AND DISCUSSION:

Single-Salt Solutions

The solubility of $CaSO_4.2H_2O$ in the different Na-salts at the various concentrations is listed in Table 1. Gypsum solubility increased with increasing electrolyte concentration in a solution with uncommon ions up to 1 M as has been noted by many other investigators (15). Among the Na-salts for the same concentrations the solubility relation for $CaSO_4.2H_2O$ was NaOAc > $NaNO_3$ > NaCl >

$NaClO_4$. The association of Ca^{2+} with OAc^- and NO_3^- to form $CaOAc^+$ and $CaNO_3^+$ has been established before, and the dissociation constants of $\underline{K}_{CaOAc^+} = 0.0575$ (11) and $\underline{K}_{CaNO_3^+} = 0.526$ (12) could explain the solubility order of gypsum in NaOAc and $NaNO_3$ solutions. If the explanation on the order of gypsum solubility in the different Na-salts is based on this kind of reasoning, then we must look for the form $CaCl^+$, since the solubility relation is NaCl > $NaClO_4$. The form $CaClO_4^+$ need not be present in the argument. In respect to the existence of the $CaCl^+$ species reports range from no complex (15) to the probability of a very weak complex (8, p. 560-561), to a recently published experimental evidence of $CaCl^+$ with a $\underline{K}_{CaCl^+} = 0.21$ (6). The values of $\underline{K}_{CaNO_3^+} = 0.526$ and $\underline{K}_{CaCl^+} = 0.21$, however, are inconsistent with the solubilities of gypsum in $NaNO_3$ and NaCl solutions observed in this experiment.

No $CaClO_4^+$ form has been reported (16, p. 317-319), and even if it did exist, the Ca^{2+} to ClO_4^- association would undoubtedly be very weak based on the inability of the strongly complex-forming transition metals to form ClO_4 complexes of any significance. Thus, in this study, $CaClO_4^+$ was assumed to be present.

The total Ca in solution from the dissolution of $CaSO_4 \cdot 2H_2O$ in $NaClO_4$ solutions was predicted assuming the presence of Na^+, $NaSO_4^-$, Ca^{2+}, $CaSO_4^o$, and ClO_4^-, but no $CaClO_4^+$ in solution. Computational results are listed in Table 1, column 7. The constants and supplemental relations used were $\underline{K}_{sp} = 2.45 \times 10^{-5}$ (10), $\underline{K}_{NaSO_4^-} = 0.19$ (9), $\underline{K}_{CaSO_4^o} = 4.90 \times 10^{-3}$ (3), the Davies equation for γ in equation [9], and $\gamma_{CaSO_4} = 1$. The computed $[Ca]_T$ compared well with the experimental values (column 2) based on the assumptions stated previously. Further improvement in the prediction was made by empirically correcting the activity coefficient of $CaSO_4^o$. This step was made in anticipation of calculating the dissociation constants of $CaOAc^+$, $CaNO_3^+$, and $CaCl^+$ which required the use of γ_{CaSO_4}. The derived relationship between γ_{CaSO_4} and ionic strength

is

$$\log \gamma_{CaSO_4} = 1.012\ \mu - 1.193\ \mu^2 + 0.289\ \mu^3. \qquad [16]$$

The computed gypsum solubility based on this equation [16] instead of using $\gamma_{CaSO_4} = 1$ is tabulated in column 8, Table 1. This form can be simplified into the relation of $\log \gamma_{CaSO_4} = -0.008 + 0.964\ \mu$ for ionic strengths less than 0.16, and when the line of best fit was forced through the log γ to μ intercept, the equation was further simplified to $\log \gamma_{CaSO_4} = 0.90\ \mu$. This form followed the relation $\log \gamma = k\mu$ reported for uncharged molecules (8, p. 532).

The activity coefficients for $CaSO_4$ computed from equation [6] were equal to 1 or larger in the 0 to 1.1 M ionic strength range. The same was true for the linear equations at the lower ionic strengths. Application of equation [16] has not been tested above 1.1 M and extrapolation should be avoided beyond this ionic strength. Yeatts and Marshall (18), on the other hand, developed the relation $\log \gamma_{CaSO_4} = -0.173\ \mu^{1/2}/(1 + 1.36\ \mu^{1/2})$ which gave γ_{CaSO_4} of 1 and smaller. They did not include the $NaSO_4^-$, $CaCl^+$, and $CaNO_3^+$ species in their systems from which the function of $\log \gamma_{CaSO_4}$ was developed.

The apparent dissociation constants for $CaCl^+$, $CaNO_3^+$, and $CaOAc^+$ are presented in Table 2. These constants were computed from gypsum solubility in NaCl, $NaNO_3$, and NaOAc (Table 1) using equations [1] through [9] developed in the theory section, along with the γ_{CaSO_4} relation of equation [16] determined empirically from gypsum solubility behavior in $NaClO_4$ solutions. For the $NaNO_3$ and NaOAc solutions, the associated Na^+ forms $NaNO_3^o$ and $NaOAc^o$, respectively, were also considered and their significance will be discussed with the solubility of gypsum in mixed Na-salt solutions.

Double-Salt Solution

The measured and computed gypsum solubility in double Na-salt systems are compared in Table 3. Solubility of $CaSO_4.2H_2O$ in the $NaClO_4$-NaCl solutions could be predicted fairly well using $\underline{K}_{CaCl^+}$ = 0.252 and no additional change was considered to adjust the computed to the experimental values. Any interaction between Na^+ and the anion of the Na-salt should become more apparent using $NaClO_4$ as the companion salt. This appeared to be the case with the $NaClO_4$-$NaNO_3$ and NaOAc mixtures. When $NaNO_3^o$ and $NaOAc^o$ associations were accounted for, the agreement between the computed and experimental solubility values was improved, particularly at the higher salt concentrations. Also, the apparent $\underline{K}_{CaNO_3^+}$ and $\underline{K}_{CaOAc^+}$ values become less Na-concentration dependent when $NaNO_3^o$ and $NaOAc^o$ were incorporated into the model (Table 2).

Multiple-Salt Solutions

Gypsum solubility was measured in more complicated systems in order to test the applicability of the technique for predicting solubility in Na-salt mixtures (Table 4). For the NaCl-$NaNO_3$-NaOAc and the $NaClO_4$-NaCl-$NaNO_3$-NaOAc mixtures, solubilities could be predicted fairly accurately at the high salt concentrations when the additional Na- to $-NO_3$ and Na- to -OAc associations were taken into account. The predicted values were consistently greater than the experimental values in the order of 1 to 4%, with the largest variation occurring at the most concentrated Na-salt mixture. For most cases, the difference was in the range of the experimental error of 1 to 2% and, consequently, no further attempt was made to improve the prediction.

The dissolved constituents of one concentration of gypsum in $NaClO_4$-NaCl-$NaNO_3$-NaOAc mixture is presented in Table 5 to show the magnitude in the concentration of each of the species. With the high amounts of Cl^-, NO_3^-, and OAc^-, the concentration of the $CaCl^+$ and $CaNO_3^+$ forms were approximately equal to the ion-pair

$CaSO_4^o$, whereas the $CaOAc^+$ was significantly larger than $CaSO_4^o$. The ionic Ca^{2+} made up about 50% of the total Ca in solution. In naturally occurring solutions such as seawater and brine which have large concentrations of Cl^-, the form $CaCl^+$ could possibly be an important constituent in solution.

The dissociation constants developed here of $\underline{K}_{CaCl^+} = 0.252$, $\underline{K}_{CaNO_3^+} = 0.167$, and $\underline{K}_{CaOAc^+} = 0.0667$ at 25 C compared with that of $\underline{K}_{CaCl^+} = 0.21$ at an unspecified temperature (6), $\underline{K}_{CaNO_3^+} = 0.52$ at 18 C (12), and $\underline{K}_{CaOAc^+} = 0.17$ (5), $\underline{K}_{CaOAc^+} = 0.075$ (1), and $\underline{K}_{CaOAc^+} = 0.056$ (11) at 25 C. The agreement was quite satisfactory considering the differences in the techniques and assumptions made in determining these constants. The dissociation constant for $NaNO_3^o$ of $\underline{K}_{NaNO_3^o} = 3.0$ compared favorably with values ranging from 2.0 to 3.2 obtained by Robinson (13), and the $\underline{K}_{NaOAc^o} = 1.5$ was the same as that of Archer and Monk (1) determined with electrometric pH measurements.

Some non-thermodynamic assumptions were required in developing the conceptual model for predicting $CaSO_4 \cdot 2H_2O$ solubility in mixed Na-salt solution at high concentrations and consequently criticisms can be justifiably raised. All attempts were made so that any empiricism invoked in this study would be consistent with existing conceptions of solution chemistry and also with the experimental observations. The basic assumptions were (a) the applicability of the Davies equation for ionic activity coefficient up to 1 $\underline{M}$, (b) the complete dissociation of $NaClO_4$ and NaCl in solution, and (c) the absence of $CaClO_4^+$ species. Associated species such as $CaCl^+$, $CaNO_3^+$, $CaOAc^+$, $NaNO_3^o$, and $NaOAc^o$ were considered present when the usual methods were not suitable for predicting gypsum solubility in mixed Na-salt solutions. The species $NaSO_4^-$ and $CaSO_4^o$ were assumed to be present. Conceivably, an alternate approach could be taken whereby corrections to the Debye-Hückel extended theory can be made to account for additional ionic interactions. However,

this approach also requires an empirical treatment. The treatment presented here can be easily visualized conceptually and at the same time easily adapted to practical situations.

Undoubtedly, arguments will be raised, for example, regarding the existence of $CaCl^+$ species, and questions raised as to whether this form is an artifact resulting from the assumptions made in computing for the dissociation constants. In the past $CaCl_2$ has been assumed to be completely dissociated at concentrations even as high as 6 M (2), and single ionic activities for Ca^{2+} and Cl^- have been computed on basis of the hydration theory. The solubility measurements of the present study make it difficult to explain fully the solubility behavior in the different Na-salt solutions without invoking association between Ca^{2+} and Cl^- that parallels the interaction of Ca^{2+} with NO_3^- and OAc^- anions. Butler (4) assigned a K_{CaCl^+} of 10 in his measurement of the standard potential of the Ca-electrode in $CaCl_2$ solutions. Even with this value of 10 vs. 0.25, the $CaCl^+$ form should become increasingly evident at the high $CaCl_2$ concentrations.

SUMMARY:

The solubility behavior of gypsum ($CaSO_4.2H_2O$) was investigated in single and mixed Na-salt solutions for developing a method for predicting its solubility at high salt concentrations. The solubility of gypsum increased with Na-salt concentration up to 1 M. and was in the order NaOAc > $NaNO_3$ > NaCl > $NaClO_4$. This behavior was explained on basis of the formation of $CaOAc^+$, $CaNO_3^+$, and $CaCl^+$. Dissociation constants of $K_{CaOAc^+} = 0.0667$, $K_{CaNO_3^+} = 0.167$, and $K_{CaCl^+} = 0.252$ were determined for the Ca-anion interactions. Associated forms $NaNO_3^o$ and $NaOAc^o$ were also considered in solutions at high concentrations, and constants of $K_{NaNO_3^o} = 3.0$ and $K_{NaOAc^o} = 1.5$ were obtained for these species. The solubility behavior of gypsum in $NaClO_4$ solutions and the Davies relation for ion activity coefficient were used to estimate an empirical function

for the activity coefficient of the neutral $CaSO_4^o$ which was $\log \gamma_{CaSO_4} = 1.012\ \mu - 1.193\ \mu^2 + 0.289\ \mu^3$.

REFERENCES:

1. Archer, D. W., and C. B. Monk. Ion-association constants of some acetates by pH (glass electrode) measurements. J. Chem. Soc. 1964:3117-3122. 1964.

2. Bates, R. G., B. R. Staple, and R. A. Robinson. Ionic hydration and single ion activities in unassociated chlorides at high ionic strengths. Anal. Chem. 42:867-871. 1970.

3. Bell, R. P., and J. H. B. George. The incomplete dissociation of some thallous and calcium salts at different temperatures. Trans. Faraday Soc. 49:619-627. 1953.

4. Butler, J. N. The standard potential of the calcium amalgam electrode. J. Electroanal. Chem. 17:309-317. 1968.

5. Colman-Porter, C. A., and C. B. Monk. Dissociation constants of the alkaline-earth salts of some monocarboxylic acids. J. Chem. Soc. 1952:4363-4368. 1952.

6. Corsaro, G. Ion strength, ion association, and solubility. J. Chem. Educ. 39:622-626. 1962.

7. Davies, C. W. Ion association. Butterworths and Co., Ltd., London. 1962. p. 39.

8. Harned, H. S., and B. B. Owen. The physical chemistry of electrolyte solutions. Reinhold Book Corp., New York. 1958. p. 532, 560-561.

9. Jenkins, I. L., and C. B. Monk. The conductances of sodium, potassium and lanthanum sulfates at 25°. J. Amer. Chem. Soc. 72:2695-2698. 1950.

10. Moreno, E. C., and G. Osborn. Solubility of gypsum and dicalcium phosphate dihydrate in the system $CaO-P_2O_5-SO_3-H_2O$ and in soils. Soil Sci. Soc. Amer. Proc. 27:614-619. 1963.

11. Nancollas, G. H. Thermodynamics of ion association. Part II. Alkaline-earth acetates and formates. J. Chem. Soc. 1956:744-749. 1956.

12. Righellato, E. C., and C. W. Davies. The extent of dissociation of salts in water. Part II. Uni-bivalent salts. Trans. Faraday Soc. 26:592-600. 1930.

13. Robinson, R. A. The osmotic and activity coefficient data of some aqueous salt solutions from vapor pressure measurements. J. Amer. Chem. Soc. 59:84-90. 1937.

14. Scarborough, J. B. Numerical mathematical analysis. John Hopkins Press. Baltimore. p. 215-223. 1966.

15. Seidell, A. Solubilities of inorganic and metal organic compounds. D. Van Nostrand Co., Inc., New York. 1953. p. 330-342.

16. Sillén, L. G., and A. E. Martell. Stability constants of metal-ion complexes. Metcalfe and Cooper, Ltd. London. 1964. p. 235-236, 317-319.

17. Tanji, K. K., and L. D. Doneen. Predictions on the solubility of gypsum in aqueous salt solutions. Water Resources Res. 2:543-548. 1966.

18. Yeatts, L. B., and W. L. Marshall. Apparent invariance of activity coefficients of calcium sulfate at constant ionic strength and temperature in the system $CaSO_4$-Na_2SO_4-$NaNO_3$-H_2O to the critical temperature of water association equilibria. J. Phys. Chem. 73:81-88. 1969.

Table 1--Solubility of gypsum ($CaSO_4 \cdot 2H_2O$) in $NaClO_4$, NaCl, $NaNO_3$ and NaOAc solutions at 25 C and predicted solubility in $NaClO_4$ solution

Salt Conc., M	$[Ca]_{total}$, M x 10^2						
	$NaClO_4$ a/	NaCl a/	$NaNO_3$ a/	NaOAc a/	pH (NaOAc)	$NaClO_4$ b/	$NaClO_4$ c/
0.025	1.744	1.790	1.797	1.817	7.125	1.80	1.72
0.050	1.891	1.941	1.977	2.057	7.325	1.98	1.88
0.075	1.998	2.096	2.161	2.246	7.472	2.13	2.02
0.100	2.120	2.215	2.264	2.449	7.574	2.27	2.13
0.200	2.469	2.705	2.804	3.037	7.818	2.66	2.48
0.300	-	3.007	3.124	-	-	-	-
0.400	2.900	3.332	3.476	4.067	8.021	3.11	2.90
0.500	3.031	3.544	-	-	-	3.24	3.03
0.600	3.165	3.822	4.014	4.904	8.243	3.34	3.13
0.700	3.281	4.029	-	-	-	3.40	3.22
0.800	3.279	4.174	4.480	5.673	8.259	3.44	3.28
1.00	3.381	4.503	4.845	6.378	8.330	3.47	3.40

a/ Measured gypsum solubility

b/ Predicted solubility based on $\gamma_{CaSO_4} = 1$

c/ Predicted solubility based on $\log \gamma_{CaSO_4} = 1.012\ \mu - 1.193\ \mu^2 + 0.289\ \mu^3$

Table 2--Apparent dissociation constants for $CaCl^+$, $CaNO_3^+$, and $CaOAc^+$ at 25 C

Salt	Apparent K_{CaX^+} x 10				
Conc., M	$CaCl^+$	$CaNO_3^+$ a/	$CaNO_3^+$ b/	$CaOAc^+$ c/	$CaOAc^+$ d/
0.025	0.88*	0.79*	0.78*	0.595*	0.592*
0.050	2.15*	1.29*	1.25*	0.641*	0.621
0.075	2.35	1.25*	1.20*	0.747	0.709
0.100	3.04	1.87	1.77	0.717	0.673
0.200	2.28	1.54	1.45	0.833	0.757
0.300	1.92	1.92	1.79	-	-
0.400	2.48	1.81	1.70	0.791	0.696
0.500	2.72	-	-	-	-
0.600	2.45	1.85	1.68	0.786	0.665
0.700	2.47	-	-	-	-
0.800	2.66	1.88	1.64	0.782	0.623
1.00	2.81	2.03	1.68	0.794	0.585
K_{CaX^+} =	0.252 ±0.031	0.184 ±0.015	0.167 ±0.011	0.0778 ±0.0033	0.0667 ±0.0051

*/ Values not used in computing means

a/ Assuming no $NaNO_3^o$

b/ $K_{NaNO_3^o} = 3.0$

c/ Assuming no $NaOAc^o$

d/ $K_{NaOAc^o} = 1.5$

Table 3--Comparison of experimental and computed gypsum solubility in two-salt mixtures

Total[a/] salt conc., M	$[Ca]_{total}$, M x 10^2							
	$NaClO_4$-NaCl		$NaClO_4$-$NaNO_3$			$NaClO_4$-NaOAc		
	Expt.	Calc.	Expt.	Calc.[b/]	Calc.[c/]	Expt.	Calc.[d/]	Calc.[e/]
0.25	2.71	2.74	2.76	2.79	2.78	2.90	3.00	3.02
0.50	3.29	3.32	3.32	3.42	3.38	3.69	3.84	3.86
0.75	3.63	3.71	3.78	3.87	3.78	4.28	4.52	4.47
1.00	3.91	4.06	4.07	4.28	4.07	4.74	5.15	4.95

a/ Solution composed of equimolar concentration of two Na-salts

b/ $K_{CaNO_3^+} = 0.184$, and assuming no $NaNO_3^o$

c/ $K_{CaNO_3^+} = 0.167$, $K_{NaNO_3^o} = 3.0$

d/ $K_{CaOAc^+} = 0.0778$, and assuming no $NaOAc^o$

e/ $K_{CaOAc^+} = 0.0667$, $K_{NaOAc^o} = 1.5$

Table 4--Comparison of experimental and computed gypsum solubility in three- and four-salt mixtures

Total salt	$[Ca]_{total}$, M x 10^2					
	$NaCl-NaNO_3-NaOAc$ a/			$NaClO_4-NaCl-NaNO_3-NaOAc$ a/		
Conc., M	Expt.	Calc. b/	Calc. c/	Expt.	Calc. b/	Calc. c/
0.10	-	-	-	2.22	2.27	2.28
0.25	2.98	3.07	3.08	2.91	3.00	2.97
0.50	3.88	3.98	3.99	3.67	3.76	3.77
0.75	4.62	4.71	4.67	4.25	4.39	4.36
1.00	5.15	5.40	5.23	4.67	4.98	4.85

a/ Solution composed of equimolar concentration of the Na-salts

b/ $K_{CaCl^+} = 0.252$, $K_{CaNO_3^+} = 0.184$, $K_{CaOAc^+} = 0.0778$, no $NaNO_3^o$ and $NaOAc^o$

c/ $K_{CaCl^+} = 0.252$, $K_{CaNO_3^+} = 0.167$, $K_{NaNO_3^o} = 3.0$; $K_{CaOAc^+} = 0.0667$; $K_{NaOAc^o} = 1.5$

Table 5--Dissolved constituents in a gypsum, Na-salt mixture for $NaClO_4 = NaCl = NaNO_3 = NaOAc = 1.25 \times 10^{-1}$ M

$[Ca]_{total}$	$= 3.77 \times 10^{-2}$ M	$[SO_4^{2-}]$	$= 2.22 \times 10^{-2}$ M
$[Ca^{2+}]$	$= 2.13 \times 10^{-2}$ M	$[Na^+]$	$= 4.731 \times 10^{-1}$ M
$[CaCl^+]$	$= 2.36 \times 10^{-3}$ M	$[NaSO_4^-]$	$= 1.26 \times 10^{-2}$ M
$[CaNO_3^+]$	$= 3.38 \times 10^{-3}$ M	$[Cl^-]$	$= 1.226 \times 10^{-1}$ M
$[CaOAc^+]$	$= 7.83 \times 10^{-3}$ M	$[NO_3^-]$	$= 1.166 \times 10^{-1}$ M
$[CaSO_4^o]$	$= 2.86 \times 10^{-3}$ M	$[OAc^-]$	$= 1.079 \times 10^{-1}$ M
$[NaNO_3^o]$	$= 5.02 \times 10^{-3}$ M	$[ClO_4^-]$	$= 1.250 \times 10^{-1}$ M
$[NaOAc^o]$	$= 9.28 \times 10^{-3}$ M	μ	$= 5.844 \times 10^{-1}$ M

$\gamma_{CaSO_4} = 1.75$; $\gamma_+ = 0.690$; $\gamma_{++} = 0.221$

PART II. THERMODYNAMIC FUNCTIONS FOR THE DISSOCIATION OF $NaHCO_3^o$, $NaCO_3^-$, H_2CO_3 AND HCO_3^-

INTRODUCTION:

The presence of the associated forms such as $NaHCO_3^o$ and $NaCO_3^-$ in Na-carbonate solutions has been demonstrated (Annual Report 1969), and their dissociation constants have been reported (8). Subsequently, the thermodynamic properties $\Delta \underline{H}$, $\Delta \underline{F}$, and $\Delta \underline{S}$ for the dissociation of $NaHCO_3^o$ and $NaCO_3^-$, together with H_2CO_3 and HCO_3^-, have been obtained.

The Harned-type electromotive cell system (5) for estimating the dissociation constant of the first ($\underline{K}_{1A}$) and second ($\underline{K}_{2A}$) dissociation constants of carbonic acid are as follows:

$$-\log \underline{K}_{1A} = \frac{(\underline{E} + \underline{E}_c - \underline{E}^o)\underline{F}}{2.303\underline{RT}} + \log \gamma_{CO_2} \underline{SP}_{CO_2} + \log \frac{[Cl^-]}{[HCO_3^-]} + \log \frac{\gamma_H \gamma_{Cl}}{\gamma_H \gamma_{HCO_3}} \quad (1)$$

and

$$-\log \underline{K}_{2A} = \frac{(\underline{E} - \underline{E}^o)\underline{F}}{2.303\underline{RT}} + \log \frac{[HCO_3^-][Cl^-]}{[CO_3^{2-}]} + \log \frac{\gamma_{HCO_3} \gamma_{Cl}}{\gamma_{CO_3}} \quad (2)$$

where $\underline{E}$ = emf of the cell, $\underline{E}_c = (-RT/2\underline{F}) \ln \underline{P}_{H_2}$, $\underline{E}^o$ = standard reference electrode potential, $\underline{R}$ = gas constant, $\underline{T}$ = Kelvin temperature, $\underline{F}$ = Faraday, $\underline{S}$ = Henry's law constant for CO_2 solubility, $\underline{P}$ = partial pressure of gas, γ = activity coefficient.

If the species $NaHCO_3^o$ and $NaCO_3^-$ are present in the carbonate solutions from which the emf's are taken, the ratios $[Cl^-]/[HCO_3^-]$ and $[HCO_3^-][Cl^-]/[CO_3^{2-}]$ need not necessarily be the carbonate stoichiometric concentration ratios. Two separate independent investigations (2, 3) have indicated the presence of Na-carbonate forms such as $NaCO_3^-$ and $NaHCO_3^o$. Harned and co-workers (4, 6)

assumed no complex or ion-pair formation in the use of these equations since there was no reason to assume it at that time. In actuality this was avoided by extrapolating to zero ionic strength to get the thermodynamic dissociation constants, $\underline{K}_{1A}$ and $\underline{K}_{2A}$. Applying an alternative computational approach (8) which made provisions for the presence of $NaHCO_3^o$ and $NaCO_3^-$ to the same set of data of Harned and co-workers (4, 6) at 25 C, the dissociation constants of $NaHCO_3^o$ and $NaCO_3^-$, and also H_2CO_3 and HCO_3^-, could be estimated simultaneously. An important feature of this technique is that the computed $\underline{K}_{1A}$ and $\underline{K}_{2A}$ values are independent of sodium and carbonate concentration or ionic strength, and, consequently removes an element of uncertainty associated with extrapolating to zero ionic strength. This procedure requires extra-thermodynamic assumptions regarding the applicability of the Debye-Hückel relation for estimating ionic activity coefficients. However, any error associated with this was minimized by using low ionic strength solutions.

PROCEDURE:

The classical experimental data of Harned and Davis (4) and Harned and Scholes (6) were used for computing the various constants. Temperature-salt concentration related values over the range of 0 to 50 C for the solubility of CO_2 in electrolyte solutions were recomputed from the data of Harned and Davis (4); the temperature dependence of the ion activity product of water and the potential of the Ag:AgCl reference electrode were obtained from Harned and Owen (5) and Bates (1), respectively; the Debye coefficients and constants used in the extended Debye-Hückel equation for the ionic activity coefficient tabulated by Kielland (7) were used.

The log $\underline{K}$'s as functions of temperature were fitted by least-squares technique to an equation of the form $\log \underline{K} = \frac{A}{T} + B + CT$; additional functions were derived from the relations $\Delta \underline{F} = -2.303\underline{RT}$

log $\underline{K}$, $\Delta\underline{H}/2.303\underline{RT}^2 = d(\log \underline{K})/d\underline{T}$, and $\Delta\underline{S} = (\Delta\underline{H} - \Delta\underline{F})/\underline{T}$ using the preceding log $\underline{K}$ relation.

RESULTS AND DISCUSSION:

The computed dissociation constants and attendant thermodynamic properties as a function of temperature for $NaHCO_3^o$, H_2CO_3, $NaCO_3^-$, and HCO_3^- are presented in Tables 1 to 4. Within each table the values computed from the experimental observations and that derived from the least-squares equation are compared side by side. The derived values for $\underline{K}_{H_2CO_3}$ (Table 2) and $\underline{K}_{HCO_3^-}$ (Table 4) computed by Harned and Davis (4) and Harned and Scholes (6) are also listed for comparison purposes.

Variation was greatest for $\underline{K}_{NaHCO_3^o}$ above 35 C (Table 1). Harned and Davis' (4) original data also indicated larger experimental variability in this temperature region. The $\underline{K}_{NaCO_3^-}$ and $\underline{K}_{NaHCO_3^o}$ values show that Na^+ is more greatly associated with CO_3^{2-} than with HCO_3^- as would be expected because of the greater charge density of CO_3^{2-} over HCO_3^-. The association of Na^+ with CO_3^{2-} and HCO_3^- is very much less than that of H^+ with these carbonates. The standard free energies of formation for the ion-pairs at 25 C are $\Delta\underline{F}^o_{NaHCO_3^o} = 203.07$ kcal/mol and $\Delta\underline{F}^o_{NaCO_3^-} = -189.50$ kcal/mol.

The computed values of $\underline{K}_{1A}$ and $\underline{K}_{2A}$ as a function of temperature and corrected for the presence of $NaHCO_3^o$ and $NaCO_3^-$ in solution (Tables 2 and 4) compare favorably with those obtained by Harned and co-workers (4, 6) using extrapolation techniques. The latter method involves some measure of compromise in that as $HCO_3^- + CO_3^{2-}$ concentrations and ionic strengths are decreased, the emf measurements become unreliable; and conversely, at high carbonate and salt concentrations, the -log $\underline{K}$ vs. ionic strength relationship becomes nonlinear due to increasing ion-pair formation, even though emf measures are stable.

The thermodynamic functions $\Delta\underline{F}$, $\Delta\underline{H}$, and $\Delta\underline{S}$ for H_2CO_3 at 25° of 8.667 kcal/mol, 2.352 kcal/mol, and -21.2 cal/mol-deg, respectively,

are similar to the values of 8.683, 1.843, and -22.9 obtained by Pitzer (9) using a calorimetric technique; for HCO_3^- these are $\Delta \underline{F}$ = 14.090 kcal/mol, $\Delta \underline{H}$ = 3.811 kcal/mol, and $\Delta \underline{S}$ = -34.5 cal/mol-deg vs. 13.983, 3.500, and -35.2, respectively, reporter by Pitzer. The $\Delta \underline{H}$'s and $\Delta \underline{S}$'s are expected to be slightly different in the comparison because of the allowance for Na-carbonate ion association in the present work.

Values for $\underline{K}_{NaHCO_3^o}$ and $\underline{K}_{NaCO_3^-}$ from other sources are available only at 25 C. Garrels *et al.* (3) reported $\underline{K}_{NaHCO_3^o}$ and $\underline{K}_{NaCO_3^-}$ of 1.82 and 0.054, respectively, and Butler and Huston (2) of 1.6 and 0.13. The two latter sets of $\underline{K}$'s were averaged from Butler and Huston's original results. In this present study, $\underline{K}_{NaHCO_3^o}$ = 0.69 and $\underline{K}_{NaCO_3^-}$ = 0.28. The differences apparently are caused by the model and experimental procedure, and most likely in the assumptions made regarding the computation of the activity coefficients of the ionic species. Regardless of which method is eventually proven the most accurate for obtaining $\underline{K}_{NaHCO_3^o}$ and $\underline{K}_{NaCO_3^-}$, the recomputed temperature dependent $\underline{K}_{H_2CO_3}$ and $\underline{K}_{HCO_3^-}$ values for carbonic acid presented here should be an improvement over the original reports of Harned and co-workers (4, 6) because extrapolation was not used.

SUMMARY:

The dissociation constants of $NaHCO_3^o$ and $NaCO_3^-$ and related thermodynamic functions were obtained for temperatures ranging from 0 to 50 C incorporating the classical experimental data of Harned and co-workers for determining the dissociation constants of H_2CO_3 and HCO_3^-. From the electromotive measurement of Na-carbonate solutions for cells without liquid junction potential, the dissociation constants for $NaHCO_3^o$, $NaCO_3^-$, H_2CO_3 and HCO_3^- were estimated simultaneously.

REFERENCES:

1. Bates, R. G. Determination of pH, theory and practice, p. 285, John Wiley, N.Y. 1965.

2. Butler, J. N., and Huston, R. Activity coefficients and ion-pairs in the systems sodium chloride-sodium bicarbonate-water and sodium chloride-sodium carbonate-water. J. Phys. Chem. 74:2976-2984. 1970.

3. Garrels, R. M., Thompson, M. E., and Siever, R. Control of carbonate solubility by carbonate complexes. Amer. J. Sci. 259:24-45. 1961.

4. Harned, H. S., and Davis, R., Jr. The ionization constant of carbonic acid in water and the solubility of carbon dioxide in water and aqueous salt solutions from 0 to 50°. J. Amer. Chem. Soc. 65:2030-2037. 1943.

5. Harned, H. S., and Owen, B. B. The physical chemistry of electrolyte solutions. pp. 690-694. Reinhold, N.Y. 1958.

6. Harned, H. S., and Scholes, S. R., Jr. The ionization constant of HCO_3 from 0 to 50°. J. Amer. Chem. Soc. 63:1706-1709. 1941.

7. Kielland, J. Individual activity coefficients of ions in aqueous solutions. J. Amer. Chem. Soc. 59:1675-1678. 1937.

8. Nakayama, F. S. Sodium bicarbonate and carbonate ion-pairs and their relation to the estimation of the first and second dissociation constants of carbonic acid. J. Phys. Chem. 74:2726-2728. 1970.

9. Pitzer, K. S. The heats of ionization of water, ammonium hydroxide, carbonic, phosphoric, and sulfuric acids. The variation of ionization constants with temperature and the entropy change with ionization. J. Amer. Chem. Soc. 63:2365-2371. 1937.

Table 1. Thermodynamic data for the dissociation reaction

$$NaHCO_3^o = Na^+ + HCO_3^-$$

Temp, °C	$-\log K_{NaHCO_3^o}$ a/	$-\log K_{NaHCO_3^o}$ b/	ΔF, c/ cal/mol	ΔH, d/ cal/mol	ΔS, e/ cal/mol-deg
0	0.375	0.368	459.7	3326.6	10.5
5	0.286	0.321	408.2	3224.4	10.1
10	0.276	0.277	358.5	3120.4	9.8
15	0.243	0.236	310.6	3014.6	9.4
20	0.260	0.198	264.6	2906.9	9.0
25	0.161	0.162	220.5	2797.3	8.6
30	0.114	0.128	178.2	2685.9	8.3
35	0.0565	0.0975	137.8	2572.6	7.9
40	0.0768	0.0691	99.2	2457.5	7.5
45	0.0200	0.0429	62.5	2340.5	7.2
50	0.0467	0.0186	27.6	2221.7	6.8

(a) Experimental observation

(b) $\log K_{NaHCO_3^o} = -\frac{1331.81}{T} + 6.7207 - 8.102 \times 10^{-3}\, T$

(c) $\Delta F^o = 6091.82 - 30.7413\, T + 3.7059 \times 10^{-2}\, T$

(d) $\Delta H^o = 6091.82 - 3.7059 \times 10^{-2}\, T$

(e) $\Delta S^o = 30.7413 - 7.4118 \times 10^{-2}\, T^2$

Table 2. Thermodynamic data for the dissociation reaction

$H_2CO_3 = H^+ + HCO_3^-$

Temp, °C	$-\log K_{1A}$ a/	$-\log K_{1A}$ b/	$-\log K_{1A}$ c/	ΔF, d/ cal/mol	ΔH, e/ cal/mol	ΔS, f/ cal/mol-deg
0	6.580	6.575	6.576	8214.6	4115.3	-15.0
5	6.520	6.518	6.516	8292.7	3774.9	-16.2
10	6.464	6.468	6.464	8377.0	3428.3	-17.5
15	6.426	6.424	6.419	8467.5	3075.5	-18.7
20	6.387	6.387	6.382	8564.1	2716.6	-19.9
25	6.358	6.355	6.351	8666.9	2351.5	-21.2
30	6.329	6.329	6.327	8775.9	1980.2	-22.4
35	6.309	6.308	6.308	8891.1	1602.7	-23.6
40	6.298	6.292	6.296	9012.4	1219.1	-24.9
45	6.293	6.280	6.289	9140.0	829.3	-26.1
50	6.265	6.274	6.287	9273.6	433.3	-27.4

(a) Experimental observation

(b) $\log K_{1A} = -\frac{2914.16}{T} + 11.4685 - 2.700 \times 10^{-2}\, T$

(c) From Harned and Davis (4); $\log K_{1A} = -\frac{3404.71}{T} + 14.8435 - 3.278 \times 10^{-2}\, T$

(d) $\Delta F^o = 13329.66 - 52.4581\, T + 0.12349\, T^2$

(e) $\Delta H^o = 13329.66 - 0.12349\, T^2$

(f) $\Delta S^o = 52.4581 - 0.24698\, T^2$

Table 3. Thermodynamic data for the dissociation reaction

$$NaCO_3^- = Na^+ + CO_3^-$$

Temp, °C	$-\log K_{NaCO_3^-}$ a/	$-\log K_{NaCO_3^-}$ b/	ΔF, c/ cal/mol	ΔH, d/ cal/mol	ΔS, e/ cal/mol-deg
0	0.767	0.767	962.1	2492.0	5.6
5	0.740	0.729	930.6	2871.0	7.0
10	0.678	0.686	892.3	3256.9	8.4
15	0.622	0.640	847.1	3649.7	9.7
20	0.575	0.590	795.0	4049.4	11.1
25	0.550	0.537	736.1	4455.9	12.5
30	0.544	0.480	670.3	4869.3	13.8
35	0.358	0.421	597.6	5289.6	15.2
40	0.356	0.359	518.0	5716.8	16.6
45	0.309	0.294	431.6	6150.8	18.0
50	0.220	0.226	338.3	6591.7	19.4

(a) Experimental observation

(b) $\log K_{NaCO_3^-} = \frac{1698.2}{T} - 15.1982 + 3.007 \times 10^{-2}\, T$

(c) $\Delta F^o = -7767.74 + 69.5181\, T - 0.1375\, T^2$

(d) $\Delta H^o = -7767.74 + 0.1375\, T^2$

(e) $\Delta S^o = -69.5181 + 0.2750\, T^2$

Table 4. Thermodynamic data for the dissociation reaction $HCO_3^- = H^+ + CO_3^{2-}$

Temp, °C	$-\log K_{2A}$ a/	$-\log K_{2A}$ b/	$-\log K_{2A}$ c/	ΔF, d/ kcal/mol	ΔH, e/ kcal/mol	ΔS, f/ cal/mol-deg
0	10.652	10.643	10.626	13.299	5.425	-28.8
5	10.560	10.566	10.554	13.446	5.113	-30.0
10	10.492	10.500	10.488	13.598	4.796	-31.1
15	10.432	10.436	10.429	13.756	4.473	-32.2
20	10.378	10.380	10.377	13.920	4.145	-33.3
25	10.334	10.330	10.330	14.090	3.811	-34.5
30	10.293	10.286	10.288	14.265	3.471	-35.6
35	10.247	10.247	10.252	14.446	3.126	-36.7
40	10.213	10.214	10.220	14.632	2.774	-37.9
45	10.185	10.185	10.193	14.825	2.418	-39.0
50	10.160	10.160	10.171	15.022	2.056	-40.1

(a) Experimental observation

(b) $\log K_{2A} = -\frac{3029.3}{T} + 7.1945 - 2.470 \times 10^{-2}\, T$

(c) From Harned and Scholes (6); $\log K_{2A} = -\frac{2902.39}{T} + 6.4980 - 2.379 \times 10^{-2}\, T$

(d) $\Delta F^o = 13856.32 - 32.9084\, T + 0.1130\, T^2$

(e) $\Delta H^o = 13856.32 - 0.1130\, T^2$

(f) $\Delta S^o = 32.9084 - 0.2260\, T^2$

PART III. THE ASSOCIATION OF CALCIUM WITH CARBONATES

INTRODUCTION:

In a recent note, Lafon (4) selected the "best" available solubility product constant, $\underline{K}_{sp}$, for calcite reported in the literature to get the concentration of Ca^{2+} in a $CaCO_3$-saturated solution which was then used to estimate the $CaCO_3^o$ concentration and its dissociation constant $\underline{K}_{CaCO_3^o} = (Ca^{2+})(CO_3^{2-})/(CaCO_3^o)$, where the parentheses represent activity. However, the best value need not necessarily be the "correct" one since the older $\underline{K}_{sp}$ values are based on the total Ca analysis. Furthermore, in order to prove the existence of $CaCO_3^o$, the choice of the constant is limited to those $\underline{K}_{sp}$ values which will yield computed $[Ca^{2+}] <$ measured $[Ca]_{total}$, where the brackets represent concentration. Theory will be developed and tested on how the dissociation constant of $CaCO_3^o$ can be determined in a saturated $CaCO_3$ solution for a model which includes the Ca-carbonate associated forms $CaCO_3^o$ and $CaHCO_3^+$ and also $CaOH^+$ without an <u>a priori</u> knowledge of $\underline{K}_{sp}$; in fact this computational technique allows the estimation of $\underline{K}_{sp}$ at the same time as $\underline{K}_{CaCO_3^o}$.

COMPUTATIONAL METHOD:

Using approximately the same theoretical starting point as Lafon (4), the mass and charge balance equations for the constituents in a saturated $CaCO_3$ solution are

$$[Ca]_{total} = [Ca^{2+}] + [CaOH^+] + [CaHCO_3^+] + [CaCO_3^o] \quad (1)$$

$$[Carbonate]_{total} = [H_2CO_3] + [HCO_3^-] + [CO_3^{2-}] + [CaHCO_3^+] + [CaCO_3^o] \quad (2)$$

$$[H^+] + 2[Ca^{2+}] + [CaOH^+] + [CaHCO_3^+] = [HCO_3^-] + 2[CO_3^{2-}] + [OH^-] \quad (3)$$

The special equilibrium condition such that $[Ca]_{total} = [Carbonate]_{total}$ (condition of minimum $CaCO_3$ solubility where no carbonate is allowed to enter nor hydrolyzed carbonate to escape) permits the equating of equations (1) and (2) to give

$$[Ca^{2+}] + [CaOH^+] = [H_2CO_3] + [HCO_3^-] + [CO_3^{2-}] \tag{4}$$

Equations (3) and (4) can be resolved into two unknown variables HCO_3^- and Ca^{2+} which can be solved simultaneously with a knowledge of the pH and the dissociation constants for H_2CO_3, HCO_3^-, $CaOH^+$, $CaHCO_3^+$, and H_2O. Subsequently, $[CaCO_3^o]$, $\underline{K}_{CaCO_3^o}$, and also $\underline{K}_{sp}$ can be estimated from the total Ca analysis and the concentration of the constituents making up (3) and (4). More specifically, rewriting equations (3) and (4) in terms of $[Ca^{2+}]$ and $[HCO_3^-]$ gives

$$\frac{(H^+)}{\gamma_H} + 2[Ca^{2+}] + \frac{[Ca^{2+}]\gamma_{Ca}\underline{K}_{H_2O}}{\underline{K}_{CaOH^+}\,\gamma_{CaOH}(H^+)} + \frac{[Ca^{2+}][HCO_3^-]\gamma_{Ca}\gamma_{HCO_3}}{\underline{K}_{CaHCO_3^+}\,\gamma_{CaHCO_3}} =$$

$$= [HCO_3^-] + \frac{2[HCO_3^-]\underline{K}_{HCO_3^-}\,\gamma_{HCO_3}}{(H^+)\gamma_{CO_3}} + \frac{\underline{K}_{H_2O}}{(H^+)\gamma_{OH}} \tag{5}$$

$$[Ca^{2+}] + \frac{[Ca^{2+}]\gamma_{Ca}\underline{K}_{H_2O}}{\underline{K}_{CaOH^+}\,\gamma_{CaOH}(H^+)} = \frac{[HCO_3^-](H^+)\gamma_{HCO_3}}{\underline{K}_{H_2CO_3}\,\gamma_{H_2CO_3}} + [HCO_3^-] +$$

$$+ \frac{[HCO_3^-]\underline{K}_{HCO_3^-}\,\gamma_{HCO_3}}{(H^+)\gamma_{CO_3}} \tag{6}$$

where $\underline{K}_{H_2O} = (H^+)(OH^-) = 1.00 \times 10^{-14}$,

$\underline{K}_{H_2CO_3} = (H^+)(HCO_3^-)/(H_2CO_3) = 4.41 \times 10^{-7}$,

$\underline{K}_{HCO_3^-} = (H^+)(CO_3^{2-})/(HCO_3^-) = 4.65 \times 10^{-11}$,

$\underline{K}_{CaHCO_3^+} = (Ca^{2+})(HCO_3^-)/(CaHCO_3^+) = 5.24 \times 10^{-2}$, and

$\underline{K}_{CaOH^+} = (Ca^{2+})(OH^-)/(CaOH^+) = 4.00 \times 10^{-2}$

and γ is the activity coefficient. Ionic charges to the species in the subscripts for the γ's have been deleted to avoid printing errors.

For the solution of equations (5) and (6), ion activity coefficients as function of ionic strength μ were calculated from the Debye-Huckel relation

$$-\log \gamma_i = Az_i^2\sqrt{\mu}/(1 + B\underline{a}_i\sqrt{\mu}) \tag{7}$$

with constants A, B, and $\underline{a}$ obtained from Kielland (3). The activity coefficients for the uncharged species $CaCO_3^o$ and H_2CO_3 were taken as 1, and also $\gamma_{CaOH} = \gamma_{OH}$, and $\gamma_{CaHCO_3} = \gamma_{HCO_3}$.

The initial ionic strength was assumed to be $3[Ca]_{total}$ to start the iterative computational process. After one preliminary computational run to solve for $[Ca^{2+}]$ and $[HCO_3^-]$, the correct version for μ was used for the model, where

$$\mu = (4[Ca^{2+}] + 4[CO_3^{2-}] + [H^+] + [OH^-] + [CaHCO_3^+] + [HCO_3^-] + [CaOH^+])/2 \tag{8}$$

The iterative computation was made on a digital computer until the constituent concentrations varied less than 0.01%.

RESULTS AND DISCUSSION:

The computational results based on the preceding theory and the saturated $CaCO_3$ solution of Grèzes and Basset (2) with $[Ca]_{total} = 1.315 \times 10^{-4}$ M and pH = 9.945 are presented in Table 1. Some of the concentrations are presented beyond the reliability of the chemical analysis. The procedure used, however, gives a method for computing simultaneously $K_{CaCO_3^o}$ and K_{sp}.

The recomputed $K_{CaCO_3^o}$ is 1.66×10^{-3} compared to that of $K_{CaCO_3^o} = 7.59 \times 10^{-4}$ obtained by Lafon (4) for the same raw data.[3] Lafon assumed that $K_{sp} = 3.98 \times 10^{-9}$ to get $[Ca^{2+}] = 1.263 \times 10^{-4}$ M and subsequently $[CaCO_3^o] = 5.2 \times 10^{-6}$ M; he also assumed the presence of no $CaOH^+$ or $CaHCO_3^+$. Under the special case of high pH, and low total Ca and carbonate concentrations, the magnitude of $[CaCO_3^o]$ is so much smaller than $[Ca^{2+}]$ or $[Ca]_{total}$ that any minor error in the measured variables is reflected by a large difference in the computed $K_{CaCO_3^o}$. In addition, for this particular experimental situation, neither the $CaHCO_3^+$ nor the $CaOH^+$ species can be neglected (Table 1).

The recomputed K_{sp} is 4.31×10^{-9} and as expected lower than the 4.4×10^{-9} value computed by Grèzes and Basset who did not account for any Ca complexing. Both are, however, significantly different from the value of 3.98×10^{-9}.

Actually, if the activity solubility product constant is known, neither the mass balance relation for the carbonate species of equation (2) nor the condition $[Ca]_{total} = [Carbonate]_{total}$ is required for computing $K_{CaCO_3^o}$. The charge balance relation as exemplified by equation (6) can be solved for either $[Ca^{2+}]$ or $[CO_3^{2-}]$ using K_{sp}, pH, and the dissociation constants of the different species. $[CaCO_3^o]$ then can be obtained from the mass balance relation for calcium in equation (1). Dissociation constants for $CaCO_3^o$ were computed using $K_{sp} = 4.31 \times 10^{-9}$ and 3.98×10^{-9} for

the rest of Grèzes and Basset's (2) data and the results are presented in Table 2. The $\underline{K}_{CaCO_3^o}$ for both cases of $\underline{K}_{sp}$'s was not constant, but increased with decreasing $[Ca]_{total}$ and increasing pH. Also, the concentration of $CaCO_3^o$ decreased progressively in a manner similar to the calcite solubility as the partial pressure of CO_2 is decreased. The value of $\underline{K}_{CaCO_3^o} = 6.07 \times 10^{-4}$ accounting for $CaHCO_3^+$ and $CaOH^+$ is different from that of 7.59×10^{-4} which was based on only the $CaCO_3^o$ form of Ca complex.

These preceding results and comparisons still do not resolve the different values of $\underline{K}_{CaCO_3^o}$ reported: 6.31×10^{-4} (1) and 3.29×10^{-5} (5). All the experiments were run in a completely different manner; namely, (a) $CaCO_3$ solution at minimum calcite solubility with no loss or gain of carbonate of Grèzes and Basset (2), (b) $CaCO_3$ solution equilibrated with known partial pressures of CO_2 of Nakayama (5), and (c) $CaCl_2$ titrated with carbonate of Garrels and Thompson (1). Experimental data were not available for case (c), but presumably a closed system was utilized. Garrels and Thompson (1) reported that measurements were made in supersaturated solutions.

We can only speculate at present on the reason or reasons for the different $\underline{K}_{CaCO_3^o}$ reported. If we attribute these to liquid junction potential error, then there are two sources for the Ca- and H-activity measurements in case (b), whereas there is only one for cases (a) and (c). With these latter two closed systems, it is essential that the total concentration of carbonates is known or that the initial concentration is not changed by CO_2 gain or loss. The data set of Grèzes and Basset (2) is actually an extrapolated value. If we assume that the measurements are essentially correct, comparison of the various experimental conditions and $\underline{K}_{CaCO_3^o}$ values indicates a pH-carbonate concentration dependency of $\underline{K}_{CaCO_3^o}$ which suggests the possibility of other Ca-bicarbonate-carbonate-hydroxide associations.

SUMMARY:

A theory was developed and tested for calculating simultaneously the dissociation constant of $CaCO_3^o$ species and the solubility product of calcite in saturated $CaCO_3$ solutions in a closed system. Comparison of the dissociation constants with other published data based on entirely different experimental conditions indicates a possibility for the existence of more complexed Ca-bicarbonate-carbonate-hydroxide associations.

REFERENCES:

1. Garrels, R. M., and Thompson, M. E. A chemical model for sea water at 25°C and one atmosphere total pressure. Amer. J. Sci. 260:57-66. 1962.

2. Grèzes, G. and Basset, M. Contribution à l'étude de la solubilité du carbonate de calcium. Compt. Rend. 260: 869-872. 1965.

3. Kielland, J. Individual activity coefficients of ions in aqueous solutions. J. Amer. Chem. Soc. 59:1675-1678. 1937.

4. Lafon, G. M. Calcium complexing with carbonate ion in aqueous solutions at 25°C and 1 atmosphere. Geochim. Cosmochim. Acta 34:935-940. 1970.

5. Nakayama, F. S. Calcium activity, complex and ion-pair in saturated $CaCO_3$ solutions. Soil Sci. 106:429-434. 1968.

PERSONNEL: F. S. Nakayama and B. A. Rasnick

CURRENT TERMINATION DATE: December 1970

Table 1. Constituent concentrations in $CaCO_3$ solution free of external CO_2, dissociation constant of $CaCO_3^o$, and solubility product of $CaCO_3$ (pH = 9.945, $[Ca]_{total} = 1.315 \times 10^{-4}$ M)

Species	Concentration, moles per liter	Species	Concentration, moles per liter
Ca^{2+}	1.284×10^{-4}	H_2CO_3	2.27×10^{-8}
$CaCO_3^o$	2.60×10^{-7}	HCO_3^-	8.978×10^{-5}
$CaOH^+$	2.68×10^{-7}	CO_3^{2-}	3.889×10^{-5}
$CaHCO_3^+$	2.04×10^{-7}	OH^-	8.977×10^{-5}

$\mu = 4.25 \times 10^{-4}$

$\gamma_H = 0.982$; $\gamma_{HCO_3} = 0.982$; $\gamma_{CO_3} = 0.928$

$\gamma_{OH} = 0.982$; $\gamma_{Ca} = 0.929$

$K_{CaCO_3^o} = 1.66 \times 10^{-3}$; $K_{sp} = 4.31 \times 10^{-9}$

Table 2. Dissociation constant of $CaCO_3^o$ in saturated calcite solution at and near its minimum solubility

$[Ca]_{total}$[a/], M/l x 10^4	pH[a/]	$K_{CaCO_3^o}$[b/], x 10^4		$[CaCO_3^o]$, M/l x 10^6		$[Ca^{2+}]$, M/l x 10^4		$[CaHCO_3^+]$, M/l x 10^7	
		A	B	A	B	A	B	A	B
2.68	8.93	9.14	2.66	4.72	14.97	2.611	2.510	21.34	19.70
1.90	9.28	9.40	3.41	4.58	11.65	1.844	1.774	9.49	8.76
1.64	9.44	19.42	4.81	2.21	8.27	1.610	1.550	6.56	6.05
1.63	9.47	8.91	3.71	4.84	10.72	1.574	1.516	6.12	5.65
1.63	9.48	7.20	3.37	5.99	11.82	1.563	1.505	5.98	5.52
1.56	9.51	17.40	4.88	2.48	8.14	1.528	1.472	5.58	5.15
1.42	9.67	14.76	5.07	2.92	7.85	1.385	1.336	3.86	3.56
1.40	9.71	12.09	4.78	3.56	8.33	1.359	1.312	3.52	3.25
1.34	9.84	12.32	5.10	3.50	7.80	1.300	1.258	2.60	2.40
1.33	9.88	12.49	5.22	3.45	7.63	1.291	1.249	2.38	2.19
1.32	9.90	15.49	5.77	2.78	6.89	1.288	1.247	2.27	2.09
1.315	9.945	16.72	6.07	2.58	6.55	1.284	1.245	2.04	1.89

a/ Data of Grèzes and Basset (2)

b/ "A" and "B" columns computed on basis of $K_{sp} = 4.31 \times 10^{-9}$ and 3.98×10^{-9}, respectively.

TITLE: MATERIALS AND METHODS FOR WATER HARVESTING AND WATER STORAGE IN THE STATE OF HAWAII

CRIS WORK UNIT: SWC-018-gG2 CODE NO.: Ariz.-WCL 65-2

INTRODUCTION:

Treatments and procedures remain the same as described in previous Annual Reports. The Maui test site was visited in June 1970 at which time all meters were cleaned and additional filter screens installed.

RESULTS AND DISCUSSION:

Kakaiau Catchment. This unit was not visited during 1970. It is assumed the catchment and reservoir are performing satisfactorily. Rainfall data forwarded monthly to the Laboratory showed 3,244 mm of rainfall were recorded for 11 months in the year. Rainfall data for July 1970 were not received.

Maui Catchments. All plots were considered in satisfactory condition when inspected in June 1970. The new water meter measuring system installed on the plots in September 1969 has not performed as expected. Trouble has been encountered with plugging of the meters on the three treated plots with grass seeds and other small debris. When the system was originally installed, a set of screens were installed in the V-shaped headboxes on each plot. These proved to be unsatisfactory. In June 1970, additional cone-shaped screens were installed in the entrance pipe to each meter. Runoff data and correspondence with maintenance personnel from East Maui Irrigation Company indicate plugging of the meters still occurs. The debris is believed to come from grasses growing around the edges of the plots. Meter plugging has not occurred on the natural grass plot. The grasses on the plot apparently filter the runoff water before it reaches the meters.

Rainfall and runoff data for the grass plot since installation of the water meter measuring system are presented in Table 1. The measurements show that over 30% of the precipitation has run off.

This is much higher than was originally expected. At the time of the original plot installation, local personnel expressed the opinion there would be no runoff from the plot.

Experimental Ditch Lining. The experimental ditch lining was inspected during the June 1970 trip. A considerable growth of nutgrass had penetrated the lining. No attempt had been made to cut or otherwise control the weed. The growth of penetrating weeds must be controlled before the asphalt-fiberglass or any other flexible membranes can be an effective liner.

SUMMARY AND CONCLUSIONS:

The Kukaiau catchment and storage unit was not inspected during the year. It is assumed the unit is performing satisfactorily.

Treatments at the Maui test site were in good condition when visited in June 1970. Meters on the three treated plots have been plugged by debris which falls on the plot and is small enough to pass through the filter screens. The plugging has not been a problem with the grass plot. Measured runoff from the grass plot since installation of the meters in September 1969 has averaged 30% of a total of 3,018 mm of precipitation.

PERSONNEL: L. E. Myers and G. W. Frasier.

CURRENT TERMINATION DATE: December 1970

Table 1. Rainfall and runoff results from the grass plot at Maui test site.

Date		Rainfall	Runoff	
Start	Stop			
		(mm)	(mm)	(%)
28 Sep 69	10 Nov 69	111.2	2.4	2.2
10 Nov 69	23 Dec 69	146.1	11.0	7.5
23 Dec 69	23 Feb 70	508.0	218.9	43.0
23 Feb 70	22 Mar 70	63.0	0	0
22 Mar 70	6 Apr 70	111.2	12.2	10.9
6 Apr 70	24 Apr 70	336.6	139.9	41.6
24 Apr 70	19 May 70	85.7	0	0
19 May 70	12 Jun 70	56.7	.9	1.6
24 Jun 70	23 Jul 70	298.5	64.2	21.5
23 Jul 70	2 Oct 70	400.0	119.4	29.9
2 Oct 70	18 Nov 70	472.5	190.2	40.2
18 Nov 70	16 Dec 70	428.6	164.6	38.0
Total		3018.1	923.7	30.6

TITLE: PHYSICAL AND CHEMICAL CHARACTERISTICS OF HYDROPHOBIC SOILS

CRIS WORK UNIT: SWC-018-gG-2 CODE NO.: Ariz.-WCL 67-2

PART I. BONDING OF ORGANIC MOLECULES TO INORGANIC SOIL AND CLAY SURFACES

INTRODUCTION:

The adsorption apparatus contrived the previous year underwent additional testing in 1970. Attention was directed toward gathering evidence of chemical bonding of organics with soil surfaces. The test results of reacting a silicone with a soil show promise and are presented here. In studies pertaining to the creation and evaluation of hydrophobic soils, one may expect to encounter chemical adsorption (Type-I isotherms), physical adsorption of water on hydrophilic surfaces (normally Type-II isotherms), physical adsorption of water on hydrophobic surfaces (normally Type-III isotherms), and possibly, occasional other types. Type of isotherm, here, refers to the general shape of the isotherm over the relative vapor pressure range of the adsorbate ($0 < p/p_o < 1$).

It is estimated, however, that 95% of all adsorption isotherms recorded are Type-II; most adsorption isotherms for hydrophilic clays and soils also are of this type. The Type-II, which describes a sigmoid, has engendered no little effort for the creation of mathematical relations which aptly describe the isotherm. Some of these relations are empirical; others, which are based on simplified scientific principles, tend toward semi-empiricism. None aptly describe the Type-II adsorption isotherm over the complete relative vapor pressure range ($0 < p/p_o < 1$). This impasse, plus a remedial need, coupled with a rather casual observation that the Fermi-Dirac statistics of quantum statistical mechanics describes a sigmoid curve, led to the development of an equation which seems uniquely well suited for describing Type-II adsorption isotherms. This report presents the equation, describes its development, and compares it to five well known adsorption equations.

THEORY:

The probability distribution (Pr) of particles among discrete energy states (E) within a system can be represented by

$$Pr = 1/[1 + \exp(\alpha + \beta E)] \qquad (1)$$

where α and β are constants related to the total number of particles and to their total energy. Equation (1), which is derived using Fermi-Dirac statistical mechanics, describes a sigmoid with Pr going to 1 or 0 (depending upon the sign of β) as E becomes infinite. Pr becomes equal to $1/[1 + \exp(\alpha)]$ as E approaches 0. The inflection of the sigmoid invariantly occurs at Pr = 1/2.

An equation which describes Type-II adsorption isotherms over a wide range of pressures must satisfy the conditions

$$W \rightarrow \infty \text{ as } p/p_o \rightarrow 1 \qquad (2a)$$

$$W \rightarrow 0 \text{ as } p/p_o \rightarrow 0 \qquad (2b)$$

and

$$d^2W/d(p/p_o)^2 = 0 \text{ for a single value of } p/p_o \text{ in the range } 0 < p/p_o < 1 \quad . \qquad (2c)$$

If, in equation (1) the relative vapor pressure (p/p_o) is substituted for the probability distribution (Pr), and the amount of adsorbed gas (W) for energy (E), one finds that only condition (2a) is satisfied. To rectify this limitation the probability and energy terms are redefined as

$$Pr = f(p/p_o) \qquad (3a)$$

and

$$E = g(W) \qquad (3b)$$

and equation (1) written in the forms

$$f(p/p_o) = 1/\ 1 + \exp[\alpha + \beta g(W)] \quad (4a)$$

$$g(W) = A + B \ln[f(p/p_o)^{-1} - 1] \quad (4b)$$

where $A = -\alpha/\beta$ and $B = 1/\beta$. It is necessary now to determine the functions $f(p/p_o)$ and $g(W)$ so as to meet all the conditions in equations (2).

If $f(p/p_o) = (p/p_o)^c$, where c is constant, condition (2c) is met since p/p_o is no longer restricted to the value of 1/2 at the inflection point. Condition (2b) is met if $g(W) = \ln W$, for $B < 0$; B is inherently negative for Type-II adsorption isotherms. These substitutions in equation (4b) lead to

$$\ln(W) = A + B \ln[(p/p_o)^{-c} - 1] \quad (5)$$

Remembering that B is always negative, it is easily shown that equation (5) meets all the conditions of (2).

PROCEDURE:

The gas adsorption apparatus used in this experiment was described in the 1970 Annual Report. Basically it controls vapor pressure using a dynamic gas flow system, and employs a micro-balance to determine adsorption. In the study on chemisorption of methyltrichlorosilane by soils, an acidic Lloyd soil, high in amorphous iron and aluminum hydroxides was dried to equilibrium weight by continually passing dried N_2 gas past the sample at 20 C. A nearly saturated atmosphere of methyltrichlorosilane was then introduced past the sample by bubbling the N_2 through the silicone liquid. When adsorption ceased, pure N_2 gas again was flowed through the system to remove any physisorbed silicone. When equilibrium weight again was attained, a water vapor adsorption isotherm was determined on the now silicone treated soil.

The procedure for fitting the proposed Type-II adsorption isotherm equation (equation 5) to experimental adsorption data employed a simple computer program. An initial value of c was chosen, A and B were calculated by least squares and the correlation coefficient r obtained. Using an iterative procedure, c was sequentially stepped until a maximum value of r was obtained for three significant figures of c. The constants A, B, and c along with the corresponding r values were computed for 41 sets (Table 1) of adsorption data. The adsorption equations (Table 2) of Brunauer, Emmett and Teller (BET); Frenkel-Halsey-Hill (FHH); Harkins and Jura (HJ); Dubinin-Kagoner (DK); and Freundlick (F) were statistically fit to the same data, and the corresponding r values obtained.

RESULTS:

Figure 1 shows that methyltrichlorosilane can be chemisorbed to soil; for this Lloyd soil the chemisorption amounted to 16.9 mg/g. The soil hydroxyl sites remaining after drying with N_2, readily reacted with the silicone as attested to by the rapid increase in weight after introduction of the reactant gas (point A). The gradual loss in weight beyond attainment of the maximum weight (40 mg/g) probably represents the loss of some residual, strongly hydrogen-bonded soil water that had now chemically reacted with the silicone, but which had not chemically cross-linked to the soil-surface hydroxyls. The continued flushing with methyltrichlorosilane gradually dissociated these strongly physisorbed molecules from the soil surface. The difference between 16.9 and 40 mg/g, thus, is due both to unreacted, physisorbed methyltrichlorisilane, and partly due to the physisorbed silicone which has chemically reacted with the small amounts of residual water remaining on the soil after the initial drying with N_2 gas. Both of these two types of molecules are swept away by the introduction of pure N_2 at point B.

After equilibrium weight again had been attained, water vapor was introduced into the system. Figure 2 shows the adsorption

isotherms for water on the Lloyd soil before and immediately after the silicone treatment. The silicone treatment has changed the water adsorption isotherm from a typical Type-II (strong physisorption) to a Type-III (hydrophobic, low surface energy).

As the relative vapor pressure was increased beyond about $p/p_o = 0.2$, large amounts of water adsorbed on the surface. In fact, beyond $p/p_o = 0.6$ the amount of water adsorbed on the silicone treated soil exceeded that on the untreated soil. This may be due in part to enhanced capillary condensation, but more likely it is due to the water reacting chemically with unreacted Cl- sites on the silicone molecules. Each silicone initially had three reactive chlorine sites - if only one or two reacted with the soil hydroxyl, then the remaining chlorines were available for reaction with the now-introduced water vapor. If the reaction indeed was between the water and the chlorine sites, it is strange that it did not proceed even at the low vapor pressures ($p/p_o < 0.1$). The anomalies warrant additional investigation.

In the search for an equation to better describe Type-II adsorption isotherms, it was found that the new equation (5) indeed described such isotherms, and did so over a wide vapor pressure range. Figure 3 which shows an adsorption and desorption isotherm of water on a soil, also shows the data replotted according to equation (5). After first computing the best fit values for the constant c, the corresponding x, y variables, i.e. $\ln [(p/p_o)^{-c} - 1)]$. and $\ln(W)$ of equation (5) were computed for each data point, and then replotted. Each computed point in the figure corresponds to the data point which is nearly vertically below or above. Equation (5) presents the adsorption data in a linear form - including the data at high and low vapor pressures, and because of the ln x, ln y feature, permits an even distribution of that data through the weight, pressure range. The computed r values for both the adsorption and desorption branches of the isotherm were better than 0.999.

Equation (5) consistently and accurately described the Type-II adsorption isotherms of clay and soil adsorbents using several adsorbates, including water, ehtylene dibromide and carbon tetrachloride (Table 1). Of the 41 data sets tested, 40 gave a correlation coefficient (r) of 0.99 or better; the one exception had an r-value of only 0.98. Correlation coefficients of the data were then determined for five other established isotherm equations (Table 2), and compared to the new equation. These data, summarily presented in Figure 4, show that none of the five established equations consistently described the adsorption isotherms as accurately as did equation (5). Of the established five, the FHH did the best, but none ever approached the ability of the new equation for describing such data.

No serious attempt has been made to date to try to assign any physical significance to the three constants (A, B, c) of the equation. No obvious relationships could be found, therefore, the equation may be strictly empirical. This is certainly worthy of additional study. The equation shows promise for predicting field water contents in either the vapor phase or the adsorbed phase - depending on the parameter which is measured; it may have utility in equations predicting vapor transfer in soils, and this general type of equation also may be adaptable to other situations where the results describe a sigmoid, e.g. soil-water potential and particle size distribution curves.

SUMMARY AND CONCLUSIONS:

Adsorption isotherm work has shown that methyltrichlorosilane can be chemically bonded to an acidic soil rich in amorphous iron and aluminum hydroxide. Water adsorption isotherms on the soil sample before and after the silicone treatment were Type-II and Type-III, respectively, showing that the silicone treatment substantially lowered the surface energy of the soil - in effect, making it water-repellent.

A new equation for describing the Type-II adsorption isotherms has been contrived. The equation in linear form is: $\ln(W) = A + B \ln [(p/p_o)^{-c} - 1]$. It was compared statistically to five other well known adsorption equations for accuracy in describing 41 adsorption isotherms of several adsorbates on soil and clay samples. The relative vapor pressure range of these 41 isotherms ranged from as low as $p/p_o = 0.0006$ to as high as $p/p_o = 0.98$. The new equation had a correlation coefficient (r) in the test for linearity of 0.99 or better, for 40 of the 41 isotherms; this was markedly better than for any of the other 5 equations tested. The new equation describes a sigmoid, has correct form at the relative vapor pressure limits (i.e., $p/p_o \rightarrow 0$, and $p/p_o \rightarrow 1$), and because of the third constant (c), permits a variant inflection point in the sigmoid. For the first time it now appears that a simple equation is available for describing well over 90% of all adsorption isotherms - and apparently can do so over practically the complete relative vapor pressure range.

PART II. Na-Ca-DEMIXING IN FREE-SWELLING MONTMORILLONITES

INTRODUCTION:

The introduction to the "demix" phase of this study was presented in the 1968 Annual Report. The preliminary experimental results did not conform to the proposed theory of swelling of such Na-, Ca-montmorillonite systems, so it was postulated that either: (1) the original x-ray data were faulty or inadequate, or (2) the theoretical models were incorrect. To resolve this impasse, supplemental x-ray diffraction analyses of the samples were run in 1970. In addition to the demix study, another critical look was directed at the physical-chemical factors controlling the free-swelling of both Na- and Li-montmorillonites. Existing equations for describing this free-swelling generally over-predicted the resultant interlayer expansion as water was added to the system. The objective was to correct the equations, if possible, through the development of improved, theoretically-based parameters. This report presents the culmination of these studies.

THEORY:

The interlayer swelling of Na-montmorillonite due to osmotic hydration is linearly related to the total water content present. This swelling has been shown (9) to closely conform to the equation:

$$d = (9.4 - uW_e/S_i) + uW_t/S_i \qquad (6)$$

where d is the d-spacing of the expanded montmorillonite in Angstroms; 9.4A is the thickness of the individual montmorillonite sheets; W_t is the total weight of water in the system (g/g); W_e is the sum of the weight of water associated with the external surfaces and with the non-free-swelling internal surfaces (g/g); S_i is the internal surface area of the free-swelling portion of the clay (m^2/g); and u is a combined constant and conversion factor equal to 2×10^4 $A \cdot m^2/g$. Equation (6) predicts a linear plot of d vs W_t provided that W_e remains constant as W_t increases.

Conceivably, converting from a pure Na-montmorillonite system to a mixed Na-, Ca-system would alter the swelling behavior of the clay. The type and extent of this alteration should depend on (1) whether the two ion types randomly mix on the exchange complex - or demix; (2) the relative proportion of Na^+ (ESP) on the exchange complex; (3) the state of hydration.

Illustrative examples of the clay swelling to be expected for several types of Na:Ca distribution were presented in the 1968 Annual Report. Swelling models were developed for (a) complete random mixing of the two cations on the exchange complex, (b) complete demixing by domains, and (c) complete demixing by alternate layers.

Earlier it had been shown that for Na- or Li-montmorillonites equation (6) predicted that plots of d-spacing (d) vs the total water content (W_t) should be linear, provided that the external water (W_e) remained constant (i.e. (W_e = a) as W_t increased. Most of the experimental swelling data closely conforms to equation (6), but when error occurs, the theoretical equation generally over-predicts

the interlayer swelling. Thus, an attempt to improve the equation was initiated.

Using mathematical deduction, it was shown that plots of d vs W_t could be linear both when $W_e = a$, as originally surmised, and, also when

$$W_e = \underline{a} + \underline{b}W_t \tag{7}$$

The $\underline{b}W_t$ term of equation (7) allows for a linear increase in external water as the total water in the system increases. This then would account for the regular over-prediction of interlayer swelling previously encountered using equation (6). Equation (6) may be corrected for the addition of the $\underline{b}W_t$ term:

$$d = [9.4 - u\underline{a}/S_i] + [u(1-b)/S_i]W_t \tag{8}$$

The plots of d vs W_t now have intercepts of $(9.4 - u\underline{a}/S_i)$ and slopes of $u(1-\underline{b})/S_i$.

The constant $\underline{a}$ in the intercept term has units of grams water per gram of total solids present, and probably corresponds to that quantity of water of hydration which does not change as W_t increases, e.g. water between non-free-swelling internal surfaces such as any vermiculite component present, or perhaps to the initial hydration of certain high-energy adsorption sites. The $\underline{b}W_t$ term provides for a linear increase in the external water of hydration as the total water in the system increases, and probably corresponds to that quantity of water associated with intra-packet regions.

The application of equation (8) to free-swelling data thus should permit a quantitative differentiation of the water of hydration between internal and external clay surfaces, and also permit a separation of the external water into a constant and a variable portion with the latter dependent upon the total water content

present. To illustrate this, a family of curves is presented in Figure 5 showing how changing the term b (holding a and S_i constant) affects the hypothetical swelling of montmorillonite. As b increases from zero, the slope of the swelling curves decreases and the proportion of water associated with external surfaces increases. Changing a or S_i would produce another family of curves.

Equation (8) now contains three unknowns: a, b and S_i, and cannot be solved solely from d vs W_t plots. A separate determination or means of accurately estimating one of the unknowns is needed. S_i seems the logical first choice for separate evaluation since means for obtaining it are readily available. Armed with a value for S_i, a and b then may be readily determined. This has been done (Table 3) for all the known data on free-swelling montmorillonites. The a and b values normally are positive and range from 0 to 0.25 for a (average 0.09) and 0 to 0.47 for b (average 0.10). The b = -0.14 value is extremely questionable - therefore, has been disregarded.

There is an overall lack of consistency in the a and b values of Table 3, which would seem to preclude their indiscriminate application to new clay-swelling situations. Concomitantly, these inconsistencies suggest either that there may be some systematic error associated with the d-spacing determinations, or that slight variations in the clay sample preparation procedures in turn affect the degree of clay swelling.

An experiment thus was designed to try to relate variation in b to variation in experimental procedure. Altering the salt concentration in the solution phase was selected since salt had already been shown to reduce swelling (10). The objective was to determine if b regularly decreased as concentration in the solution phase decreased - with the intent of extrapolating the b values to zero salt content.

PROCEDURE:

The experimental procedures and clay samples for the "demix" study were the same as outlined in the 1968 Annual Report, except that the d-spacings were determined using a different x-ray diffractometer.

A subsample of Na-Wyoming bentonite from the "demix" study was used in the study to confirm the validity of the corrected free-swelling equation. The Na-bentonite for this study was split into four subsamples, dried over P_2O_5, then each subsample was rehydrated to 1g H_2O/g clay using one each of the four NaCl solutions: 0.100, 0.010, 0.100 or 0.300 N. Each clay-salt combination was thoroughly mixed in a vial, stoppered to eliminate evaporation, then stored for two weeks with occasional mixing.

The four subsamples described previously were then all further subdivided into approximately one gram clay samples, and each of the four sets was then diluted with increasing amounts of deionized water. Again, the samples were mixed, stoppered, and equilibrated for two weeks. The d-spacings were determined on these clay pastes using the same low-angle techniques previously described.

RESULTS:

The plots of d-spacing versus total water content (W_t) for the higher ESP values studied are shown in Figure 6. The slopes at ESP = 91 and ESP = 50 were nearly the same, at approximately u/800 m^2/g. As noted previously, such behavior indicates random mixing of exchangeable cations on the exchange complex. Further support for random mixing of the Na- and Ca-ions at ESP = 57% and higher was provided by the complete absence of any detectable 20A phase at the higher water contents, i.e. greater than approximately 1.25 g/g.

There was definite evidence, however, of cation demixing at ESP levels of 38 and 29%. The x-ray diffractograms in this range gave peaks for two repeat spacings, one at or near 20A corresponding to a Ca-phase, and another, a low-angle peak corresponding to a Na-phase. The slopes of the swelling lines in this ESP range were also substantially greater than u/800. Although ion demixing definitely occurred, the extent of this demixing was far from complete. For complete demixing, the slopes of the ESP 38 and 29% samples should have been approximately u/300 and u/240, respectively, rather than u/660 and u/400 shown in Figure 6. The Na-ions apparently exerted

an undue influence in promoting this free-swelling. The observation that no 20A phase existed for ESP levels greater than 57% was further evidence for the enhanced influence of Na-ions in dominating the swelling behavior of the system.

The lines through the low-angle (high d-spacing) data points at ESP 29 and ESP 38 in Figure 6 were drawn by visual inspection only. The x-ray data were not of sufficient quality to justify the use of statistics to establish exact slopes and intercepts. The intercepts selected (10A) were a compromise between the domain demixing and the alternate layer demixing hypotheses. The x-ray techniques used in this experiment thus did not permit establishing whether the demixing was by domain or by alternate layers. Hopefully, improved low-angle x-ray diffraction techniques will be developed to aid in resolving this issue.

The initial nonlinear portion of the swelling curves at ESP 29 and ESP 38 in Figure 6 apparently represents a "jump" at the point of initiation of osmotic swelling in the systems. This behavior is similar to the "jump" in spacing recorded by Norrish (10) and others (9, 11) for homoionic Na-Wyoming bentonite. However, for homoionic Na-bentonite, the recorded jump was only from about 20A to 35A, whereas for the two mixed-ion clays, it was from 20A to 50A and from 20A to 120A, respectively. The presence of some Ca-ions in predominantly Na-saturated regions probably increases Coulombic forces, so that a greater swelling potential was necessary before these regions could "jump" into the osmotic swelling region.

X-ray diffractograms for a sample with ESP of 12 showed evidence for only the 20A spacing of completely hydrated Ca-montmorillonite. Admittedly, small quantities of free-swelling Na-clay in a predominantly Ca-saturated system could go undetected using the method. However, these data, when coupled with those of previous investigators, suggest that at low ESP values mixed-ion clays exist as tactoids, with the interlayer exchange sites predominantly Ca-saturated, and with the external exchange sites predominantly Na-saturated.

The experimental results pertaining to the effects of salt on the swelling of a Na-montmorillonite are shown in Figure 7. The d-spacing is a linear function of total water content (W_t), at least for the three most dilute salt concentration series. Surprisingly, the two most dilute solution series of 0.001 and 0.010 N had identical b values, and equally surprising, that value was zero. The original intent of relating b to salt concentration thus was thwarted.

However, increasing the salt content of the initial sample to 0.1 N did retard interlayer swelling throughout the dilution range tested (b = 0.18). Increasing concentration of 0.3 N collapsed the clay to the meta-stable 20A phase, but osmotic swelling was initiated in this sample by dilution with water. A b value of 0.25 is listed for this 0.3 N series, even though no definite linear swelling region existed. Thus, the b value has seemingly cycled for approximately b = 0.1 for a zero salt content (Table 3), then decreased to b = 0 for a low salt content, only to increase again to b = 0.18 and .26 as salt content increases still farther. The rationale for relating this apparent cycling of b as a function of salt content to clay physical or chemical properties is obscure.

This seeming inconsistency in the b value, coupled with those already shown in the data in Table 3, suggests that the causal agents of these inconsistencies may be variations in experimental techniques of clay preparation or possible errors associated with the d-spacing determinations, or possibly other unknown factors. Obviously, further closely controlled and meticulously accurate experimentation is called for.

The b value, if determinable, provides a means for establishing the proportion of the total water of hydration that is associated with external and non-free-swelling surfaces, i.e. $(a + bW_t)/W_t$. The b value, if controllable at zero or some consistent value by manipulation of clay preparation procedures, provides a means for extremely accurate determination of the internal surface area of

these free-swelling clays and thus should lead to accurate quantitative determination of the free-swelling clay portion in clay type mixtures. Of course, if one is content with about 15 to 20% accuracy in the determination of internal surface area using this swelling technique, one may simply assume $\underline{b} = 0$; or one may acquire a bit more superficial sophistication ($\pm$ 10% accuracy) by assuming that for most Na- and Li-montmorillonites $b = 0.10$. Certainly this matter of fitting theoretically sound equations to free-swelling data plots is not completely resolved.

SUMMARY AND CONCLUSIONS:

Hypothetical models for the crystalline, interlayer swelling of mixed-ion (Na^+ and Ca^{2+} saturated) montmorillonites in water were developed for two types of cationic distributions on the clay minerals: namely, for complete demixing and for complete random mixing of cations. In addition, the model for demixing was expanded to include both the alternate layering of Ca- and Na-saturated platelets and the complete demixing of cations into separate Na- and Ca-domains. The theoretical development is based on the accepted principles of limited interlayer swelling (10A maximum) for Ca-montmorillonite, and free-swelling for Na-montmorillonite as the water content of the system is increased beyond approximately 120%. Experimental measurements of interlayer swelling using a low-angle x-ray diffraction technique showed that the relative distribution of Na^+ and Ca^{2+} ions on the clay exchange complex was a function of the exchangeable sodium percentage (ESP): (1) the two cations were randomly mixed for ESP values greater than approximately 50%; (2) they were partially demixed for ESP values between approximately 50 and 15%; and (3) for ESP values less than approximately 10 to 15% no cation demixing in interlayer regions was evident, but the results did suggest that the interlayer exchange complex was predominantly Ca-saturated and the exchange complex on external surfaces was predominantly Na-saturated. Although the experimental techniques could establish that demixing occurred within certain ranges of ESP values,

it was not sensitive enough to differentiate between demixing by domains and demixing by alternate layers.

The consequences of such demixing of exchangeable cations on clay may include soil structural alteration through preferential erosion of any Na-clay portion; also, localized demixing could influence ion diffusion, water movement, shrink-swell properties and dispersion of soil materials.

Also, an equation was presented which describes the linear expansion of free-swelling Na- and Li-saturated montmorillonite clays in water. An attempt was made to relate the slope-intercept terms of these d-spacings versus total water content plots to theoretically acceptable parameters. Basically, provision was accorded for the presence of a measurable portion of the total water present being associated with non-free-swelling mineral surfaces: (1) a constant, normally small portion being relegated to the intercept term of the equation, and (2) a portion which increases proportionately as the total water content increases, being relegated to the slope term. The equation thus permits a quantitative differentiation of the water of clay-swelling between internal and external clay surface positions, and further differentiates the external water into a fixed, hygroscopic portion and a portion which increases proportionately as the total water in the system increases.

REFERENCES:

1. Martin, R. T. Water vapor sorption on kaolinite: Hysteresis. Clays and Clay Minerals 6:259-277. 1959.

2. Jurinak, J. J. Multilayer adsorption of water by kaolinite. Soil Sci. Soc. Am. Proc., 27:269-272. 1963.

3. Hill, K. J. PhD Thesis, London. In Adsorption, Surface Area and Porosity, Gregg, S. J., and Sing, K. S. W., pp. 100-101. Academic Press, London. 1967.

4. Orchiston, H. D. Adsorption of water vapor: II. Clays at 25 C. Soil Sci. 78:463-480. 1954.

5. Orchiston, H. D. Adsorption of water vapor: I. Soils at 25 C. Soil Sci. 76:453-465. 1953.

6. Gary, J. W., Kohl, R. A., and Taylor, S. A. Water adsorption by dry soil and its thermodynamic functions. Soil Sci. Soc. Am. Proc. 28:309-314. 1964.

7. Jurinak, J. J., and Volman, D. H. Application of the BET equation to ethylene dibromide adsorption by soils. Soil Sci. 83:487-496. 1956.

8. Jackson, R. D. Water vapor diffusion in relatively dry soil: III. Steady-state experiments. Soil Sci. Soc. Am. Proc. 28: 467-470. 1964.

9. Fink, D. H., Rich, C. I., and Thomas, G. W. Determination of internal surface area, external water, and amount of montmorillonite in clay-water systems. Soil Sci. 105:71-77. 1968.

10. Norrish, K. The swelling of montmorillonite. Disc. Faraday Soc. 18:120-134. 1954.

11. Foster, W. R., Savins, J. G., and Waite, J. M. Lattice expansion and rheological behavior relationships in water-montmorillonite systems. Clays and Clay Minerals 3:296-316. 1954.

12. Hight, R., Jr., et al. Small angle x-ray scattering from montmorillonite clay suspensions: II. J. Chem. Phys. 37: 502-510. 1962.

PERSONNEL: Dwayne H. Fink, R. D. Jackson and F. S. Nakayama.

CURRENT TERMINATION DATE: December 1971.

Table 1. Sources of the 41 adsorption isotherms used in this study; inc.: adsorbate, adsorbent, pressure range covered, and number of data points for each.

Ref. adsorbate adsorbent	p/p_o range	n 4/
Martin (1); H_2O 1/		
Li-kaolinite	0.003-0.92	20
Na-kaolinite	0.002-0.77	25
Jurinak (2); H_2O 1/		
Li, Ba, Ca, Al-kaolinite	0.2-0.97	10
Na, Li (Peerless)-kaolinite	0.2-0.9	8
Hill (3); CCl_4 2/		
kaolinite	0.04-0.8	22
Orchiston (4); H_2O 2/		
unheated:		
Ariz. montmorillonite, illite, green sand,	0.1-0.9	9
silica gel	0.1-0.8	8
heated (600 C):		
mont., illite,	0.1-0.8	8
green sand,	0.1-0.4	4
silica gel	0.1-0.5	5
Orchiston (5); H_2O 1/		
7 soils	0.081-0.842	14
Cary et al. (6); H_2O 1/		
Millville soil		
14.8 C	0.0012-0.98	21
24.8 C	0.0006-0.88	15
34.8 C	0.0002-0.65	15
Jurinak & Volman (7); EDB 2/		
5 soils	0.1-0.9	9
1 soil	0.1-0.6	
Jackson (8); H_2O 3/		
2 soils, 3 isotherms	0.118-0.97	11
2 soils, 5 isotherms	0.03-0.84	13

1/ published data
2/ from published smoothed curve
3/ some data not previously published
4/ number of data points

Table 2. Equations for describing Type-II adsorption isotherms

Equation	Linear form
[5]	$\ln W = A + B \ln [(p/p_o)^{-c} - 1]$
BET	$p/W(p_o - p) = A + B(p/p_o)$
FHH	$\ln W = A + B \ln[\ln(p_o/p)]$
HJ	$W^{-2} = A + B \ln(p/p_o)$
DK	$\ln W = A + B \ln(p_o/p)$
F	$\ln W = A + B \ln(p/p_o)$

Table 3. Parameters for describing free-swelling data using equation (8)

Reference	Clay Mineral	Montmorillonite	Internal Surface Area Theoretical	Internal Surface Area Swelling*	b**	a**
		%	m^2/g	m^2/g		g/g
F.R.T. (9)	Na-Wyoming bentonite	100	746	826	0.10	0.12
F.S.W. (11)	"	100	746	833	0.10	0.20
N. (10)	"	100	746	896	0.17	0.09
H.H.D.S. (12)	"	100	746	1417	0.47	0.00
F.R.T. (9)	(plus kaolinite)	90	671	685	0.02	0.05
F.R.T.	"	70	522	456	-0.14	0.25
F.R.T.	"	50	373	368	-0.01	0.12
F.R.T.	"	30	224	229	0.02	0.12
F.R.T.	Na-hectorite	100	765	759	-0.01	0.11
F.R.T.	Li-Wyoming bentonite	100	757	858	0.12	0.12
F.S.W. (11)	"	100	757	731	-0.03	0.13
F.R.T. (9)	Li-Otay bentonite	100	762	955	0.20	0.01
F.R.T.	Li-hectorite	100	771	886	0.13	0.02
F.R.T.	Li-nontronite	100	687	757	0.09	0.09

*Computed from swelling data using equation (8), assuming b = 0.

**Computed from swelling data using equation (8), assuming the theoretical planar surface area for S_i.

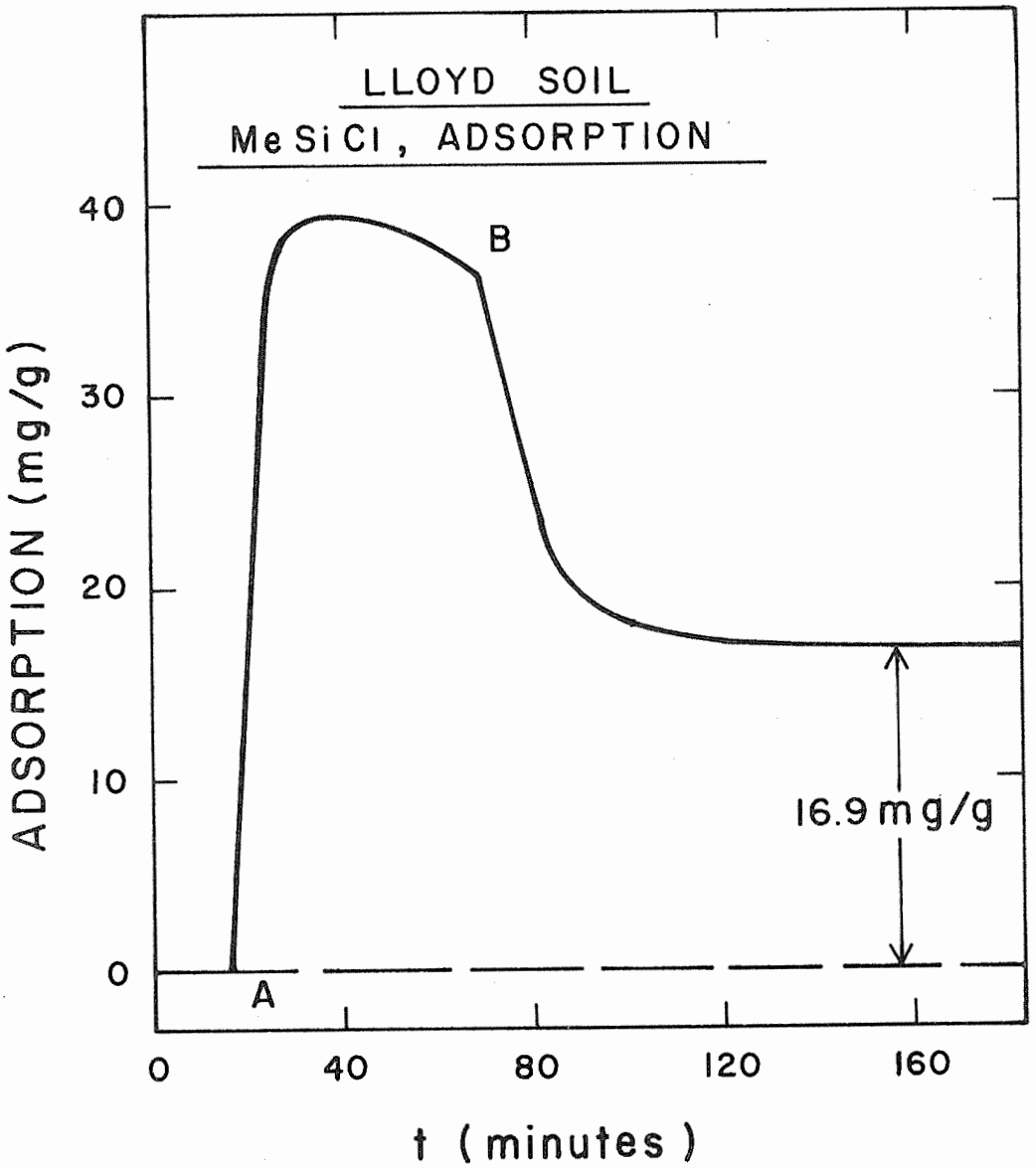

Figure 1. Adsorption - rate study of methyltrichlorosilane on Lloyd soil: N_2 gas only from t_o to point A; N_2 carrier plus M_e S_i Cl_3 from A to B; N_2 gas only beyond point B.

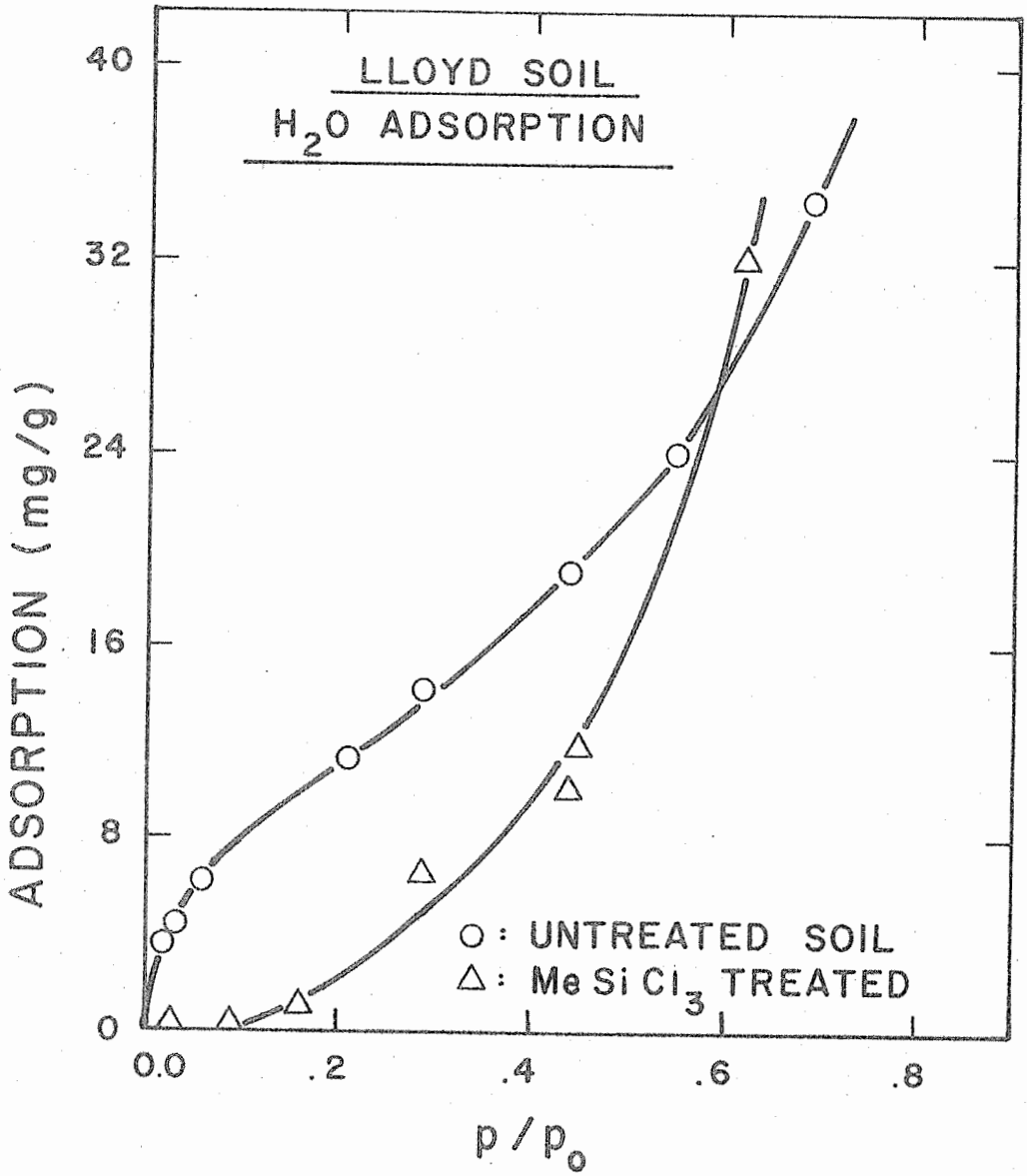

Figure 2. Adsorption isotherms of water on a Lloyd soil before and after treatment with methyltrichlorosilane.

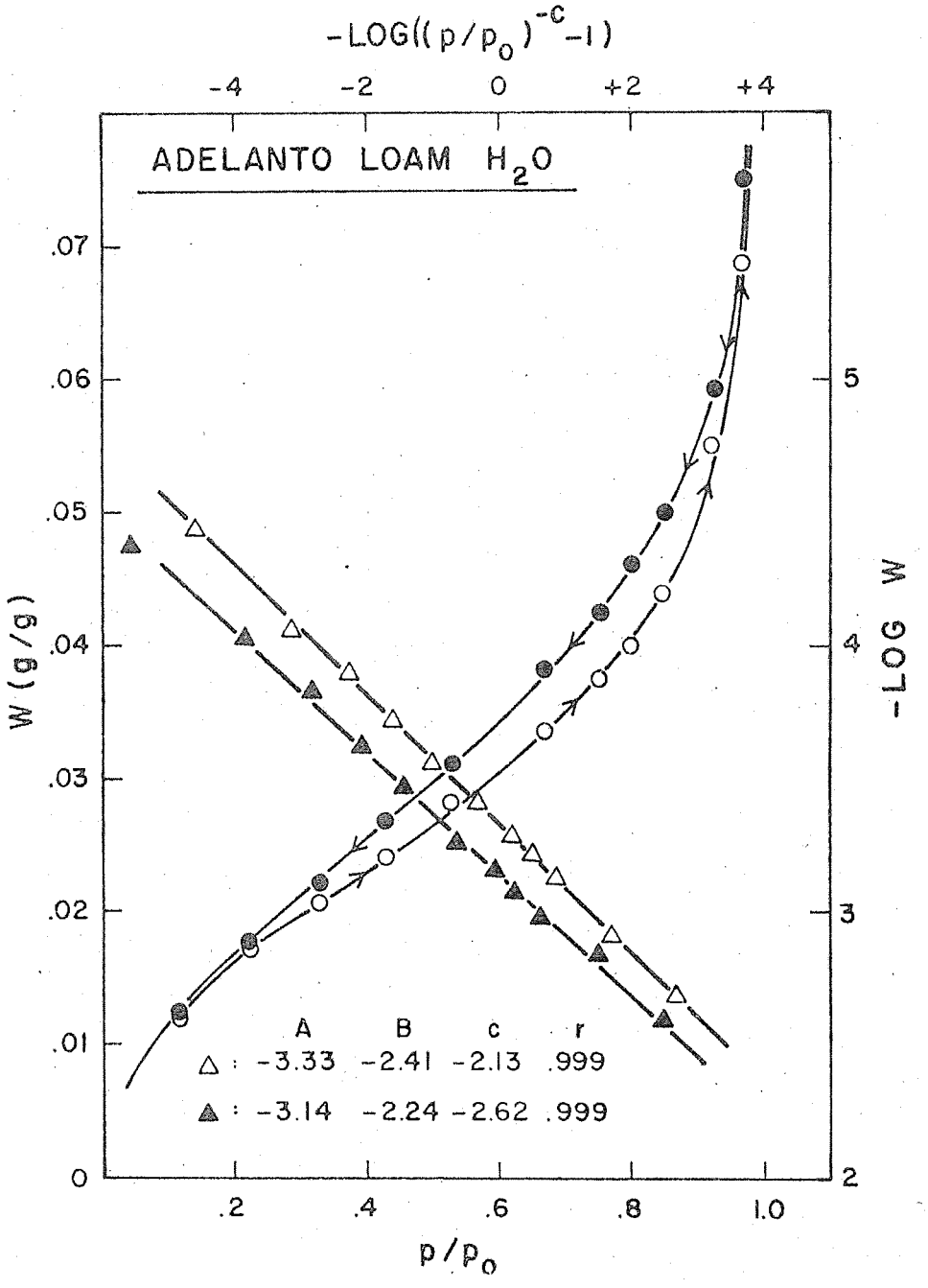

Figure 3. The adsorption-desorption isotherms of water on an Adelanto loam soil plotted as amount adsorbed versus relative vapor pressure, and then replotted according to the proposed log functions.

ADSORPTION EQUATIONS

CORRELATION COEFFICIENT (r)	[5]	BET	FHH	HJ	DK	F
1.00	40	4	15	11	0	13
.99	1	3	13	0	1	7
.98		4	7	11	6	8
.96		9	3	7	2	6
.94		5	2	4	5	1
.92		2	1	0	5	2
.90		9		6	17	4
.80		4		0	5	
.70		1		2		
<.70						

Figure 4. Distribution of the linear correlation coefficients (r) of best fit for six equations used for describing the adsorption isotherms of 41 clay and soil adsorbents.

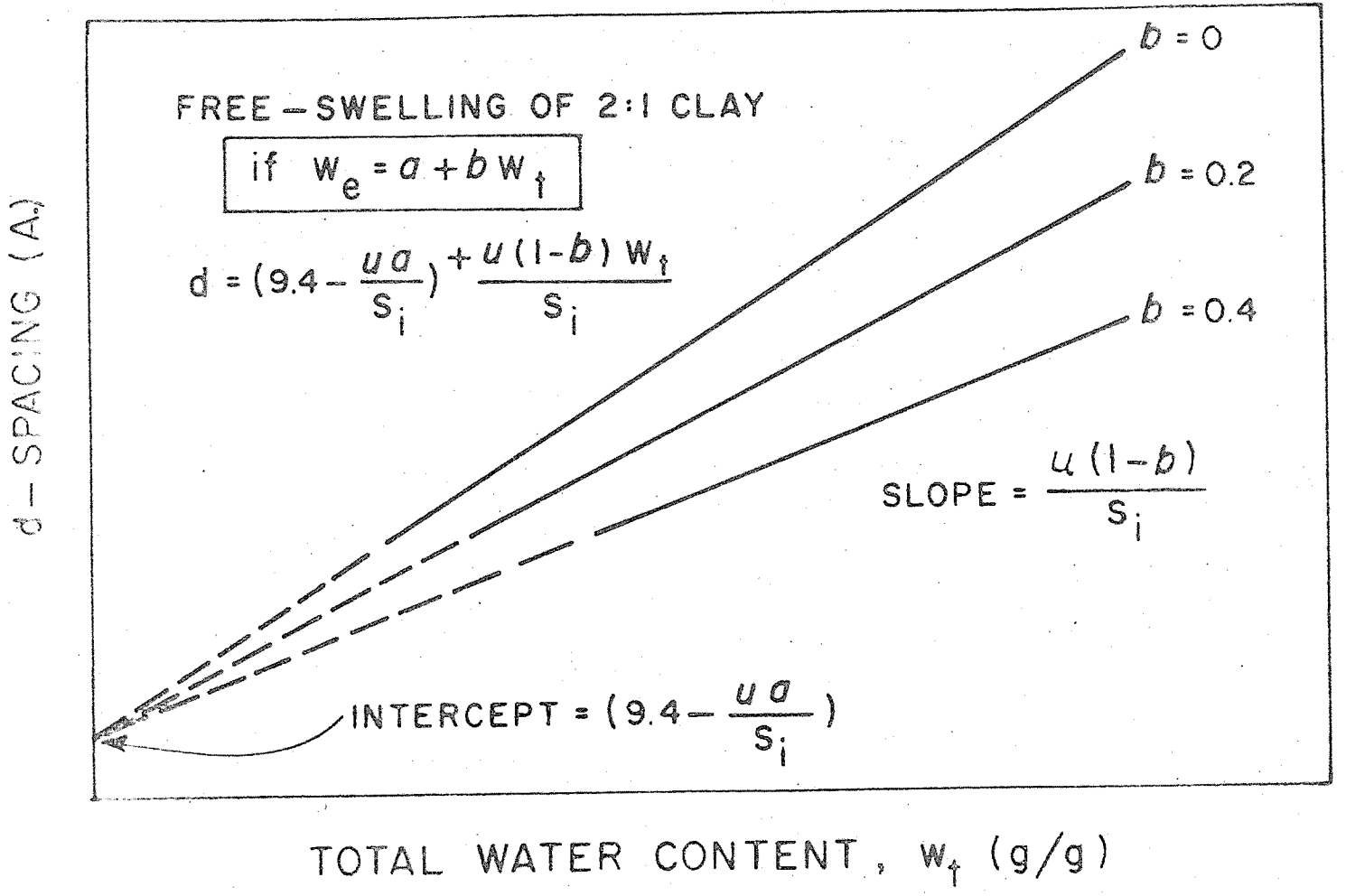

Figure 5. Hypothetical free-swelling curves of a montmorillonite as a function of increasing b, assuming a remains constant.

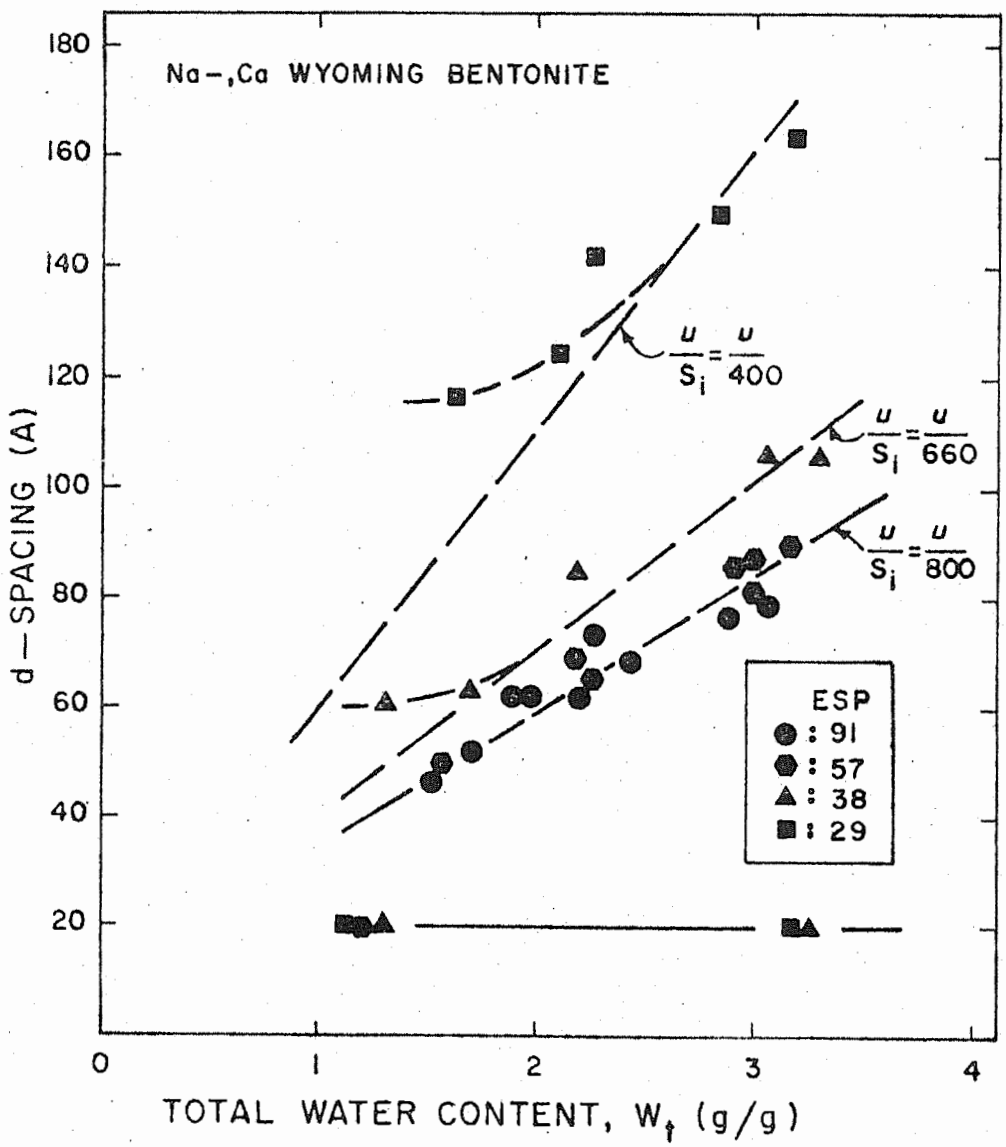

Figure 6. Swelling of Na-, Ca-Wyoming bentonite in water systems as affected by ESP and degree of demixing of the two exchangeable-cation types.

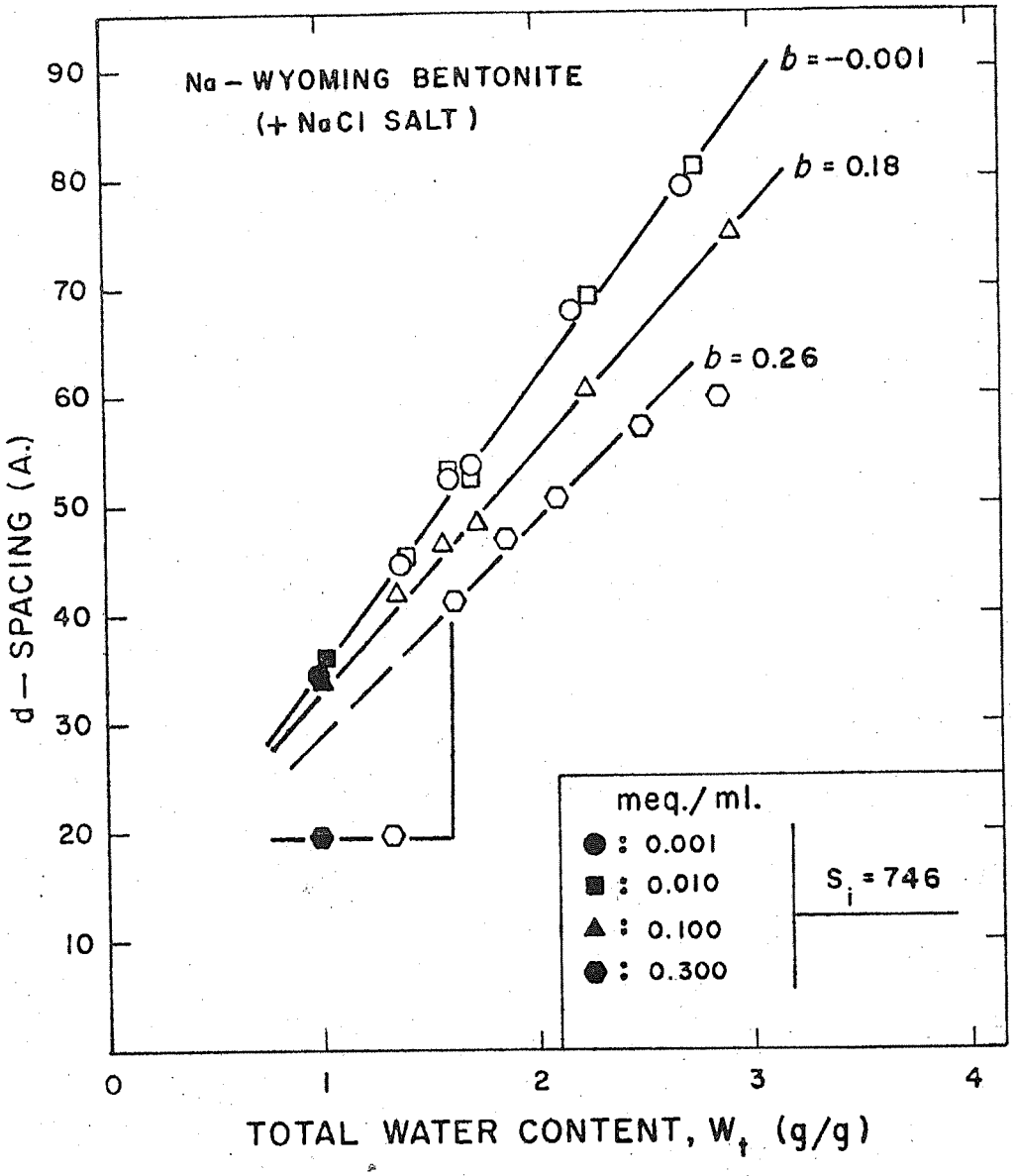

Figure 7. Free-swelling of a Na-Wyoming bentonite in salt solutions. Closed symbols denote starting salt concentrations, open symbols denote increasing dilutions of original samples with distilled water.

TITLE: THE USE OF FLOATING SOLID AND GRANULAR MATERIALS TO REDUCE EVAPORATION FROM WATER SURFACES

CRIS WORK UNIT: SWC-018-gG-2 CODE NO.: Ariz.-WCL-67-3

INTRODUCTION:

The search for practical floating materials to reduce evaporation losses was continued during 1970 (see 1968, 1969 Annual Reports WCL 67-3). An experiment was conducted to determine the efficiency and durability of three samples of wax chips. A sample of foamed butyl rubber was also tested to compare its efficiency with two other previously tested butyl covers.

PROCEDURE:

The experiments were conducted from 8 June to 9 November 1970 on four insulated evaporation tanks. One tank was left open and used as a reference throughout the experiments.

During the first experiment, three wax samples supplied by Mobil Oil Corporation were tested. The samples were white and consisted of individual particles 2.5 cm × 2.5 cm × 0.3 cm thick, or smaller. One sample was a regular hot-melt wax, and the other two were pigmented, containing either calcium carbonate or flocculent diatomacious clay as the pigment. These three samples were placed on tanks 4, 3, and 1, respectively, on 8 June, and evaporation measurements were recorded until 1 September.

The second experiment began on 8 September and continued until 9 November. In this experiment a sheet of white, or cream colored, foamed butyl rubber supplied by Segmented Swimming Pools, Ltd. was compared with covers of green foamed butyl and white butyl. The covers were placed on tanks 3, 1, and 4, respectively, and evaporation measurements recorded.

RESULTS AND DISCUSSION:

Both pigmented wax samples covered about 40% of the surface area of the tanks, and reduced evaporation by 25% during the first week. The regular hot-melt wax covered about 90% of the surface, and reduced evaporation 38% during the same period. After five weeks

the efficiency of all three samples had decreased such that all were essentially the same (16-19%). At the conclusion of the study, a total of 12 weeks, the efficiency of the regular hot-melt wax was only 11%. The efficiency of the two pigmented samples remained essentially constant after five weeks, ending at 18-20%.

In all cases the reduction in efficiency was probably due to oxidation of the wax when exposed to the elements; the hot-melt wax being particularily susceptible. The final efficiencies were not of sufficient magnitude to warrant further testing of these samples. Other types of wax are being procured for testing which do not oxidize as rapidly and should be more efficient.

The purpose of the second experiment was to compare the Segmented Swimming Pool (SSP) foamed butyl cover against some previously tested covers of high efficiency. At the end of the nine week study period, efficiencies of 71, 74, and 74% were obtained for the green, SSP, and white butyl covers, respectively, The area covered was also essentially the same in all cases (81% $\pm$ 1%). A highly efficient cover of this type could be useful in reducing evaporation losses if a method was developed to prevent wind damage, and if the cost was low enough. At the present time the SSP material costs $\$3.09/m^2$. This means that if it was assumed that one meter of water per unit area per year was saved, the cost of the saved water would be about $10/1,000 gallons. Since the cover is supposed to last for 20 years, this cost would be reduced to $.50/1,000 gallons. The high initial cost and relatively high average cost of water provided by this cover would limit its use to only a few locations.

SUMMARY AND CONCLUSIONS:

The evaporation reduction efficiency of three wax samples tested decreased from initial values of 24, 25, and 38% to values of 17, 16, and 19%, respectively, after six weeks. Final efficiencies after 12 weeks were 20, 18, and 11%, respectively. The

decrease was probably due to oxidation of the wax. Since the overall efficiency of these materials was so low, no further tests are planned; however, other types of wax will be tested.

A cream colored, foamed butyl cover was very efficient in reducing evaporation (74% with 81% covered) and compared closely with green and white butyl covers previously tested.

PERSONNEL: Keith R. Cooley

CURRENT TERMINATION DATE: December 1970.

TITLE: EVAPORATION OF WATER FROM SOIL

CRIS WORK UNIT: SWC-018-gG-2 CODE NO.: Ariz.-WCL-68-1

INTRODUCTION:

The objective and need for the research documented in this outline appears in the USWCL 1969 Annual Report. A field experiment was conducted during 1970 in which soil-water content and soil temperatures were measured as a function of depth and time under high evaporating conditions. This experiment is described in Part I. The 1969 report covered the laboratory phase of the development of a gamma-ray transmission apparatus for measuring soil-water content in the field. The development has been essentially completed and the field results are presented as Part II of this report. Preliminary work on a detailed experiment to delineate water movement by diffusion and mass flow through mulches is reported in Part III.

PART I. SOIL-WATER CONTENT AND TEMPERATURE CHANGES WITH DEPTH AND TIME DURING EVAPORATION.

Initially, after a rain or an irrigation, the evaporation loss of water from a bare soil is controlled largely by meteorological conditions. As the surface dries the rate of water movement to the soil surface becomes the predominant factor determining the rate of water loss. The rate of water movement is dependent upon soil-water content and temperature. As evaporation proceeds, the soil-water content decreases, decreasing the rate of water movement. Temperature gradients, in general, cause water to flow downward during the day and upward at night. The net effect of water content and temperature gradients on the evaporation of water from soil is very complex. This report describes an experiment in which water content and temperature were measured as a function of time and depth, along with various meteorological parameters. Some background experiments on evaporation of water from bare soil (lysimeter studies) are given on pages 151-182 of the 1961 Annual Report of the USWCL.

EQUIPMENT AND PROCEDURES:

The experiment was conducted in the lysimeter field at the U. S. Water Conservation Laboratory. Location of instruments and soil sampling sites are shown in Figure 1. On 10 July 1970, basins 2 and 3 and lysimeters 2 and 3 were flooded with water to an average depth of about 10 cm. This irrigation took approximately 3 hours. Basin 1 and lysimeter 1 remained dry.

Various sensors were placed in locations 9 through 14 (Figure 1) and were interrogated and recorded every half hour, the information being punched on paper tape. Site #9 contained 4 miniature net radiometers, two at 20 cm above the soil surface and two at 50 cm above the surface. An inverted Epley pyroheliometer was located at site 10 to measure reflected short wave radiation. Soil temperatures with copper constantan thermocouples were measured at location 11. Included were two thermocouples at the soil surface, two at 1-cm depth, two at 2-cm depth, one thermocouple at 3 cm, two at 4 cm, and one at each of the following depths: 5 cm, 7 cm, 8 cm, 10 cm, 16 cm, 32 cm, 64 cm, and 128 cm.

In basin 3, incoming short wave radiation was recorded at site #12, while vapor pressure and air temperature were measured at 20 and 50 cm above the soil surface at site 13. In addition, at site 13, two experimental hemispherical radiometers were placed at an elevation of 215 cm above the soil surface. Windspeed at 10, 45, 85, and 170 cm was measured at site 14.

Gravimetric soil samples were taken each half-hour period starting at 0530, 11 July 1970, and ending at 2200, 17 July 1970.

Soil samples were taken in sites 4 through 8 in basin 2 in the following manner. An Oakfield probe was pushed into the soil to a depth of 10 cm on the hour and to a depth of 4 cm on the half-hour. Then the soil core was sliced into 1-cm increments starting from the top. The five samples at each depth for each time period were placed in a container for gravimetric water content determination. All samples were taken at random in the five sites.

Soils were dried for 12 hours in a forced draft oven at 104 C.

Bulk density samples were also taken using the Oakfield probe and the soil sampler described in the U. S. Salinity Handbook 60. Both pieces of equipment yielded similar bulk densities with depth.

RESULTS AND DISCUSSION:

Although the plots were first sampled on 11 July, results reported here are from 0100 12 July until 2200 17 July, the period of most rapid drying. We are concerned here with evaporation during the period that the rate of movement of soil-water is the controlling mechanism in the evaporation process.

In the first analysis of the data, gravimetric water content at each depth was plotted as a function of time. These data were then smoothed by drawing the best fit line, as determined visually, through the points. Volumetric water content was determined by multiplying the gravimetric water content at any time obtained from the smooth line and multiplying it by the appropriate bulk density. By this technique, values of volumetric water content with time for various soil depths were obtained.

Water contents at three depths are presented in Figure 2. The diurnal drying and partial rewetting is evident from the curves, especially for the 0-1 cm. On 12 July, the second day after irrigation, the water content in the 0-1 layer decreased by 50%, from .265 to .135, within a period of 10 hours. Rewetting during the following 5 hours brought the water content up to .177. The amount of drying and rewetting during a 24-hour period decreased with increasing time. On 12 and 13 July the minimum water content at all three depths occurred at nearly the same time, 1800-1900. On 16 and 17 July the minimum does not occur at the same time for the three depths, but shifts to an earlier time in the 0-1 layer and to later times in the other two. This results because, at the lower water contents, water movement is predominantly in the vapor phase.

The temperatures at the surface and at 1 and 2 cm are presented in Figure 3. The maximum and the minimum soil temperatures progressively increase over the time of the experiment. The temperature decreases with depth during the day and increases with depth at night. The crossover occurs between 0600 and 0700 in the morning and 1800-1900 during the evening.

With the water content data in Figure 2, and evaporation data from the lysimeters, the flux of water at 1, 2, and 3 cm depth was calculated. The lysimeter yields the flux at the surface in cm hr^{-1}. The flux at 1 cm was obtained by subtracting the water content change (loss or gain) during the corresponding hour period from the flux at the surface. Similarly, the water content change per hour in the 1-2 cm layer was subtracted from the flux at 1 cm to obtain the flux at 2 cm. Figure 4 presents the flux data for 0, 1, and 2 cm depths. The flux at the surface follows the diurnal trend discussed in the 1961 Annual Report, pp 151-182. The flux at 1 cm (f_1) and 2 cm (f_2) generally follows the flux at 0 cm (f_0) during the morning hours, but is considerably different during the evening. For example, at 1800 hours on 12 July f_1 and f_2 reach a minimum. After increasing for an hour or so they again decrease, but are consistently higher than f_0. The minimum in f_1 at 1800 corresponds with the minimum in water content at that time (Figure 2) and the time at which the temperature at the surface became less than the temperature at 1 cm. At this time the temperature gradient, which had been in the direction to reduce the upward flux, reversed direction and began aiding the upward flux. The time of the reversal of the temperature gradient occurred at the same time as the f_1 and f_2 minimum on 12 July, and at the time that f_1 and f_2 became greater than f_0 on 13 through 17 of July. It is evident that temperature and temperature gradients play large roles in the movement of water in the surface layers of a field soil. These phenomena will be studied in detail during 1971. It is planned to apply the theory of the simultaneous transfer of water and heat to these data.

Several of the equations that utilize meteorological parameters to calculate evaporation require a knowledge of the vapor pressure at the soil surface. This is usually estimated by calculating the saturated vapor pressure at the temperature of the surface. This is a reasonable estimate if the soil surface does not dry to the point that the vapor pressure in the soil pores is less than saturated. For the soil used in this experiment, this would occur when the water content was below about 0.14. Figure 2 shows that the average water content in the 0-1 cm layer is below 0.14 over most of the time of this experiment. However, the average water content in the 0-1 cm layer does not represent the water content at the surface. In the course of this study a method of estimating the water content in the 0-0.1 cm layer evolved.

By plotting f_0, f_1, f_2 and f_3 as a function of depth and interpolating the flux at 0.1 cm ($f_{0.1}$) and at, say, 0.5 cm ($f_{0.5}$) can be estimated. Now the water content change in the 0-0.1 cm layer over an hour period is $(f_0 - f_{0.1}) \times 10$, and at 0.5 cm $(f_0 - f_{0.5}) \times 2$. If the water content in the 0-0.1 and 0-0.5 layers are known at any one time, the water content at all other times can be calculated. These calculations were made and are presented in Figure 5. It was assumed that the water content at 0100-0500 on 12 July was constant from 0 to 1 cm. The water contents in these layers vary dramatically with time of day. By 1400 on 12 July the water content in the 0-0.1 layer is below 0.14. After 1200 on 14 July the range is from 0.005 to 0.04 volume fraction. This corresponds to a relative vapor pressure range of 0.02 to 0.5.

The ability of estimating the water content at 0-0.1 cm allows us to estimate the vapor pressure in this layer. In the first approximation this can be considered the vapor pressure of the surface. Relative vapor pressure versus water content has been determined for Adelanto loam, the soil used in this experiment. Such data are presented on page 27-31 of the 1963 Annual Report of the U. S. Water Conservation Laboratory. Results reported

under WCL 67-2 elsewhere in this report give an equation that describes this relationship very well. With that equation, the saturated vapor pressure calculated from surface temperature measurements and the estimated surface water content, the vapor pressure of the surface can be calculated. During 1971 these calculations will be completed and the resulting information used in meteorological equations to predict evaporation of water from soil.

PART II. FIELD MEASUREMENT OF SOIL-WATER CONTENT BY GAMMA-RAY TRANSMISSION COMPENSATED FOR TEMPERATURE FLUCTUATIONS

The 1969 Annual Report described the use of a spectrum stabilizer to compensate for the horizontal shift of the peak pulse height. During 1970 a means of compensating for the vertical pulse height shift was devised. Briefly, this consists of measuring the detector probe temperature and adjusting the count rate by using a previously measured count-rate, temperature relationship. With these developments the gamma rig was field tested. The following discussion presents the results of these tests. For details of equipment and procedures, see the 1969 Annual Report.

RESULTS AND DISCUSSION:

The equipment and the experimental site were calibrated by scanning the soil profile with gamma rays and by obtaining concurrent gravimetric samples. The samples were taken in 1-cm increments to a depth of 10 cm with an Oakfield probe. Samples at each depth were taken from three locations (all within 1 m of the gamma equipment) and were composited to obtain representative gravimetric water content data. Initially, samples were taken at 0630, 0700, 0800, 1130, and 1500 on 15 September 1970 in a relatively dry soil (θ_w between 0.02 and 0.11). After the sampling at 1500, the area around the gamma rig was flooded to a water depth of about 4-5 cm and count-rates through water were taken.

On 17 September 1970, two days after irrigation, soil samples were taken at 0700, 1200, and 1500 hours. During the sampling

periods the gamma rig scanned and recorded the count-rate through the soil profile in 1-cm increments to a depth of 10 cm, counting for 100 seconds at each depth. Between soil sampling times, the count-rate in air was recorded almost continuously, and energy spectrums were obtained periodically. The detector probe temperature was recorded every 5 minutes throughout the experiment.

The energy spectrum in air determined at three different probe temperatures is shown in Figure 6. Over the temperature range of 17.6 to 42.2 C, the pulse height spectrum did not shift along the baseline. However, the count-rate at the peak pulse height decreased with increasing temperature. The differences in peak count-rates as a result of temperature changes exceed the error limits determined by counting statistics ($\pm 2\sigma = \pm 940$ cpm). Evidently, the spectrum-stabilizing equipment adequately compensates for temperature-induced horizontal energy spectrum shifts, but not for vertical peak height changes.

The temperature dependency of the peak count-rate is presented more explicitly in Figure 7 where peak count-rates are plotted versus measured probe temperatures for two different gain settings. These data are for both warming and cooling of the detector probe. The best-fit line for each set of data was determined by least squares analysis. The slopes of the two curves are nearly the same, but the intercepts are different. This linear relationship is valid over the temperature range we measured; however, more recent data indicate a leveling off of this curve at temperatures less than 15 C.

These results show that the peak count-rate in air, I_o, is inversely proportional to detector probe temperature. The average temperature coefficient for our equipment (-0.35%/^{o}C) is similar to the data obtained by others (-0.5%/^{o}C). This inverse relationship and the probe temperature at the time of scanning the soil profile must be known in order to calculate bulk density or water content. On one measurement day the probe temperature during one scan of the soil profile changed 3 C and from morning to afternoon

changed 23 C. For our equipment the I_o versus temperature relationship does not change as long as no adjustments are made in the baseline voltage and window width.

From the gravimetric water content values and concurrently determined count-rates, the bulk densities at each centimeter depth were calculated for the eight sampling times. The average of the eight densities at each depth was not significantly different from the average of two densities, one obtained from the dry soil and one from the wet soil. A plot of these two calculated bulk densities in the top 10 cm of the soil profile is shown in Figure 8. The line represents the average density used to calculate soil-water contents for the remaining six sampling times. These results indicate that at least two sets of soil samples should be taken to calibrate the equipment and experimental site.

Assuming that I_o was not temperature dependent, and using the I_o obtained at the beginning of the experiment, values of θ_w were calculated. Curve A in Figure 9 shows a plot of the gravimetric versus gamma θ_w for this case. Using linear regression analysis, the slope of the line is 0.908 $\pm$ 0.127, the intercept 0.011 $\pm$ 0.002, and the resulting value of "t" for the t-test is 7.1 (the slope being significantly different from zero). The confidence limit for these data at the 95% level is $\pm$ 0.035, and the average difference between gamma and gravimetric water content for all 59 samples is 0.018.

Taking into account the temperature effect on peak count-rate (from Figure 7), the data were recalculated and are presented in Figure 9, Curve B. The slope of the line is 1.048 $\pm$ 0.084, the intercept is -0.005 $\pm$ 0.002, and t = 12.5. The confidence limit is $\pm$ 0.023 at the 95% level. The average difference for all samples is 0.009, a significant improvement over the 0.018-value where temperature was not taken into account.

Another approach for calculating water content with the gamma data is to measure I_o immediately prior to each scan of the soil

profile. This takes into account the temperature effect on peak count-rate, although not as nicely as the data shown in Figure 7. This approach assumes that the probe temperature does not change significantly during the subsequent scanning of the soil profile. Data calculated for this case are shown in Figure 9, Curve C. The slope of the line is 0.923 $\pm$ 0.028, the intercept 0.016 $\pm$ 0.001, and t = 32.6. The confidence limit is $\pm$ 0.023 at the 95% level, and the average difference for all samples is 0.010.

The confidence limit and the average deviation for the data shown on Curves B and C in Figure 9 are the same. Thus, either method should yield equal accuracy. The method chosen will depend on whether it is easier to obtain the relationship between probe temperature and peak count-rate or to measure the peak count-rate in air immediately prior to each scan of the soil profile. For the latter case, the total scan time should be of short duration so that the probe temperature change is small during the scan.

The precision of measurement is influenced only by the error in counting I_o and I. To assess the errors involved in the calculation of density and water content from the accuracy in determining count-rates, data were used from the 4- to 5-cm depth taken at 1500 on 15 September 1970. From these data (θ_w (gravimetric) = 0.101, I_o = 213,878 cpm, and I = 44,142 cpm), the density was calculated for all combinations of error in I_o and I (2σ = twice the standard deviation). Using the average density, ρ_s = 1.685 g cm^{-3}, both the gravimetric and volumetric water contents were then calculated (Table 1). Maximum deviation is; density $\pm$ 0.015 g cm^{-3}, volumetric water content $\pm$ 0.015, and gravimetric water content $\pm$ 0.009.

Counting error may be reduced by obtaining more counts at each measurement site. This may be done by (1) moving the source and detector closer together; (2) increasing the source strength; or (3) increasing the counting time. Moving the source or detector closer together will result in a smaller portion of soil being

sampled and increase the influence of the access tubes on the sampling area. The necessity of keeping the access tubes a reasonable distance apart and as small as possible precludes the use of lead shielding material. Thus, for health safety, the source strength should be small. An increase in source strength does not produce a proportional decrease in error. For example, if the I_o and I values used in computing the data for Table 1 were increased by a factor of 5 the maximum deviation in θ_v would be $\pm$ 0.007, a reduction by a factor of about 2. Increasing the counting time will improve counting statistics but may result in larger probe temperature variations.

It is apparent that the effect of temperature on peak count-rate must be accounted for in order to obtain reasonably accurate soil-water content data under natural field conditions. If this is done, absolute gravimetric water content can be measured with an average difference between gamma and gravimetric values of 0.009 for the equipment and experimental conditions used here. The optimum source strength, counting time, and distance between access tubes must be determined for each experimental situation.

PART III. DIFFUSION COEFFICIENT FOR WATER VAPOR THROUGH MULCHES UNDER FIELD CONDITIONS.

To understand fully the process of soil-water evaporation in the later stages of drying, one must first understand the mechanisms by which gaseous exchange occurs between soil and atmosphere. Romell (7 [as described by Keen (5)]) concluded, primarily from inductive reasoning, that diffusion is the most important mechanism in this exchange. Recently, however, evidence has appeared which suggests that air turbulence may also have an important influence, at least, under some conditions. Hanks and Woodruff (3) observed that evaporation through soil, gravel, and straw mulches increased with wind velocity in their wind tunnel. Holmes, Greacen, and Gurr (4) also using a wind tunnel, found that evaporation was affected by surface tilth (and, hence, from inference, also by

surface roughness and the subsequent nature of air turbulence). Benoit and Kirkham (2) and Acharya and Prihar (1) observed increases in evaporation rate when air movement was increased over soil columns having a soil mulch. Kimball and Lemon (6) found that heptane vapor movement through coarse gravel and straw was increased greatly by air turbulence under natural field conditions, but their data were too scattered to draw any firm conclusions about movement in finer textured materials.

Thus, there are several indications that air turbulence above the soil can significantly increase the rate of gas movement in soil. This study was initiated to determine more precisely how much gas movement can be increased by air turbulence under field conditions.

The procedure to identify the effects of air turbulence will consist of applying mulches to three weighing lysimeters and then observing the rates of water loss through the mulches. Concurrent measurements of air temperature, air vapor pressure, wind velocity and soil temperature at the soil-mulch interface will permit the amount of water vapor loss attributable to molecular diffusion to be calculated. Then the differences between calculated and observed losses will be attributed to air turbulence (or to another mass flow mechanism if there should be large differences which do not correlate with wind velocity).

To date, progress has been confined to assembling the mulch materials. They have various pore sizes and geometries so that differences in the effects of air turbulences may be observed among several porous media. Table 2 lists the mulches to be used.

The glass beads were purchased from a manufacturing company. The soil aggregates have been sieved from Adelanto loam. The glass bead aggregates were vastly more difficult to obtain. They were made by first heating layers of 0.047-0.084 mm diameter glass beads in a pan slowly in a muffle furnace up to approximately 605 C at which temperature the beads fused to form porous "cakes." After

slowly cooling, the cakes were broken into smaller chunks with a meat tenderizer, and then they were further reduced in size by grinding in a Wylie mill. The aggregates of the desired size range were sieved out using a mechanical shaker.

All of the mulches have been treated with a water-repellent material, trichlorosilane, so that they will not conduct liquid water from moist soil beneath them to their upper surface. This will assure that all water lost from the lysimeters will have to move in the vapor phase through the mulch.

SUMMARY AND CONCLUSIONS:

Evaporation of water from bare soil was studied during an intensive field experiment conducted in July 1970. Soil-water content and temperature were measured as a function of time and depth for 6 days after an irrigation. Pertinent meteorological parameters were also measured. Water content was measured in 1-cm increments to 10 cms gravimetrically. These data, along with the total evaporative loss as measured by lysimeters allowed the calculation of soil-water flux at several depths within the soil. Using the flux data a method was devised to calculate soil water contents in increments as small as 0.1 cm. This development allows the estimation of water content, and thus vapor pressure, at the soil surface. Vapor pressures thus calculated can be used in meteorological equations that predict evaporation. The water content, water flux, and temperature data will be used to test the applicability of the theory of simultaneous flow of water and heat to the movement of water to an evaporating surface under natural conditions.

Subsequent to the July experiment the development of a gamma-ray transmission technique to measure soil water content under natural conditions was completed. The technique compensates for temperature changes in two ways. An electronic spectrum stabilizer is used in conjunction with the nuclear counting equipment to adjust for temperature-induced horizontal shifts in the energy spectrum, and a measured relationship between peak count-rate and temperature

is used to compensate for vertical shifts of the energy peak. During a particular experiment the detector probe temperature varied 23 C, the gravimetric water content ranged from 0.021 to 0.186, and the average deviation between gravimetric and gamma-ray measured values was 0.009. Automatic, continuously repeated scanning of the soil profile is accomplished with a programmable controller that controls sequentially the positioning, measurement, recording and repositioning of the gamma ray system.

An experiment to determine the relative magnitude of diffusion and mass flow mechanisms in the evaporation process is under way. The rates of water vapor through mulches applied to weighing lysimeters will be measured and compared to the loss attributable to molecular diffusion alone. Preparation of mulches of several different pore sizes and geometries has been completed.

REFERENCES:

1. Acharya, C. L., and Prihar, S. S. Vapor losses through soil mulch at different wind velocities. Agron. J. 61:666-668. 1969.

2. Benoit, G. R., and Kirkham, D. The effect of soil surface conditions on evaporation of water. Soil Sci. Soc. Amer. Proc. 27:495-498. 1963.

3. Hanks, R. J., and Woodruff, N. P. Influence of wind on water vapor transfer through soil, gravel, and straw mulches. Soil Sci. 86:160-164. 1958.

4. Holmes, J. W., Greacen, E. L., and Gurr, C. G. The evaporation of water from bare soils with different tilths. Trans. Int. Congr. Soil Sci., 7th Congr. Madison. 1:188-194. 1960.

5. Keen, B. A. The physical properties of soil. Longmans, Green, and Co., New York, 380 pp. 1931.

6. Kimball, B. A., and Lemon, E. R. Air turbulence effects upon soil gas exchange. Soil Sci. Soc. Amer. Proc. 35(1). 1971

7. Romell, L. G. Luftvaxlingen i marken s. ekol. falstor. Medd. Stat. Skogsforsoki 19:125-359. 1922.

PERSONNEL: Ray D. Jackson, Robert J. Reginato, and Bruce A. Kimball.

CURRENT TERMINATION DATE: December 1970.

Table 1. Calculated soil densities and water contents associated with accuracy in determining count rates. 1/

		Density ($g\ cm^{-3}$)	θ_w 2/	θ_v 2/
I_o	I	1.685	0.101	0.170
$I_o + 2\sigma$	$I + 2\sigma$	1.680	0.098	0.164
$I_o + 2\sigma$	$I - 2\sigma$	1.700	0.110	0.185
$I_o - 2\sigma$	$I + 2\sigma$	1.670	0.092	0.155
$I_o - 2\sigma$	$I - 2\sigma$	1.691	0.104	0.176
$I_o + 2\sigma$	I	1.690	0.104	0.174
$I_o - 2\sigma$	I	1.680	0.098	0.165
I_o	$I + 2\sigma$	1.675	0.095	0.160
I_o	$I - 2\sigma$	1.695	0.107	0.180

1/ For calculations: θ_w (gravimetric) = 0.101, I_o = 213,878 cpm, I = 44,142 cpm, $x\mu_w$ = 0.9357 $cm^3 g^{-1}$, σ = (total counts)$^{\frac{1}{2}}$.

2/ Water contents were calculated using ρ_s = 1.685 $g\ cm^{-3}$.

Table 2. Mulch materials to be applied to the lysimeters.

Experiment No.	Lysimeter No. 1	2	3
1	1.65-2.37 mm glass beads	0.84-1.65 mm glass beads	0.41-0.84 mm glass beads
2	0.84-1.65 mm glass bead aggregates	0.84-1.65 mm glass beads	0.84-1.65 mm soil aggregates
3	loam soil	0.41-0.84 mm soil aggregates	0.84-1.65 mm soil aggregates

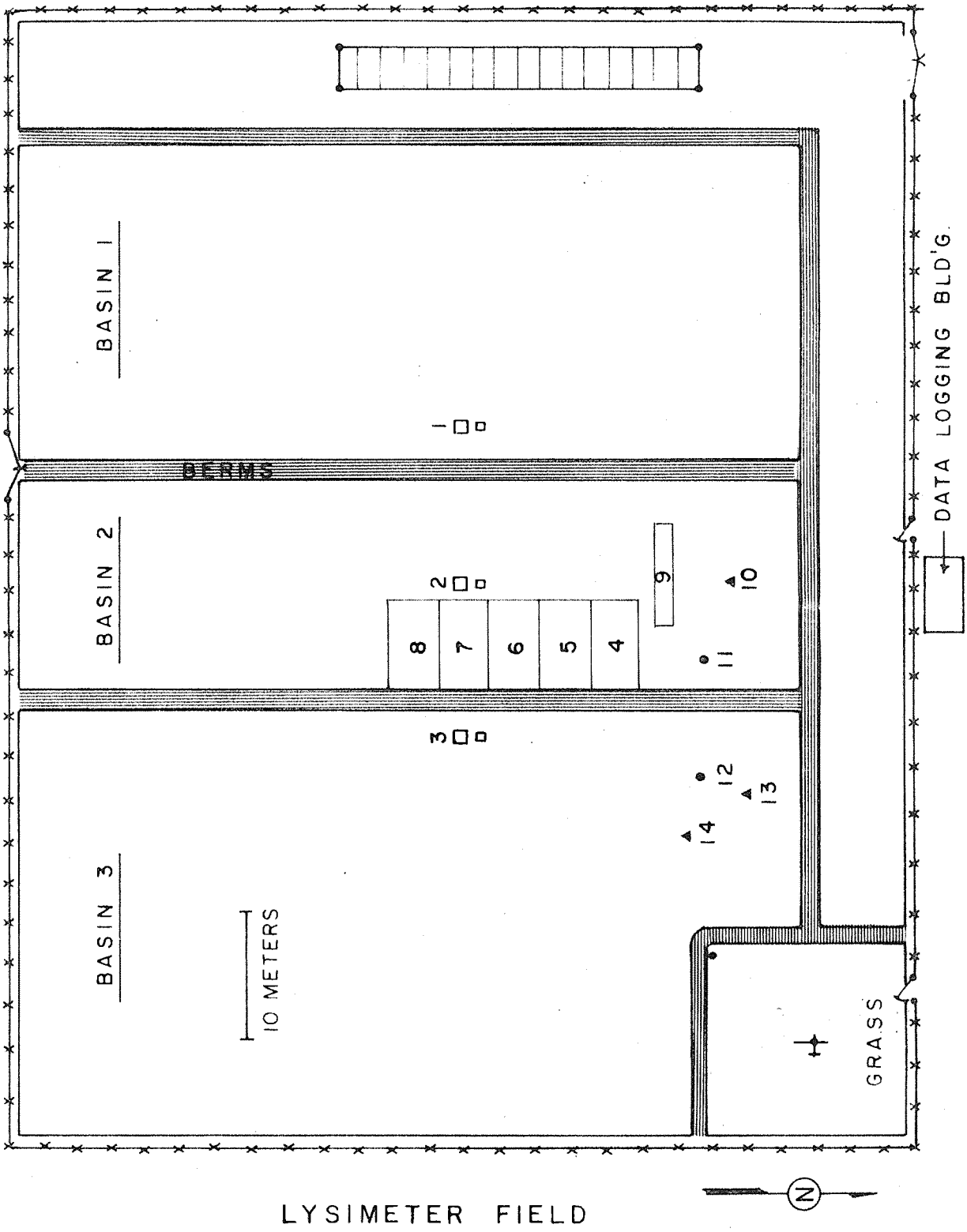

Figure 1. Diagram of experimental field showing the location at which various measurements were made.

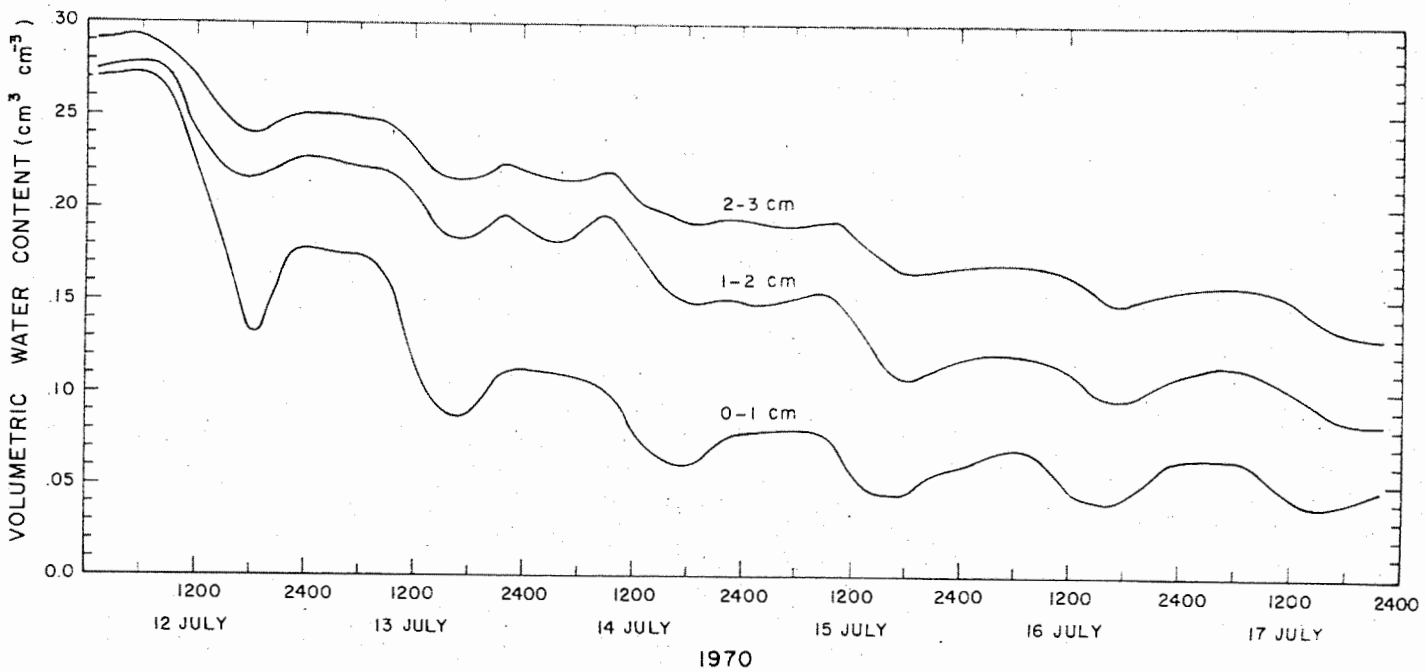

Figure 2. Smoothed volumetric water contents at three depths for the 6-day drying period.

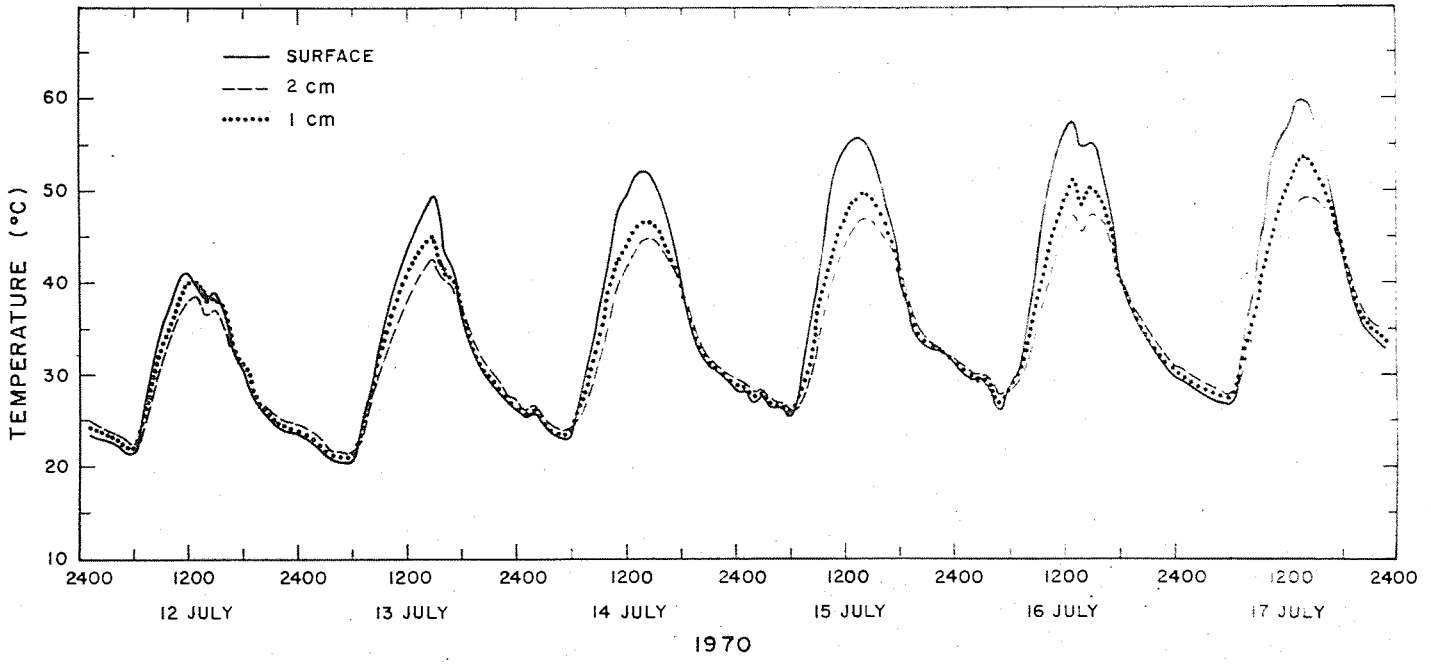

Figure 3. Soil temperatures at three depths for the 6-day drying period.

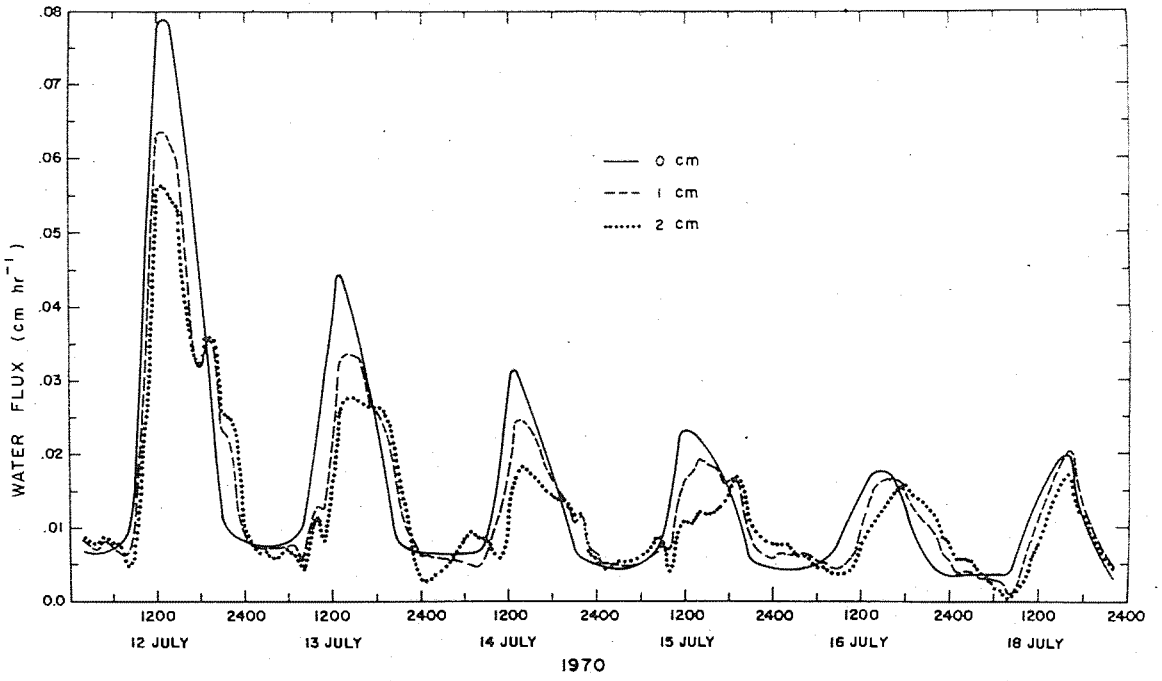

Figure 4. Water flux at depths of 0, 1, and 2 cm.

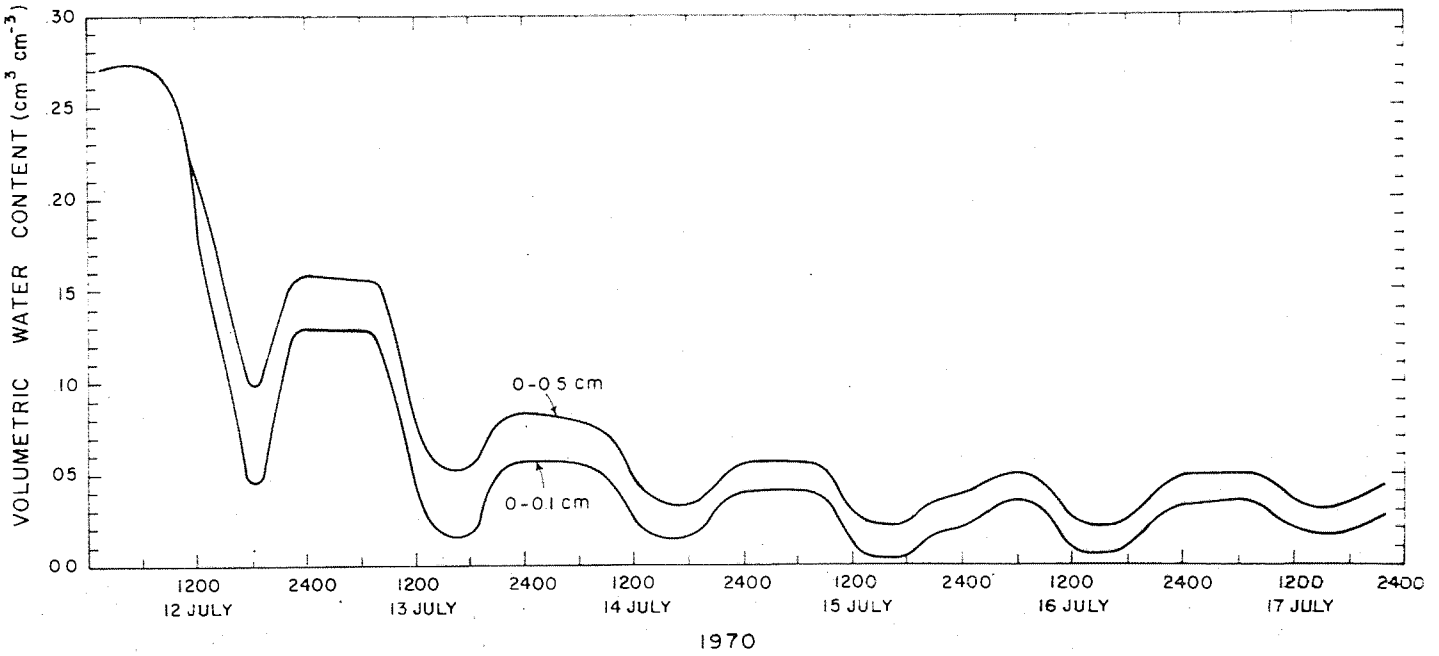

Figure 5. Calculated water contents at intervals of 0-0.5 and 0-0.1 cm.

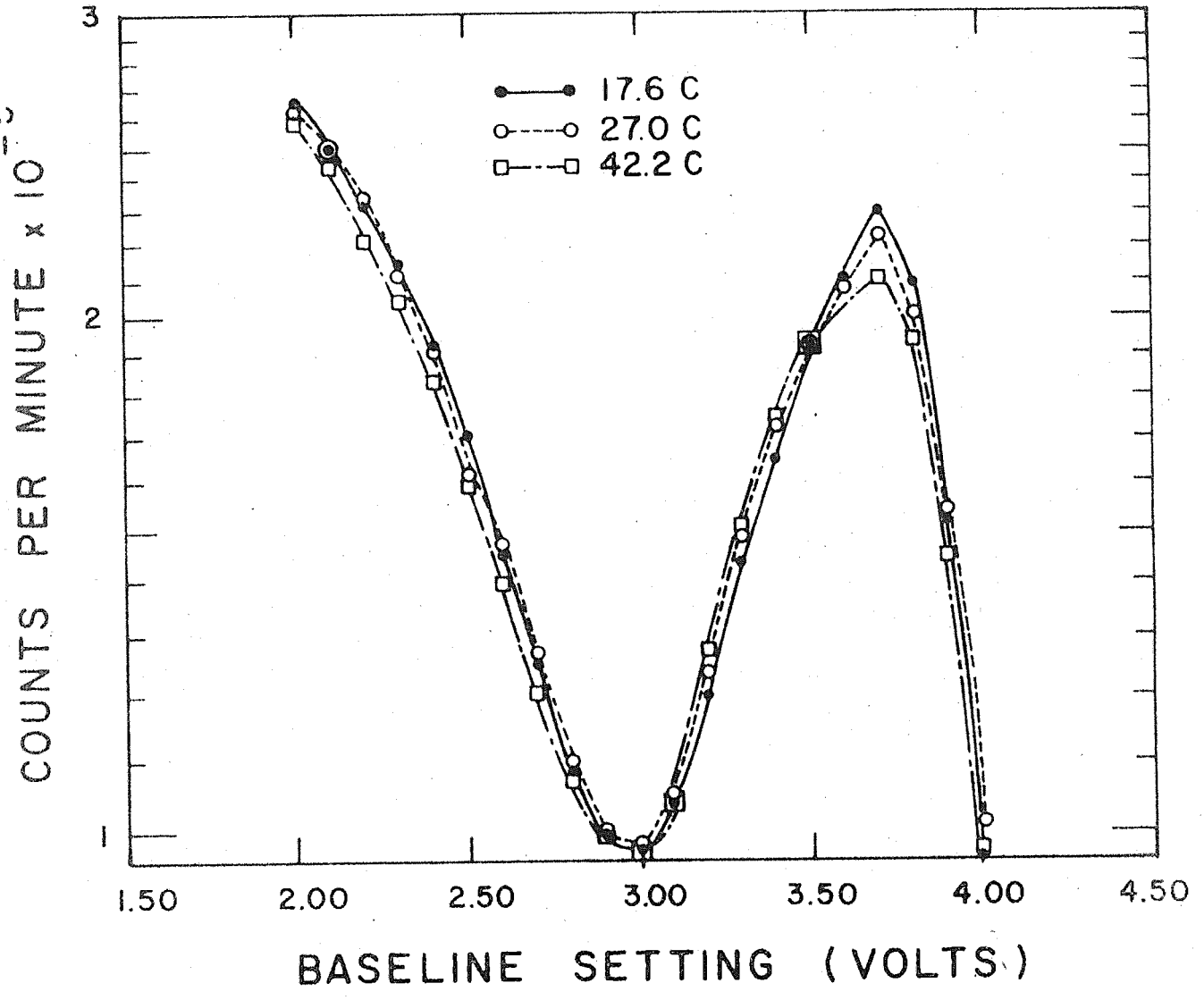

Figure 6. Energy spectrum of ^{137}Cs as a function of the detector probe temperature obtained with stabilized nuclear counting equipment.

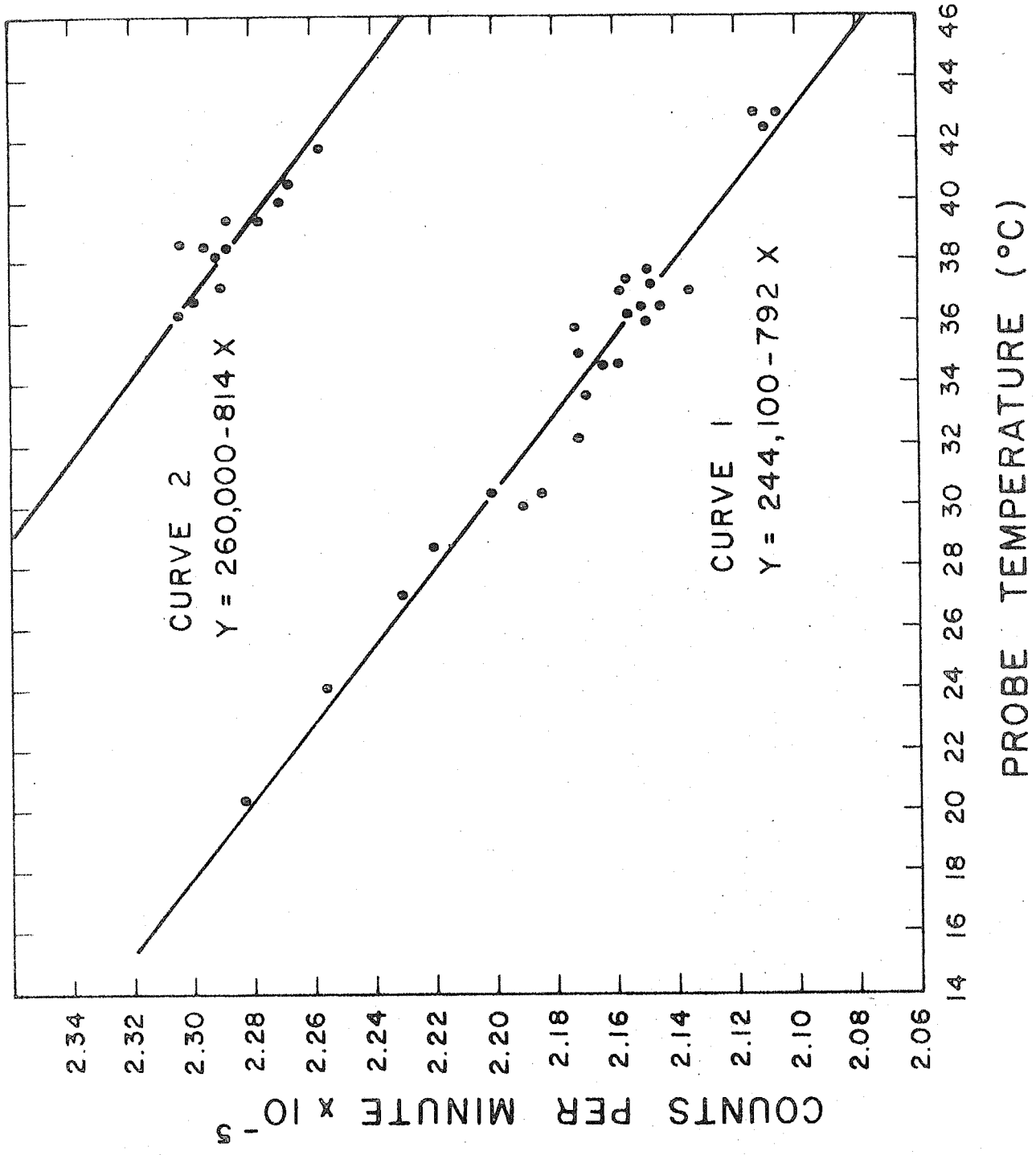

Figure 7. Peak count-rate in air as a function of detector probe temperature.

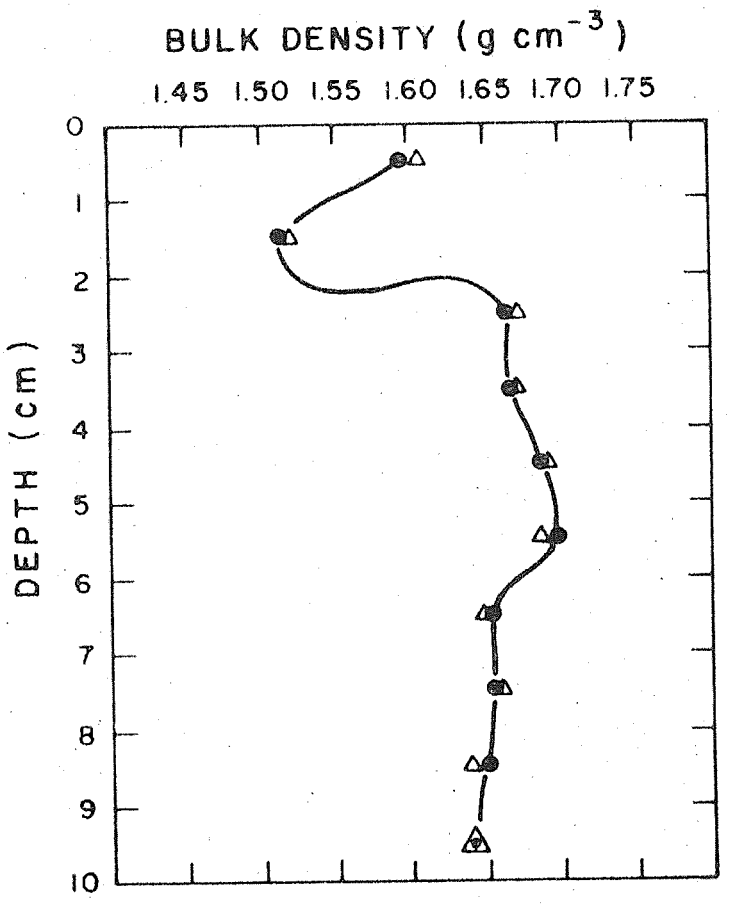

Figure 8. Bulk density calculated from the average of two (●) and of eight (▲) soil samples versus soil depth.

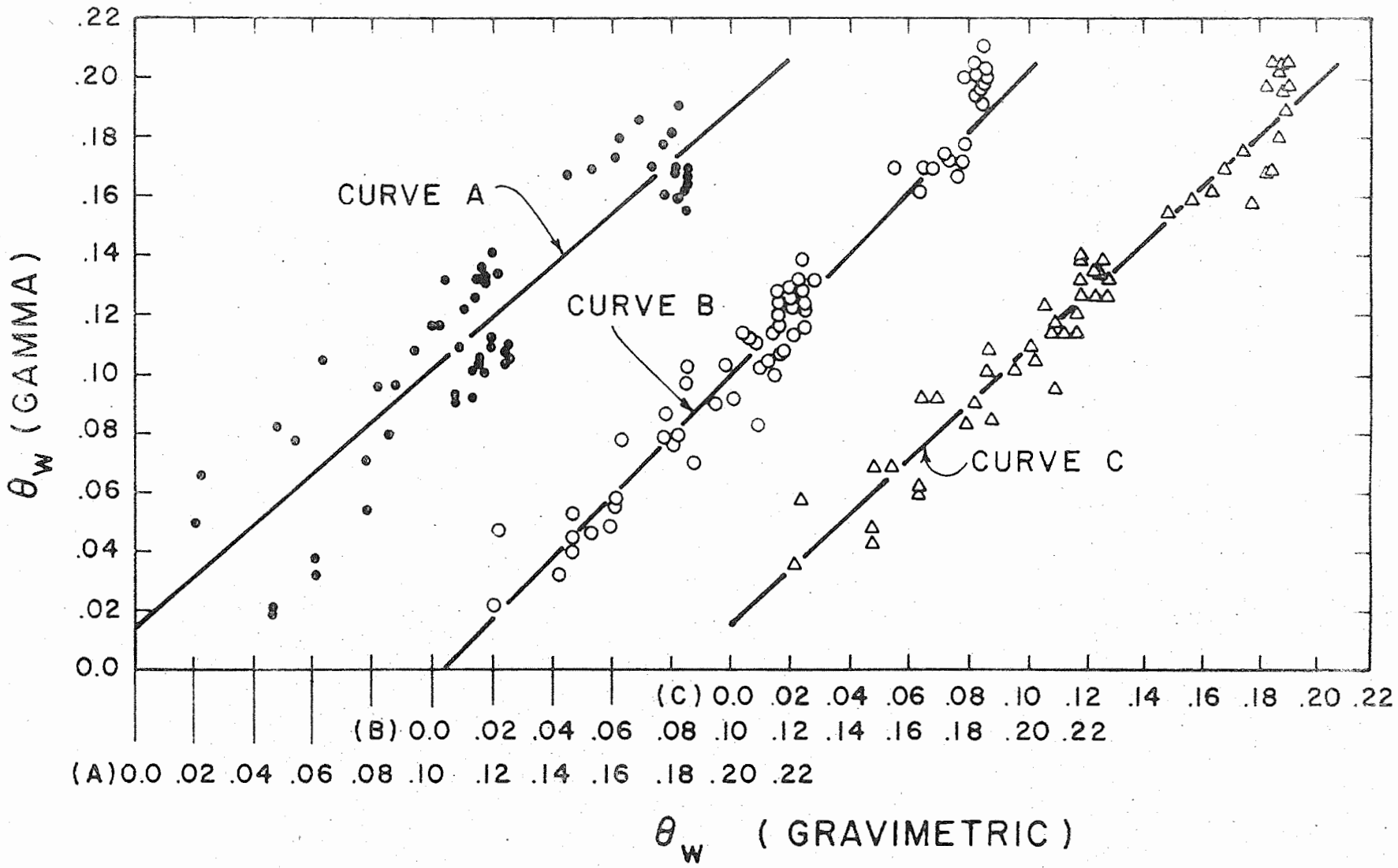

Figure 9. Calculated (by gamma transmission) versus measured gravimetric water content. "A" -- data neglecting temperature effects on probe performance. "B" -- data when relationship between count-rate and probe temperature is used. "C" -- data when I_o for each profile scan is used.

TITLE: FABRICATED-IN-PLACE, REINFORCED LININGS AND GROUND COVERS

CRIS WORK UNIT: SWC-018-gG-2 CODE NO.: Ariz.-WCL 68-2

INTRODUCTION:

Studies were continued using the pressure plate assembly to determine the maximum head of water that various treatments on different types of reinforcing materials are capable of supporting without leakage. Limited studies were conducted to determine lap joint strength, tensile strength and puncture resistance of asphalt treated fiberglass. New field installations consisted of a small holding pond at the Granite Reef test site and an ornamental fish pond in South Phoenix. Laboratory personnel assisted and instructed at the installation of two operational catchments installed by the Bureau of Land Management near Safford, Arizona.

PROCEDURE:

Procedures remained the same as described in the 1969 Annual Report with the following addition.

Strength of Material Studies. The lap joint strength and tensile strength of asphalt treated fiberglass was measured with the Dillon testing machine. The fiberglass matting was cut into strips 122 cm long and 10.2 cm wide. The strips were laid on a sand base and the asphalt applied by brushing. Lap joints 10.2 cm wide were made by placing ends of strips together before the asphalt had set. After curing outdoors the required length of time the asphalt-fiberglass strips were placed in the testing machine, with the clamps 25 cm apart, and pulled to failure of material or lap. Traverse speed of testing machine was 5.1 cm per min. All treatments were run in duplicate.

In the puncture resistance studies the fiberglass was treated on small soil trays 12.1 cm × 38.8 cm × 5.1 cm filled with soil. After curing, the samples were placed in the testing machine and a 2.54 cm × 2.54 cm square foot forced into the surface at a rate of .64 cm per min.

RESULTS AND DISCUSSION:

Strength of Material Studies. The lap and tensile strength studies were conducted using 1 oz per ft^2 and 1.5 oz per ft^2 chopped fiberglass matting. Cationic asphalt emulsion SSKH was brushed on at a rate of 1.4 kg asphalt m^2 and cured for periods of 1, 2 and 4 weeks. The results of these tests are presented in Table 1. The higher lap strength at one week compared to the tensile strength is a result of the increased thickness at the lap joint. All lap joints with 2 or more weeks curing were stronger than the material.

Puncture resistance tests on the two fiberglass thicknesses failed to damage the asphalt-fiberglass matting when the foot was pushed in .64 cm. Additional tests will be run with the foot penetrating to greater depths.

Pressure Plate Studies. Over 140 separate samples were tested on the pressure plates. This included 20 asphaltic treatments on four fiberglass materials. Several treatments were able to hold pressures equivalent to 14 feet of water. No treatment was consistently able to support pressures equivalent to over 20 feet of water. Apparently the asphalt undergoes a "cold flow" movement at these pressures and small holes develop. Studies are being conducted to develop coatings which are harder and will resist flowing under the higher pressures.

Field Studies. A report on the performance of the experimental asphalt-fiberglass ditch lining on Maui, Hawaii is given in Annual Report section titled "Materials and Methods for Water Harvesting and Water Storage in the State of Hawaii." The asphalt-fiberglass catchment at the Maui test site was in excellent condition when last inspected in June 1970. The Whitlock Peak operational catchment of asphalt-fiberglass in southeastern Arizona is reported to be in excellent condition. Bureau of Land Management personnel were sufficiently pleased with the performance of the Whitlock catchment that they installed two new catchments in September 1970 using asphalt-fiberglass. Each of these catchments of 10,000 ft^2 were installed by six men in approximately six hours.

A small, irregularly shaped, ornamental fish pond was lined with asphalt-fiberglass in January 1970. The pond, approximately 3 feet deep with a surface area of 5000 ft^2 was lined by five men in four hours. Seepage measurements one year later show a total loss, including evaporation, of 4 mm per day. A second small pond of 500 ft^2 at the Granite Reef testing site was lined by three men in one hour. This pond is used as a collection reservoir for a small watershed and is dry the majority of the year.

SUMMARY AND CONCLUSIONS:

Laboratory studies were conducted to measure the lap joint and tensile strength of asphalt treated fiberglass. After one week curing, tensile strength of the fiberglass was greater than 2 kg per cm width. All lap joints were stronger than the tensile strength of the asphalt fiberglass. Pushing a 1 inch square foot, 1/4 inch into samples of asphalt fiberglass supported on soil caused no significant damage to the material.

Pressure plate studies have shown pressures equivalent to 14 feet of water can be supported by asphalt fiberglass linings. Pressures greater than 20 feet of water usually cause the linings to fail. Apparently the higher pressures force the asphalt to cold flow causing small holes to form. Studies are being conducted to develop surface treatments which will prevent this cold flow movement.

Field installations of asphalt-fiberglass lined catchments and reservoirs are all performing satisfactorily. The performance of existing asphalt-fiberglass units was a major factor in the Bureau of Land Management installing two new operational units of asphalt fiberglass in southeastern Arizona.

PERSONNEL: G. W. Frasier and L. E. Myers.

CURRENT TERMINATION DATE: July 1971.

Table 1. Lap and tensile strength of asphalt-fiberglass lining materials.

Curing Time	Lap Strength		Tensile Strength	
	1.0 oz ft^{-2}	1.5 oz ft^{-2}	1.0 oz ft^{-2}	1.5 oz ft^{-2}
(weeks)	(kg/cm width)	(kg/cm width)	(kg/cm width)	(kg/cm width)
1	4.7	6.3	2.3	3.4
2	> 3.6 1/	> 6.3 1/	3.6	6.3
4	> 4.0 1/	> 8.0 1/	4.0	8.0

1/ Material adjacent to lap joint failed.

TITLE: CONSUMPTIVE USE OF WATER BY CROPS IN ARIZONA

CRIS WORK UNIT: SWC-019-gG-3 CODE NO.: Ariz.-WCL 58-2

INTRODUCTION:

See Annual Report 1969, Page 12-1.

OBJECTIVES:

1. To measure the consumptive use for the new varieties of wheat and barley.

2. To check the need for a fall irrigation or late irrigation near harvest, resulting from earlier planting dates and variety changes.

3. To make Piche evaporimeter measurements for possible correlation with consumptive use.

PROCEDURE:

The experiment was located on two borders, F47 and F48, (0.42 acres), at the University of Arizona Mesa Experiment Farm, Mesa, Arizona. Five varieties of wheat -- Sonora 64, Maricopa, Siete Cerros, Inia 66, and Ramona 50 -- and three varieties of barley -- Arimar, Hembar, and Arivat -- were planted 18 November 1969 in a randomized, split plot, six replication design. A precision planter was used, planting in rows 12 inches apart. Each plot was 6 rows wide and 30 ft long. The Sonora 64, Inia 66, and Ramona 50 were planted at a rate of 44 lbs to the acre. All other varieties were planted at the rate of 35 lbs to the acre. The seed bed had previously been fertilized with 200 lbs of nitrate, 50 lbs of phosphate, and had been irrigated about 12 days before planting. Soil moisture samples were obtained at the planting date, before and after each irrigation, at 10-day intervals throughout the growing season, and at the harvest date. Yields were measured on the two inside rows of each plot on 20 ft of row. Heads were hand cut and threshed with a plot thresher.

Timing of irrigations was based mainly on previous studies and close observation of the soil moisture measurements.

RESULTS AND DISCUSSION:

A good stand was obtained on all varieties. Temperatures were above normal in November and December, and with numerous small rains amounting to 0.8 inches, excellent growth occurred. Above-normal temperatures continued through January and February with less than normal rainfall. Because of the excellent growth and lack of normal rainfall, the first irrigation was given on 10 February. The second irrigation was not given until 20 March. During the period between the two irrigations, 2.03 inches of rain fell. The third irrigation was given on 7 April, and a fourth irrigation was given on 28 April to all varieties of the wheat except the Ramona.

Temperatures in April were lower than normal, by as much as 10 degrees in the last two weeks. This coincided with the peak consumptive use period for both barley and wheat. Consumptive use was about 2 inches lower in 1969-70 than in 1968-69 (Table 1). These lower temperatures may have affected the lower consumptive use.

SUMMARY AND CONCLUSIONS:

Yields of all varieties of barley showed considerable increase over yields in 1968-69 (Table 2). The fact that the barley did not lodge this year undoubtedly contributed to the improved yield.

Sonora 64 wheat showed some increase in yield over 1968-69, probably due to the higher seeding rate. However, overall wheat yields were down from 1968-69. Yields of all the Mexican varieties showed a similar trend.

Table 1 shows the average consumptive use for barley and wheat to be 22.10 and 25.40 inches, respectively. This compares to 26.6 and 27.3 inches as measured last year. Consumptive use for barley in the University of Arizona Agricultural Extension Service Bulletin TP-169 is 25.3 inches, which is very close to the two-year average as measured for the new varieties. The figure reported in TP-169 for wheat is 22.9 inches. This figure should be increased by at least 3 inches. It is also interesting to note that Sonora 64 uses less

water than the other high-yielding varieties. It was also noted that Sonora 64 was shorter in height and appeared to produce much less plant material.

PERSONNEL: L. J. Erie, D. A. Bucks, and O. F. French

CURRENT TERMINATION DATE: December 1970.

Table 1. Consumptive Use (inches) -- Barley and Wheat -- 1969-70

BARLEY *		WHEAT **	
Variety	Inches	Variety	Inches
Arimar	22.67	Inia 66	25.93
Arivat	21.59	Maricopa	26.30
Hembar	22.05	Ramona *	21.42
		Siete Cerros	26.64
		Sonora 64	23.17

* Three irrigations

** Four irrigations

Table 2. Average Yield (gms per plot) * -- Barley and Wheat -- 1969-70

BARLEY		WHEAT	
Variety	Yield	Variety	Yield
Arimar	2259	Inia 66	2054
Arivat	2517	Maricopa	2209
Hembar	1875	Ramona **	-----
		Siete Cerros	2018
		Sonora 64	2057

* Yield is the mean of 6 reps. Multiply gms. X 2.40 to get lbs per acre.

** No yield, due to excessive bird damage.

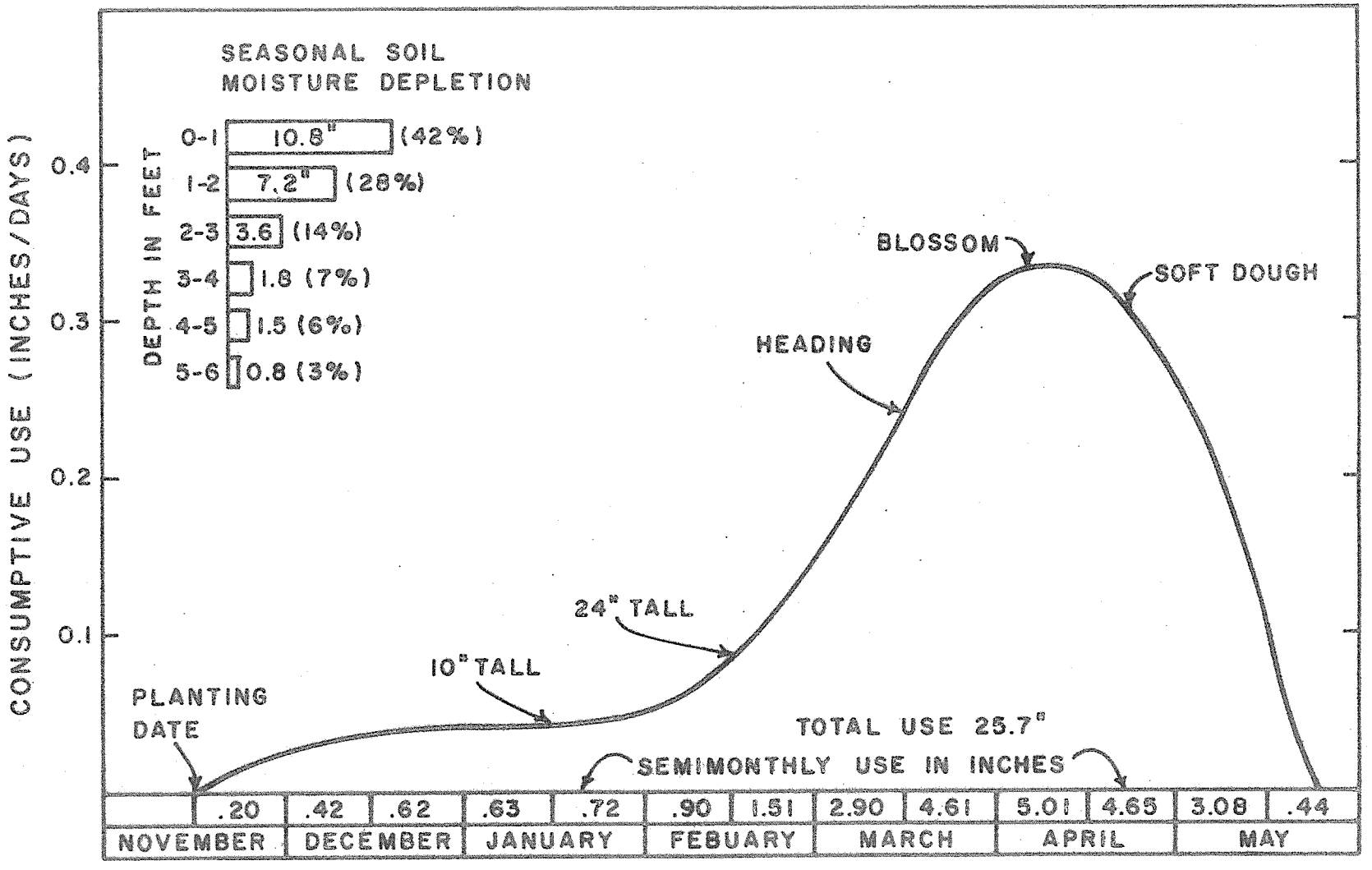

Fig. 1. Consumptive use for wheat (Maricopa) at Mesa, Arizona. 1969-70.

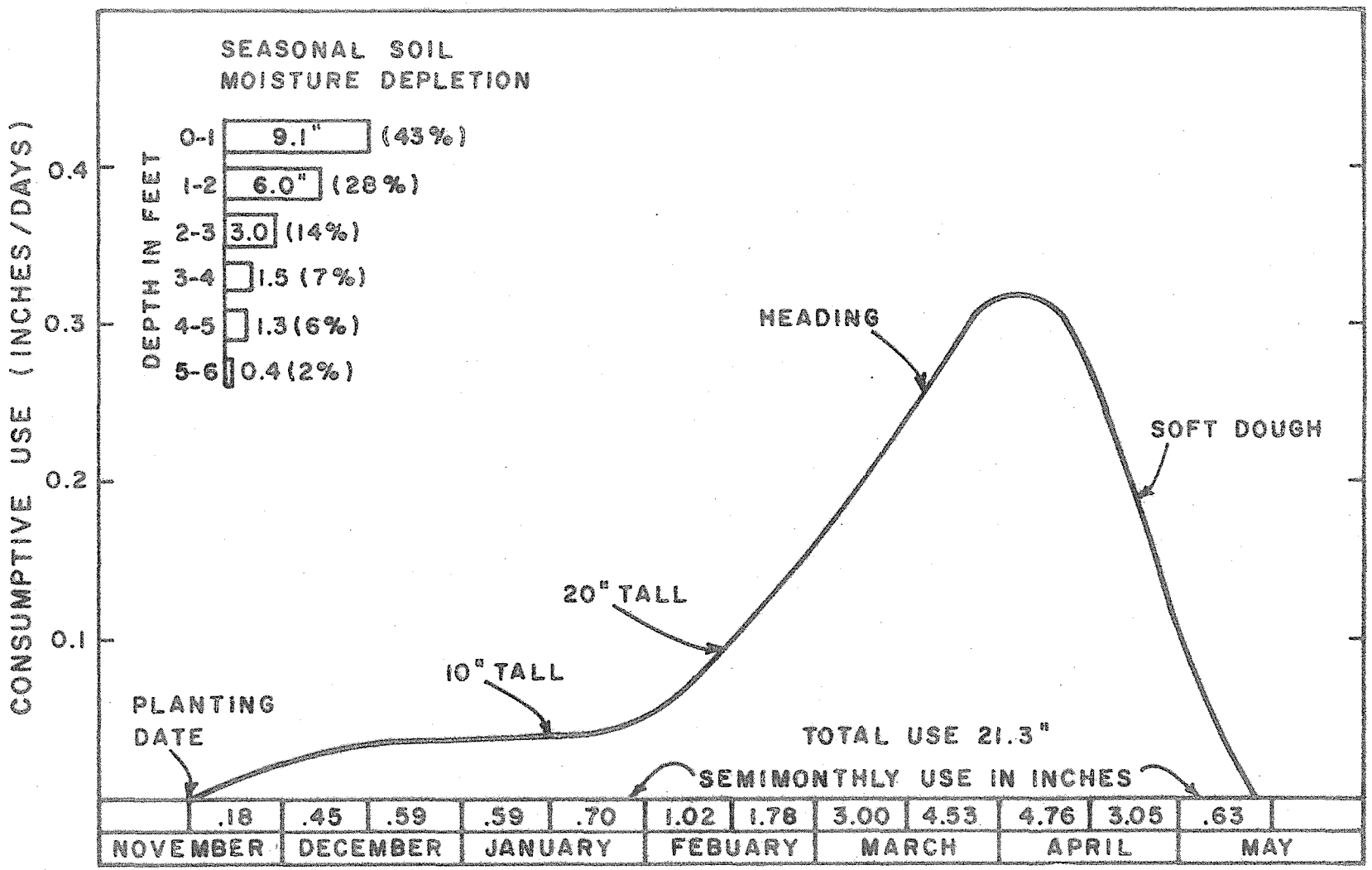

Fig. 2. Consumptive use for barley (Arivat) at Mesa, Arizona. 1969-70.

TITLE: PLANT RESPONSE TO CHANGES IN EVAPORATIVE DEMAND AND SOIL WATER POTENTIAL, AS SHOWN BY MEASUREMENTS OF LEAF RESISTANCE, TRANSPIRATION, LEAF TEMPERATURE, AND LEAF WATER CONTENT.

CRIS WORK UNIT: SWC-019-gG-3 CODE NO.: Ariz.-WCL-62-10

PART I. THE WATER USE EFFICIENCY OF AGAVE AND OPUNTIA PLANTS IN THE DESERT.

INTRODUCTION:

Two previous Annual Reports (1967, 1968) have described this project. After 21 months of growth on a moderately wet irrigation regime, on 14 July 1970 the agaves were put on wet versus dry treatments to determine the effect of two levels of soil water content on water use efficiency. At this time one-half of the 24 plants per plot was harvested to measure water use efficiency under the preconditioning regime. The present objective is to irrigate the wet treatment plants frequently enough to avoid any large rise in soil water tension, but with such small increments of water, usually 10 mm, that the yearly total application, including both irrigation and rainfall, will be no more than 610 mm (2 ft).

Conversely, the dry treatment will be subjected to an increased stress by being limited to a total water application of about one-half that of the wet treatment. The effect on growth will be measured by periodic counts of new leaves and successive harvests of the lower leaves, and eventually by a complete harvest of the 12 remaining plants in each of the two agave plots. The opuntia plants had not made sufficient growth to initiate dry vs. wet treatments by 14 July, and therefore still are being irrigated on a preconditioning schedule.

RESULTS AND DISCUSSION:

Irrigation. From 10 October 1969 through 14 July 1970, 18 irrigations were given to both agave plots, all but three of the water applications consisting of 10-mm increments, as recommended

in last year's Annual Report. Table 1 shows the monthly values of both irrigation and rainfall. For the 9-month period the total application was 349 mm. Projected to a yearly basis, this rate would be 465 mm, considerably less than the 686 mm applied the previous year, and yet sufficient to maintain a good growth rate. This increase in efficiency of application presumably was due to less deep percolation with 10-mm than with 20-mm irrigations. As shown in Table 2, the wet treatment was given 290 mm of irrigation water as compared to 60 mm for the dry treatment, from 15 July, the beginning of differential irrigation, through 30 November 1970, the time at which a "trimming up" harvest of only the lower, senescing leaves was made. Each irrigation except that on 16 July (20 mm) consisted of a 10-mm increment. Added to the rainfall, the total water application for the wet treatment was 374 mm, as compared to 144 mm for the dry treatment.

Because of what apparently was a developing sodium burn on some of the opuntias, both plots (No. 2 and 3) were given gypsum and two more irrigations than the agave plots (No. 1 and 4), for a total of 240 mm of irrigation water from 10 October 1969 through 14 July 1970. Also, from 15 July through 30 November plot 2, the south plot, was given numerous supplemental irrigations in an attempt to maintain the soil water content close to that of plot 3, the north plot, although no "wet" vs. "dry" treatments had been started for opuntia. This more liberal schedule consisted of 27 irrigations (totaling 280 mm) for plot 2 as compared to only 14 for plot 3 (totaling 140 mm) in addition to the 84 mm of rainfall during the period. No quantitative evaluation of the relative growth in the two opuntia plots was possible, but the plants appeared to progress in a similar manner.

The differential irrigation of opuntia during the preconditioning period was tried in an attempt to avoid the prevalent difference in soil water content occurring when identical amounts of water were applied to north and south plots. This same

difference is shown by the north vs. the south plot of agave (Figure 1), where the north plot (No. 1) stayed near 13% water content, but the south plot (No. 4) at only 9%, under the same irrigation regime. A texture analysis of the soils in plot No. 3 and 4 at three depths, 0-10 cm, 10-20 cm, and 20-30 cm revealed no significant differences with either depth or plot; the values for both plots ranged from 5 to 8% clay, 13-15% fine silt, 25-31% coarse silt, and 49-59% sand, which classifies the soils as a sandy loam. Moreover, the amount of particles larger than 2 mm did not vary between plots. As of now, the difference in water holding capacity is unexplainable. A tenuous hypothesis would be a structural difference, but no evidence for this is at hand.

Soil Water Content (θ_v). As mentioned in last year's report, both agave plots were given a total water application of 686 mm for the first year, during which time 179 new leaves developed in plot 1 (north plot), and 175 in plot 4. Since both plots initially had 24 transplants with the same aggregate weight, and since the number of new leaves was almost the same during a year's growth, it was assumed that the gain in weight was equal under the preconditioning irrigation schedule specified above. Therefore, equal amounts of irrigation water per plot were continued for another 9 months, although neutron meter readings had been showing a higher soil water content in plot 1 than in plot 4.

That the differences were not negligible is shown graphically in Figure 1. Also quite apparent is the high sensitivity of the neutron method to small changes in θ_v. The first prominent peak in θ_v occurs because a heavier than normal irrigation (20 mm) on 26 February was followed by two heavy rains on 2 and 3 March, totaling 39 mm, and then a third rain of 15 mm on 5 March.
Shallow applications (10 mm) cause an increase in θ_v of about 1.5%, whereas 20-mm applications raise θ_v by about 3%, the amplitude depending somewhat on the season. The two plots maintained a remarkably consistent difference in θ_v while the preconditioning period

was in effect. After 14 July the decreasing irrigation frequency for the "dry" plot (No. 1) was just beginning to pull down θ_v from its characteristically high value of about 13.5%, when a heavy rain (63 mm) on 6 September sent θ_v up to the highest point of the year, 23.2 percent on 11 September. From this point a slow decline set in, lasting until late October when the 12% value prior to the rain was regained. No irrigation was given to the "dry" plot between 24 August and 10 November.

Seven irrigations on the "wet" plot (No. 4) between 14 July and the middle of August, as well as 10 mm of rain succeeded in raising θ_v somewhat - from about 8.5% during June and early July to an average of 9.5% from the middle of July to the middle of August. Then θ_v started to fall off, despite 10-mm irrigations on 21, 24 and 31 August. The heavy rain in early September raised θ_v to 12.5% briefly. From this time on, frequent additional 10-mm irrigations succeeded in gradually building up θ_v with no difficulty, the values averaging around 13% for most of October. During November and December, a decreasing frequency of application resulted in a tapering off to around 9%. This value is not considered as limiting growth, since no new leaves emerge during the winter months. When growth starts again, differential irrigation will be resumed.

Gravimetric Sampling. Intensive gravimetric sampling of the soil in plot 4 (agave) was carried out over a 3-day period in August 1970, with the following objectives: (1) to verify the readings of the neutron meter, in view of the possible limitation imposed by monitoring θ_v at a shallow depth (20 cm) that may permit escape of neutrons to the air, (2) to determine the depth of water penetration from the usual shallow irrigation (10 mm) and to find out if daily evaporation is a significant fraction of the total application, and (3) to ascertain the irrigation frequency needed to maintain θ_v at a level consistent with a "wet" treatment.

Five sites within the 20 m^2 plot were sampled with an Oakfield probe. Two cores were taken at each site at depths of 0-10 cm, 10-20 cm, and 20-30 cm. Samples were collected just before an irrigation. Water was applied rapidly and uniformly, 10 mm being put on from 1025 to 1030 on 18 August, designated as the reference time (T_o). Subsequent 5-replicate samples were taken at T_o + 0.73, 2, 24, 48, and 72 hours, respectively. The data are shown in Table 3. Later, bulk density measurements were made for the three sampling depths, and a texture analysis also was made from soil at the five sites. These samplings indicated that 70% of the water applied was retained in the 0-10 cm layer, 26% in the 10-20 cm level, and only 4% in the 20-30 cm level, when the half-time for soil sampling was 0.73 hour after T_o.

Use of the appropriate bulk density for each layer resulted in a calculated gain in θ_v of 235 liters, as compared to the 200 $\pm$ 1 liters actually applied. This overestimate may be due to too high a bulk density value or to a nonuniform distribution of water over the plot. However, five sites were averaged for both θ_v and bulk density.

The chief value of this calculation is to show that under normal conditions there is no deep percolation. Table 3 does show, however, that there is a redistribution of water occurring from the first sampling (T_o + 0.73 hour, when 90% of the surface water had infiltrated) to the second time (T_o + 2 hours). This depletion of the upper layer amounted to 2.1%, whereas the corresponding gain by the two lower layers totaled 1.8%. The small difference could be attributed to evaporation, but it is more likely to be experimental error. The significant points are that no water moved below the root zone and that beyond two hours there was no further gain by the lowermost layer, but rather a loss after 24 hours to the upper levels.

In an effort to check the validity of the neutron readings taken at the 20-cm depth (the only level corresponding to the bulk

of the agave roots), Table 4 was constructed, comparing gravimetric and neutron meter results. Although the neutron meter is seen to respond to irrigation, the change is small, and both the absolute value of θ_v and the change are not quite equal to the corresponding values of gravimetric data, or to averages of different depths. In general, however, it can be concluded that the neutron meter readings are only somewhat below the true values.

Actual versus Potential Evapotranspiration. A Young pan 2 m away from the plots was used for an estimate of potential evaporation (E_o). Table 5 shows that during the time of gravimetric sampling E_o was 0.27 mm/hour. If it is assumed that evapotranspiration (ET) from the agave plot can be found reliably by calculating the difference between the amount of depletion in θ_v of the upper level and the gain by both lower levels, ET was 0.24 mm/hour, essentially equal to E_o. This is reasonable, since the surface temperature of the wetted soil was slightly higher than that of the water surface in the Young pan, and since 70% of the water applied stayed near the surface for more than an hour. As mentioned earlier, though, this computation may be straining the accuracy of the data, in view of the short interval and consequent small change. On the other hand, over periods of a day or more the method should be valid. Such a comparison shows that ET from the agave plot is less than half of the potential rate even in the first 24 hours (Table 5). Over the 3-day period ET was only 10.9 mm as compared to 34.1 mm for E_o, showing that a decline in capillary conductivity presumably was limiting ET. Nevertheless, the standard irrigation is seen to last only for about three days in hot weather. The schedule actually adopted for the wet treatment beyond 14 July made use of the data concerning ET, in that it consisted of two irrigations per week during hot, rainless weather.

Plant Growth During the Preconditioning Period.

A. Opuntia

As of 14 July 1970, when one-half of the agaves was

harvested from plot No. 1 and 4, the opuntias had not grown sufficiently to justify the start of a drying cycle. As mentioned in last year's report, the opuntia plants in plot 2 had developed 32 new pads in one year, as compared to 43 in plot 3, as of October 1969. By May 1970, 41 more pads had developed in plot 2, and 59 in plot 3. Nevertheless, ground cover was poor, due mainly to an initial number of only 12 plants per plot instead of the 24 for agave. Moreover, an apparent sodium burn caused the loss of several opuntia pads. Therefore, it was decided not to begin differential irrigation treatments on opuntia, but rather to extend the preconditioning period. The preconditioning was modified in an attempt to maintain θ_v in plots 2 and 3 closer together than previously, in an attempt to equalize the production of new pads per plot. This necessitated giving considerably more irrigations to plot 2 (south plot) than plot 3.

B. Agave

(1) Leaf Growth. Although the number of new leaves formed in the two plots was essentially equal during the first year (Table 6), four successive leaf counts during the next 39 weeks of the preconditioning period gave an average of 20% more new leaves in plot 4 than plot 1. This happened despite the same irrigation regime in both plots and a significantly higher θ_v in plot 1 than plot 4. Even though leaf number may not necessarily be proportional to fresh weight gain, it ordinarily is a good indication of growth. When the increase in fresh weight was determined by harvesting 12 of the 24 plants in each agave plot, the one in which leaf growth had been 20% better, plot 4, gained much less than plot 1, which is a paradox.

During the 19-week period from 14 July to 23 November plot 4 again produced the larger number of new leaves, just as it had done four times previously. Therefore, this fact by itself is no indication of an influence of the wet treatment (higher frequency irrigation schedule) on growth. However, on 23 November the ratio

of plot 4 to plot 1 was the highest it had ever been (1.38). Such a high ratio is evidence that the differential irrigation schedule in effect for 19 weeks probably was taking effect. It cannot be determined if the high ratio is due to a stimulation of leaf growth by the wet treatment as compared to the previous moderately wet schedule or to an inhibition of leaf formation on the dry treatment. Later leaf counts during good growing weather should help determine the answer. Also, periodic leaf harvests from the bottom of the plant should correlate with the moisture level of the soil.

Over the 21-month preconditioning period plot 4 gained 35 kg (from an initial fresh weight of 9845 g to a weight of 44750 g on 14 July 1970). In contrast, although in plot 1 the initial weight of the 12 plants was only slightly more than that of plot 4 (11987 g), the final weight was much more (68250 g), a gain of 56 kg. This large difference in favor of plot 1 is hard to reconcile with the equality of leaf production during the first year and the repeated measurements of leaf count in favor of plot 4. However, a correlation that probably is significant in explaining the results is the persistently higher θ_v in plot 1 than in plot 4, even under the same irrigation regime (Figure 1). The higher θ_v presumably would be associated with a lower soil water tension and therefore be conducive to improved growth, manifested in fresh weight gain.

(2) Water Use Efficiency. Over the 1.75-year preconditioning period both plots 1 and 4 received the same total water application of 1035 mm, made up of 390 mm of rain and 645 mm of irrigation water (34 applications, mostly in 10-mm increments). The fresh weight gain of 56 kg from one-half the plot (No. 1) can be thought of as having been produced on one-half the total water application, or 517.5 mm. These data give a water use efficiency (WUE) of 5.4 kg m^{-3} of water for plot 1. For plot 4 the yield of only 35 kg for the same amount of water (517.5 mm) gives a WUE of

3.4 kg m^{-3}.

For comparison, a calculation of the WUE of alfalfa grown in the Salt River Valley, Arizona is made, as follows: total ET for one year is 7500 m^3 (from L. J. Erie's consumptive use data, 73 inches per year). Total yield of fresh weight, estimated from an air-dry weight of 10 tons per acre, is 40 tons per acre, or 36280 kg. Therefore WUE = 4.8 kg m^{-3}. This computation indicates that even at an early stage of growth, the WUE of agave is on a par with that of alfalfa, a crop that is believed to represent quite a challenging comparison. As the agaves grow larger, forming a canopy, less surface evaporation should occur, with the likelihood that the same or even less irrigation water will be required, even from larger plants, in view of the agave's capability of daytime stomatal closure. Also, production should increase as further growth by both the original plants and the offshoots occurs. Therefore, WUE can be expected to increase with time.

SUMMARY AND CONCLUSIONS:

Reducing the amount of irrigation water from 20 to 10 mm as the standard application during the nine months that made up the second part of the preconditioning period succeeded in decreasing the total water application (rain plus irrigation) from 686 mm per year to a prorated yearly value of 465 mm for the agaves. The opuntias were given two more irrigations than the agaves to help correct a sodium burn. On 14 July differential irrigations were begun for agave, with the objective of maintaining a fast growth rate in the wet treatment. This was done by increasing irrigation frequency to maintain a low soil water tension in the root zone. The goal is not to exceed 610 mm total water application per year for the wet treatment, as compared to about half as much for the dry treatment.

Yield over the 21-month preconditioning period was greatly different on the two agave plots. There was a fresh weight gain of 56 kg for plot 1 (12 of the original 24 plants being harvested);

plot 4 gained only 35 kg, despite the fact that the first year's increase in leaf number was equal in both plots and that leaf growth rate during the nine months before harvest was 20% greater in plot 4 than plot 1. The greater gain in fresh weight in plot 1 was positively correlated with the consistently higher soil water content in plot 1 than plot 4, despite equal irrigations. In the 21-month preconditioning period 1035 mm of water was applied to both plots, giving a calculated water use efficiency of 5.4 kg m^{-3} for plot 1, and 3.4 kg m^{-3} for plot 4. These values compare favorably with that for alfalfa, 4.8 kg m^{-3}.

Intensive gravimetric sampling over a 3-day period established that (1) the neutron meter readings taken at 20 cm are highly responsive to changes in soil water content, but slightly below the true moisture value, (2) no percolation occurs below the 30-cm depth from the standard 10-mm irrigation, and (3) evapotranspiration drops below the potential rate 24 hours after irrigation, and (4) during hot weather the 10 mm of added water is depleted in about three days, thus requiring frequent irrigations to maintain a wet treatment.

Present plans are to continue the wet and dry treatments as already described, making periodic leaf counts and small leaf harvests from the lower part of the plant for determination of the gain in fresh weight with time. Knowledge of the total water application at any harvest time will permit successive calculations of water use efficiency. It is believed desirable to make a large enough number of these measurements for the total weight gain to be great in proportion to the initial fresh weight on 14 July, in order to minimize the effect of possible errors in estimating initial fresh weight of the 12 plants left after the preconditioning harvest.

PART II. AUGMENTED WATER STORAGE IN SAND BY SUB-SURFACE BARRIERS, AS RELATED TO POTATO PRODUCTION.

The objective of the preliminary research reported here was to augment available water storage in sand by placement of sub-surface barriers of water-repellent material to minimize water losses due to deep percolation. Low cost materials which achieve this goal can be expected to bring about an increase in water use efficiency, either by lowering the water requirement or by enhancing crop growth on a given amount of water. Sprayable silicones show promise of meeting both the economic and technological requirements for success, and were used as sub-surface barriers to increase the growth of potatoes.

PROCEDURE AND RESULTS:

A pit was excavated in the lysimeter field at this Laboratory. It was 80 ft long by 10 ft wide by 3.5 ft deep, sloping to 4 ft at the north end. The pit was lined with butyl rubber sheeting, and was provided with a gravel-covered tile drain over its whole length, and a sump at the lower end, equipped with a drainage pump. The pit was filled with river sand closely simulating Superstition sand, and irrigated heavily with tap water for consolidation, levelling, and leaching; then the drainage water was pumped out.

Treatments. Treatment (A) was a control, a conventional potato bed with no sub-surface barrier (other than the butyl lining 3.5 ft below). Treatment (B) was a deeply placed barrier with the silicone layer being parallel to and 18 inches below the ground surface, in addition to forming the sloping walls and ends of a "tub" whose bottom was 7 ft long by 4 ft wide; the overall volume was approximately 500 liters. Treatment (D) was a shallow barrier in the form of a "vee" whose apex was 10 inches below the ground level, directly below the center of the irrigation furrow. Since the furrow was 4 inches deep, the depth of sand over the apex of the barrier was only 6 inches. The upraised segments of the "vee," each 12 inches long, were set apart at a 75°-angle, and thus formed

a shallow tray that would store a small amount of water, but would function primarily in shunting water sideways, for efficient application of small amounts.

Potato Bedshaping and Planting. After the surface of the sand was levelled, the beds were shaped by excavation and use of a template dragged along the 9-ft rows. The barrier was made by spraying R-20, a commercial silicone liquid that forms a thin, water-repellent layer after curing. When the layer had dried, sand was put back in place, recommended amounts of nitrogen and phosphorous fertilizers were added, and the seed pieces were planted at the overall ground level and covered with sand. The variety was Pontiac, a red-skinned potato grown locally. Seed pieces had been treated with a fungicide, and were planted 6 inches apart in the row, two rows to a bed, on 18 March 1970. Additional nitrogen was applied on 13 May; both nitrogen and potassium were applied on 18 and 25 May and on 8 June.

Irrigation. Over the 13-week growing period 20 irrigations were given to treatments (B) and (D), and 21 to (A), the control, beginning on 18 March. Criteria for irrigation were: (1) plant appearance, (2) previous scheduling experience, and (3) tensiometer readings at the 6-inch depth. Irrometer tensions 24 hours after irrigation were 6 cb, and were allowed to rise to 10 cb before irrigation. From a determination of the soil water characteristic curve supplemented by a sunflower wilting point, it was calculated that the range in soil water tension from 6 to 10 cb represents a depletion of about one-half of the available water. The irrometers were in line with the seed pieces. During irrigation, water was applied at a rate high enough to build up a 10-cm head in the furrow, and was run long enough to move across a 43-cm distance to the irrometer cup and lower the tension from 10 cb to zero. This criterion usually was met by application of 500 liters (ℓ) to (A) and (B), and 300 ℓ to (D). On occasion much larger irrigations were given to induce subbing to a point 20 cm beyond the center of

the row. The total quantity of water applied was 18.1 m^3 for (A), 12.0 m^3 for (B), and 11.8 m^3 for (D). Since these volumes were applied to the same area for all treatments (4.74 m^2), the equivalent surface depth was 383 cm for (A), 253 cm for (B), and 249 cm for (D). These are large amounts of water, as might be expected for a sandy soil in a hot, dry climate. Nevertheless, in both (B) and (D) treatments the silicone barrier reduced the irrigation requirement about 35% below that of the control.

The salt content of the irrigation water was low, averaging 0.80 mmho cm^{-1} (510 ppm) over the whole season. Frequent pumping out of the drainage water combined with considerable leaching maintained the effluent almost as low as the irrigation water, 0.88 mmho cm^{-1} (565 ppm). After nitrogen fertilization a slight rise in electrical conductivity was noted.

Soil Water Content by Weight (θ_w). That the barrier was effective in augmenting θ_w is shown in Table 7. The data for 24 March represent a dry situation, six days after irrigation, in contrast to the three other dates, where θ_w is the value 24 hours after irrigation. At the three depths on all four dates θ_w was higher in (B) than (A), the overall average difference being 2.4%. Although seemingly small, this difference is enough to lower soil water tension from 7 to 5 cb. This may be sufficient when integrated over a long period to increase growth at the low tension, in view of the extreme sensitivity of growth to low tissue water potential.

Growth and Yield. Late planting may have reduced yields. The yield of ungraded tubers, in grams per plot, was: (A) 2556, (B) 8164, and (D) 4182. The silicone barriers in treatments (B) and (D) not only reduced the irrigation requirement, but also increased the yield. The term "water use efficiency" takes both factors into consideration. The water use efficiency, in kg yield per m^3 of water applied, was: (A) 0.1, (B) 0.7, and (D) 0.4.

SUMMARY AND CONCLUSIONS:

It appears obvious from these preliminary results that silicone barriers do enhance soil water storage in sand, and that even a small augmentation can increase yields. However, the comparative yields may be somewhat misleading, since the relative standings may be affected by irrigation scheduling. For example, a greater number of smaller irrigations than were given in this experiment might have improved the yield of the control more than that of treatments (B) and (D). Despite these qualifications, these data demonstrate the potential of silicone barriers to increase water use efficiency economically.

PERSONNEL: William L. Ehrler

CURRENT TERMINATION DATE: December 1970

Table 1. Monthly amounts of water received by the two agave plots at Granite Reef from 10 Oct 1969 through 14 Jul 1970, in millimeters.

Month	By Irrigation	By Rainfall	Total
Oct	10	10.8	20.8
Nov	-	19.6	19.6
Dec	-	28.2	28.2
Jan	20	1.9	21.9
Feb	20	9.4	29.4
Mar	-	62.5	62.5
Apr	60	3.6	63.6
May	40	-	40.0
Jun	50	-	50.0
Jul (1-14)	10	2.8	12.8
TOTAL	210	138.8	348.8

Table 2. Monthly amounts of water received by the wet and dry treatments of agave at Granite Reef from 15 Jul through 30 Nov 1970, in millimeters.

	By Irrigation		By Rainfall	Total	
Month	Wet Trt.	Dry Trt.	(Both Trts.)	Wet Trt.	Dry Trt.
Jul (15-31)	50	10	3.3	53.3	13.3
Aug	60	40	10.2	70.2	50.2
Sep	50	-	64.2	114.2	64.2
Oct	90	-	4.7	94.7	4.7
Nov	40	10	1.8	41.8	11.8
TOTAL	290	60	84.2	374.2	144.2

Table 3. Profile changes in soil water content, percent by volume, (θ_v) after a 5-minute application of 10 mm of water to agave plot 4 on 18 Aug 1970.

Depth (cm)	θ_v, Mean of two cores at five sites						Percent of total gain at T_o + 0.73 hr
	T_o - 0.5 hr	T_o + 0.73 hr	T_o + 2 hr	T_o + 24 hr	T_o + 48 hr	T_o + 72 hr	
0-10	7.0	15.3	13.2	9.5	8.2	7.2	70
10-20	7.6	10.7	12.0	11.5	10.4	8.7	26
20-30	7.8	8.2	8.7	8.7	8.5	7.1	4

Table 4. Profile changes in soil water content in agave plot 4 at Granite Reef as measured gravimetrically and with a neutron meter, in response to a 10-mm irrigation on 18 Aug 1970.

	Soil water content, percent by volume*						
	Gravimetric						
Depth (cm)	Before Irrig	After Irrig	Gain	Probe midpoint depth (cm)	Before Irrig	After Irrig	Gain
0-10	7.0	15.3	8.3	10	7.2	9.3	2.1
10-20	7.6	10.7	3.1	20	9.2	9.6	0.4
20-30	7.8	8.2	0.4	30	9.2	9.4	0.2
Mean of 0-30	7.5	11.4	3.9				
Mean of 10-30	7.7	9.4	1.7				

*Gravimetric values converted to a volumetric basis by use of the following bulk densities: 1.72 for 0-10 cm depth, 1.85 for 10-20 cm, and 1.74 for 20-30 cm.

Table 5. Potential evaporation (E_o), measured with a Young pan at Granite Reef, as compared with ET from agave plot 4.

Date	Time	Pan level, cm	Interval (hr)	E_o (mm)	E_o mm/hr	E_o mm/24 hr	ET mm/hr	ET mm/24 hr
18 Aug 70	1032	51.18						
	1222	51.13	1.83	0.5	0.27		0.24	
	1310	51.10	0.80	0.3	0.38			
19	1025	50.10	23.87	10.8	0.45	10.8		4.2
20	1025	48.80	24.00	13.0	0.54	13.0		2.6
	1225	48.77	2.0	0.3	0.15			
	1328	57.03	(pan refilled)					
21	1025	56.13	21.0	9.0	0.43	10.3		4.1

Table 6. Growth rate of agave at Granite Reef before and after initiation of the wet vs. dry irrigation regimes on 14 July 1970.

Date	No. of new leaves		No. of Weeks	New leaves per week		Plot 4 / Plot 1
	Plot 1	Plot 4		Plot 1	Plot 4	
10 Oct 68	Reference date			(Mod. wet)		
10 Oct 69	179	175	52.0	3.4	3.4	1.00
13 Feb 70	47	60	15.4	3.0	3.9	1.30
09 Apr	44	52	7.8	5.6	6.7	1.20
08 May	20	24	4.1	4.9	5.8	1.18
13 Jul	90	99	9.6	9.4	10.3	1.10
14 Jul	ONE HALF OF THE 24 PLANTS PER PLOT REMOVED			(Dry)	(Wet)	
23 Nov	45	62	19.0	2.4	3.3	1.38

Table 7. Soil water content, percent by weight, at three depths under the surface of the potato irrigation furrow at four sampling dates.

Depth (cm)	24 March Treatment A	B	D	26 March Treatment A	B	D
2.5-10	4.2	7.3	6.8	5.8	7.6	11.4
10-18	5.4	9.2	-	8.0	8.9	-
18-25	6.0	11.7	-	8.5	12.2	-
$\bar{X}$	5.2	9.4	-	7.4	9.6	-

Depth (cm)	4 April Treatment A	B	D	17 April Treatment A	B	D
2.5-10	4.9	8.7	7.5	5.4	6.4	9.2
10-18	5.7	7.2	-	7.4	7.6	-
18-25	5.9	6.1	-	7.1	9.9	-
$\bar{X}$	5.5	7.3	-	6.6	8.0	-

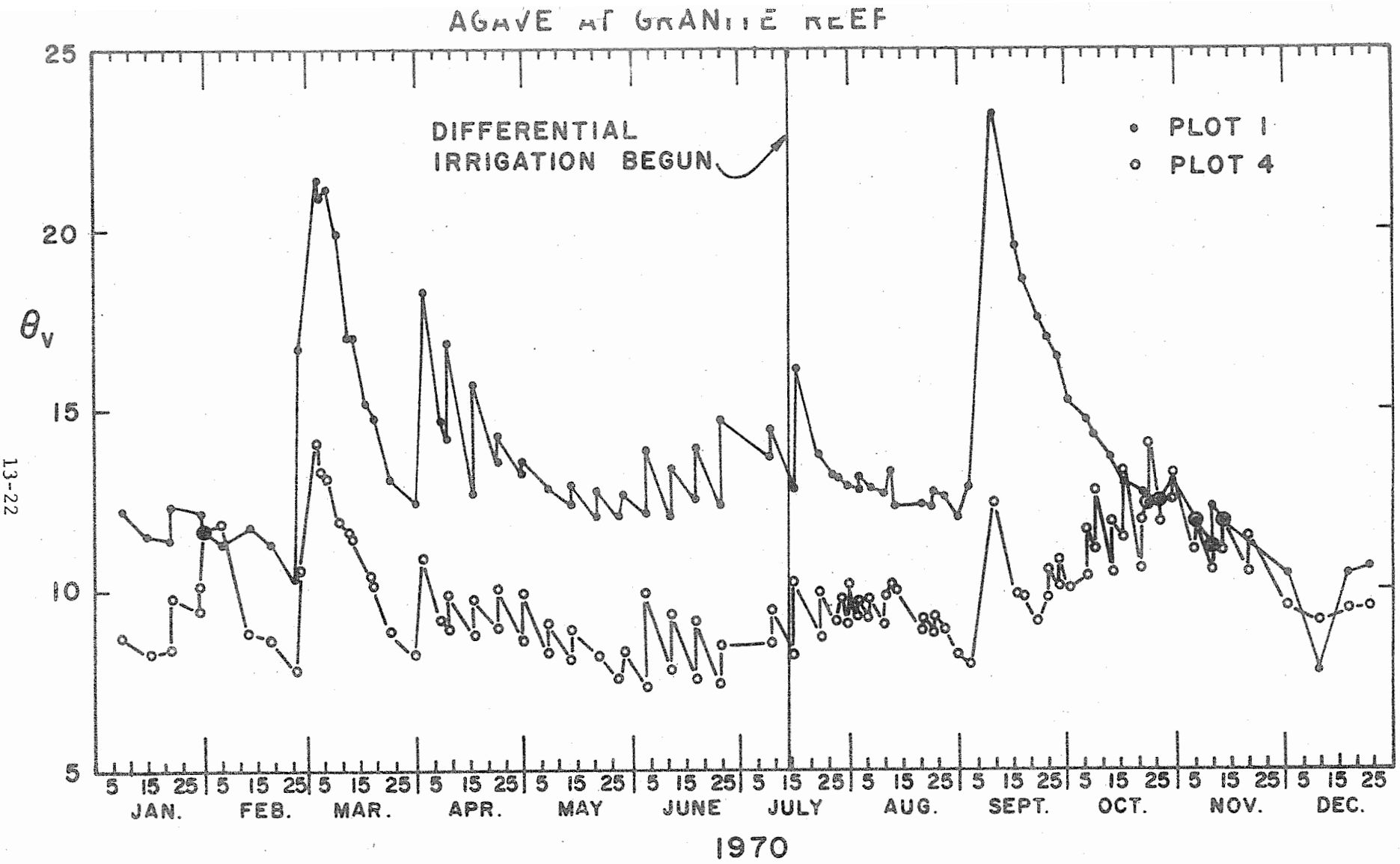

Figure 1. Changes in soil water content by volume (θ_v) at 20 cm as measured with a neutron meter in agave plot No. 1 and 4 in response to rainfall and differential irrigation levels.

TITLE: IRRIGATION OUTLET STRUCTURE TO DISTRIBUTE WATER ONTO EROSIVE SOILS.

CRIS WORK UNIT: SWC-019-gG-3 CODE NO.: Ariz.-WCL-66-2

INTRODUCTION:

For need of study, see Annual Report, 1966.

OBJECTIVES:

1. To obtain design criteria for low-cost irrigation outlets that will distribute large streams of water without excessive erosion.

PROCEDURE:

The major activity on this project has been to construct outlets at farm sites where erosion problems exist, observe their operation, determine their weaknesses, then repair or reconstruct them and continue to observe their performance and longevity.

In 1970, a new structure was built on the Wheeler Ranch near Tacna, Arizona. A very serious erosion problem existed, associated with a jack gate normally discharging about 17 cfs into a bermudagrass field. A semi-circular dissipator wall, 1 ft high, equipped with a 4 ft apron, was constructed of concrete. To date, erosion seems to be eliminated.

The SS-2 asphalt structure on the Spencer and Spencer Ranch was rebuilt after bermudagrass and sand burrs penetrated through the asphalt. A clay emulsion was placed over the SS-2. No visible signs of breakthrough of weeds have been observed, to date.

Most of the five structures on the Fred Enke Ranch were repaired. Damage was due to machinery, and design seemed to be adequate.

The Cannon Ranch structures have been in for more than five years. Machinery cannot reach these structures, but bermudagrass is abundant and has caused separations where concrete has been

poured at different times. Since 1965, aprons have been attached to the poxes in such a way that this problem is now virtually eliminated. These structures will be changed and repaired to alleviate the bermudagrass problem.

The structures on the Currie, Woodhouse, Naquin and Spaar ranches seem to be designed properly, and only machinery damage has been noted. The Woodhouse structures are in conjunction with jack gates. Length of run studies on the Woodhouse and Spaar ranches, which are dead level, were conducted in 1970.

SUMMARY AND CONCLUSIONS:

Structure inspections this year showed that dissipator boxes will discharge non-erosive streams of water when they are properly attached with appropriate components.

Properly designed structures did not fail because of normal wear, but because of damage by machinery. Structures associated with the jack gates have not been installed long enough to test whether or not our design is correct. The structures we built have stopped the erosion, and hopefully the operators will relevel and fill the area that was eroded before the structures were built. Then, we can properly evaluate our structures and make any necessary changes.

PERSONNEL: L. J. Erie, J. A. Replogle, D. A. Bucks, and O. F. French

CURRENT TERMINATION DATE: December 1970.

TITLE: FLOW MEASUREMENTS IN OPEN CHANNELS WITH CRITICAL DEPTH FLUMES

CRIS WORK UNIT: SWC-019-gG-3 CODE NO.: Ariz.-WCL 67-1

INTRODUCTION:

Previous reports (see Annual Reports for 1966-1969) summarized the results of studies on several critical-depth flumes with throat sections that were trapezoidal, triangular or circular. The technical paper "Flow Measurement with Critical-Depth Flumes," presented in April, 1969, before the VII Congress of the International Commission on Irrigation and Drainage, Mexico City, was subsequently followed by a presentation in July, 1970, before the American Society of Agricultural Engineers. The paper title was "Critical Depth Flumes for Determining Flow in Canals and Natural Channels." While the first paper presents some theoretical aspects for predicting the calibration results for flumes and also summarizes the effects of installation anomalies, the second paper proposed sizes for several common ditch shapes frequently constructed.

Several more flumes have been designed for other agencies, three of which have been constructed.

Five more flumes have been constructed to check a variety of aspects including the effects of roughness in the throat and its relation to throat length and shape, bringing the total of flume shapes calibrated to ten.

PROCEDURE:

The laboratory calibration was made as previously described using a gravimetric (weighing) system to determine discharge rates. Head in the flumes was referenced to the bottom of the outlet end of the throat section, but was measured in the approach section of the flume. Because the cross-sectional area of the flow in the throat of the flume is of primary importance, some changes in selecting the reference point were made to improve this area determination. A template was accurately cut to the

intended shape of the flume throat. The template with known cross-sectional area was placed in the flume throat and the reference computed from the top of the known area template. This method produced a better computation of actual flow area available than might be obtained by reference to a single point on the flume floor, especially if the flume floor is irregular. For triangular and trapezoidal throats the template was trimmed at the corners in order to allow the confining walls to define the area. The slight fillets in the corners as constructed represented negligible area errors.

Noting the problems involved in correctly predicting low flows by the boundary-layer thickness method described in Annual Report, 1969, the computer was used to evaluate other models of friction accounting. Considerable improvement, applicable to all shapes tested and to several flumes calibrated by others resulted from evaluating the friction as if it were the total drag on flat plates. The only problem to date involves under-predicting the discharge for a triangular throated flume with a narrow opening (30°). A logical explanation appears to be that the drag does not develop as predicted because of mutual interference near the sharp bottom corner.

COMPUTATIONAL DERIVATIONS AND PROCEDURES:

The boundary layer thickness method discussed in Annual Report, 1969, worked for most flumes but gave some problems at low flows. Since it was based on adjusting the flow area to account for the maximum thickness of the boundary layer, it proved inconvenient to introduce other effects such as location of the depth sensing and length of the transition. Recourse to boundary drag concepts allows one to make computations as detailed as desired. However, many compromises between the advances in modern boundary layer theory and the application to the present problem were made because in most cases the precise

roughness properties of the walls were not known to a degree that justified an extremely rigorous computational procedure. Fortunately, high precision in the estimate of this roughness and in the computation of the friction loss was not required to predict flume calibrations to about $\pm$ 2% over a low flow to high flow ratio of more than 1 to 100.

The method of predicting boundary drag is developed from the concepts presented in Schlichting (4) for one side of a flat plate held parallel to the general flow of a fluid.

Using the principles of fluid dynamics, the throat section of the flume can be conceived as a flat plate warped into the geometrical shape of the throat. A fluid flowing through the throat will create a drag on the inside surface. This force, D, is assumed equal to the drag created by the flow of fluid along one side of a flat plate held parallel to a fluid flow and is given by

$$D = C_F \rho \frac{V^2}{2} PL \qquad (1)$$

where C_F is the total drag coefficient, ρ is the mass density of the fluid, V is the average fluid velocity, and the plate surface area is given by the product of the wetted perimeter, P, and the throat length, L.

The boundary layer is assumed to begin its development at the leading edge of the plate, or in this application, at the entrance to the flume throat. Further, the boundary layer is assumed to have a laminar region extending from the leading edge to some critical Reynolds Number, R_c, based on length, X_c, from the leading edge, after which the drag will be determined by turbulent boundary layer concepts. The existence of the laminar section causes the total drag to decrease, and, following Prandtl (Schlichting (4) p. 538), the decrease can be estimated if it is

assumed that, in the section beyond the point of transition, the turbulent boundary layer behaves as if it were turbulent from the leading edge. Thus, it is necessary to subtract the turbulent drag up to the point of transition and to add the laminar drag for the same length.

The corrected total drag coefficient, C_F', for a given flume throat can then be shown to be

$$C_F' = C_F - \frac{R_c}{R_L} [C_{F,t} - C_{F,l}] \qquad (2)$$

where $C_{F,t}$ and $C_{F,l}$ denote the coefficient of turbulent and laminar skin friction, respectively, for the total drag up to X_c where transition occurs (i.e. at R_c), R_L is the length Reynolds Number based on the entire throat length, L_3, and C_F is the coefficient of total skin friction based on turbulent flow also over the entire length, L_3.

No completely comprehensive method for reliably predicting R_c is available. Schlichting (4, p.379) estimates it to range from 3.5×10^5 to about 10^6, but Harrison (2) used a range from 3×10^5 to 3×10^6. Smooth boundaries and low turbulence intensities would tend to delay the transition. If, however, R_c is a function of relative roughness alone, the concept of permissible roughness may be used (Schlichting (4, p.559)) to estimate R_c. A linear empirical relationship was chosen that would keep R_c in the range suggested by Schlichting (4) for most flume throat lengths likely to be encountered, i.e. R_c should not exceed 10^6 even for smooth glass flumes with throat lengths of 10 ft. The relation chosen was

$$R_c = 350{,}000 + L_3/K \ . \qquad (3)$$

Having estimated R_c, it is then possible to solve for $C_{F,t}$, $C_{F,l}$, and hence C_F' using the "Coefficient of Total Skin Friction Diagram" (Harrison (2)), or by iteratively solving the equation

$$C_F = \frac{0.544\sqrt{C_F}}{5.61\ C_F^{0.5} - 0.638 - \log_e \left[\frac{1}{R_L C_F} + \frac{1}{4.84\ C_F^{0.5}\ L_3/K}\right]} \tag{4}$$

for both C_F and $C_{F,t}$, the latter simply by substituting $C_{F,t}$, R_c, and X_c for C_F, R_L, and L_3, respectively. ($X_c = R_c\ \nu/V_3$, where ν is the fluid kinematic viscosity.)

The value for $C_{F,l}$ is obtained from Schlichting (4, p. 122-123) for the laminar region of the boundary layer development, or

$$C_{F,l} = 1.328/R_c^{0.5} \tag{5}$$

When the estimated value for R_c exceeds R_L, the C_F' is given by equation (5) with C_F and R_L replacing $C_{F,l}$ and R_c respectively. Equation (1) can then be solved with $C_F = C_F'$.

The drag force can be represented in terms of head loss by observing that the drag force is retarding a volume of water with weight γ per unit volume moving under the influence of an energy gradient such that it loses H head in a distance L or

$$D = \gamma\ AL\ \frac{H}{L} \tag{6}$$

Thus

$$H = \frac{D}{\gamma A}\ . \tag{7}$$

The same result can be obtained from work and power considerations, since from the power standpoint

$$P = \gamma QH = \text{Force} \times \text{Velocity} \tag{8}$$

or

$$\gamma QH = D \times \frac{Q}{A} \tag{9}$$

and

$$H = \frac{D}{\gamma A} \tag{10}$$

Other minor drag-force losses include those in the approach section from the point of depth measurement to the entrance of the converging section, and those through the converging section. These are approximated by using an average drag coefficient of 0.0235 and an average wetted perimeter in the converging section based on the entrance area and an estimated exit area. The exit area depth was calculated to be equal to the critical depth, Y_3, in the throat, plus about 5/8 of the difference between the upstream depth Y_1 and the critical depth, Y_3.

The sum of these head-loss estimates were then included in the general iteration equations for the flumes (see Annual Reports 1966-1969).

THE EVALUATION OF THE ENERGY DISTRIBUTION COEFFICIENT

Yet another factor requires evaluation for precision flume-calibration predictions. This is the energy-distribution coefficient, α, which really corrects for the errors introduced by the method of calculation. Since the average velocity is used throughout the computation, whenever there is a velocity gradient the energy computed using the average velocity in the flow section will be less than the actual energy represented by the integral of the point velocities. For convenience in computation, the average velocity is traditionally used and a coefficient, α, slightly greater than unity is introduced.

Attempts by Robinson and Chamberlain (3) to measure the velocity distribution in the throats of flumes indicated that the velocity distribution coefficient (for the throat section, designated herein as α_3) was essentially unity. However, the measurements were made in flows where the throat length was on the order of one or two times the flow depth. This could be expected in converging flows where the opportunity to develop a stable flow profile is limited by throat length. At low flow rates, where the throat is ten to thirty times the flow depth, a fully developed flow profile may likely be present, and the velocity distribution coefficient may approach the value frequently associated with long prismatic open channels, 1.04. This is also the value used to compute the energy in the approach section of the flume since it is assumed that the approach section is long enough to develop the flow profile.

It appears logical that α_3 should be a function of (a) length for flow development, (b) roughness in the throat, and (c) the cross-sectional shape of the throat.

Cross-sectional shape might be characterized by the hydraulic radius or by a width to depth ratio, although the former, if not perfect, is probably better than the latter and has the advantage of some type of rational transfer of wide channel and pipe results to the present problem. This will become more apparent in the following development.

Chow (1, p.29) presents the approximate formulas for α derived for a logarithmic distribution in a wide channel

$$\alpha_3 = 1 + 3E^2 - 2E^3 \qquad (11)$$

See Chow P 211, 8, 168
Schlichting P.537
or Harrison Eq 2

where: $E = (v_{max}/\bar{v}) - 1$, or in terms of fully developed flow, $E = 0.8831^{0.5} = 0.8834C_F^{0.5} = 1.77\ C_F^{0.5}$. ($C_F$ should be used rather than C_F' since maximum development of the boundary layer

properties are of primary concern in evaluating E). Thus, roughness of the flume throat, and to a certain extent, the flow regime, laminar, transitional, or turbulent, is reflected.

The above development is for wide channels, and some consideration of cross-sectional shape is needed. Recourse to laminar flows in wide rectangular channels and circular channels flowing half-full should provide a representative range of α values for relative comparison. Laminar flows in pipes have an α value of 2.00 while that for wide channels is 1.54 (Chow (1, p. 154)). While not in any way rigorous, a similar deviation from unity due to shape might be applied to the wide turbulent flows. Using the hydraulic radius, R, to represent the channel shape factor, we find that R = d for very wide rectangular channels and R = d/2 for semi-circular channels where d represents the flow depth measured at the centerline of the flow cross section. In the throat, the ratio of average depth D_3 to the hydraulic radius in the throat, R_3, D_3/R_3, goes from 1 to 1.57 as α_3 goes from 1.54 to 2.00 for the wide channel and semi-circular channel, respectively, or an increase above unity of 0.54 and 1.00, or (1.0 - 0.54)/0.54 = 0.85 increase. A corresponding relationship for the turbulent case can be approximated between $(\alpha_3 - 1)$ and R_3/D_3 by the linear equation

$$(\alpha_3 - 1) = [3E^2 - 2E^3]\,[1.5D_3/R_3 - 0.5] \tag{12}$$

or

$$\alpha_3 = 1 + [3E^2 - 2E^3]\,[1.5D_3/R_3 - 0.5] \tag{13}$$

Another modification should be evident. If the throat is too short to produce fully developed flow (in pipe flow, at least 10 diameters and in many cases 100 diameters are required) then

some discounting of both the shape effect and the flow profile effect on α_3 should be made. Some consideration is made in the Reynolds Number when evaluating C_F, but the effect is actually in the wrong direction in that short throat lengths tend to decrease the Reynolds Number, increasing C_F and thus the calculated α_3 value. This can be rationalized by recalling that the relationships between E, f, and C_F are based on developed turbulent flow. An apparently reasonable assumption is that nearly fully developed flow exists when the throat length exceeds the equivalent of 10 pipe diameters or about 40 R, and that full discounting of all deviations from unity should prevail when the throat length is less than about 2 R_3. (The Robinson and Chamberlain (3) data support~~s~~ this.) Again using a linear function to interpolate between these two extremes, the discounting factor should range between 0 and 1 for R_3 between about 2 and 42, respectively or

$$\text{discounting factor} = 0.025\ R_3 - 0.05 \tag{14}$$

The final computation of α_3 then becomes

$$\alpha_3 = 1 + [3E^2 - 2E^3]\ [1.5\ D_c/R_3 - 0.5]\ [0.025\ R_3 - 0.05] \tag{15}$$

RESULTS:

As formulated in the above equations, the entire deviation in discharge from an ideal flow must be accountable in terms of H_f, α_3, α, none of which are convenient to measure accurately in the flumes. However, as stated before, high accuracy in these estimates is not required to satisfactorily evaluate the departure from the predicted calibration for an ideal frictionless flow through the flume. Recourse to evaluating the relations lies in examining the success with which the equation can predict the calibration for a variety of flumes that have been carefully tested.

To aid evaluation of the computational procedure, the ten flume shapes and sizes calibrated in the laboratory were each subjected to computer analysis. A calibration table was first computed for an ideal, frictionless flow through each flume. Then, the computations were repeated incorporating a series of specified roughnesses and the velocity distribution coefficients. For purposes of comparison, a type of calibration coefficient was computed as the quotient of the computed real flow discharge based on frictional estimates, Q, and the ideal flow discharge, Q_i, or Q/Q_i. The laboratory measured discharges can be likewise compared to Q_i and plotted among the curves based on the specified roughness values. The test of the procedure then is shown by how well the laboratory data is fitted by an appropriate, or reasonable, roughness-based curve. The roughness heights should correspond to handbook values listed for the type of construction material used in the particular flume.

The flume calibrations were satisfactorily predicted to $\pm$ 2%, as can be observed in Figures 1, 2, and 3, except for the long-throated rectangular flume, Figure 1, where errors of approximately 5% are noted for flow depths of about 1/3 ft. Thus, when friction effects dominate as in this case, inaccuracies in H_f become observably significant.

In another instance, not plotted, a narrow-throated triangular flume (30° opening) consistently discharged about 3% more than predicted. A possible source for discrepancy may lie in the assumption that the flume can be warped into the desired throat shape and still be treated as a flat plate. If this is the case, then the effects of two 90° bends must be considered for the rectangular flume as opposed to two much less radical bends on the trapezoidal flume of the same throat length. The latter was predicted satisfactorily.

In the case of the triangular flumes, the sharp bend at the bottom and the resulting close proximity of the walls probably do violate the assumptions of a flat plate. Another possibility is that the effective throat length is reduced because critical depth does not occur at the end of the throat as assumed because of the boundary layer obstruction to the flow. In the case of the triangular flumes better agreement is achieved if L_3 is reduced 25 to 50%.

Examination of the relative effects of long throat lengths illustrates the desirability of keeping the throat length at a minimum. For example in Figure 1, the basic difference between the group of curves, a, and the group, b, is the throat length. In the shorter 3-ft. length flume, a roughness change, from K = 0.00005 ft to 0.0005 ft, due to weathering of the construction materials will cause a change of about 1% in discharge. In the 8-ft length flume, the change would be nearly 2%. Similar comparisons for the flumes in Figures 2 and 3 can be made.

SUMMARY AND CONCLUSIONS:

Investigation of the variables affecting the calibration prediction of critical-depth flumes was continued in the laboratory and by mathematical modeling on a computer. The boundary-layer thickness modeling method previously reported was abandoned in favor of a boundary-layer, drag-force, modeling technique that is more versatile and more capable of adaptation to a wide variety of roughness characteristics in the flumes and to a variety of cross-sectional shapes.

The method involved applying principles of hydrodynamics to the calculation of the drag force exerted by a flowing fluid on one side of a flat plate which is then warped to form the flume throat. This drag is converted to energy loss through the flume and incorporated into the appropriate form of the energy equations for predicting the flume calibrations.

The method was applied to ten flumes constructed and calibrated in the laboratory; two 1 ft wide rectangular throated flumes, one with 3-ft and one with 8-ft throat lengths; two trapezoidal-throated flumes, both with 1:1 side slopes, but one had a 0.4 ft wide throat and was hydraulically smooth while the other had a 0.9 ft wide throat that was raised 0.5 ft above the approach section of the flume and was rough surfaced; and six triangular flumes with openings of 90°, 90°, 60°, 60°, 53°, and 30°, respectively, throat lengths varying from 1 to 8 ft, and roughness heights ranging from hydraulically smooth to 0.005 ft.

All flume calibrations were satisfactorily predicted to $\pm$ 2% over the entire test range except for the low flows in the long-throated rectangular flume when errors exceeded 5% at flow depths below 0.3 ft and in the 30° triangular-throated flume where the discharge was underpredicted by about 3% over the entire test range. The rectangular-throated flume indicates that there are limitations on the method especially when the throat length is greater than 30 times the depth of flow in the throat. The possible source for error in both instances may be the fact that no allowance for the sharp corners is made since the predictions for the less radically warped cases of the trapezoidal-throated flumes with two 135° corners are satisfactory.

Future efforts will be directed toward solving field problems of depth sensing, sedimentation effects, and the magnitude of changes in calibration due to partial submergence.

REFERENCES:

1. Chow, Ven Te, Open-Channel Hydraulics. McGraw-Hill Book Company, Inc., New York, 1959.

2. Harrison, Anthony J. M., Boundary-layer displacement thickness on flat plates. Proc. Amer. Soc. Civil Engin. 93(HY4):79-91. 1967.

3. Robinson, A. R. and Chamberlain, A. R. Trapezoidal flumes for open-channel flow measurements. Trans. Amer. Soc. Agric. Engin. 3(2):120-124, 128. 1960.

4. Schlichting, Hermann. Boundary Layer Theory. McGraw-Hill Book Co., Inc., New York, 4th Edition, 1960.

PERSONNEL: J. A. Replogle

CURRENT TERMINATION DATE: December 1970

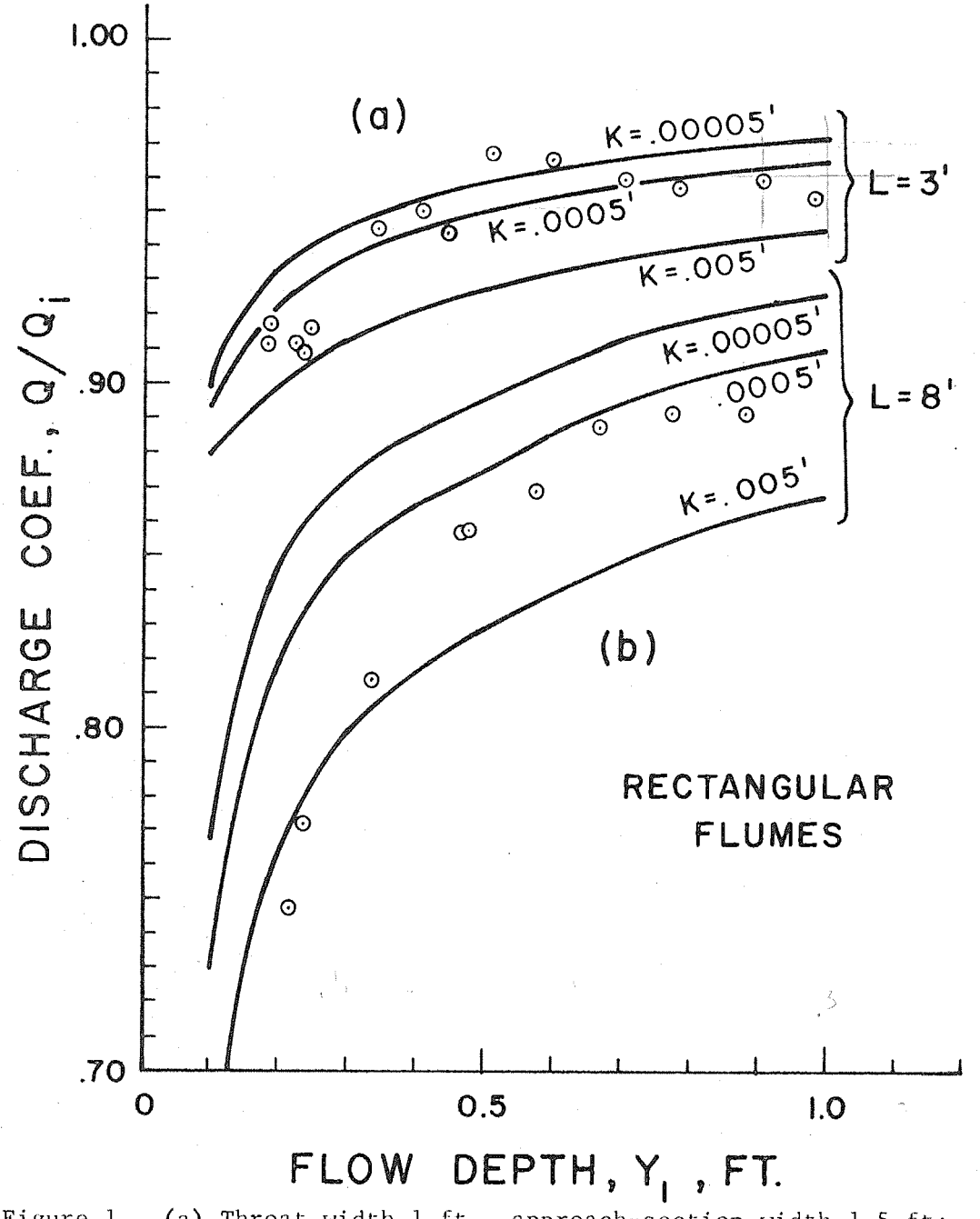

Figure 1. (a) Throat width 1 ft, approach-section width 1.5 ft; converging section length 1.5 ft; zero sill height in throat, galvanized sheet metal construction.
(b) Identical to (2) except throat length, L, is 8 ft as indicated.

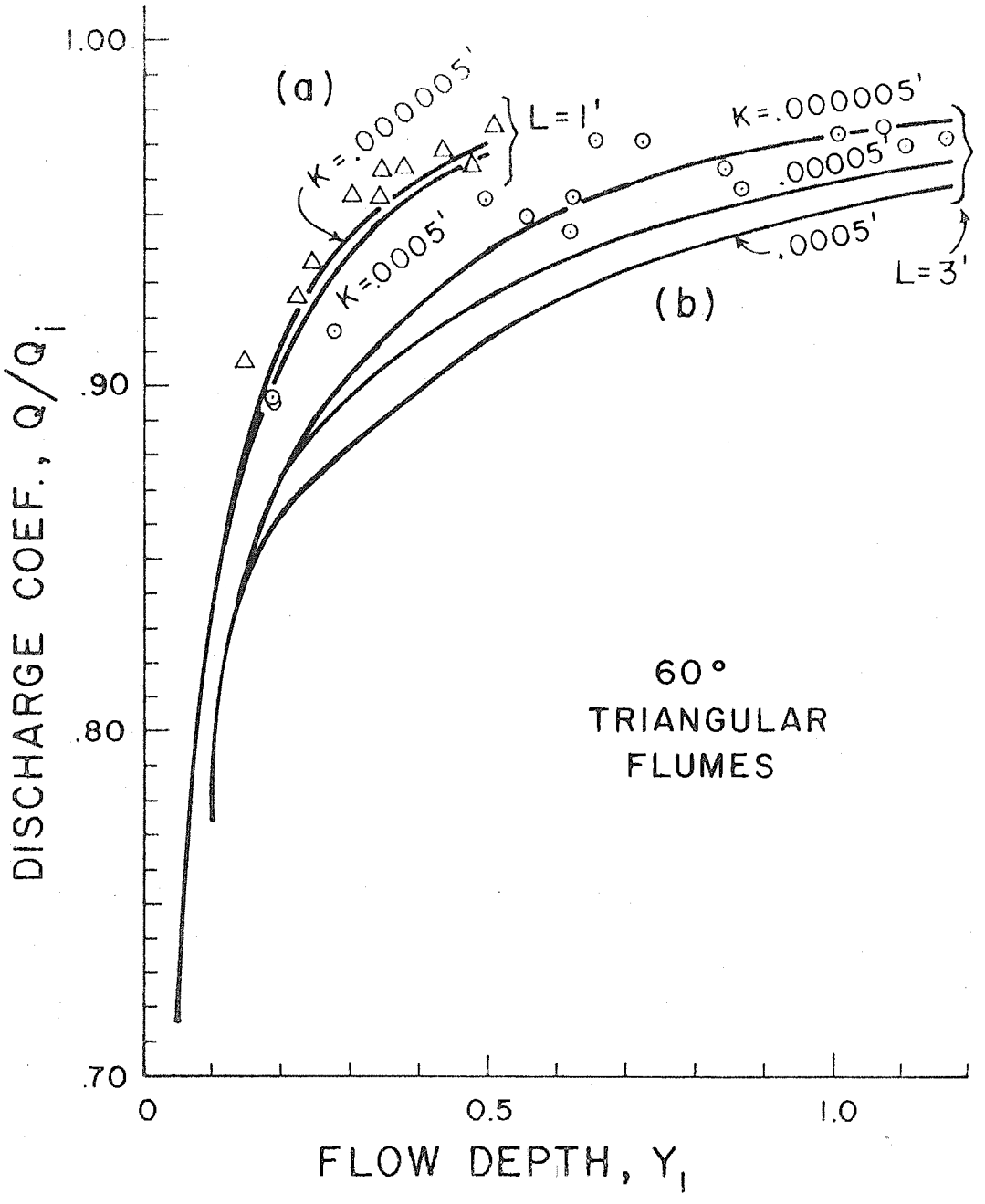

Figure 2. (a) Throat opening, 60°; approach-section, 60° sideslopes and 0.167 ft bottom width; converging section 0.582 ft long; zero sill height in throat; aluminum sheet metal construction. (b) Throat opening, 60°; approach-section, 60° sideslopes and 0.667 ft bottom width; converging section, 2 ft long; zero sill height; fiberglass construction.

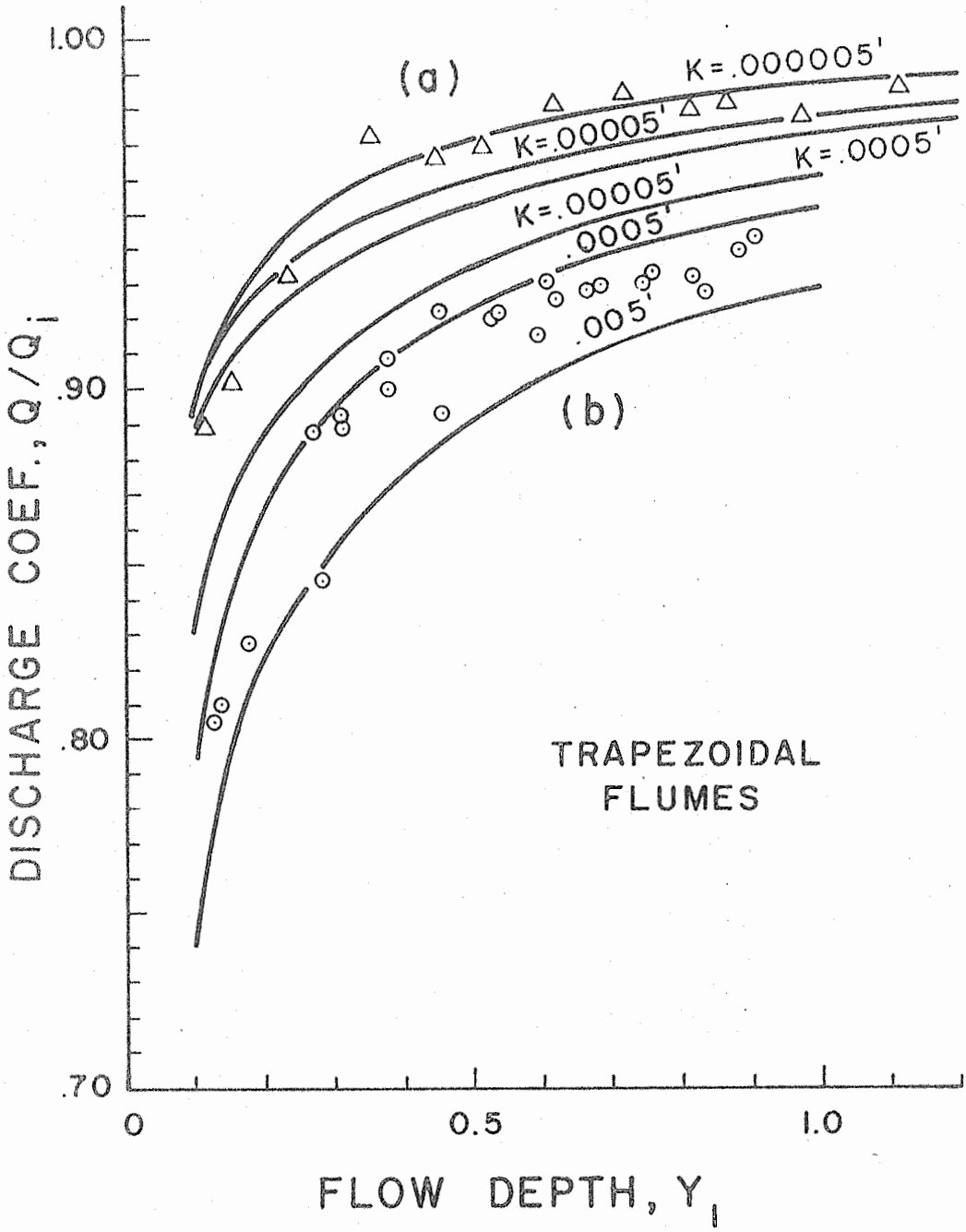

Figure 3. (a) Throat opening, 1:1 sideslopes and 0.333 bottom width; throat length, 3 ft; approach-section, 1:1 sideslopes and 0.833 bottom width; converging section, 3 ft long; zero sill height; sanded and varnished fiberboard construction. (b) Throat opening, 1:1 sideslopes and 0.962 bottom width; throat length, 8 ft; approach section, 1:1 sideslopes and 1 ft bottom width; converging section, 3 ft long; sill height, 0.463 ft; sheet aluminum construction, coated with fiberglass and asphalt mix.

TITLE: ASSESSING THE ENERGY ENVIRONMENT OF PLANTS

CRIS WORK UNIT: SWC-019-gG-3 CODE NO.: Ariz.-WCL-68-5

INTRODUCTION:

The emphasis this year in assessing the energy environment of plants dealt mostly with matters of instrumentation. Work of this nature was conducted in six major areas: net radiation, atmospheric thermal radiation, solar radiation, infrared emittance, energy balance, and soil heat flux.

PROCEDURES AND RESULTS:

A simple technique for the long-wave calibration of net and one-way radiation probes was developed. Materials required for the method are inexpensive and easily assembled. Calibrations of several Fritschen-type net radiometers obtained by the new technique and by a chamber technique agreed to within better than $\pm$ 3%. The new technique thus appears to be a simple, trustworthy alternative to the much more involved chamber technique of long-wave calibration.

Many commercially available net radiometers using polyethylene shields to protect their sensing surfaces have 5% of these surfaces covered with a highly reflective white paint. The purpose of this paint is to reduce the sensitivities of these instruments to short-wave radiation and make them equal to a supposedly lower long-wave radiation sensitivity. Rederivations of the net long-wave radiation equations for the calibration chambers of Funk and Fritschen, who pioneered in the construction and evaluation of these instruments, indicate, however, that certain approximations made in the original derivations completely account for the original 5% discrepancy. New experiments verified these findings and demonstrated the equality of short- and long-wave calibration constants for polyethylene-shielded net radiometers without the customary 5% areal covering of white paint.

Theoretical considerations indicated that for surfaces with temperatures significantly different from that of the ambient air,

net radiation measurements become increasingly less representative of surface conditions with increasing height above the surface. For a dry, bare soil on a clear summer day at Phoenix, significant errors were noted at a height of only 50 cm. An experiment was thus designed to see how low the net radiometers could be lowered before their shadows became an important factor. For a Fritschen-type net radiometer, it was found that the optimum vertical location was 25 $\pm$ 5 cm.

A study was carried out to determine the effect of screen-level air temperature upon net radiation. It was found, in general, that net radiation decreases with decreasing temperature to about 0 C, whereupon any additional air temperature decrease results in an increase in net radiation.

A Fritschen-type net radiometer was converted to a hemispherical radiometer by the spray application of black paint to the lower polyethylene dome and the utilization of a second polyethylene layer to secure three fine thermocouples in close proximity to the inwardlying radiating paint surface. All theoretical and experimental work conducted with the new radiometer indicated that it performed properly under both laboratory and field conditions. The instrument measures the total influx of solar and atmospheric thermal radiation.

A radiation balance and modified radiation balance method were used to determine hourly and daily values of atmospheric thermal radiation on three clear and three cloudy days during February and March 1970 at Phoenix, Arizona. The radiation balance was utilized over surfaces of bare soil, bermudagrass, and open water; while the modified radiation balance was utilized over the open water surface only. It differed from the pure radiation balance method in that net radiation was calculated as the residual in the energy equation rather than being measured.

The values of atmospheric thermal radiation thus obtained were compared to values obtained from measurements of incoming,

all-wave radiation minus incoming solar radiation. From this analysis it appeared that the best alternative to the semi-direct measurement of atmospheric thermal radiation was the radiation balance over the bare soil surface. Results from this method were of sufficient accuracy, even on an hourly basis, for most research studies, and were even better on a daily basis. Radiation balances over grass and water surfaces were somewhat less satisfactory, but still better than the modified radiation balance method.

Measurements of direct and diffuse solar radiation, surface temperature and vapor pressure, and atmospheric dust content were made at two localities on the outskirts of Phoenix, Arizona. On two days of light air pollution with different dust contents, but nearly identical amounts of precipitable water aloft, total transmittances of the atmosphere for solar radiation were nearly identical, while ratios of diffuse to direct solar radiation were quite different. The utility of diffuse skylight measurements to provide a detailed characterization of light to moderate particulate air pollution episodes was thereby demonstrated.

Methods for modifying polyethylene-shielded net radiometers to measure solar radiation underwater were developed. Five specific modifications were made and tested for use in determining both down-welling and up-welling radiation. All five modifications appeared to be successful in both applications. A field trial of the instruments indicated that they yielded a logarithmic extinction relation in very turbid water with the up-welling radiation being equal to about 2.2% of the down-welling radiation at any level.

A new technique for measuring infrared emittances of terrestrial surfaces was developed. It is based upon the derived prediction that when surfaces of identical temperature are viewed through an aperture of an enveloping blackbody cavity of different temperature, the output of the infrared thermometer is a linear function of surface emittance. This relation was verified

experimentally and a simple approximate technique consequently developed, where the internal cavity of the infrared thermometer head serves as the blackbody cavity.

An extensive amount of energy balance data obtained over a variety of different surfaces and climatic conditions was analyzed to yield evaluative information with respect to the "heating coefficient" of Monteith and Szeicz and the "long-wave exchange coefficient" of Gay. The results indicated that both of these parameters were less than adequate in both a statistical and descriptive context.

An alternative approach to that currently in general useage for the measurement of conductive heat flux in soils was developed. It has only one general requirement, and that is that the thermal conductivity of the heat flux plate be as great as possible. It is based upon a new technique for the calibration of heat flux plates whereby a heat radiation method is used to calibrate the heat flux plate in terms of the heat passing through the plate itself and not through any surrounding medium. A method was also developed to obtain geometry factors for any heat flux plate, and it would appear that once it is utilized with a highly conductive heat flux plate, a simple formula may yield geometry factors quite accurately in the future. The complete concept appears to be sound in all respects and should allow the measurement of conductive heat flux in soils to be made with uncertainties of only a very few percent.

SUMMARY AND CONCLUSIONS:

A simple technique for the long-wave calibration of net and one-way radiation probes was developed. It was demonstrated that polyethylene-shielded net radiometers do not require any white paint on their sensing surfaces. Net radiometers of the size of the Fritschen and Funk types were found to give the best readings at a height of 25 $\pm$ 5 cm, when the underlying surface is of a temperature significantly different from that of the ambient air.

It was found, in general, that net radiation decreases with decreasing temperature to about 0 C, whereupon any additional air temperature decrease results in an increase in net radiation.

A Fritschen-type net radiometer was converted to a hemispherical radiometer. A radiation balance over bare soil gave the next best approximation of atmospheric thermal radiation. Diffuse skylight measurements were found to be very characteristic of the atmospheric dust content. Polyethylene-shielded net radiometers were also converted to underwater use.

A new technique for measuring infrared emittances of terrestrial surfaces was developed. An extensive amount of energy balance data was analyzed to evaluate the "heating coefficient" and the "long-wave exchange coefficient." Finally, a new approach to the measurement of soil conductive heat flux was developed and partially tested.

PERSONNEL: S. B. Idso

CURRENT TERMINATION DATE: 1971

TITLE: COMPUTER SIMULATION OF GREENHOUSES

CRIS WORK UNIT: SWC-019-gG-3 CODE NO.: Ariz.-WCL-70-1

INTRODUCTION:

It is well known from greenhouse and growth chamber studies that CO_2 fertilization will substantially increase the yields of almost all crops. However, attempts to fertilize with CO_2 in normal field culture have resulted in failure because turbulent exchange is so rapid in an open field that almost all of the CO_2 released has been lost to the atmosphere. Many greenhouses currently employ CO_2 fertilization on a regular basis. However, the effectiveness of the practice has been limited because at high light intensities when CO_2 fertilization should be most effective, the greenhouses have had to be ventilated to lower the inside temperature, and much CO_2 has been lost [Kretchman and Howlett (2)]. If, however, a means could be found to economically control the temperature of a greenhouse under high light conditions without resorting to any form of ventilation, CO_2 fertilization could be practiced more advantageously. In addition, crops could then be grown with almost zero water use, a feature which would make such a system particularly attractive to arid regions.

The benefits to mankind stemming from the development of a practical temperature control for a sealed greenhouse could be very great indeed. As a first stage in the research and development of such a control, this project was initiated with the following two objectives: (1) Develop a computer program which can simulate all significant heat exchange processes occurring in a greenhouse; and (2) Run the program with various sets of experimental parameters for the optical and thermal properties of greenhouse walls to try to find new ways to provide suitable closed environments for plant growth.

During the past year, Objective 1 has been attained.

PROCEDURE:

A computer program was developed which simulates all the

significant heat exchange processes or fluxes occurring in a greenhouse. As described by Kimball (1), the fluxes were formulated in the program in terms of known weather and greenhouse parameters and unknown temperatures and vapor pressures. The unknown temperatures and vapor pressures were then calculated from the solution to a set of simultaneous energy balance equations which were written to describe the balance of energy at several locations in a greenhouse. The model is designed to be flexible so that both conventional and unusual thermal and optical properties of the greenhouse walls and methods of heating and cooling can be simulated and their effects on the greenhouse environment evaluated.

Temperature, vapor pressure, and radiation observations were made in the glass greenhouse located at the U.S. Water Conservation Laboratory, Phoenix, Arizona in order to obtain physical data against which to compare the model [Kimball (1)]. The measurements were taken on 22 June 1970 when the greenhouse was evaporatively cooled, on 23 June 1970 when the evaporative coolers were turned off, and on 25 June 1970 when the greenhouse was again evaporatively cooled, but had had a coarse cloth sun screen placed over the top. No crop was present in the greenhouse during the time the measurements were taken, and it was assumed that no significant evaporation occurred from the dry gravel, concrete, and wooden bench surfaces which constituted the "soil" surface.

RESULTS AND DISCUSSION:

Generally, the observed and predicted values agreed closely. However, the model did tend to underestimate air temperatures slightly and to overestimate soil surface temperatures on all three days, indicating that perhaps larger values should have been used for an inside convective transfer coefficient. The computed and observed radiation fluxes agreed closely except just before noon on 23 June 1970, when a period of cloudiness decreased all the observed values and except for the inside solar radiation on 25 June 1970. In the latter case, the fabric shade apparently absorbed more than

50% (the value used in the model) of the incident solar radiation during most of the day. Then, starting at 1500, the sun shone directly on the solarimeter through an unshaded west end. Since the computed and observed temperatures agreed closely, the radiation entering the unshaded east and west ends of the experimental greenhouse apparently balanced the extra radiation allowed to pass through the fabric shade due to the low percent absorption value used for the model greenhouse. Additional data are needed in order to predict the inside convective transfer coefficients more accurately, and to test the model with a vegetative canopy, but the evidence indicates that the present model can accurately predict the heating and cooling requirements of a greenhouse for a wide range of greenhouse properties and environmental conditions. During the coming year, the program will be run using various sets of optical and thermal properties for greenhouse walls to try to find new ways to provide suitable closed environments for plant growth in accordance with Objective 2 of this research outline.

SUMMARY AND CONCLUSIONS:

The energy balance of a greenhouse was simulated with a digital computer program. The fluxes of solar radiation were calculated from sun angle equations and the optical properties of the greenhouse walls and vegetation. The thermal radiative, sensible, latent, and conductive heat fluxes were modeled by mathematical equations in terms of unknown temperatures and vapor pressures. Provision was made for the introduction of externally imposed heating or cooling fluxes. Energy balance equations were then developed for various locations in the greenhouse where the sum of the fluxes at that location should be zero. The equations were solved by an iterative procedure to obtain the unknown temperatures and vapor pressures.

Measurements of temperatures and radiation fluxes were obtained in a glass greenhouse to provide physical data with which to compare values predicted by the model. The greenhouse was

alternatively 1) evaporatively cooled and not shaded, 2) not cooled and not shaded, and 3) cooled and shaded, each treatment lasting one day. The observed and predicted values agreed closely for each of these extremely different treatments. It is concluded that the model can accurately predict the heating and cooling requirements of a greenhouse for a wide range of greenhouse properties and environmental conditions.

REFERENCES:

1. Kimball, B. A. Simulation of the energy balance of a greenhouse. Agron J. Submitted. 1971.

2. Kretchman, D. W. and Howlett, F. S. CO_2 enrichment for vegetable production. Trans. Am. Soc. Agric. Eng. 13:252-255. 1970.

PERSONNEL: B. A. Kimball

CURRENT TERMINATION DATE: 1973

TITLE: DESIGN AND PERFORMANCE OF TRICKLE IRRIGATION SYSTEMS

CRIS WORK UNIT: SWC-019-gG-3 CODE NO.: Ariz.-WCL-70-3

INTRODUCTION:

A new method of water application -- trickle irrigation -- has aroused considerable interest because of possibly increased water-use efficiency, reduced labor requirements, and improved crop production. The ultimate capabilities of trickle irrigation systems are to apply the desired quantity of water evenly, frequently, and automatically. Trickle irrigation delivers water by means of a small perforation, nozzle, or applicator in a plastic pipe, capable of being spaced as desired, and discharges water through these outlets at fairly low rates. A trickle irrigation system is usually planned to be above ground, although this same equipment may be used underground (subsurface irrigation); however, the latter may be more susceptible to clogging.

At present, trickle irrigation is in the developmental stages. Researchers and some commercial enterprises have found three problems in subsurface and trickle irrigation to be the most difficult -- the variability of discharge rates from supposedly identical orifices or applicators, differences in uniformity of water application along a lateral line because of velocity and pressure changes, and clogging of orifices. To date, very little information is available on optimum design of discharge rates from outlets, operating pressures, spacing of outlets, length of lateral line, and water quality requirements.

The initial objective of this study is to develop improved principles and methods for designing trickle irrigation systems. First, the design of an appropriate outlet or applicator which reduces clogging and nonuniformity of discharge rates will be investigated. Lastly, criteria for managing trickle irrigation systems for increased water use efficiency, improved crop production, and salinity control will be investigated.

RESULTS AND DISCUSSION:

Theoretical Considerations: The hydraulics of the flow for a trickle irrigation pipeline can be described as spatial varied closed-conduit flow. Investigation of the energy equation reveals that the distribution of flow is determined by the change in velocity and friction loss as the quantity of flow decreases along the lateral. As a part of the fluid volume is being discharged through the outlets, the velocity head decreases, causing an increase in pressure as predicted by the energy equation. Oppositely, the head loss due to friction causes a reduction in pressure. Friction loss between outlets will vary with the velocity and coefficient of friction between each outlet. The magnitude of these two values will determine whether there will be an increase or decrease of pressure at the end of the lateral. For trickle irrigation systems, the velocity head is usually small compared to the friction loss head; thus pressure normally decreases in the direction of flow.

Design Considerations: Before an improved trickle irrigation system can be designed, a number of hydraulic factors need to be considered. Some of these criteria are: (1) the desired range of discharge rates, (2) the desired range of operating pressures, (3) the optimum spacing of orifices, and (4) the maximum length of lateral line.

Discharge rates usually range from 0.5 - 3.0 gals per hour for trickle irrigation systems. It is evident that the smaller the discharge rate, the smaller the required component parts of the system; i.e., pump size, header lines, and lateral line dimensions. On the other hand, clogging problems could be reduced by using larger orifices with higher discharge rates to shorten operation time and increase the velocity in the lateral line.

If it is assumed that all the water should be supplied to the plant on the day it is required, it would be sufficient to supply a quantity of 0.5 inch per day on the hottest day of the year in

Arizona to meet the maximum evapotranspiration of an unspecified crop. The quantity of water required would be 13,600 gals per acre per day. Suppose that a minumum number of applicators for a tree crop is 200 applicators per acre, and the maximum number of applicators required for a vegetable crop is 6,500 applicators per acre. Therefore, the theoretical output per applicator would be 68 gals per day for the tree crop, and 2 gals per day for the vegetable crop. Realizing that the application time for the system can be varied, it would be possible to apply 2.8 gals per hour for 24 hours on the tree crop, and 2.0 gals per hour for 1 hour on the vegetable crop. Assuming that each applicator waters a 2 ft circle (or approximately 4 sq ft), a soil intake rate of at least 1 inch per hour would be required.

The feasible range of operating pressures, optimum spacing of orifices, and the maximum length of lateral depend, of course, on the outlet design and the field situation. However, operating pressures above 10 psi may cause erosive water jets from discharge orifices, unless the outlet has an expensive protective cover or a flow-spreading device. As for minimum pressures, laboratory experience would suggest that pressures below 1 to 2 psi result in fluctuating discharge rates. It is also anticipated that the system should include the capabilities for applying a higher-than-normal pressure to facilitate flushing the system. Concerning orifice spacings, indications are that spacings less than 40 inches are satisfactory and that closer orifice spacings along the lateral may be desirable for specific crops and soil types. Lastly, the length of lateral line in the past has been limited to less than 300 ft.

A theoretical analysis by computer of the flow characteristics along the lateral line was completed, assuming a 2 gal per hour discharge rate, a 2 psi minimum pressure, a 2 ft orifice spacing, and a 300 ft lateral line. At present, modifications in assumed hydraulic criteria and design principles and methods are being

considered for obtaining uniform discharge rates from trickle irrigation systems.

Outlet Discharge: Studies are being conducted to determine the coefficient of discharge and the variability of discharge rates to be expected for three types of outlets -- plain perforations, plastic nozzle inserts, and metal inserts. The test results to date are given in Table 1, showing the discharge variabilities and discharge coefficients determined in the laboratory.

Plain perforations were made by drilling and punching holes into polyethylene, rigid polyvinyl chloride, flexible polyvinyl chloride, and acrylonitrile-butadiene-styrene (ABS) plastic pipe. From visual inspection, drilled holes, which were constructed by drilling from the inside into a patch cut from a section of ABS pipe, appeared to be free from loose fibers and burrs. Drilling was accomplished with a slow spiral drill, 5400 rpm drill speed, slow feed speed, water as a coolant, and drilled into a wood dowel. Clean-appearing holes were made in ABS pipe using a small diameter punch constructed from a hypodermic needle -- outside diameter, 0.025 inch -- with the end cut flat and the cutting edge ground to a fine outside edge. The plastic nozzle tested was a molded plastic insert of 0.021 inch inside diameter. The metal inserts tested were a brass bushing insert with a 0.028 inch drilled hole and a stainless steel hypodermic needle insert of 0.020 inch inside diameter, with a 0.2 inch orifice length projecting into the pipe. The variability of discharge rates appears to be improved by using plastic nozzles or metal inserts rather than the plain perforations.

The test facility constructed in the laboratory included a reinforced plastic filter with an activated charcoal cartridge of a 1 micron rating, a pressurized water tank to reduce pressure surges, a pressure regulator, and a precision needle flow valve to provide a constant-head water supply. A mercury manometer, with 0.05 psi subdivisions, was used for head measurements. The test lines were

48 inches long with outlets spaced 4 inches apart. The discharge was collected in 10 vertical, calibrated Pyrex tubes, 48 inches in length and 22 mm in diameter. A stop watch was used to time the flow into the tubes, while the supply pressure was constant within 0.1 psi during a run. The velocity of flow in the test line was not of sufficient magnitude to warrant consideration of friction losses within the short pipe length.

SUMMARY AND CONCLUSIONS:

A new method of water application -- trickle irrigation -- has aroused considerable interest because of possible increased water-use efficiency, reduced labor requirements, and improved crop production. A study was initiated in 1971 to develop improved principles and methods for designing trickle irrigation systems. The effectiveness of the systems is dependent upon the extent that uniform discharge rates can be obtained from outlets and that variations of discharge rates along the trickle lateral can be reduced. Studies are being conducted to determine the variability of discharge rates to be expected for three types of outlets -- plain perforations, plastic nozzle inserts, and metal inserts. The plastic nozzles and metal inserts appear promising. A theoretical analysis of the flow characteristics along the lateral line was initiated. Modifications in hydraulic criteria and design principles are being considered for obtaining uniform discharge rates from trickle irrigation systems.

PERSONNEL: D. A. Bucks, L. J. Erie, J. A. Replogle, and L. E. Myers.

CURRENT TERMINATION DATE: October 1973.

Table 1. Discharge Rates for Trickle Irrigation Outlets

Outlet Description	Head at the Outlet (ft)	Discharge Rates Mean (gph)	Discharge Rates Standard Deviation (gph)	Coefficient of Variability (± %)	Coefficient of Discharge
Plastic Drill Patch .028 inch diameter	4.62	1.49	.174	11.7	.76
	6.93	1.86	.225	12.1	
	9.24	2.13	.265	12.4	
	13.86	2.62	.345	13.2	
	18.48	3.02	.412	13.7	
	23.11	3.34	.543	16.2	
Punched Hole .025 inch diameter	4.62	.763	.047	6.2	.47
	6.93	.905	.078	8.6	
	9.24	1.05	.090	8.5	
Plastic Nozzle .021 inch diameter	4.62	1.05	.042	4.0	.94
	6.93	1.28	.054	4.2	
	9.24	1.49	.066	4.4	
Brass Insert .028 inch diameter	4.62	1.77	.053	3.0	.91
	6.93	2.22	.066	3.0	
	9.24	2.60	.076	2.9	
Hypodermic Needle Insert .020 inch diameter	4.62	.634	.022	3.4	.65
	6.93	.802	.026	3.2	
	9.24	.917	.026	2.8	
	13.86	1.14	.040	3.5	
	18.48	1.34	.052	3.9	
	23.11	1.51	.058	3.9	

APPENDIX I

SUMMATION OF IMPORTANT FINDINGS

SWC-012-gG-1 METHODS FOR WATER QUALITY IMPROVEMENT AND ITS STORAGE UNDERGROUND

The rise of the groundwater mound in relation to recharge rate remained essentially unchanged after 3.3 years of groundwater recharge with secondary sewage effluent in which a depth of 862 ft of effluent was applied. Thus, the hydraulic conductivity of the aquifer beneath the 10-ft deep water table remained constant, and clogging of the deeper soil materials, which could restrict the useful life of a recharge system for renovating waste water, did not take place. (WCL 67-4)

The nitrogen content of the soil below recharge basins intermittently inundated with secondary sewage effluent showed no change in 1970, when 400 ft of effluent moved into the soil, and was only 0.1 mg per gram of dry soil higher than that of the virgin soil outside the basins. This amount of nitrogen can only account for a small fraction of the nitrogen removed from the effluent as it seeped through the soil. Thus, the main mechanism for nitrogen removal must have been biodenitrification. (WCL 67-4)

Much nitrogen removal previously thought to occur during flooding of recharge basins with sewage effluent may actually be due to denitrification during the drying period. An environment suitable for denitrification was maintained in laboratory soil columns during a 10-day dry period following flooding with secondary sewage effluent. Measurements showed that half of a 250-cm soil column remained in a reduced condition even though the soil was drained. This same anaerobic environment may persist in the field during drying periods as well as during inundation and allow continuous denitrification. Chemical oxygen demand reduction under these reduced conditions was equal to that under aerobic conditions, indicating

that the efficiency of organic carbon removal would not be affected by maintaining anaerobic zones. (WCL 68-3)

Intermittent flooding appears to be a requirement for consistent removal of large amounts of nitrogen from sewage water by soils during groundwater recharge. Soil columns which had lost their capacity for nitrogen removal during 120 days of continuous flooding were then placed on an intermittent flooding schedule. The capacity to remove nitrogen from sewage water was restored after the columns released stored nitrogen during the first few cycles of flooding and drying. The amount of nitrogen removal after the rejuvenation was more than could be explained by the freeing of adsorption sites. The alternate flooding and drying must, therefore, be required to develop the proper biological environment for nitrogen removal. (WCL 68-3)

The solubility of gypsum in mixed-salt solutions of high concentrations could be predicted more accurately by accounting for the interaction of Ca^{2+} with the acetate, chloride, and nitrate anions. New dissociation constants for these interactions were established through experimental and theoretical treatment of the anomalous solubility behavior of gypsum in single Na-salt solutions. These constants are of value for understanding the basic phenomenon involving cation-anion interactions and also for characterizing gypsum solubility in saline irrigation and groundwaters, and sea water. The presence of Ca^{2+} association involving more complicated bicarbonate-carbonate-hydroxyl species than previously considered were indicated from computer analysis of Ca^{2+} interaction in different types of $CaCO_3$-solution systems. An entirely different type of Ca species distribution is indicated for the acidic, calcareous, and alkaline soil systems, thus affecting the availability and precipitation behavior of Ca in a variety of ways. (WCL 64-6)

An equation was developed theoretically which relates the free-swelling of montmorillonite clays to their water content and surface area. All the known published, pertinent clay-swelling data were tested and were found to conform to the new equation. The theoretically based parameters of the equation should permit its use for studying a host of physical-chemical properties of clays and soils, including: clay surface area determinations, qualitative and quantitative clay mineral identification in clay type mixtures, surface charge density evaluations, studying the distribution of exchangeable cations on clays, and quantitatively discerning between the water hydrating the non-swelling edge or peripheral surfaces and that associated with the swelling clay surface portion. (WCL 67-2)

X-ray studies of the swelling behavior of various mixtures of sodium and calcium montmorillonite revealed that when 50 percent or more of the clay is in the sodium form, these two cations become homogeneously distributed throughout, and the clay swells as if it were all the sodium form. But when calcium-clay is the predominant form, these two cation types become demixed into separate regions. This demixing limits the swelling of the calcium clay portion, but permits complete free-swelling of the sodium clay portions as water is added to the system. The consequences of such demixing of cations on clay may include soil structural alteration through preferential erosion of any sodium portion; also, localized demixing could influence ion diffusion, water movement, and other physical-chemical properties of clays and soils. (WCL 67-2)

A new type of equation has been developed for describing the physical adsorption of water vapor and other gases on solid surfaces. The equation, which describes sigmoidal or S-shaped curves, evolved after a series of mathematical manipulations of the parameters of another sigmoidal equation -- that from the field of statistical quantum mechanics. The new equation was tested statistically on a large number of such adsorption isotherms of soil and clay minerals, and was compared to five other well-known adsorption equations. The new equation was markedly superior to any of the other five in describing such adsorption data. Potential applications for such an equation include predicting the soil water content and/or the relative humidity of soils under natural field conditions, and evaluating water vapor movement in such soils. (WCL 67-2)

The gamma-ray transmission technique for measuring soil water content was modified for use under field conditions. The modification involved compensating for the effect of temperature on the gamma-ray detector assembly. In conjunction with a programmable controller, the system continuously and repeatedly scans preset increments of the soil profile to determine soil-water content. This development

greatly increases field measurement capabilities in studies of the evaporation of water from and the infiltration of water into soil. (WCL 68-1)

Fabricated in place, asphalt-fiberglass linings have proven to be excellent materials for constructing water harvesting catchments on difficult sites. Fiberglass matting is laid over the soil and sprayed with asphalt emulsion. After curing for a few days a seal-coat of asphalt-clay roofing emulsion is applied. A 10,000 ft^2 installation requires less than 30 man-hours. Three catchments have been installed on sites so rough that butyl rubber or any other elastomeric or plastic materials could not have been used. The asphalt-fiberglass is easily installed, is highly resistant to damage by animals or wind, and costs less than half the cost of butyl rubber. This material will allow the development of livestock water supplies at many sites where previously available materials would have required prohibitive construction costs. (WCL 68-2)

SWC-019-gG-3 EFFICIENT IRRIGATION AND AGRICULTURAL WATER USE

Field studies have shown that the new short straw varieties of Mexican wheats yield about 250 lbs of grain per inch of water evaporated as compared to 100 lbs of grain for the older varieties. Sonora 64, Siete Cerros, and Inia 66 required less than 10 percent more water than the older varieties, but yielded about 2-1/2 times more grain. These studies show that tremendous improvement in water use efficiency can be achieved through the development of improved crop varieties. (WCL 58-2)

The water-use efficiency (WUE) of agave (Century plant) in the desert (Granite Reef) was 4.4 kg of fresh weight m^{-3}, a mean of two plots, over a 21-month preconditioning period. This value, attained with a total water application, including rainfall, of 591 mm per year (less than 2 ft), equals the WUE of high-producing alfalfa, which requires 1854 mm per year (6^{+} ft) in a similar environment. Such efficient water use by agave depends on responses typical of succulents, featuring daytime stomatal closure and dark fixation of carbon dioxide. Enhancement of such processes in agronomic crops may be obligatory for economical production as irrigation costs rise. (WCL 62-10)

The energy balance of a greenhouse was successfully simulated with a digital computer program. Results computed from the program agreed closely with values observed in a glasshouse for a wide range of different conditions. This agreement is important because it gives confidence that the computer program can now be used to simulate unorthodox greenhouse constructions. Thus, various untested and untried methods of achieving greenhouse temperature control can now be simulated in an attempt to find an economically practical method to grow plants in a closed environment with almost zero water consumption and with CO_2 fertilization to increase yields. (WCL 70-1)

PL 480 PROJECTS

A10-SWC-20 BIOLOGY AND CONSUMPTIVE WATER USE OF RANGE PLANTS UNDER DESERT CONDITIONS

This project received additional funding in November 1969 to finance additional field work and preparation of final report, but no progress reports were received during 1970. Accordingly, research findings during 1970 are not known at this time.

A10-SWC-75 INFILTRATION AND RAINFALL RUNOFF AS AFFECTED BY NATURAL AND ARTIFICIAL SURFACE CRUSTS

Collection of meaningful data has been delayed by problems in obtaining equipment. No significant research findings for 1970 are available at this time.

APPENDIX II

LIST OF PUBLICATIONS PUBLISHED AND MANUSCRIPTS PREPARED IN 1970

		MS No.
SWC-012-gG-1	Methods for water quality improvement and its storage underground.	
Published:		
	Bouwer, Herman. Groundwater recharge design for renovating waste waters. Jour. Sanitary Engin. Div., Amer. Soc. Civil Engin. Proc. 96(SA 1):59-74. 1970.	285
	Bouwer, Herman. Water quality aspects of intermittent infiltration systems using secondary sewage effluent. Artificial Groundwater Recharge Conf. Proc., Paper 8. Univ. of Reading, England. Sept. 1970.	310
	Bouwer, Herman. Closure: Salt balance, irrigation efficiency, and drainage design. Jour. Irrig. and Drain. Div., Amer. Soc. Civil Engin. Proc. 96(IR 3): 349-351. 1970.	316
Prepared:		
	Bouwer, Herman. Digest: Salt balance, irrigation efficiency, and drainage design. Trans., Amer. Soc. Civil Engin. (Submitted for publication).	317
	Bouwer, Herman. Waste water purification. Chap. in McGraw-Hill Yearbook of Science and Technology, 1971. (In press).	324
	Bouwer, Herman. Digest: Groundwater recharge design for renovating wastewater. Trans., Amer. Soc. Civil Engin. (Submitted for publication).	333

MS No.

Bouwer, Herman, and Lance, J. C. Reclaiming municipal waste water by groundwater recharge. Amer. Assoc. Adv. Sci. Symp. on Urbanization of Arid Lands Proc., Chicago, Illinois. December 1970. (In press) 331

Bouwer, Herman, and Mann, Russel F. Agricultural and urban waste water reuse. Presented at Amer. Soc. Civil Engin. Water Resources Engin. Conf., Phoenix, Arizona, January 11-15, 1971. (Approved for preprint distribution). 346

Lance, J. C. Nitrogen removal from waste water by chemical and biological reactions in the soil. Jour. Water Pollution Control Fed. (Submitted for publication). 336

		MS No.
SWC-018-gG-2	Increasing and conserving farm water supplies.	

Published:

Bouwer, Herman and Rice, R. C. Closure: Salt penetration technique for seepage measurement. Jour. Irrig. and Drain. Div., Amer. Soc. Civil Engin. Proc. 96(IR 3):344. 1970.	314
Cooley, Keith R. Energy relationships in the design of floating covers for evaporation reduction. Water Resources Res. 6(3):717-727. June 1970.	302
Cooley, Keith R. Evaporation from open water surfaces in Arizona. Univ. of Ariz. College of Agric. Exten. Serv. Folder 159. April 1970.	304
Cooley, Keith R. Rainfall-runoff relationships for natural and lined-channel watersheds. Symp. of ARS-SCS Workshop on Hydrologic Models Proc., Tucson, Arizona, 16-19 March 1970. Section 35, Pp. 1-11.	308
Fink, Dwayne H. Water repellency and infiltration resistance of organic-film coated soils. Soil Sci. Soc. Amer. Proc. 34(2):189-194. 1970.	290
Frasier, Gary W., and Myers, L. E. Protective spray coatings for water harvesting catchments. Trans., Amer. Soc. Agric. Engin. 93(3):292-294. 1970.	274
Jackson, R. D., and Whisler, Frank D. Equations for approximating vertical non-steady-state drainage of soil columns. Soil Sci. Soc. Amer. Proc. 34(5):715-718. 1970.	291

MS No.

Kimball, Bruce A., and Lemon, E. R. Spectra of air pressure fluctuations at the soil surface. Jour. Geophys. Res. 75(33):6771-6777. 1970. 321

Myers, Lloyd E. Opportunities for water salvage. Civil Engin. 40(1):41-44. 1970. 283

Myers, Lloyd E., and Frasier, Gary W. Evaporation reduction with floating granular materials. Jour. Irrig. and Drain. Div., Amer. Soc. Civil Engin. Proc. 96(IR 4):425-436. 1970. 295

Nakayama, F. S. Hydrolysis of sodium carbonate. Jour. Chem. Ed. 47(1):67-68. 1970. 269

Nakayama, F. S. Hydrolysis of $CaCO_3$, Na_2CO_3 and $NAHCO_3$ and their combinations in the presence and absence of external CO_2 source. Soil Sci. 109(6):391-398. 1970. 294

Nakayama, F. S. Sodium bicarbonate and carbonate ion-pairs and their relation to the estimation of the first and second dissociation constants of carbonic acid. Jour. Phys. Chem. 74(13):2726. 1970. 305

Reginato, R. J., and Stout, Karl. Temperature stabilization of Gamma Ray transmission equipment. Soil Sci. Soc. Amer. Proc. (NOTE) 34:152-153. 1970. 288

Whisler, Frank D., and Bouwer, Herman. Comparison of methods for calculating vertical drainage and infiltration for soils. Jour. Hydrol. X(1):1-19. 1970. 280

Whisler, Frank D., Klute, Arnold, and Millington, R. J. Analysis of radial, steady-state solution and solute flow. Soil Sci. Soc. Amer. Proc. 34(3):382-387. 1970. 298

	MS No.
Prepared:	
Bouwer, Herman. Digest: Planning and interpreting soil permeability measurements. Trans., Amer. Soc. Civil Engin. (Submitted for publication).	313
Bouwer, Herman, and Rice, R. C. Digest: Salt penetration technique for seepage measurements. Trans., Amer. Soc. Civil Engin. (Submitted for publication).	315
Bruce, R. R., and Whisler, Frank D. Infiltration of water into layered field soils. Trans., Joint Meeting, Commissions I and VI, Internatl. Soil Sci. Soc., Israel, August 1971. (Submitted for presentation and publication).	345
Cooley, Keith R., and Idso, S. B. Atmospheric thermal radiation: An isolated anomaly. Jour. Atmos. Sci. (NOTE). (Submitted for publication).	326
Cooley, Keith R., and Idso, S. B. A comparison of energy balance methods for estimating atmospheric thermal radiation. Water Resources Res. (Submitted for publication).	329
Frasier, Gary W. Optimum design of water harvesting structures by computer. USDA-ARS 41-175. (In press).	330
Kimball, Bruce A., and Lemon, E. R. Air turbulence effects upon soil gas exchange. Soil Sci. Soc. Amer. Proc. (Submitted for publication).	320
Kimball, Bruce A., and Lemon, E. R. Theory of soil air movement due to pressure fluctuations. Agric. Meteor. (Submitted for publication).	332

MS No.

Myers, Lloyd E. Digest: Opportunities for water salvage. Trans., Amer. Soc. Civil Engin. (Submitted for publication). 311

Nakayama, F. S. Thermodynamic functions for the dissociation of $NaHCO_3^o$, $NaCO_3^-$, H_2CO_3, and HCO_3^-. Jour. Inorg. & Nucl. Chem. (Submitted for publication). 309

Nakayama, F. S. The possibility of bicarbonate and carbonate association with potassium in carbonate solution. (Approved for publication). 318

Nakayama, F. S. Problems associated with the determination and application of the solubility product constant. Soil Sci. Soc. Amer. Proc. (Submitted for publication). 341

Nielsen, D. R., Jackson, R. D., Cary, J. W., and Evans, D. D., Editors. SOIL WATER. Univ. of California, Davis. (In press). 339

Reginato, R. J., and Jackson, R. D. Field measurement of soil-water content by Gamma-ray transmission compensated for temperature fluctuations. Soil Sci. Soc. Amer. Proc. (Submitted for publication). 343

Whisler, F. D., and Watson, K. K. Digest: Analysis of infiltration into draining porous media. Trans., Amer. Soc. Civil Engin. (Submitted for publication). 328

MS No.

SWC-019-gG-3 Efficient irrigation and agricultural water use.

Published:

Idso, S. B. The transmittance of the atmosphere for solar radiation on individual clear days. Jour. Appl. Meteorol. 9(2):239-241. 1970. 287

Idso, S. B. The relative sensitivities of polyethylene-shielded net radiometers for short- and long-wave radiation. Rev. Sci. Instr. 41(7):939-943. 1970. 301

Idso, S. B., Baker, D. G., and Blad, B. L. Reply to discussion of "Relation of radiation fluxes over natural surfaces". Qtrly. Jour. Royal Meteorol. Soc. 96(410): 765-767. 1970. 325

Idso, S. B., and DeWit, C. T. Light relations in plant canopies. Appl. Optics 9(1):177-184. 1970. 279

Idso, S. B., and Kangieser, P. C. Seasonal changes in the vertical distribution of dust in the lower troposphere. Jour. Geophys. Res. 75(12):2179-2184. 1970. 296

Replogle, J. A. Flow meters for water resources management. Water Resources Bul. 6(3):345-374. 1970. 306

Prepared:

Erie, L. J., Replogle, J. A., and French, O. F. Non-erosive field turnout structures to distribute large streams of irrigation water. (Approved for publication). 312

Idso, S. B. A simple technique for the calibration of long-wave radiation probes. Agric. Meteorol. (Submitted for publication). 307

MS No.

Idso, S. B. Relations between net and solar radiation. Jour. Meteorol. Soc. Japan. (In press). 322

Idso, S. B. Transformation of a net radiometer into a hemispherical radiometer. Agric. Meteorol. (In press). 323

Idso, S. B. Modifications of shielded net radiometers to measure solar radiation profiles in water. Limnology and Oceanography. (Submitted for publication). 337

Idso, S. B. The utility of diffuse skylight measurements in characterizing low levels of particulate air pollution. Atmos. Environ. (In press). 338

Idso, S. B. Evaporation suppression by solar radiation reflection. Jour. Geophys. Res. (In press). 340

Idso, S. B. Possible effects of global temperature change on earth's vegetation. In "Man's Impact on the Global Environment: Tech. Vol. II". Mass. Inst. Tech. Press. (In press). 342

Idso, S. B., and Blad, Blaine L. The effect of air temperature upon net and solar radiation. Jour. Appl. Meteorol. (Submitted for publication). 344

Idso, S. B., and Cooley, K. R. The vertical location of net radiometers. I. The effects of the underlying air layer. Agric. Meteorol. (Submitted for publication). 334

Idso, S. B., and Cooley, K. R. The vertical location of net radiometers. II. The effect of the net radiometer on the underlying surface. Agric. Meteorol. (Submitted for publication). 335

MS No.

Jensen, Marvin and Erie, L. J.
Irrigation and water management.
Chap. 8 in "Advances in Sugar Beet
Production: Principles and Practices".
Ortho Div., Chevron Chem. Co. (In press). 319

Replogle, John A. Critical-depth flumes
for flow determinations in canals and
open channels. Trans., Amer. Soc.
Agric. Engin. (Submitted for publication). 327

APPENDIX III

SUMMARY TABLE OF STATUS OF RESEARCH OUTLINES

	Title	Code
SWC-012-gG-1	Methods for water quality improvement and its storage underground	
Ariz.-WCL 66-1	Experimental and analytical studies of the flow and oxygen regimes in soil intermittently inundated with low quality water	B
Ariz.-WCL 67-4	Waste-water renovation by spreading treated sewage for groundwater recharge	B
Ariz.-WCL 68-3	Column studies of the chemical, physical, and biological processes of wastewater renovation by percolation through the soil	B
Ariz.-WCL 70-2	Characterization of the soil microflora and biological processes occurring in soil used for waste water renovation	B

	Title	Code
SWC-018-gG-2	Increasing and conserving farm water supplies	
Ariz.-WCL 60-7	Soil treatment to reduce infiltration and increase precipitation runoff	B
Ariz.-WCL 61-4	Measurement and calculation of unsaturated conductivity and soil water diffusivity	C
Ariz.-WCL 64-3	Clay dispersants for the reduction of seepage losses from reservoirs	C
Ariz.-WCL 64-4	Water-borne sealants to reduce seepage losses from unlined channels and reservoirs	C
Ariz.-WCL 64-6	Dispersion and flocculation of soil and clay materials as related to the Na and Ca status of the ambient solution	B
Ariz.-WCL 65-2	Materials and methods for water harvesting and water storage in the State of Hawaii	B
Ariz.-WCL 66-3	Study of unsaturated two-dimensional soil water flow using an analogue computer	C
Ariz.-WCL 67-2	Physical and chemical characteristics of hydrophobic soils	B
Ariz.-WCL 67-3	Use of floating solid and granular materials to reduce evaporation from water surfaces	B
Ariz.-WCL 68-1	Evaporation of water from soil	B
Ariz.-WCL 68-2	Fabricated-in-place, reinforced reservoir linings	B

	Title	Code
SWC-019-gG-3	Efficient irrigation and agricultural water use	
Ariz.-WCL 58-2	Consumptive use of water by crops grown in Arizona	B
Ariz.-WCL 62-10	Plant response to changes in evaporative demand and soil water potential, as shown by measurements of leaf resistance, transpiration, leaf temperature, and leaf water content	B
Ariz.-WCL 65-3	Integrating velocity profile meters	C
Ariz.-WCL 66-2	Irrigation outlet structures to distribute water onto erosive soils	B
Ariz.-WCL 66-4	Automation of water distribution systems for surface irrigation	C
Ariz.-WCL 67-1	Flow measurement in open channels with critical depth flumes	B
Ariz.-WCL 68-4	Water stresses in plants	C
Ariz.-WCL 68-5	Assessing the energy environment of plants	B
Ariz.-WCL 68-6	Simulation of plant communities for determining water use efficiency	C
Ariz.-WCL 70-1	Computer simulation of greenhouses	B
Ariz.-WCL 70-3	Design and performance of trickle irrigation systems	B

	Title	Code
PL-480 Projects		
A10-SWC-20	Biology and consumptive water use of range plants under desert conditions	B
A10-SWC-75	Infiltration and rainfall runoff as affected by natural and artificial surface crusts	B
E30-SWC-4	Influence of irrigation on changes of physical properties of soil	A